

RESEARCH AND TECHNOLOGY

(NASA-TN-102150) RESEARCH AND TECHNOLOGY AT
KENNEDY SPACE CENTER, JANUARY, 1968
(NASA) 133 P

NOV-11-68

05/99 UNCLAS
0110825

NASA Technical Memorandum 102150



1968 ANNUAL REPORT

John F. Kennedy
Space Center

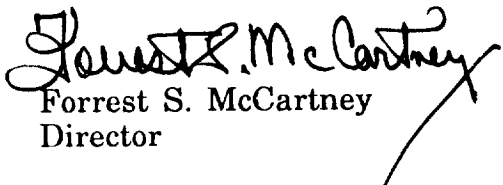
"Journey to Venus: The Magellan Expedition" - gouache rendering by Lew Wallace, Boeing Aerospace Operations, Inc., shows deployment of a spacecraft equipped with imaging radar to map the surface of Venus.

**Research and Technology
1989 Annual Report
of the John F. Kennedy
Space Center**

FOREWORD

As the NASA Center responsible for assembly, checkout, servicing, launch, recovery, and operational support of Space Transportation System elements and payloads, the John F. Kennedy Space Center is placing increasing emphasis on its research and technology program. In addition to strengthening those areas of engineering and operations technology that contribute to safer, more efficient, and more economical execution of our current mission, we are developing the technological tools needed to execute the Center's mission relative to future programs. The Engineering Development Directorate and the Biomedical Operations and Research Office, encompassing most of the laboratories and other Center resources that are key elements of the research and technology program, are responsible for implementation of the majority of the projects in this Kennedy Space Center 1989 Annual Report.

Thomas M. Hammond, Technology Utilization Officer, PT-PMO-A, (407) 867-3017, is responsible for publication of this report and should be contacted for any desired information regarding the Center-wide research and technology program.


Forrest S. McCartney
Director

AVAILABILITY INFORMATION

For additional information on any individual report, contact the person identified following the article. Commercial telephone users can dial the listed extension preceded by area code 407. Telephone users with access to the Federal Telecommunications System can dial the extension preceded by 823.

CONTENTS

MECHANICS, STRUCTURES, AND CRYOGENICS	1
Prediction of the Frictional Pressure Drop in Fully Developed, Annular Liquid/Vapor Flow in Straight Ducts Under a Zero-Gravity Environment	3
<i>Based upon a prediction method developed by the University of Illinois and KSC, a step-by-step procedure for calculating frictional pressure drop in liquid/vapor duct flow in zero gravity is presented.</i>	
Comparison of Analytical Methods for Calculation of Wind Loads	5
<i>An analytical comparison between various building codes and standards was conducted to determine which one calculated larger wind load pressures.</i>	
Prediction of Near-Field Acoustic Environments for Advanced Launch Systems	7
<i>For the design of launch pad structures, an empirical computer-driven mathematical approach is developed to model the acoustical pressure (near) field of rocket engine exhausts.</i>	
Fluid Dynamics of Phase Separation in a Field of Centrifugal Acceleration	9
<i>By studying the behavior of two fluids of similar densities in a centrifugal flow, the equations for phase separation in a reduced gravity condition can be determined.</i>	
Advanced Liquid Hydrogen Transfer Line	10
<i>A new design of vacuum-jacketed liquid hydrogen lines uses its own generated gaseous hydrogen boiloff to increase line insulation quality by reducing the heat transfer rate.</i>	
Structural Loads in an Acoustic Field	11
<i>A new method is established for computing generalized modal loads in an acoustic field defined by a distribution of correlated pressures.</i>	
MATERIALS SCIENCE	14
Protective Coating Systems for the Space Transportation System Launch Environment	16
<i>Top coatings, for protection of zinc-rich primers (applied to launch site structures and equipment) from the acidic residues produced by solid rocket boosters, are undergoing a five-year, harsh-environment exposure program.</i>	

CONTENTS (Cont)

Corrosion of Convolute Metal Flexible Hoses	16
<i>Exposure of a number of alloys to a salt and acid environment has resulted in selecting Hastelloy C-22 as the optimum material for fabricating convolute metal flex hoses. A simple electrical impedance test may be the key for measuring an alloy's susceptibility to acid- and salt-induced corrosion.</i>	
Permeability of Polymers to Organic Liquid and Condensable Gases	17
<i>To find the optimum clothing/chemical combinations, protective polymeric-based protective clothing (including the Propellant Handlers Ensemble) is being subjected to various chemicals to determine breakthrough and steady-state permeation rates.</i>	
Protective Coating Systems for Repaired Carbon Steel Surfaces	17
<i>New metal coating products are undergoing laboratory and field evaluation tests to determine their ability to protect less-than-perfect prepared carbon steel from the KSC marine and launch environment.</i>	
Development of New Flooring Materials for Clean Rooms and Launch Site Facilities	18
<i>A formulation of chemically resistant polymers, conductive fillers, flame retardant activities, and structural adhesives is a potential replacement for PVC tiles or poured-epoxy, clean-room flooring if manufacturing problems can be solved and if field testing is successful.</i>	
Conductive Organic Polymers as Corrosion Control Coatings	19
<i>An evaluation program is in progress to answer the question: Can electrically conductive organic polymers protect steel structures from the launch site corrosion forces better than the currently used inorganic zinc-rich coatings?</i>	
Ignition of Metals in High-Pressure Oxygen	19
<i>Tests are being conducted in a high-pressure oxygen environment on various metals and metal alloys to determine their susceptibility to ignition propagation.</i>	
Thermal Tile Bonding Inspection Using Gamma Ray Scattering	20
<i>Gamma ray backscatter radiometry is being developed for inspecting thermal tile bonding integrity.</i>	
Laser Acoustic Thermal Protection System (TPS) Bond Assessment Study	20
<i>A noncontacting laser acoustic sensor to assess the integrity of tile bonding in the Shuttle thermal protection system is in the evaluation phase.</i>	

CONTENTS (Cont)

INSTRUMENTATION AND DATA ACQUISITION	22
Long-Term Testing of Transducers	24
<i>With the exception of analysis of malfunctions, the transducer long-term environmental test program is totally automated in its data acquisition, reduction, and retrieval functions.</i>	
Liquid Air Level Indicator for Portable SCBA Dewars	26
<i>A transducer capable of accurately measuring the level of liquid air remaining in the dewar vessel of a liquid air pack, independent of its orientation, is undergoing static and dynamic testing.</i>	
Automated Laboratory for Evaluation and Qualification of Transducers	28
<i>Automating qualification procedures has resulted in adding environmental testing to the incoming transducer acceptance test program.</i>	
Fast-Response Instrumentation Van	29
<i>A self-sufficient step van recently furnished with instrumentation signal conditioners has recording equipment that can support temporary and remote testing rapidly and with minimum setup time.</i>	
Precision Laser Tracking System II (PLTS II) System Development	30
<i>The global positioning system (GPS) and an infrared tracking system are capable of calibrating the Shuttle Microwave Scanning Beam Landing System in a cost-effective manner.</i>	
Handbook of Strain Gage Application Techniques	32
<i>A handbook to help engineers in the selection and application of strain gages is in the developmental stage.</i>	
Field Portable Biomedical Instrumentation System	33
<i>Prototype portable instrumentation is monitoring the parameters of physiologic heat stress of fire rescue men performing simulated rescues in the field.</i>	
Orbiter Tire Leak Rate Detection System	33
<i>Instrumentation that is capable of rapidly measuring a pressure drop of 0.23 psi/day is needed to establish Orbiter tire leak rates.</i>	
Instrumented Torque Wrench System (INTOWS)	34
<i>A torque wrench instrumented with strain gages and connected to a hand-held microprocessor that records such data as torque values and operator/tool certification status may replace the conventional inspection verification methods in some applications.</i>	

CONTENTS (Cont)

COMMUNICATIONS AND CONTROL	36
DC to 150-Megabits-Per-Second Fiber Optic Link Development	37
<i>A prototype DC to 150-megabits-per-second fiber optic link has been improved and repackaged and is undergoing a 13-kilometer field test.</i>	
BIOSCIENCES	38
Controlled Ecological Life Support System (CELSS) Breadboard Project	40
<i>Initial biomass production chamber experiments demonstrate that the chamber is an excellent facility for studying plant community biological processes.</i>	
Aquaculture Research	40
<i>As a part of biomass production, research efforts are underway to produce fish protein from the inedible biomass byproducts.</i>	
Kennedy Space Center Firefighters Occupational Performance Test Validation Program	41
<i>The results of a Combat Task Test (CTT) performed by a nonfirefighter group indicate that standardized fitness tests can predict performance on some CTT tasks and that test predictors were amenable to exercise training.</i>	
Tuskegee University Project	42
<i>All aspects of the sweet potato physiology are being studied to understand its production processes and its nutritional qualities.</i>	
Biomass Production Research	43
<i>The influence of carbon dioxide concentrations and the spectral content and photoperiod of plant lighting are being studied to optimize the production of soybean plants.</i>	
Orbiter Environmental Simulator	43
<i>A plant growth chamber is operated to simulate the Orbiter's environment by using actual Orbiter flight data to control (via a computer) the chambers.</i>	
Biomass Processing Research	44
<i>Development continues on the conversion processes for transforming biomass production chamber crop harvest residues into edible products.</i>	

CONTENTS (Cont)

EPCOT Project	45
<i>The plant nutrient delivery system in the NASA/EPCOT project is now automated for the generation of plant growth data.</i>	
Tubular Membrane Plant Growth Unit	46
<i>Work continues on optimizing the nutrient delivery system design of an automated prototype flight plant growth unit.</i>	
Space Biology Plant Research	47
<i>A research program has commenced in a new physiology/biochemistry laboratory to study the effects of microgravity on plant metabolism.</i>	
A New Technique for the Demonstration of Fiber-Type-Specific Capillarization in Skeletal Muscle	48
<i>A simple, cost-effective procedure for characterizing a single transverse section of skeletal muscle has been developed.</i>	
Environmental Monitoring	49
<i>The state of the KSC environmental work is synopsized.</i>	
Prototype Devices for Plant Growth	52
<i>Small business firms are developing the necessary specialized tools that control and monitor plant growth chambers to produce simulated environments.</i>	
Human Physiology Research Projects: Blood Pressure Control	53
<i>Test results suggest that adjusting the body fluid volume may have little effect on the ability of the carotid-cardiac baroreflex to reduce orthostatic hypotension (low blood pressure) caused by long exposure to microgravity.</i>	
HAZARDOUS EMISSIONS AND CONTAMINATION MONITORING	54
Real-Time Hydrazine Monitoring Using Surface-Enhanced Raman Spectroscopy (SERS)	56
<i>Applying the technique of surface-enhanced Raman spectroscopy to hypergolic vapor detection may provide a sensitive, fast-responding, qualitative, and quantitative real-time monitor.</i>	
Hydrogen Sulfide and Ammonia Effects on the ESI 7000 Series of Hypergolic Fuel Vapor Sensors	58
<i>Test results show that hydrogen sulfide is a suitable candidate for use as a test surrogate gas for monomethylhydrazine in a hypergolic vapor detection analyzer.</i>	

CONTENTS (Cont)

Field Testing of the Citrate Sampler	60
<i>A citrate sampling badge design used for hydrazine detection has been modified to negate interferent problems and is ready for field use.</i>	
Relative Humidity Compensation for an Infrared Total Hydrocarbon Monitor	60
<i>A calibration procedure has been developed for a total hydrocarbon monitor that compensates for the monitor's inherent response to ambient water vapor.</i>	
Photoionization Detection of Hydrazine	65
<i>Test results show that commercial photoionization detectors are best suited to detect hydrazines in clean-room environments (low contamination and constant humidity).</i>	
Enhancements to the Hypergolic Vapor Detection System	68
<i>Hypergolic vapor detection colyzers will be modified to eliminate a single-point failure in the sample delivery circuit and to add a remote functional check capability to the electrochemical sensing cell.</i>	
A Feasibility Study of an Ion Mobility Spectrometer (IMS) for Hydrazine Vapor Detection	71
<i>A commercial ion mobility spectrometer, capable of detecting low monomethyl-hydrazine concentrations, may be used as a KSC portable vapor detector if the recovery time and ammonia interference can be reduced.</i>	
Evaluation of Quick-Response Oxygen Analyzers	73
<i>For detecting oxygen deficiencies, an investigation program has been initiated to identify a monitor that complies with a 10-second response requirement.</i>	
Development of an Improved Particle Counter Calibration System	73
<i>An aerosol generation system is being developed that will produce streams of particles with known size and a concentration in the 0.5- to 5.0-micron range.</i>	
Multispectral Imaging of Hydrogen Flames	75
<i>A prototype hydrogen flame imaging system can detect and distinguish infrared heat sources and then translate that information onto an ordinary operational television CRT.</i>	
Hypergolic Vapor Generation and Validation	76
<i>A hypergolic vapor generator and sophisticated vapor delivery system are required to accurately calibrate toxic vapor detection instrumentation.</i>	
Preliminary Evaluation of Commercial Hypergolic Fuel Vapor Sensors	78
<i>Through an evaluation and development program, efforts are underway to identify a new, technically advanced generation of hypergolic vapor detection instrumentation.</i>	

CONTENTS (Cont)

Advanced Hazardous Gas Detection System (AHGDS)	83
<i>A new mass spectrometer developed for submarines is under test and evaluation and may be the analyzer selected for the next generation of hazardous gas detection systems.</i>	
Color Chemistry of Hydrazine Detection	84
<i>The presence of monomethylhydrazine in the parts-per-billion range can be detected in real time using colorimetric chemistry techniques.</i>	
GMD Badge Test	85
<i>Two colorimetric dosimeter models using different chemical detection approaches were successfully tested for their ability to detect hydrazines.</i>	
Rocket Engine Leak Detection Mass Spectrometer (RELDMS)	86
<i>A project to demonstrate the capability for building a fast, lightweight, flight-qualified mass spectrometer leak detector that can be located close to potential leak sources (such as rocket engines) has been initiated.</i>	
Evaluation of Ammonia Sensors for Toxic and Flammable Concentrations	87
<i>An evaluation program has been initiated to evaluate off-the-shelf monitors that are capable of detecting low (threshold limit value) and high (flammable level) concentrations of anhydrous ammonia.</i>	
METEOROLOGY	89
Simulated Lightning for Research Studies	90
<i>A high-energy Marx generator will be used to generate a simulated lightning-derived electromagnetic field and to simulate lightning strikes on lightning-protected structures.</i>	
Short-Term Forecasts Using Wind Divergence	91
<i>When analyzed, a dense set of wind observations is an aid in predicting summer thunderstorms.</i>	
Kennedy Atmospheric Boundary Layer Experiment (KABLE)	94
<i>Meteorological data collection and analysis improve sea breeze predictability and verify/improve the transport and diffusion algorithms being used at KSC/CCAFS launch sites.</i>	
Forecasting Cloud Growth Using Satellite Sounding	95
<i>Geostationary satellites can take many more temperature and moisture profiles of the cloud environment than conventional earth stations. The operational utility of these profiles is being studied.</i>	

CONTENTS (Cont)

AUTONOMOUS SYSTEMS	98
Artificial Intelligence Mass Spectrometer (AIMS)	100
<i>Artificial intelligence (knowledge-based) technology is being developed for monitoring, analyzing, and displaying data from a hazardous gas detection system's mass spectrometer.</i>	
Remote Maintenance Monitoring System	101
<i>An expert system maintenance tool, consisting of data acquisition components implanted in a multicomputer system, a data retrieval network, and expert system software resident in a host maintenance processor, is capable of anticipating or detecting impending failures and hard failures.</i>	
Intelligent Launch Decision Support System (ILDSS)	107
<i>A knowledge-based software tool is being developed to support the NASA test director's decisionmaking process and its impact to the critical time elements of the launch countdown on and after the T-9 minute milestone.</i>	
Automated Tile Inspection	109
<i>A robotic system with a laser end effector successfully demonstrates that the Space Shuttle thermal tiles critical step-and-gap measurements can be totally automated.</i>	
Remotely Operated Umbilical System Development	110
<i>A robotic mechanism and sensor system is being developed to remotely mate a pair of large-capacity umbilical connections under spacecraft dynamics.</i>	
Automated Radiator Inspection	112
<i>A program is being initiated to develop a highly accurate robotic system integrated with an inspection sensor that can spatially locate damages to Orbiter radiator panels.</i>	
Checkout, Control, and Monitor Subsystem (CCMS) Operations Analyst (OPERA) Expert System	113
<i>An integrated set of expert systems is being developed to automate and standardize the isolation and correction of problems occurring in a complex distributed computer network.</i>	
Automatic Test Expert Aid System Environment (AT-EASE)	119
<i>A "smart" front end has been incorporated into automatic test equipment (ATE) systems and provides automated generation of test program sets for printed circuit board testing and validation.</i>	
Human Factors and Expert Systems	121
<i>Expert systems technology is being applied to developing explosive hazard classifications for energetic materials used in rocket and gun propulsion systems.</i>	

CONTENTS (Cont)

Knowledge-Based Autonomous Test Engineer (KATE) 122
KATE, the generic model-based expert system shell that was successfully demonstrated during Shuttle liquid oxygen loading operations, is now being applied to new checkout and launch domains.

TECHNOLOGY UTILIZATION 125

Feasibility Analysis of a High-Efficiency Dehumidifier/Air Conditioner Using Heat Pipes 126
Heat pipes are used as a heat feedback device to reduce the power consumption of air conditioning systems.

Development of a Digital Hearing Aid 127
Customizing the physical and acoustical parameters of hearing aids to the needs of users by use of digital circuitry and adaptive fitting procedures results in an improved design.

Mechanics, Structures, and Cryogenics

The sheer magnitude of the mechanical systems and attendant structures at the John F. Kennedy Space Center (KSC) requires unique facilities and equipment to solve design and operations problems or to advance the state of the art in mechanical and civil engineering. Three major areas that support the mechanics, structures, and cryogenic design and research effort are: (1) the Launch Equipment Test Facility, which is the primary testbed for full-scale, proof-of-concept testing of the umbilicals, service arms, holddown posts, and other ground-to-vehicle electrical and fluid connections used at the launch site ; (2) the computer-aided design and computer-aided engineering facility, where modeling is accomplished via an extensive design software library; (3) the Prototype Laboratory, which provides the services and tools to rapidly convert the engineering designs to hardware; and (4) the academic community in which conceptual design and theoretical analyses are performed.

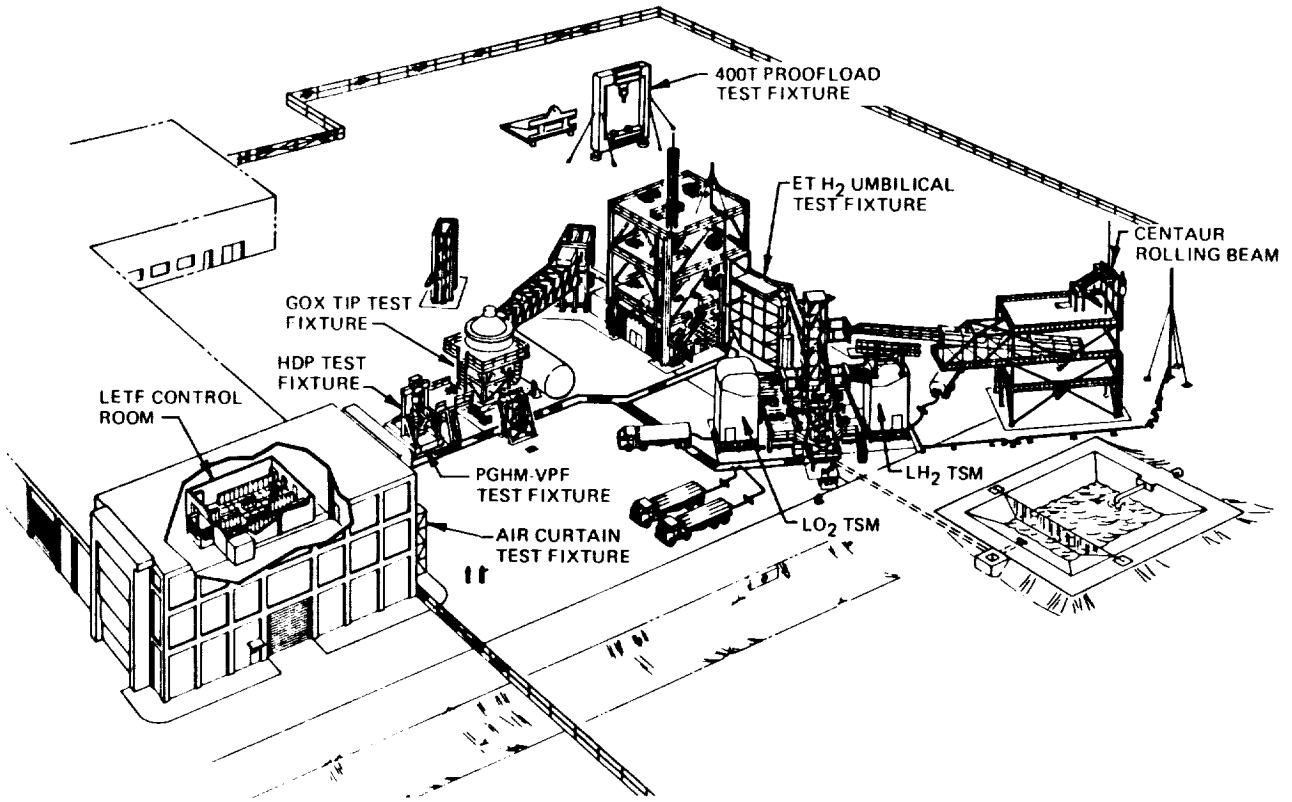
The Launch Equipment Test Facility

The Launch Equipment Test Facility is a unique engineering complex dedicated to the development and qualification testing of virtually all the NASA launch equipment mechanisms. The facility's test fixtures and supporting electrical/electronic systems have the capability to simulate

launch-site conditions such as cryogenic loading and flow, pyrotechnic operation, random motion, abort motion, lift-off motion, and other phenomena associated with launch operations. An extensive measurement system is available to obtain, record, display, and analyze the data associated with the testing. The facility also supports development and qualification testing of fluid system valves and other components, free-fall restraints, and load-bearing fixtures and lifting slings.

The Prototype Laboratory

The Prototype Laboratory provides KSC with a civil-service-staffed facility that has the capability to develop, fabricate, modify, model, breadboard, and/or test all manner of electrical and mechanical passive or active components, subsystems, and systems on a nonproduction or limited-production basis. The technical staff has the versatility to work from rough sketches as well as from formal engineering drawings. The laboratory is composed of a mechanical department (including metal working, sheet metal forming, welding, and high-pressure areas), a woodworking and model-making department, an electrical/electronic department, an instrumentation department, and a personal computer board fabrication department capable of fabricating single- or doubled-sided printed circuit boards from customer-supplied positives or negatives.



Launch Equipment Test Facility



Prototype Laboratory

Prediction of the Frictional Pressure Drop in Fully Developed, Annular Liquid/Vapor Flow in Straight Ducts Under a Zero-Gravity Environment

Background

Two prediction methods for the frictional pressure drop in turbulent, fully developed, liquid/vapor flow in straight ducts have been developed for a zero-gravity (0-g) application. The first method is for the dispersed flow regime, and the second is for the annular/flow regime. Both methods are based on experiments conducted on earth using a simultaneous flow of water and n-butyl benzoate, which are neutrally buoyant, and are guided by theoretical analysis.

For the flow of dispersed bubbles in liquids, the frictional pressure drop in 0-g is identical to the drop due to liquid flowing alone at the same total volumetric rate of the liquid and vapor combined. Hence, one may simply measure the pressure drop due to the liquid-alone flow in a duct of the same cross section and surface roughness as that to be used in 0-g. Alternatively, the desired pressure drop can be calculated from a suitable empirical correlation for single-phase flow.

For the annular liquid/vapor flow, the determination of the frictional pressure drop in 0-g would require experimentation using water and benzoate at flow rates that satisfy certain matching conditions (explained in detail in the following section), and then the desired pressure drop of the annular liquid/vapor flow in 0-g can be related to the measured pressure drop for the benzoate/water flow in 1-g.

Procedure

The following is a step-by-step procedure for the determination of the frictional pressure drop in a fully developed, annular

liquid vapor pipe flow in zero gravity.

Given: Total mass flow rate \dot{M} and vapor quality x of a specified fluid flowing in a straight pipe of inside diameter $2r_0$.

1. Compute the mass flow rate of the annular (film) liquid \dot{M}_F and of the core vapor \dot{M}_C :

$$\dot{M}_F = \dot{M}(1-x) \quad (1a)$$

$$\dot{M}_C = \dot{M}x \quad (1b)$$

2. Calculate the film Reynolds number Re_F and the core Reynolds number Re_C according to:

$$Re_F = \frac{2\dot{M}_F}{\pi r_0 \mu_F} \quad (2a)[A.7]^*$$

$$Re_C = \frac{2\dot{M}_C}{\pi r_0 \mu_C} \quad (2b)[A.8]$$

Comment: Both Re_F and Re_C are based on superficial velocities. For clarity and convenience, the properties associated with the annular (film) and core fluid of the liquid/vapor system in 0-g and of the benzoate/water system on earth are designated by the following subscripts:

* Alphanumeric in square bracket denotes the equation number from the Final Report for the period 23 August 1988 to 22 August 1989, Contract NAS10-11153 (MOD5).

	Liquid/Vapor Flow in 0-g	Benzoate/Water Flow in 1-g
Annular (film) fluid	L (liquid)	B(benzoate)
Core fluid	G (vapor)	W (water)

Thus, $Re_F = Re_L$ and $Re_C = Re_G$ for the liquid/vapor system, and $Re_F = Re_B$ and $Re_C = Re_W$ for the benzoate/water system. The Reynolds numbers for the benzoate flow Re_B and for the water flow Re_W are also based on the superficial velocities; that is,

$$Re_B = \frac{2\dot{M}_B}{\pi(r_o)_{B/W}\mu_B} \quad (3a)$$

$$Re_W = \frac{2\dot{M}_W}{\pi(r_o)_{B/W}\mu_W} \quad (3b)$$

where $(r_o)_{B/W}$ is the inside radius of the pipe used in the benzoate/water system.

3. The matching condition is:

$$\left[\frac{(0.707 Re_B^{0.5})^{2.5} + (0.0379 Re_B^{0.9})^{2.5}}{(0.707 Re_L^{0.5})^{2.5} + (0.0379 Re_L^{0.9})^{2.5}} \right]^{0.4} \left(\frac{Re_G}{Re_W} \right)^{0.9} = \frac{\mu_L}{\mu_G} \frac{\mu_W}{\mu_B} \left(\frac{\rho_G}{\rho_L} \right)^{1/2} \quad (4)[A.18c]$$

At room temperature, $\mu_w/\mu_B = 0.286$, and the right hand side of equation (4) is completely determined by the ratio of the viscosity of the liquid and of the vapor and by the ratio of their densities. Thus, for a given liquid/vapor system, it is a known quantity. Either Re_w or Re_B can be selected, and the other is to be determined from equation (4). Major factors to be considered in the selection are the

capacity of the flow facility available and the high cost of benzoate. In this experimentation, Re_w is selected, and Re_B is then calculated from equation (4).

4. Annular benzoate/water flow experiments are conducted using the just-determined Re_w and Re_B . The corresponding mass flow rates are:

$$\dot{M}_W = \frac{\pi}{2} (r_o)_{B/W} \mu_W Re_W \quad (5a)$$

$$\dot{M}_B = \frac{\pi}{2} (r_o)_{B/W} \mu_B Re_B \quad (5b)$$

The frictional pressure drop over a suitable length of the fully developed region of the benzoate/water flow is measured. The pressure gradient so determined is denoted by:

$$(dP/dz)_{(R/B/W)}$$

5. The desired frictional pressure gradient for the liquid/vapor flow in 0-g, $(dP/dz)_{(R/L/G)}$, is related to $(dP/dz)_{(R/B/W)}$ according to:

$$\left(\frac{dP}{dz} \right)_{(R/L/G)} / \left(\frac{dP}{dz} \right)_{(R/B/W)} = \left(\frac{Re_G}{Re_W} \right)^{1.8} \cdot \left(\frac{\mu_G}{\mu_W} \right)^2 \cdot \frac{\rho_W}{\rho_G} \cdot \left[\frac{r_o (B/W)}{r_o (L/G)} \right]^3 \quad (6)$$

Numerical Example

It is desired to predict the frictional pressure drop due to the flow of refrigerant R11 in a 12.7-mm smooth pipe at a total flow rate of 0.0906 kgs⁻¹ and a vapor quality of 0.3. The saturated liquid/vapor flow is at 290 K. The relevant properties are:

$$\rho_L = 1495.3 \text{ kg/m}^3, \quad \rho_G = 4.639 \text{ kg/m}^3$$

$$\mu_L = 454 \times 10^{-6} \text{ Pa}\cdot\text{s}, \quad \mu_G = 10.63 \times 10^{-6} \text{ Pa}\cdot\text{s}$$

The existing benzoate/water system has a 15.4 mm inside diameter smooth tube and was operated at 286.5 K. Thus, the relevant properties are:

$$\rho_B = 1,000 \text{ kg/m}^3, \quad \rho_w = 999.3 \text{ kg/m}^3$$

$$\mu_B = 4.14 \times 10^{-3} \text{ Pa}\cdot\text{s}, \quad \mu_w = 1.185 \times 10^{-3} \text{ Pa}\cdot\text{s}$$

Accordingly, the dimensionless group on the right hand side of equation (4) has the value:

$$\frac{\mu_L}{\mu_G} \frac{\mu_w}{\mu_B} \left(\frac{\rho_G}{\rho_L} \right)^{1/2} = 0.681$$

$$1. \dot{M}_F = \dot{M}_L = 0.0906 \times (1 - 0.3) = 0.0634 \text{ kgs}^{-1}$$

$$\dot{M}_C = \dot{M}_G = 0.0906 \times 0.3 = 0.0272 \text{ kgs}^{-1}$$

$$2. \text{Re}_F = \text{Re}_L = \frac{2 \times 0.0634}{\pi \times 6.35 \times 10^{-3} \times 454 \times 10^{-6}} = 1.40 \times 10^4$$

$$\text{Re}_C = \text{Re}_G = \frac{2 \times 0.0272}{\pi \times 6.35 \times 10^{-3} \times 10.63 \times 10^{-6}} = 2.565 \times 10^5$$

3. Select $\text{Re}_w = 25,000$, Re_B is then determined from:

$$\left[\frac{(0.707 \text{Re}_w^{0.5})^{2.5} + (0.0379 \text{Re}_B^{0.9})^{2.5}}{(0.707(1.40 \times 10^4)^{0.5})^{2.5} + (0.0379(1.40 \times 10^4)^{0.9})^{2.5}} \right]^{0.4} \left(\frac{2.565 \times 10^5}{2.5 \times 10^4} \right)^{0.9} = 0.681$$

$$\therefore \text{Re}_B = 503$$

$$4. \dot{M}_w = \frac{\pi}{2} \times (7.7 \times 10^{-3}) \times 1.185 \times 10^{-3} \times 25,000 = 0.3583 \text{ kgs}^{-1}$$

$$\dot{M}_B = \frac{\pi}{2} \times (7.7 \times 10^{-3}) \times 4.14 \times 10^{-3} \times 503 = 0.02518 \text{ kgs}^{-1}$$

5. Measured $(\Delta P)_{(R/B/W)}$ is 431.7 mm H₂O over a length of 1.829 m in the fully developed region of the benzoate/water flow.

6. Predicted $(\Delta P)_{(R/L/G)}$ for the liquid/vapor flow in 0-g over the same length is:

$$431.7 \times \left(\frac{2.565 \times 10^5}{2.5 \times 10^4} \right)^{1.8} \left(\frac{10.63 \times 10^{-6}}{1.185 \times 10^{-3}} \right)^2 \left(\frac{999.3}{4.639} \right) \left(\frac{15.4}{12.7} \right)^3 = 881.7 \text{ mm H}_2\text{O}$$

Contact:

F. N. Lin, 867-4181, DM-MED-11

Participating Organization:

University of Illinois (Dr. B. T. Chao)

NASA Headquarters Sponsor:

Office of Space Flight

Comparison of Analytical Methods for Calculation of Wind Loads

In the process of revising KSC-STD-Z-0004, Standard for the Design of Structural Steel Buildings and Other Steel Structures, four building codes that determine the wind load pressures on buildings or structures were considered. An analysis was conducted to determine which code mathematically produces the largest wind load pressures. The methods specified in ASCE Paper No. 3269, ANSI A58.1-1982, The Standard Building Code, and the Uniform Building Code were analyzed using various hurricane speeds to determine the differences in the calculated

results. The winds used for the analysis ranged from 100 to 125 miles per hour and were applied inland from the shoreline of a large body of water (such as an enormous lake or the ocean) a distance of 1,500 feet or ten times the height of the building or structure considered. The wind velocity envelope ranged from 30 to 500 feet. In order to compare the various methods, a four-sided building or structure with vertically oriented walls was considered. Only primary frames and systems were taken into account, and only the windward and leeward sides were analyzed. Roofs were not considered in order to reduce the number of graphs produced.

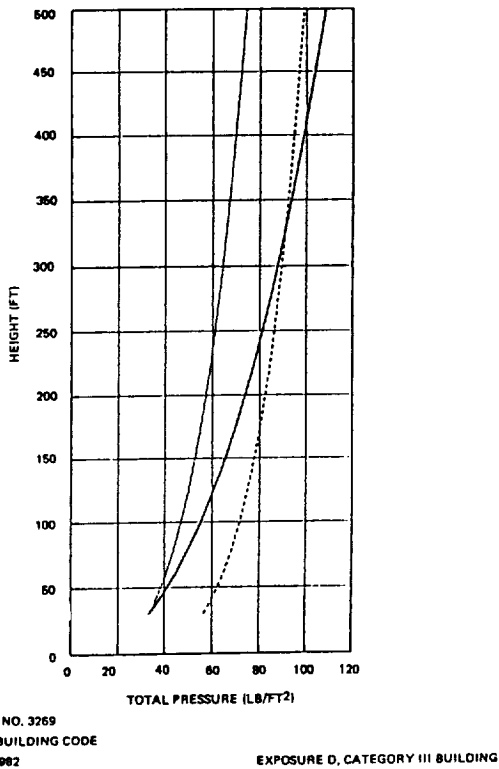
Upon investigation, it was determined that the Uniform Building Code (1982 edition) did not encompass winds coming off a large body of water and, therefore, was excluded on the basis of nonconformity to the project's problem statement. The remaining three methods were then analytically compared using a spreadsheet

program to produce output tables containing wind velocity at a height of 30 feet, steady-state total pressure, peak total pressure, and wind velocity at discrete heights (which is apparent in the table "Wind Pressure and Wind Velocity for 100 Miles per Hour at 33 Feet"). The output of the spreadsheet was then passed to a presentation/graphical program, which generated a series of graphs. The graphs then permitted easy visual comparison of wind velocity profile and wind pressure changes (see the figure "Height Versus Total Pressure: Wind Velocity 100 Miles per Hour at 33 Feet").

The results of the analysis indicated that for a building or structure less than or equal to 250 feet in height acted upon by a wind of 115 miles per hour or more, the method specified in ANSI A58.1-1982 calculates a larger wind load pressure than the other methods. For a building or structure between 250 and 500 feet tall acted upon by a wind ranging from 100 to

*Wind Pressure and Wind Velocity for 100 Miles per Hour at 33 Feet
(Exposure D, Category III Building)*

Height, Z (ft)	ASCI Paper No. 3269 Steady-State Total Pressure (psf)	ANSI A58.1-1982 Steady-State Total Pressure (psf)	Standard Building Code Steady-State Total Pressure (psf)	ASCE Paper No. 3269 Peak Total Pressure (psf)	ANSE A58.1-1982 Peak Total Pressure (psf)	ASCE Paper No. 3269 Velocity Profile (mph)	ANSI A58.1-1982 Velocity Profile (mph)
30.00	33.25	56.34	33.28	40.24	63.10	100.00	99.05
33.00	34.61	57.43	34.20	41.70	64.05	102.02	100.00
40.00	37.53	59.68	36.13	44.83	66.04	106.24	101.94
60.00	44.51	64.72	40.57	52.21	70.44	115.69	106.16
80.00	50.23	68.56	44.04	58.17	73.76	122.91	109.26
100.00	55.18	71.69	46.94	63.25	76.45	128.81	111.72
120.00	59.57	74.35	49.45	67.74	78.73	133.85	113.78
140.00	63.56	76.68	51.68	71.78	80.72	138.26	115.55
160.00	67.24	78.75	53.69	75.47	82.48	142.19	117.10
180.00	70.65	80.63	55.53	78.88	84.07	145.76	118.49
200.00	73.85	82.34	57.23	82.07	85.53	149.02	119.74
220.00	76.87	83.93	58.80	85.06	86.86	152.04	120.89
240.00	79.74	85.40	60.28	87.89	88.10	154.85	121.95
260.00	82.47	86.78	61.68	90.57	89.26	157.48	122.93
280.00	85.08	88.08	63.00	93.13	90.35	159.95	123.84
300.00	87.58	89.30	64.25	95.57	91.37	162.29	124.70
320.00	89.99	90.46	65.45	97.92	92.34	164.51	125.51
340.00	92.32	91.56	66.59	100.18	93.26	166.62	126.27
360.00	94.56	92.62	67.69	102.35	94.14	168.63	126.99
380.00	96.74	93.62	68.74	104.45	94.98	170.56	127.68
400.00	98.85	94.59	69.76	106.48	95.78	172.41	128.34
420.00	100.90	95.52	70.74	108.45	96.55	174.19	128.97
440.00	102.89	96.41	71.68	110.37	97.29	175.90	129.57
460.00	104.83	97.27	72.60	112.23	98.01	177.55	130.14
480.00	106.72	98.10	73.49	114.03	98.70	179.15	130.70
500.00	108.57	98.91	74.35	115.80	99.36	180.69	131.23



Background

During a space vehicle launch, vibrations are induced in structural elements that are exposed to the brief but intense acoustic pressure waves. The noise-induced vibrations may lead to fatigue failures of ground structures or malfunctions of equipment in the vicinity of the launch pad. Since most structural and equipment problems due to the acoustic field occur in the proximity of the source (less than 1,200 feet), the near-field noise is of particular significance. Accurate knowledge of near-field acoustics is required to determine its effect on launch equipment and to develop vibration and acoustic test specifications.

The near-field noise of modern rocket engines is complex. Besides its highly directional nature, the noise field is complicated by mixing flows from homogenous and nonhomogenous engine clusters, exhaust deflectors, the effects of shielding, and water steam clouds. Empirical methods, used to predict near-field acoustics based on exhaust flow parameters and source allocation techniques, involve assumptions of noise directivity. Since the mechanism of directivity has not been fully validated for supersonic exhausts, empirical methods of predictions lead to inaccuracies. Moreover, these prediction methods require computation of the total sound power at each frequency, and they assume the existence of a single-peaked power spectrum that is normally used for far-field applications, while measurements show multip peaked near-field power spectra shapes (typical of Shuttle and Saturn V noise measurements).

ALS near-field predictions posed several unique problems not fully addressed before. The first problem was the lack of an accurate definition of acoustic efficiency, which was essential to estimate acoustic power from rocket propulsive power. Since measurement of acoustic efficiency was not possible with the existing state of the art,

Height Versus Total Pressure: Wind Velocity 100 Miles per Hour at 33 Feet

110 miles per hour, there is no clear choice of which method to use. For these cases, factors that must be considered are the steady-state or peak wind velocity, the geographic location, the distance from a large open body of water, and the expected design life and its risk factor.

Contact:

D. J. Minderman, 867-2906, DM-MED-33

NASA Headquarters Sponsor:
 Office of Space Flight

Prediction of Near-Field Acoustic Environments for Advanced Launch Systems

Objective

To predict the launch-induced near-field acoustics of eight advanced launch system (ALS) vehicles currently under study by several contractors for the United States Air Force (USAF).

empirical equations were sought from scientific literature. The existing empirical equations were unsuitable for the computation of acoustic efficiencies of high-thrust rocket engines in ALS vehicles. Secondly, an accurate definition of near- and far-field regimes was also lacking but essential. This definition was necessary to confirm the applicability of far-field generalized and single-peaked power spectrum for near-field predictions. The last problem addressed was the manner in which effective diameter and effective velocities were defined for the computation of the Strouhal number. The Strouhal number has been the principal similarity parameter used in scaling of rocket-noise spectra in the past. The existing definitions of the effective diameter and velocity were limited to either a single engine or clusters of similar engines. These techniques were not suitable for nonhomogenous engine clusters of some ALS vehicles. A consistent definition of the Strouhal number was also essential for separating similar engine clusters [space Shuttle main engine (SSME) and solid rocket booster (SRB)] from a nonhomogenous cluster (Shuttle) for scaling.

Approach

In general, existing prediction methods can be categorized as noise-origin or noise-source based, requiring directivity assumptions. The proposed scaling method, however, focuses on the sound at the receiver. ALS predictions were made at exactly the same locations where acoustic data from similar vehicles was available, thereby eliminating assumptions of atmospheric attenuation, launch pad configuration, and directivity. Liquid (SSME), excess (Shuttle plus SSME) and total Shuttle (Shuttle only) models were developed after separating the SSME and SRB components from the total Shuttle acoustics. Near-field acoustic environments of ALS vehicles were predicted using these models.

Analysis of Shuttle and Saturn V near-field data lead to several noteworthy obser-

vations. First, vehicle- and distance-independent single-peaked spectra were observed for distances beyond 600 feet. For distances within 600 feet, Shuttle and Saturn V spectra exhibited strong vehicle and distance dependence. In other words, dissimilar shapes of Shuttle and Saturn V power spectra in the near-field required a greater emphasis on the nature of the propulsion system in the selection of the source vehicle for predictions. Similarities in ALS and Shuttle propulsion systems resulted in the use of Shuttle rather than Saturn V acoustic measurements in the proposed scaling method.

Measurements of Shuttle acoustics at lift-off are composed of data from liquid and solid engine components. Separation of SSME and SRB components from the total Shuttle acoustic power required definition of acoustic efficiencies for SSME's and SRB's. An empirical relation to estimate acoustic efficiency values from the engine Mach number has been developed. Higher values of acoustic efficiencies were found to be associated with higher engine exhaust velocities. Since predictions relied on scaling of acoustic powers, only the ratios rather than the absolute values of acoustic efficiencies are of consequence.

Once the overall acoustic power was determined, the next requirement involved a frequency resolution of this power. Early attempts were based on the concept of the Strouhal number, $S=f*De/V$, as the principal similarity parameter for predicting noise spectra of new vehicles. Unique problems surfaced during the computation of the equivalent diameter, De , in this equation of the Strouhal number. The formal method of computing an equivalent diameter of an engine cluster, $De=\sqrt{n}*Di$, was found to be inaccurate. A generalized method of computing an effective diameter of nonhomogenous engines, which converges to a single-engine diameter for homogenous clusters, has been derived. This revised definition of the effective diameter was vital in the compu-

tation of consistent Strouhal numbers for homogenous and nonhomogenous engine clusters of ALS vehicles.

Similarity concepts used by existing methods were based on the premise that the noise field for rockets is similar when exhaust flow is similar. The present effort, on the other hand, relied on a premise that required the equality of power spectra at the same Strouhal number for vehicles of equal acoustic power. Since the measurements and predictions were at similar locations, the two premises can be considered identical. However, the latter premise was found to be inaccurate at the high-frequency end of the spectra, despite the use of revised effective engine diameter in computations. Therefore, a shift-attenuation was necessary to obtain the desired accuracy.

Results

An acoustic power scaling technique has been developed to predict the near-field acoustic environment of new launch vehicles. The important feature of the developed method is that it is based on measurements that define absolute values, while other parameters that are rather difficult to define enter only as ratios between the new (ALS) and source vehicles. This technique uses measured power spectra from similar vehicles at several locations in the near-field. The predicted near-field environment is defined in terms of an overall sound pressure level (OASPL) and its frequency spectrum. OASPL is obtained by scaling acoustic powers of the two vehicles with the related frequency spectrum defined by a Strouhal-number-based shift attenuation. Results of this study and an extensive documentation of the development effort are contained in KSC-DM-3327, "Near-Field Acoustic Environment Predictions for Advanced Launch Systems."

Contact:

R. E. Caimi, 867-4181, DM-MED-11

Participating Organization:

Boeing Aerospace Operations, Engineering Support Contract (R.N. Margasahayam and V. Sepcenko)

NASA Headquarters Sponsor:

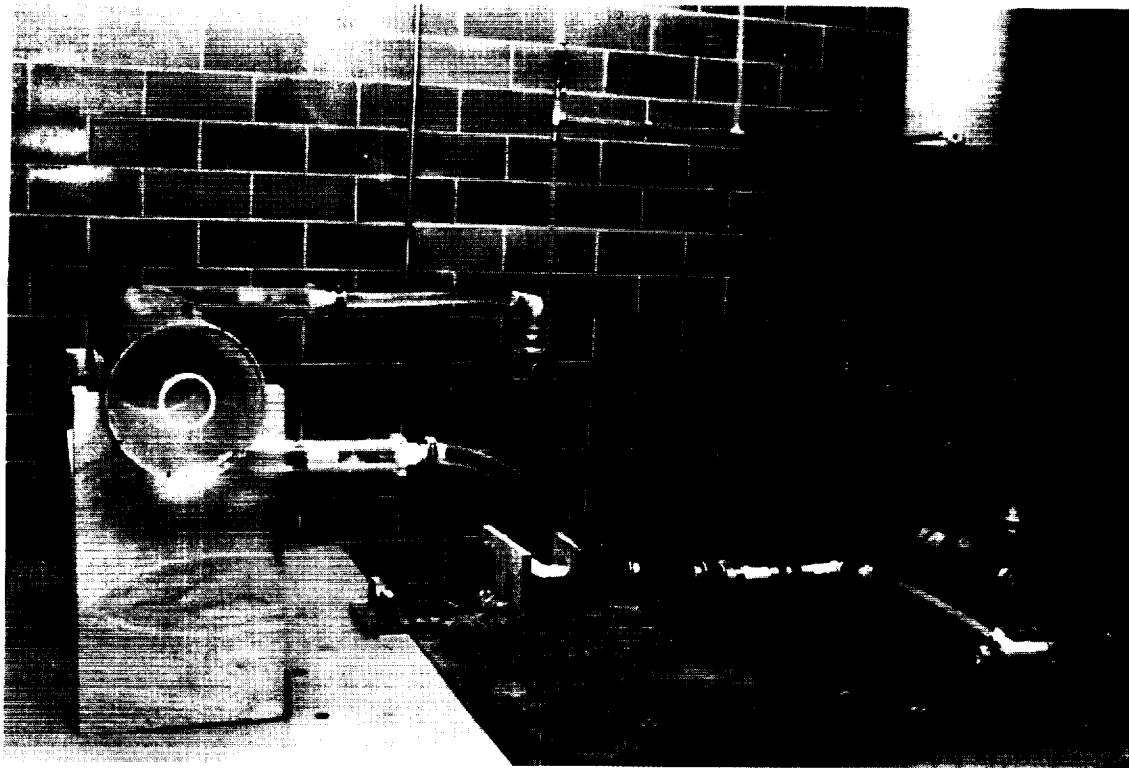
Office of Space Flight

Fluid Dynamics of Phase Separation in a Field of Centrifugal Acceleration

This study, being performed under a grant to Clemson University, covers an analysis, a test model fabrication, and a test program to determine a means of phase separation of cryogenic fluids in both normal and reduced gravitational fields using centrifugal force to achieve phase separation. The study will provide information that will enable the transfer of cryogenics through pipe lines in reduced-gravity environments. Two fluids of nearly the same density are being used to cause the fluid with the greater density to respond as if it were in a reduced-gravity environment.

A side view of the model built for the first phase of the study is shown in the figure "Fluid Dynamics of Phase Separation in a Field of Centrifugal Acceleration Model." The cylinder is located on the left side of the figure in a cradle. A centrifugal pump, flowmeter, throttle valve, and pressure relief valve are shown in the inlet line. A laser is part of the measurement system shown on the table. The tank on the wall, in the right corner of the figure, is used to fill the system.

The first phase of the study will provide two-dimensional measurements and equations using a laser. A second phase is being planned to build and test a centrifugal accelerator model using hologram measurements to determine the three-dimensional parameters affecting phase separation in a reduced-gravity environment.



*Fluid Dynamics of Phase Separation in a
Field of Centrifugal Acceleration Model*

Contact:

F. S. Howard, 867-4181, DM-MED-11

Participating Organization:

Clemson University (Dr. R. Kumar)

NASA Headquarters Sponsor:

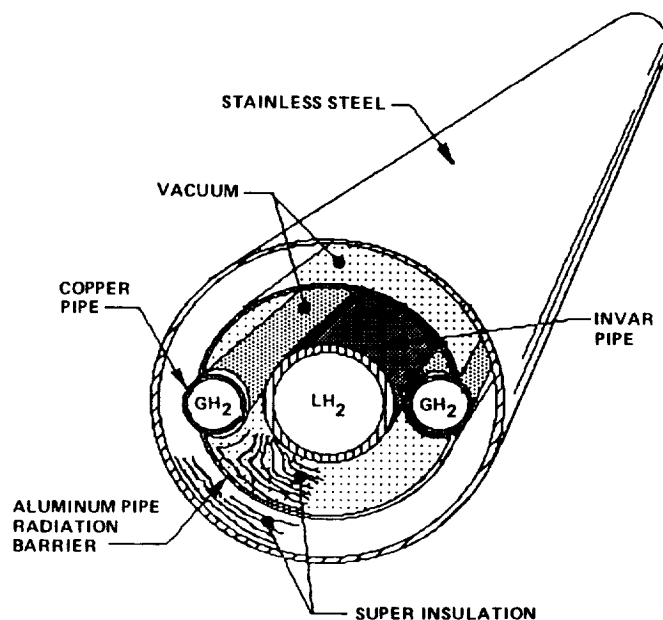
Office of Space Flight

Advanced Liquid Hydrogen Transfer Line

The purpose of the advanced liquid hydrogen transfer pipe is to enable the transfer of liquid hydrogen over long distances. With a conventional vacuum-jacketed transfer pipe, the liquid hydrogen boiloff increases vapor formation, which in turn increases the liquid hydrogen flow velocity. An increase in the liquid hydrogen flow rate causes an additional heat input from the friction of the fluid transfer. This additional heat causes additional vaporization and an additional increase in the flow rate, making it difficult to trans-

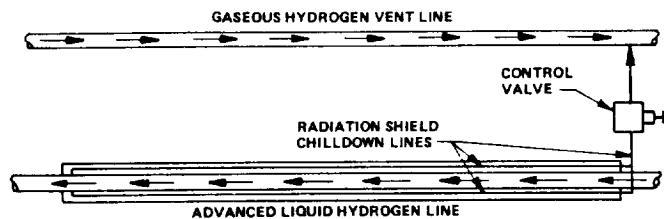
fer liquid hydrogen over long distances.

A cross section of the advanced liquid hydrogen transfer pipe is shown in the figure "Advanced Vacuum-Jacketed Transfer Pipe." The advanced liquid hydrogen



Advanced Vacuum-Jacketed Transfer Pipe

transfer pipe vents some of the liquid from each section into two small lines attached to a radiation heat transfer barrier. A section of the advanced line without end closures is shown in the figure "Flow Diagram of Advanced Liquid Hydrogen Transfer Pipe." The shield runs the length of each section of the pipe, and the gas is vented into a vent line that is piped to a burn stack or hydrogen refrigerator for reliquefaction.



Flow Diagram of Advanced Liquid Hydrogen Transfer Pipe

As heat transfers from the outside wall of the pipe to the liquid hydrogen line, it has to transfer through a super insulation wrap, consisting of layers of aluminized Mylar and foam in a vacuum, to the radiation barrier. Since this barrier is cooled to nearly the same temperature as the liquid hydrogen pipe, heat transfer from the radiation barrier through additional super insulation to the liquid hydrogen line is insignificant. The heat transfer path becomes more restrictive by causing heat to pass from the outer wall to the shield by radiation and from the shield to the cooling lines by conduction.

A section of pipe was procured from CVI, Incorporated. Boiloff tests were begun October 23, 1989. The total of the liquid required to chill down the radiation barrier and the liquid boiled from the main line is less than the boiloff from a conventional vacuum-jacketed line.

Contact:
F. S. Howard, 867-4181, DM-MED-11

Participating Organization:
The University of North Carolina,
Charlotte (P. Wang)

NASA Headquarters Sponsor:
Office of Space Flight

Structural Loads in an Acoustic Field

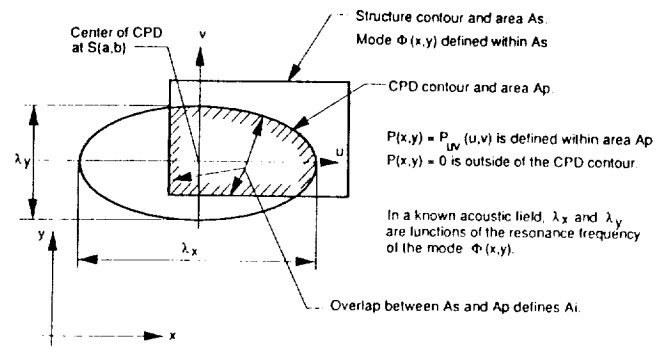
During a launch of a space vehicle, a relatively brief but intense pressure transient is generated by the rocket exhausts. The vibration response of a structure to this transient depends on the vibroacoustic coupling between the structure and the transient acoustic field. The vibroacoustic coupling is the reason why two close and seemingly similar structures may respond and vibrate differently during a launch; one structure may survive, the other may fail. All structures located at the launch pads at KSC must survive this intense pressure transient in order to perform critical servicing functions for launches and to provide rapid turnarounds between launches. This project was established in order to define a generalized method for calculation of loads induced by the vibroacoustic environment during launch.

The analysis and design of launch-supporting structures for strength to withstand vibration are multidiscipline tasks involving both theoretical analyses and experimental data. The design process requires a definition of the transient acoustic field, using quantities and parameters that cannot be directly measured but require a substantial analytical effort to extract them from data that have been measured. The problem is further complicated by the random nature of the measurements; data from each launch are unique and require the use of statistical concepts for their interpretation and application in the design.

An outline of a recommended design procedure for structures subjected to intense acoustic pressures on and near the launch pad was first published at KSC in September 1987 in technical report KSC-DM-3147, "Procedure and Criteria for

Conducting a Dynamic Response Analysis of Orbiter Weather Protection System on LC-39B Fixed Service Structure." In this report, a launch-generated acoustic field was defined by means of response spectra and pressure correlation lengths (PCL's); both functions were derived from multiple sets of simultaneous measurements collected during past Shuttle launches. PCL's, together with analytically obtained modal parameters of a structure, provide a quantitative definition of vibroacoustic coupling and an estimate of structural response based on response spectra.

The design procedure in KSC-DM-3147 recommended for the Orbiter Weather Protection System deviated from the previous method, which was based on pressure power spectra as a source of dynamic excitation. This change in methods was necessitated by a number of factors documented by KSC-DM-3147, among which were the need for a greater prediction accuracy and a straightforward method for computation of the peak modal response. KSC-DM-3147 provided only a generalized



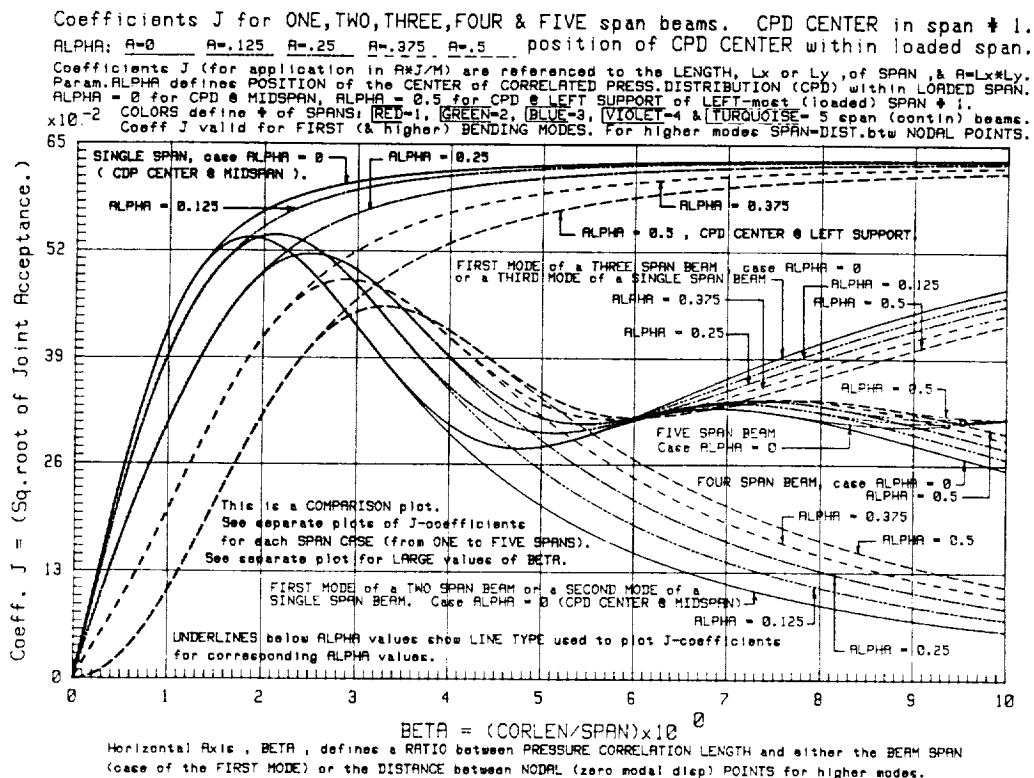
$$\text{Problem: } AJ = \int_{A_i} \Phi(x,y) P(x,y) dA$$

Find a position of S(a,b) relative to the mode $\Phi(x,y)$ such that AJ becomes an extreme [maximum or minimum depending on the sign of $\Phi(x,y)$].

AJ is a measure of vibroacoustic coupling.

Illustration of a Vibroacoustic Coupling for a Planar Structure

formulation of the vibroacoustic coupling for the computation of generalized modal loads for application in response spectra. The problem of vibroacoustic coupling is addressed in depth in the followup report KSC-DM-3265, "Computation of Generalized Modal Loads in an Acoustic Field



Example of a Joint Acceptance Diagram

Defined by a Distribution of Correlated Pressures," published in August 1989. The figure "Illustration of a Vibroacoustic Coupling for a Planar Structure" shows a mathematical formulation of the problem.

For a general case of a vibration mode, the computation of joint acceptance (AJ) coefficient extremes has to be made by numerical calculations. A general case requires a trial-and-error process because the AJ function may have multiple extremes within almost any region of the mode. The extremes depend on the position of the correlated pressure distribution (CPD) center relative to the mode. The position resulting in the absolute extreme is seldom obvious. In order to simplify

cumbersome computations, diagrams of AJ-coefficients were plotted for a few types of simple structures (KSC-DM-3265). These diagrams allow explicit solutions. An example of a diagram is shown in the figure "Example of a Joint Acceptance Diagram." Numerical examples illustrating the application of the method utilizing the diagrams in the response analysis are provided in KSC-DM-3265.

Contact:

L. L. Schultz, 867-7584, DM-MED-33

Participating Organization:

Boeing Aerospace Operations, Engineering Support Contract (V. Sepcenko)

NASA Headquarters Sponsor:

Office of Space Flight

Materials Science

Materials science investigations are conducted in three well-equipped and well-staffed laboratories at the John F. Kennedy Space Center (KSC).

The Microchemical Analysis Laboratory

The Microchemical Analysis Laboratory employs high technology instruments, such as the electron microprobe, scanning electron microscope, infrared spectrophotometer, and mass spectrometer/gas chromatograph, as well as classical analytical methods to identify a variety of different materials. One basic function of the laboratory is to chemically identify any fluid or solid material down to the parts-per-billion range. A second basic function is to provide the investigative effort necessary to understand and solve chemical problems associated with the selection and application of materials in aerospace systems. Typical subjects for analysis are the Shuttle thermal protection system, aircraft materials (such as alloys and soft goods), and the environmental effects of launch operations.

The Materials Testing Laboratory

The Materials Testing Laboratory in-

cludes materials and environmental testing facilities, a liquid oxygen impact testing facility, and an environmental exposure test site along the Atlantic Ocean. This laboratory provides the investigative effort necessary to understand and solve technical problems associated with the selection and application of materials (such as plastics, elastomers, metals, and lubricants) used in flight hardware, ground support equipment, and facility systems.

The Malfunction Analysis Laboratory

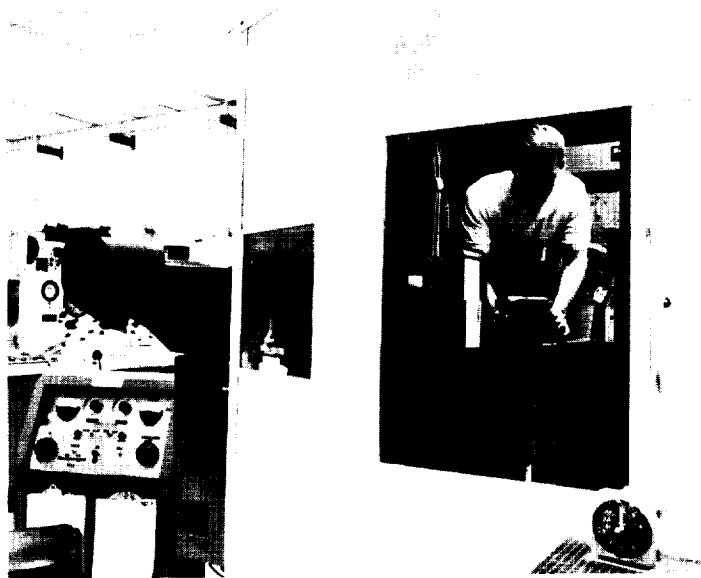
The Malfunction Analysis Laboratory provides the investigative capabilities to determine, on a rapid turn-a-round basis, the causes of failures related to ground support equipment and flight hardware. The malfunction analysis process is conducted in the electrical/electronics, mechanical/fluid, metallurgical, and metrological laboratories, with supporting expert services within each of these areas. After the completion of an investigation, the engineer or physicist makes recommendations for preventing similar occurrences and, if necessary, devises a research program with the goal of preventing future failures.



Microchemical Analysis Laboratory

ORIGINAL PAGE
BLACK AND WHITE PHOTOGRAPH

Materials Testing Laboratory



Malfunction Analysis Laboratory

Protective Coating Systems for the Space Transportation System Launch Environment

Zinc-rich coating systems exposed to the Space Transportation System (STS) launch environment at KSC have been suffering premature failure due to the highly acidic residue produced by the solid rocket boosters. Early attempts at topcoating these zinc-rich coatings with a thin film to increase their chemical resistance have produced only marginal results.

Topcoat systems are being tested to improve coating performance for exposure to KSC's harsh environment. The present study focuses on using thicker film topcoats over the zinc-rich primers to improve the chemical resistance to both a marine atmosphere and highly acidic residues.

In 1986, 119 materials producing 67 coating systems were exposed to atmospheric contaminants at the KSC beach corrosion site with concurrent applications of an acid slurry made of hydrochloric acid (HCl) and alumina (Al_2O_3). The slurry was applied to the test panels with no subsequent washdown to simulate the worst-case scenario experienced at the launch sites.

The current test will be conducted for five years to determine the suitability of the topcoat systems. The panels have been judged for performance at 6, 12, 18, and 36 months. The last evaluation will occur at 60 months, which will be followed by a final report. During this five-year period, there will have been approximately 130 applications of the acid slurry.

The panels are approaching the 40-month point of exposure. The results of the 18-month evaluation were published in February 1988 under document number MTB-268-86B. The 36-month evaluation revealed that topcoat performance was generally poorer than the untopcoated condition. Several manufacturer's topcoat

products are, however, performing very well. This result has prompted consideration to prepare a list, for incorporation into KSC-STD-C-0001, that includes approved topcoat products for use when topcoats are required and specified for launch structures and ground support equipment at KSC.

Contact:

L. G. MacDowell, 867-2906, DM-MSL-2

NASA Headquarters Sponsor:

Office of Space Flight

Corrosion of Convuluted Metal Flexible Hoses

Various cryogenic supply lines and hypergol lines at the Shuttle launch site use convuluted flexible hoses and bellows constructed of type 304L stainless steel. The extremely corrosive Space Transportation System (STS) launch environment, composed of sodium chloride (NaCl) and hydrochloric acid (HCl), has caused rapid pitting and failure of these flexible hoses; this leads to loss of vacuum with resulting high boiloff of the cryogenics.

In 1987, a project was initiated to identify a more corrosion-resistant alloy for this service. After testing 19 corrosion-resistant alloys for pitting resistance, the study quickly focused on the nickel-based alloys such as Hastelloy and Inconel. These alloys were chosen on the basis of their reported resistance to acid/chloride environments.

The first-year results were published under document number MTB-325-87A. Several alloys, such as Inco G-3, Inconel 625, and Hastelloy C-4, C-22, and C-276, performed well. After evaluation of all mechanical data and corrosion tests, Hastelloy C-22 was determined to be the most acceptable alloy for use in the STS launch environment. Samples of all alloys continue to be exposed to salt fog/acid slurry and

beach exposure testing to gain valuable long-term exposure data.

During the summer of 1989, testing continued on the 19 alloys to determine the possibility of using alternating current impedance techniques to assess corrosion resistance. The alloys were tested in three electrolytes: neutral 3.55 percent NaCl, 3.55 percent NaCl and 0.1 normal HCl, and 3.55 percent NaCl and 1.0 normal HCl. The acidic electrolytes were used to simulate conditions that exist in the STS launch environment. Preliminary data suggests that this technique may prove to be a valuable tool in rapidly screening metal alloys for relative corrosion resistance. The study will continue using this technique to determine its correlation with actual field exposure results. The preliminary data was published under document number MTB-610-89.

Contact:

L. G. MacDowell, 867-2906, DM-MSL-2

NASA Headquarters Sponsor:

Office of Space Flight

Permeability of Polymers to Organic Liquid and Condensable Gases

Workers involved in the production, use, and transportation of hazardous chemicals may be exposed to numerous chemicals capable of causing harm to the human body. The effects of these chemicals can range from acute trauma, such as skin irritation and burns, to chronic degenerative diseases, such as cancer or emphysema. Since engineering and administrative controls may not eliminate all possible exposure, attention must be given to reducing the potential for direct contact through the use of polymeric-based protective clothing that resists permeation, penetration, and degradation.

Permeation tests are being performed by Tuskegee University to evaluate the protec-

tion afforded by various fabrics used for protective clothing. This evaluation determines the breakthrough time and the steady-state permeation rate for particular chemical/clothing combinations. Materials of interest are nitrile rubber, butyl rubber, Neoprene, poly(vinyl alcohol), poly(vinyl chloride), latex rubber, and chlorobutyl rubber coated Nomex fabric. Chemicals of interest for evaluation of the fabric include nitrogen tetroxide, hydrazine, monomethylhydrazine, hexane, toluene, dimethylformamide, 1,1,1-trichloroethane, benzene, and ethyl acetate.

The test matrix has been expanded to include additional gloves and chemicals used routinely in the processing of Orbiters, external tanks, and solid rocket boosters in the Shuttle program.

This study was recently extended to include a search to identify a fabric to replace the chlorobutyl rubber coated Nomex fabrics used in the current Propellant Handlers Ensemble (PHE). This study is a joint effort between the Texas Research Institute Austin, Inc., and Tuskegee University. It is anticipated that a new lighter weight, more chemical resistant, lower maintenance fabric will be identified for the production of a third-generation PHE.

Contact:

C. J. Bryan, 867-4344, DM-MSL-2

NASA Headquarters Sponsor:

Office of Space Flight / Office of Equal Opportunity Program

Protective Coating Systems for Repaired Carbon Steel Surfaces

In the past, maintenance repair of corroded carbon steel surfaces required the use of abrasive blasting to adequately clean and prepare the metal surface for application of protective coatings. Recent advances in coating technology promises acceptable protective coating performance when surface

preparations are less than perfect. The present study focuses on new products and techniques that may reduce the level of surface cleanliness required for corrosion protection in many areas at KSC.

The coatings being tested in this study include epoxy mastics, moisture-cured urethanes, chemical conversion coatings, and any other type of repair coating identified during the course of the program. The study compares the performance of previously rusted panels that have been mechanically prepared using four methods and two initial conditions. The four mechanical methods used are power wire brush, pneumatic needle gun, sanding disk, and coarse wheel grinder. The two initial conditions used are to prepare the panels with water washing or without water washing prior to mechanical cleaning.

The initial screening of the many products was accomplished by exposing the prepared panels to 2,000 hours in the salt fog chamber. The initial results of this screening procedure indicate varying performances of the coatings of the same generic type. This result has considerably reduced the final list of products to be tested. Further results show that the "rust converter" type coatings provide little protection in an aggressive atmosphere and should not be considered for use at KSC. Following this screening procedure, the materials list and preparation methods will be evaluated to determine which combinations will be used in a final test exposure sequence. After preparation of all test panels using the decisive materials and methods, two different exposure conditions will be used to determine coating performance. Duplicate test panels will be exposed at the beach corrosion site and in the laboratory to search for a possible correlation.

Panels exposed at the beach corrosion site and the laboratory will undergo solid rocket booster (SRB) effluent testing to simulate the conditions at the launch site. The SRB effluent tests will be accomplished

by dropping simulated effluent onto two-thirds of the panels every two or three weeks. Panels at the beach will be inspected after 1, 3, 6, 12, 18, 36, and 60 months and rated for rusting on a scale from 1 to 10 in accordance with ASTM D610. An expanded test plan is available under document number MTB-144-88.

Contact:

L. G. MacDowell, 867-2906, DM-MSL-2

NASA Headquarters Sponsor:

Office of Space Flight

Development of New Flooring Materials for Clean Rooms and Launch Site Facilities

NASA utilizes one of two different static-dissipating floor coverings in Shuttle assembly areas: flexible poly(vinyl chloride) (PVC) tiling or poured epoxy floor covering. Both have disadvantages associated with their use. The flexible vinyl tiling, which is currently the floor covering of choice, fails NASA's outgassing tests due to the plasticizer component within the formulation. The plasticizer can volatilize at room temperature and then recondense on sensitive optical surfaces, leading to contamination problems. Although there are static-dissipating vinyl tiles commercially available, none have qualified following outgassing tests. Disadvantages associated with the poured epoxy floor coverings are dusting, chalking, and repair difficulties.

A Small Business Innovative Research (SBIR) contract identified chemically resistant polymers, conductive fillers, flame retardant additives, and structural adhesives that could be used as formulation components in a specialized floor covering for installation at NASA launch site facilities, which would eliminate or minimize the current flooring inadequacies.

As a result of experimentation, a conductive fiber was determined to be the most efficient filler giving the most consistent

results. Surface and volume resistivities of 10^6 to 10^8 ohms per square were achieved consistently.

Sample formulations passed outgassing and hypergolic resistance tests at Kennedy Space Center. Work is now progressing on process problems associated with the uniform dispersion of the conductive component in the polymer matrix. The next milestone in the program is the production of sufficient flooring material to permit the installation of a test floor (500 square feet) at KSC for evaluation under conditions of actual use.

Contact:

C. J. Bryan, 867-4344, DM-MSL-2

*NASA Headquarters Sponsor:
Office of Space Flight*

Conductive Organic Polymers as Corrosion Control Coatings

Electrically conductive polymers are under evaluation as protective coatings for ground support equipment and structures at KSC. For over 20 years, inorganic zinc-rich coatings have been utilized for protection of launch structures. The zinc portion of these currently used coatings, however, is attacked by the high concentrations of hydrochloric acid released during a Space Shuttle launch. The search for a coating with resistance to hydrochloric acid and to corrosion has focused on conductive polymers.

A conjunctive research effort is in progress at KSC and the Los Alamos National Laboratory in which several classes of conductive polymers are being studied for suitability in corrosion protective coatings. This research involves synthesis, polymerization, development of coatings, and testing of the coatings. The classes of materials under study are polyaniline, polybenzimidazole, polyphenylquinoxaline, polyimide, polyisoimide, polypyrrone, polypyrrole, and polythiophene. Once a polymer is prepared,

testing is carried out in Zone 2 and Zone 3 environments. The Zone 2 environment consists of exposure to a 350 °C temperature for 30 minutes, hot hydrochloric acid and aluminum oxide, water, and sodium chloride. The Zone 3 environment consists of exposure to a 66 °C temperature, hydrochloric acid, water, and sodium chloride.

Several candidate materials have been identified thus far as suitable for further testing as corrosion protective coatings. Additional work is in progress to improve adhesion of the coatings to steel. Coated steel panels utilizing these candidate coatings will undergo accelerated corrosion testing, beach exposure testing, wear resistance testing, and launch exposure testing.

Contact:

K. G. Thompson, 867-4344, DM-MSL-2

*NASA Headquarters Sponsor:
Office of Space Flight*

Ignition of Metals in High-Pressure Oxygen

During the past several years, the White Sands Test Facility (WSTF) of the Johnson Space Center has developed three methods to evaluate the flammability and ignition properties of metals in pressurized oxygen. WSTF is now evaluating the metals used in existing KSC oxygen systems in support of Space Shuttle operations and several other metals being considered for new systems.

The three test methods developed by WSTF are: rubbing friction, particle impact, and promoted ignition. The metals being evaluated include several stainless steels, a carbon steel typically used in vacuum storage vessels, nickel, several nickel/copper alloys, and several nickel/chromium alloys.

The particle impact tests were conducted using sand, rust, and iron particles. Ignitions were obtained only with the iron

particles, which suggests that the ignition of the particles themselves plays an important role in the ignition of metals. In these tests, the particle size was kept constant, and the oxygen pressure and velocity were the variables.

The promoted ignition tests have been completed. The nickel/copper alloys were the most resistant to ignition and burning while the iron-based alloys ignited and burned easily. Titanium ignited and burned at subambient pressures. The nickel/chromium alloys were found to be much more resistant to ignition and flame propagation than were the 300-series stainless steel alloys currently being used in KSC systems. The stainless steel alloys were found to ignite and burn completely at 1,000 pounds per square inch absolute (psia). The nickel/chromium alloys ignited at 2,500 psia but self-extinguished after burning approximately 1-1/2 inches of the 6-inch test length. Testing at 3,500 and 4,500 psia is continuing. Corrosion tests on the nickel/chromium alloys showed these materials to be very resistant to the KSC Shuttle launch environment, which could result in significant savings in maintenance costs if these newly identified alloys can be used in future systems.

In the rubbing and friction tests, it was found that most materials were harder to ignite at high oxygen pressures than at low oxygen pressures. This is thought to be due to either: (1) the increased thermal conductivity of oxygen at higher pressures, thus conducting the frictional heat away from the test specimens, or (2) the formation of oxide coatings that lubricate the rubbing surfaces and slow the diffusion of oxygen to the active sites.

Contact:

C. J. Bryan, 867-4344, DM-MSL-2

*NASA Headquarters Sponsor:
Office of Space Flight*

Thermal Tile Bonding Inspection Using Gamma Ray Scattering

In Phase I of the project, the potential for reliable nondestructive inspection of adhesion of Space Shuttle thermal protection system (TPS) tiles using gamma ray backscatter radiometry was evaluated. Monoenergetic gamma rays, using sodium iodide spectrometry, provided system response to density changes in the sensitive areas formed at the bonded surfaces. Based on Phase I results, the combination of precise collimation with energy resolution promises a greater sensitivity to voids and microinclusions for this technique than could be achieved with x-ray backscatter tomography. Features less than 0.001 inch can be resolved with this technique. Results also support development of a small, portable inspection system able to rapidly detect voids in the silicone adhesive without applying an external force or vibration. Both computer and bench-scale modeling confirmed the feasibility of this technique.

Contact:

N. P. Salvail, 867-4614, DM-MSL-2

Participating Organization:

Spire Corporation

NASA Headquarters Sponsor:

Office of Space Flight

Laser Acoustic Thermal Protection System (TPS) Bond Assessment Study

A new approach is being developed for the inspection of bonds in difficult-to-inspect materials. Researchers at the Idaho National Energy Laboratory (INEL) are under a NASA contract with KSC to demonstrate the feasibility of using a noncontacting laser acoustic sensor to assess the bond condition of the thermal protection tiles used on Space Shuttle Orbiters. The concept or physics behind the bond assessment is fairly simple. The assumption is that bonded materials will

vibrate in a slightly different manner than unbonded materials when they are gently excited by a known impulse. By proper selection of the excitation and use of a very sensitive laser measurement of a tile's displacement, it is possible to determine whether or not the tile is properly bonded. In some sense, the technique is an amplification and quantification of the "Tap Test" used in many areas of inspection.

This research has been under way for over three years. The study has shown that there are several well-characterized features in the dynamic response of thermal tiles that can be associated with the degree of bond. In addition, a laser acoustic sensor system has been developed and patented. The sensor can make measurements off of dark, diffusely reflecting surfaces, such as the thermal tile's borosilicate glass coating, at distances up to 10 meters. Most of the work to date has been conducted on tile geometries similar to the "acreage" tiles that cover much of the underbodies of Orbiters. Field tests were

conducted at the Orbiter Processing Facility in July 1988. These tests showed that tile response was similar to responses measured in the laboratory but that ambient motion of the Orbiter was greater than anticipated and would require some modification of the sensor.

Work is continuing on this project with a "blind" test of the technique being discussed as a next step. The remaining technical issues for development of a prototype are sensor modifications, inclusion of more tile geometries and variables into the database, and development of a simulation tool to model the vibrational response under varying conditions.

Contact:

J. W. Larson, 867-3423, SI-PEI-1A

Participating Organization:

*Idaho National Energy Laboratory
(B. Barna)*

NASA Headquarters Sponsor:

Office of Space Flight

Instrumentation and Data Acquisition

The measuring systems that monitor every facet of the Shuttle checkout and launch process (including non-Shuttle tests) must be more reliable than the systems they monitor. The instrumentation and data acquisition laboratories have the responsibility to ensure that the John F. Kennedy Space Center (KSC) is provided with the latest technology in monitoring hardware and techniques.

The Transducer and Sensor Laboratory

The Transducer and Sensor Laboratory is the focal point for Centerwide ground support equipment and institutional utility system's instrumentation research and development. The activities include: developing new families of instrumentation using internal resources and the resources of industry and academia; publishing design and procurement specifications; performing comprehensive evaluation, qualification, and long-term environmental testing for prototype and off-the-shelf hardware; developing and qualifying signal conditioning or hardware interface electronics; and providing common or special instrumentation components for special test programs.

The Landing Aids and Security Instrumentation Laboratory

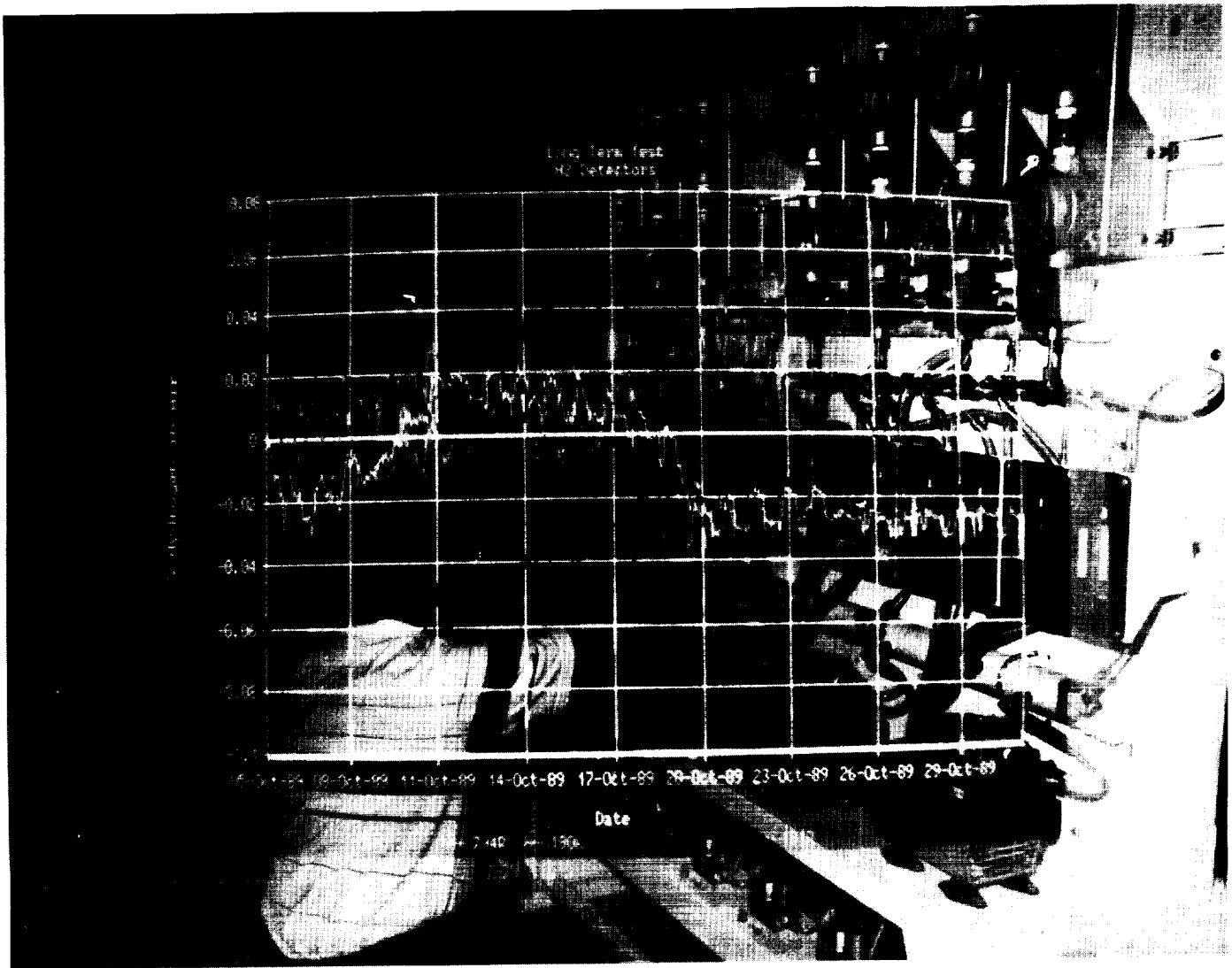
The Landing Aids and Security Instru-

mentation Laboratory develops the flight test instrumentation used in the checkout and calibration of the Microwave Scanning Beam Landing System (MSBLS) and the Tactical Air Navigation (TACAN) system. Current work is concentrated on applying the Global Positioning System (GPS) navigation signals to the calibration of the landing aids systems. Other supporting work includes developing a pilot display and evaluating an infrared tracking system. The second function of the laboratory is to develop both intrusion and personnel access security systems.

The Data Acquisition Development Laboratory

The Data Acquisition Development Laboratory is responsible for applying the latest technology to the data acquisition process. The two data acquisition systems currently supporting the KSC ground instrumentation are: (1) the Launch Complex 39 Permanent Measuring System (PMS), which collects the environmental and special measurements data generated during Shuttle launches, and (2) the Launch Equipment Test Facility (LETf) mobile van, which monitors ground support equipment verification tests.

ORIGINAL PAGE
BLACK AND WHITE PHOTOGRAPH



Transducer and Sensor Laboratory

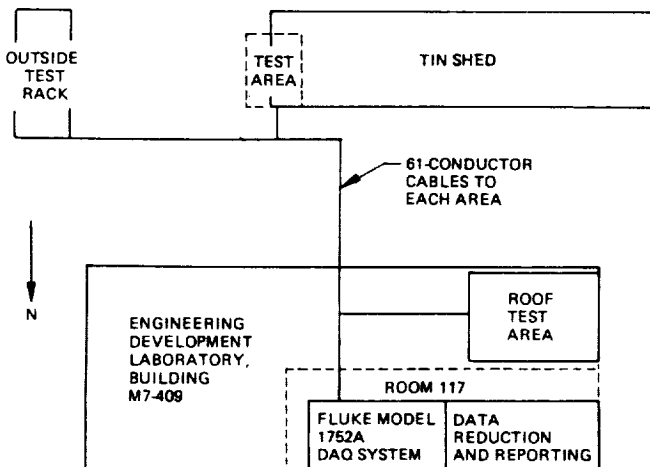
Long-Term Testing of Transducers

As part of the qualification of transducers in the Evaluation and Qualification Laboratory, there was a need to test them in the actual environment in which they will be used at KSC. Two types of testing were necessary:

1. Exception monitoring: tests devised to monitor zero drift or the conditions that should exist when the transducer is not stimulated.
2. Active tests: tests designed to monitor the transducer under stimulation.

Three sites in the vicinity of the Engineering Development Laboratory (EDL) were chosen to perform the long-term testing. The sites were the roof of the EDL, both an inside and outside area at a tin shed behind the EDL, and an outside test rack located near the tin shed (see the figure "Long-Term Testing Sites").

After the site selection, one 61-conductor cable was run from each area to room 117, the Evaluation and Qualification Laboratory of the EDL. Breakout terminal boxes were then made at the sites so transducers of any type could be efficiently installed or removed.



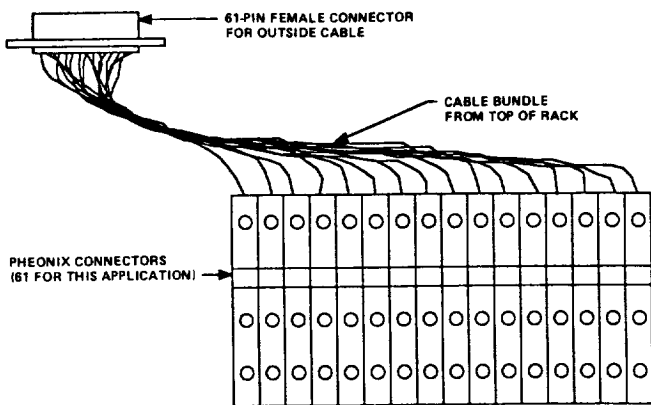
Long-Term Testing Sites

In room 117, a data acquisition/data reduction system was used to record the history and produce the necessary reports. This was accomplished using a Fluke Model 1752A as the data acquisition subsystem and an MS-DOS-compatible computer as the data reduction subsystem. The 61-conductor cables were brought into the top of the racks from the outside test areas.

It was decided that exception monitoring would be performed 24 hours a day and active tests would be performed once every 24-hour period. During exception monitoring, data/conditions would be recorded once an hour. This would keep the mass storage requirements within reasonable limits. The active test data would be stored on a floppy disk and the exception monitoring data stored on a hard disk. Based on these requirements, the system was configured to perform the following:

1. Record exception monitoring data once an hour. Only the reading taken on the hour is recorded on disk. The file containing this data is noted on the printout along with the date and time. At the same time, if an error occurs during the hour, the channel number, value of the data, and high/low values are printed. This means that only the last error value is printed; however, the operator is informed of a problem without creating a mass storage or printer paper problem.
2. Perform active tests and record the data on a floppy disk for later reduction. Any exceptions noted during the running of the test are immediately printed on the printer in the same format in which the exceptions were noted during exception monitoring.

The design shown in the figure "Terminal Breakout Drawing" was selected for the input cabling so that maximum versatility would be achieved. The design used Phoenix connectors in a one-in-two-out



Terminal Breakout Drawing

configuration; this allowed the same signal to be used in more than one place for parallel system testing and troubleshooting. Since the data acquisition subsystem used the same screw-type terminals, this allowed the installation and removal of a sensor with a screwdriver and a pair of wire strippers.

The software was written to meet the following criteria:

1. Perform exception monitoring and record any exceptions. The only software change required to activate exception monitoring for a channel was the changing of three variables. Changing one variable activated exception monitoring; the other two variables provided the high and low limits to be monitored.
2. Ensure that exception monitoring could not be stopped accidentally. This was handled by requiring the operator to go through three distinct screens to exit the program. Any error on these screens returns the program to the monitoring mode.
3. Require the shortest possible time to activate a new item and deactivate an old item. The requirement for the shortest activation time was fulfilled by having all screen labels ready with periods instead of charac-

ters; thus, to change the screen, the operator defines the page to be used and replaces the periods with the desired characters.

4. Perform active tests on transducers. The capability of performing active tests depended too much on the type of transducer being installed, so this requirement was the most difficult to fulfill. It was necessary to write a new software module for each type of transducer. The integration of this new module was made simple by having the active test performed at the same time each day.
5. Enable the simple addition/deletion of active test modules. This was facilitated by use of the Phoenix screw-type connectors.
6. Perform a manual active test without recording the results or triggering an exception. The manual test capability was achieved by using the active test module with touch-screen buttons already written into the software as the activation device.
7. Display 64 channels of data on a 15-line cathode-ray tube (CRT). In order to show 64 channels of data on a 15-line screen, a paging format was chosen. An index page was also generated to allow the operator to see what options are available and on what pages.
8. Simple to operate. Simplicity of operation was accomplished by writing a short autostart file on the data acquisition system. This means that the operator only needs to press the restart button and the system will automatically initialize all the desired channels and exception monitoring and will display the index page. A separate page was created to transfer the recorded data to the data reduction system; this page

gives the directions required to do this.

9. Minimize the required laboratory floor space. The need for a keyboard was removed by using the Fluke Model 1752 Touchscreen Toolbox for all screen entries. This enabled the entire acquisition and reduction system to fit into two racks in room 117.

Contact:

R. M. Howard, 867-3185, DL-ESS-23

Participating Organization:

Boeing Aerospace Operations, Engineering Support Contract (R. T. Deyoe)

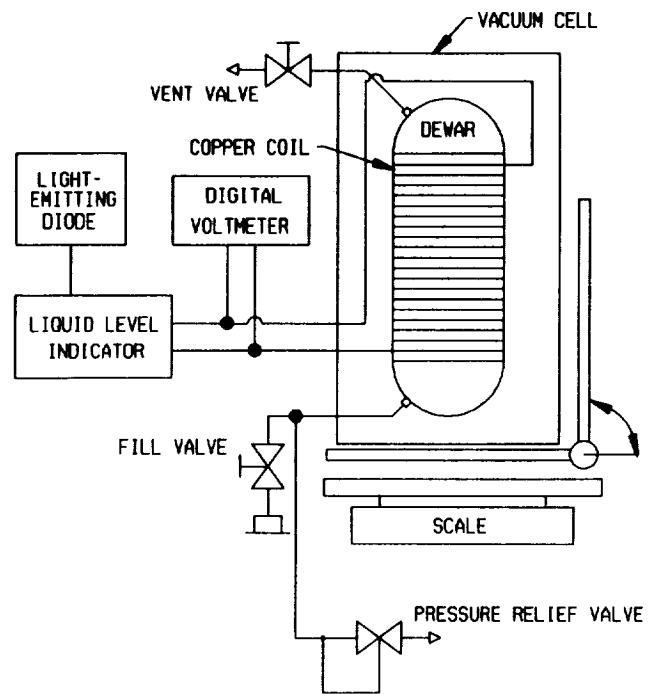
NASA Headquarters Sponsor:

Office of Space Flight

Liquid Air Level Indicator for Portable SCBA Dewars

A typical self-contained breathing apparatus (SCBA) consists mainly of a pressurized air source, a one- or two-stage pressure regulator, hoses, gages, and a face mask to provide air to the user. A major safety component of an SCBA is a low-level indicator/alarm. This device performs two functions: (1) it allows the wearer to monitor the amount of air left in the SCBA and (2) it sounds an alarm when 25 percent of the air is left so the wearer can egress to a safe atmosphere.

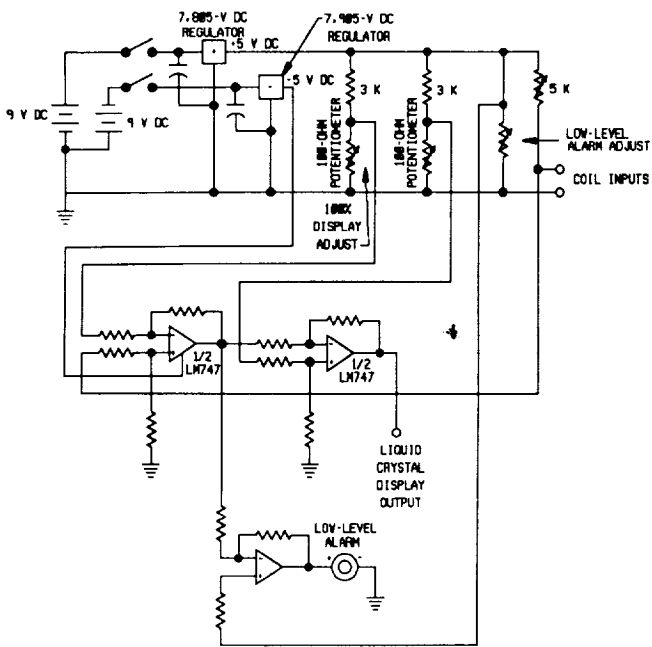
At the John F. Kennedy Space Center (KSC), a liquid air pack (LAP) self-contained breathing apparatus is used by the closeout crew and fire rescue teams to rescue disabled astronauts in the event of a launch pad emergency. Although designed for a 1-hour duration, the LAP is rated at 45 minutes and uses an electronic timer to sound a low-level alarm. A drawback with the timer is that it is not activated by a direct measurement of the amount of liquid air in the dewar. The liquid air level is related to the type of



Liquid Level Indicator Dynamic Test Schematic

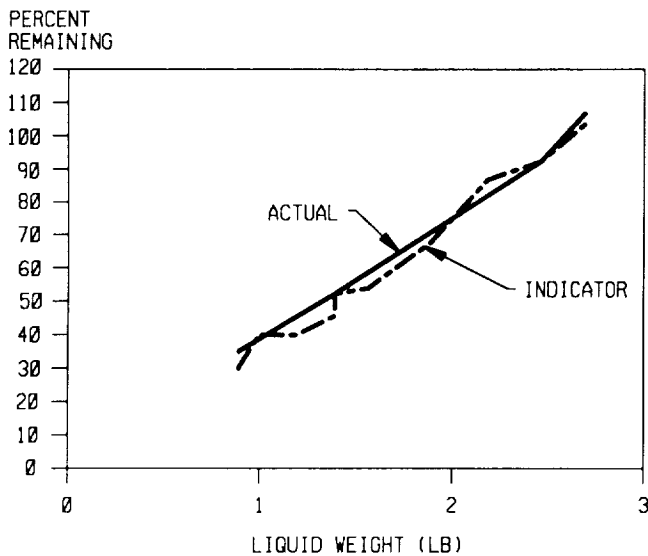
usage; for example, a sitting or walking man will use less air than one climbing stairs or running. Therefore, the timer is set at a conservative period for safety (33.75 minutes, leaving 11.25 minutes or 25 percent of the time for egress).

A method of direct liquid-air-level measurement would allow the LAP to be upgraded to its original design duration. NASA Engineering Development is working on an electrical resistance/temperature device to measure the amount of liquid air in the LAP dewar. This liquid level indicator (LLI) uses a 30-mil diameter insulated copper wire that is wound around the outer surface of an experimental dewar's inner vessel. The copper wire coil is connected to the LLI electronics, which measures electrical resistance (ohms). When liquid air is used from the dewar, the temperature of the coil and its electrical resistance increase. This increase in resistance is correlated by the LLI to the drop in weight of the liquid air. The output is read in the percentage of liquid air remaining.



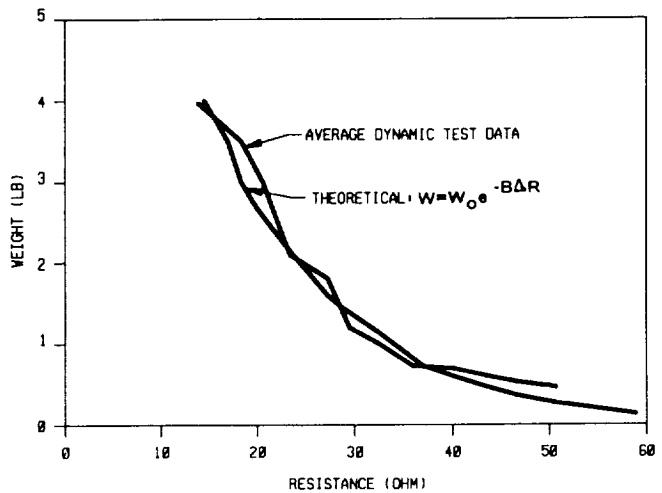
Liquid Level Indicator

Testing of the prototype LLI apparatus in both a static mode (the dewar is vertical and stationary) and a dynamic mode (the dewar orientation varies randomly between the vertical and horizontal) has been completed. In these tests, liquid nitrogen (LN₂) was used to simulate liquid air. The inner dewar vessel/coil assembly was encapsulated by a Plexiglas vacuum



RANGE 20 TO 50.9 OHMS

Indicator Dynamic Test



Actual Versus Theoretical Measurements

cell to reduce the thermal transfer to the LN₂. Air use was simulated by allowing the LN₂ to vent to ambient through a 1/4-inch tube. The actual weight of LN₂ in the dewar was measured by a 0- to 200-pound scale during each test.

Measurements by the LLI and the actual percent weight of LN₂ in the dewar agree well. The LLI tracked the amount of LN₂ regardless of the dewar's orientation or motion. The decrease of LN₂ weight in the dynamic tests (which model actual use) closely follows an exponential equation:

$$W = W_0 e^{-B \Delta R}$$

The constant B is an empirical term in units of ohms⁻¹, and ΔR is the change in electrical resistance.

The next phase of testing, which will begin in January 1990, involves interfacing the LLI with a LAP unit for both laboratory and field testing. This testing will allow evaluation of the LLI under conditions that approximate actual use. The laboratory testing will involve repeating the static and dynamic tests with a breathing machine to simulate human respiration. The field tests will have a test subject wear the modified LAP and per-

form exercises to simulate actual rescue operations.

Contacts:

*M. Hogue, 867-7960, DM-MED-41
D. McLaughlin, 867-7287, DM-MED-2*

*NASA Headquarters Sponsor:
Office of Commercial Programs*

Automated Laboratory for Evaluation and Qualification of Transducers

In an effort to standardize transducers used at KSC, it was necessary to set up a testing area to perform qualification tests. Since a production calibration facility would not normally run these tests, this led to the need for an Evaluation and Qualification Laboratory at KSC to be responsible for these functions.

Qualification of a transducer involves verifying its ability to withstand environmental parameters (temperature, vibration, electrical, and atmospheric) specified by the manufacturer or by a NASA system engineer. Once a transducer's ability to withstand these parameters has been verified, the manufacturer is given as a suggested source for purchase in the specifications. Qualification also involves the continued testing of a family of transducers to the parameters listed under the original evaluation to determine if the whole family of devices is deteriorating to such an extent that industry must be searched for replacement sensors.

Since manpower to perform qualifications testing is limited, it was decided to automate the laboratory. Several major decisions for selection of equipment had to be made; equipment was needed for control of laboratory standards and for measurement and data reduction systems.

An MS-DOS-based personal computer was selected as the laboratory controller

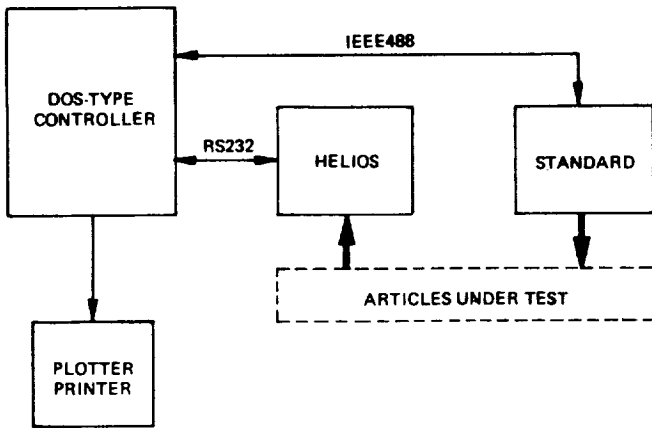
because it can be modified for use by the addition of a few special-purpose boards and has a low acquisition cost.

The IEEE488 bus was selected to control the laboratory standards, since this was what most manufacturers provide as the computer interface. Also, there were many plug-in boards (most of which had libraries of software to link with Quick Basic) on the market to customize the MS-DOS-based computer as an IEEE488 controller.

A system called Helios, which is manufactured by John Fluke Manufacturing, was selected as the data acquisition system. This selection was made based on several factors:

1. **System accuracy.** Since the laboratory would be responsible for evaluating transducers that may find their way into critical applications, it was necessary to get the highest turn-down ratios possible from a traceability standpoint. Helios provides a 0.005 percent reading plus or minus 7-microvolt direct current accuracy on the 64-millivolt direct current range with a resolution of 0.6 microvolts.
2. **Versatility.** Using available boards, the system can be configured to acquire a variety of data, such as resistance, temperature (both resistance thermal detector and thermocouple), voltage, current, and strain.
3. **Ease of use.** Use of the Helios Toolbox software, which links with Quick Basic, allows software to be written that can acquire the data and load the output directly into Lotus files for data reduction without the need of a separate machine and all the inherent interface problems.

In the block diagram "Typical Test Bench," the Standard could be pressure, vacuum, temperature, or any other discipline required at KSC. The Standard and



Typical Test Bench

Helios are used in the acquisition of data. The printer and plotter are used for data reduction and reporting.

Through the use of ovens, shaker tables, and other environmental test equipment, parameters such as nonlinearity, repeatability, and hysteresis can be determined at the extremes to which the transducer may be subjected. In addition to the laboratory tests, the sensor will be placed in an outdoor setting for a period of time to test its ability to withstand the actual KSC environment.

Establishing the automated qualification laboratory will ensure that sensors purchased for critical functions meet specification requirements and that specifications define the most appropriate transducers available.

Contact:

R. M. Howard, 867-3185, DL-ESS-23

Participating Organization:

Boeing Aerospace Operations, Engineering Support Contract (R. T. Deyoe)

NASA Headquarters Sponsor:

Office of Space Flight

Fast-Response Instrumentation Van

Some testing performed by KSC must be conducted at remote sites because the test

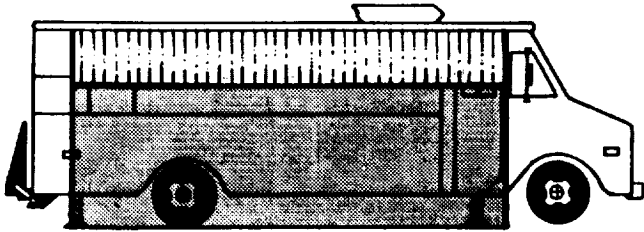
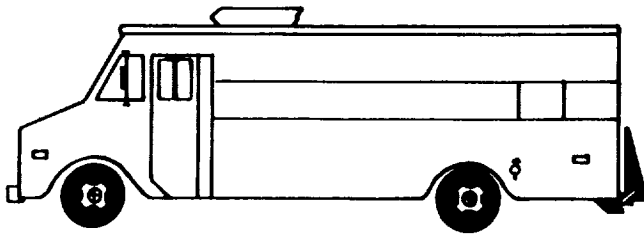
articles are remotely located or the test is hazardous; these areas lack adequate shelter for instrumentation equipment. To remedy this situation, KSC is developing an instrumentation van that can be used to support testing at remote locations.

The vehicle is a 1987 Chevrolet step van. The van is powered from a 120-volt alternating current, three-phase, 60-ampere facility or by generator power. It is outfitted with internal and external lighting, three removable equipment racks, air conditioning, hydraulic power levelers, a one-half ton lift gate, a trailer hitch, and a retractable awning with mosquito netting.

The van is being equipped to provide measurement and data processing capability for support of small tests. The van configuration will be flexible depending on the test requirements. The standard configuration for the van will accommodate 48 channels of data input with some expansion capability available. The rack configurations will accommodate 24 channels of signal conditioning amplifiers, 20 channels of O-graph recording, 16 channels of strip chart recording, 32 channels of multiplexed pulse code modulation (PCM) data, 14 tracks of direct recording on magnetic tape with the capability of adding 8 channels of strip chart recording and 14 tracks of direct/FM recording on magnetic tapes.

All of the equipment within the van will be computer controlled via an IEEE-488 bus. A Macintosh II, in conjunction with National Instrument's Labview software, will be used as the computer controller. Analog data acquisition and analysis may also be handled by the Macintosh II computer.

The frequency response capabilities vary depending upon the data acquisition components used. High-level data may be recorded directly on magnetic tape (FM) for direct current to 500-kilohertz frequency response. The frequency response of other



Fast-Response Instrumentation Van

system components varies from direct current to 100 hertz (strip chart), from direct current to 5 kilohertz (O-graph), and from direct current to 10 kilohertz (signal conditioning amplifier). The Macintosh II computer can digitize at a 100,000-samples-per-second rate (multiplexed). The van's test support capabilities also include obtaining the proper sensors and calibrating, installing, and functionally checking them prior to a test.

The Fast-Response Instrumentation Van is still in development; however, it has supported one test for the U.S. Air Force involving recording transient pressures and accelerations during the failure of a pressure vessel pressurized to its burst point. In the future, the van will also provide support capability of fabrication and verification for Advanced Launch System facilities and systems.

Contact:

M. M. Scott, Jr., 867-3185, DL-ESS-23

Participating Organization:

Boeing Aerospace Operations, Engineering Support Contract (J. C. Ake)

NASA Headquarters Sponsor:

Office of Space Flight

Precision Laser Tracking System II (PLTS II) System Development

System Description

The Ground Support Equipment Branch of the Engineering Development Directorate working with the Instrumentation and Measurements Branch of the Ground Engineering Directorate is developing a replacement for the Precision Laser Tracking System (PLTS). The PLTS tests and verifies the Microwave Scanning Beam Landing System (MSBLS) at the three primary Shuttle landing facilities: White Sands Space Harbor (WSSH), White Sands, New Mexico; Edwards Air Force Base (EAFB), California; and John F. Kennedy Space Center (KSC), Florida. This process of calibration and verification of the MSBLS is referred to as "commissioning" and is required to be performed once a year. The MSBLS has been established at additional landing sites at Zaragoza and Moron, Spain; Ben-Guerir, Morocco; Banjul, Gambia; Hickam Air Force Base, Hawaii; and Anderson Air Force Base, Guam.

The original PLTS consists of a 40-foot trailer that houses a laser-positioning system which tracks a test aircraft as it makes various approaches to the landing site. The PLTS provides a nine-track, 1,600-bits-per-inch digital tape containing the position data of the approaching aircraft with respect to time. Aboard the aircraft is a pallet containing MSBLS receivers and transmitters and a data acquisition and formatting computer. This computer collects the MSBLS data and formats it onto a nine-track, 1,600-bits-per-inch digital tape and transmits this data to the ground for recording on instrumentation recorders (back-up data). After a number of test flights, the two digital tapes are then processed by another computer that computes the errors in the MSBLS so that corrections can be made to the MSBLS, usually repositioning the

elevation and azimuth antennas. If corrections are made, additional flights are required to verify the error has been removed.

New System Development

The development of a new system to replace the PLTS has concentrated on the use of the Department of Defense Global Positioning System (GPS) for tracking a test aircraft as it approaches a landing site. The GPS baseline constellation of 24 satellites operates in 12-hour orbits at an altitude of 20,183 kilometers (10,898 nanometers) and provides visibility of 6 to 11 satellites at 5 degrees above the horizon to users located anywhere in the world at any given time. The position determinations are based on the measurement of the transit time of radio frequency signals from four satellites of the total constellation.

A second tracking system, called MINILIR, is also being developed and will be used to supplement the GPS tracking system. MINILIR, an infrared tracking system manufactured by Societe Anonyme de Telecommunications (SAT), Paris, France, automatically tracks an infrared source and provides azimuth and elevation data that establishes the trajectory of the infrared source.

GPS System Description

A GPS receiver is located on the test aircraft with the MSBLS receiver and a computer for data processing. The GPS signals from the constellation of satellites enable the GPS receiver to compute the location of the aircraft as it makes its approach to the landing site. The data from the GPS receiver is sent directly to a computer located on the aircraft, which also receives data from the MSBLS. The data from the GPS and MSBLS are compared, and the errors in azimuth, elevation, and distance are plotted on a cathode-ray tube in real-time for the operator. For reference purposes, the plotted data can be dumped by the operator to a graphics

printer. The operator can then direct the technicians to adjust the MSBLS, if required, and direct the pilot to re-fly the approach to check the MSBLS and verify if further adjustment is necessary. The GPS and MSBLS data from all flights are also stored for near real-time retrieval and posttest processing and analysis. In addition, this system can be used to check the MSBLS transmitter's power during the flight.

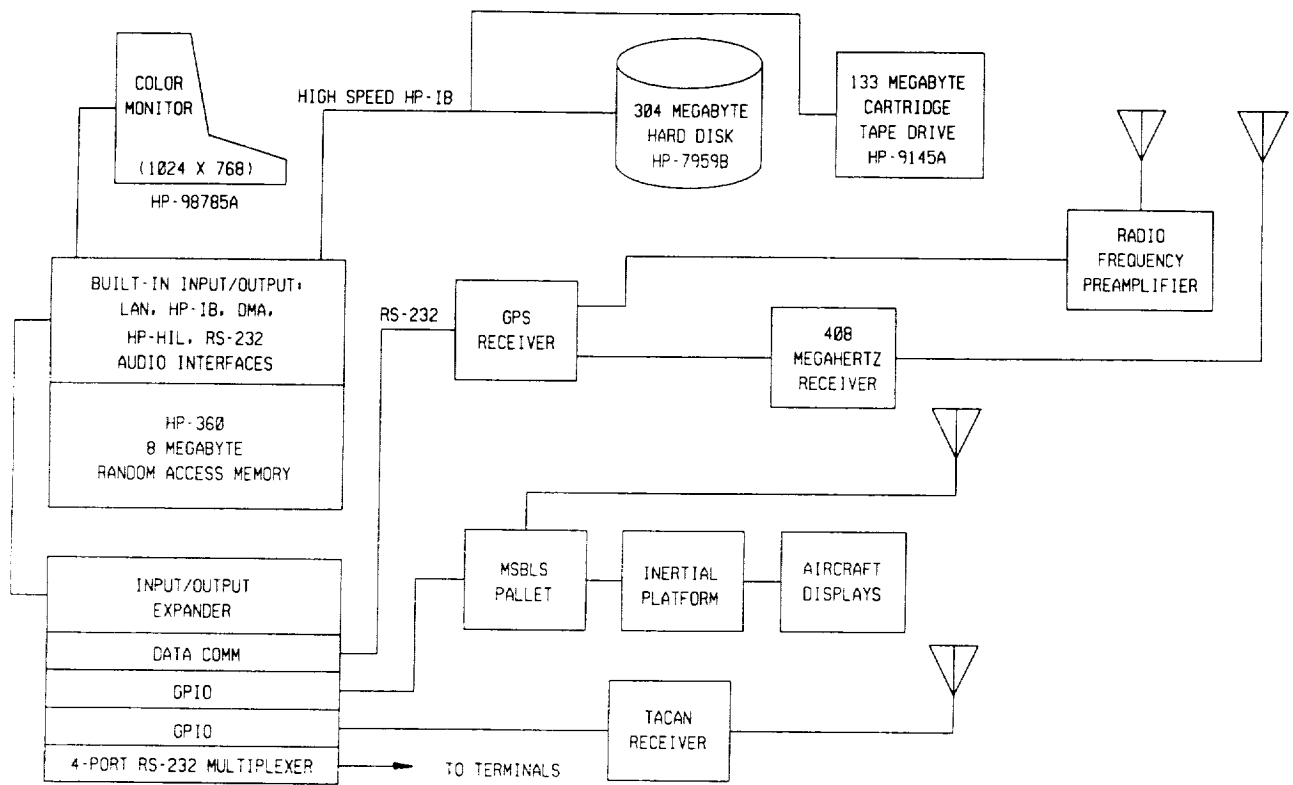
MINILIR System Description

The MINILIR system consists of a telescope with an infrared detector and servomechanisms, infrared signal processing and data encoding equipment, a satellite time code receiver, and a computer. This system can automatically track an infrared source and provide azimuth and elevation data, along with the time of day, for the trajectory of an object with respect to a fixed point on the ground.

The MINILIR system operates much like the original PLTS and provides a backup method for flight verification. The system is used to track the test aircraft's landing light (only one landing light is turned on) as it makes an approach to the landing site. The system provides the trajectory data on a floppy disk, which is played back into the GPS/MSBLS computer and compared to the MSBLS data recorded during a corresponding flight.

System Expansion

In addition to the GPS and MSBLS data input, two more data sources are being added to the system for data processing. The first new source is the pitch, roll, and yaw data of the aircraft, which will be derived from an inertial platform that will be added to the MSBLS pallet. The platform data is used to refine the GPS data and increase the accuracy of the measurement. The second source of data is from a Tactical Air Command and Navigation System (TACAN) receiver, which is used to verify the TACAN installation at the differ-



GPS/MSBLS Data Processor

ent landing sites. The certification of the TACAN is presently contracted to the Federal Aviation Administration (FAA) for the Space Shuttle landing sites and is a yearly requirement.

At the present time, the MINILIR data has to rely on the MSBLS distance measuring equipment (DME) data for distance information for the comparative calculations. A radio frequency range finder will be added to the MINILIR system, which will enable the MINILIR to determine the distance of the aircraft from the MINILIR. This additional data will make the MINILIR a totally independent system for measuring aircraft position.

Aircraft position at the beginning of a test run and throughout the test will be made available to the aircraft pilot through a real-time display. GPS data will be used to show the pilot where his aircraft is in relation to the runway, where the test run is to start and end, and the path he is to follow during the test.

Contact:

M. M. Scott, Jr., 867-3475, DL-ESS-23

Participating Organization:

Boeing Aerospace Operations, Engineering Support Contract (T. Erdogan)

NASA Headquarters Sponsor:

Office of Space Flight

Handbook of Strain Gage Application Techniques

Strain gages are widely used at KSC for structural analysis, recording of launch effects, and tensioning of critical bolts. Because of the highly sensitive nature of strain gages, errors can easily be introduced into the measurements. To minimize these potential errors, care must be taken in selecting the type of gage used for a particular application, the mounting method employed, the orientation of the gage, and signal conditioning. Proper use of strain gages cannot be ensured by existing systems of specifications or by other

means that are effective for other types of transducers. There exists the need to distill the knowledge of strain gages and to transfer the knowledge effectively to the many end-users at KSC.

This project will produce a handbook that fully addresses the practical aspects of the installation of strain gages and strain gage instrumentation to enable KSC engineers to properly design and use strain gages and interpret the data gathered by them. The first phase of the project, researching scientific literature and performing extensive hardware laboratory research to develop a full understanding of the state of the art in strain gage usage, is underway. A full understanding of pitfalls, sources of error, and environmental effects are being derived. This knowledge will be formulated into a handbook which will receive extensive review by the KSC user community. This approach will ensure a handbook is produced that meets the needs of KSC mechanical and electrical engineers. The handbook will be published in late 1991.

Contact:

R. M. Howard, 867-3185, DL-ESS-23

Participating Organization:

Boeing Aerospace Operations, Engineering Support Contract (J. C. Ake)

NASA Headquarters Sponsor:

Office of Space Flight

Field Portable Biomedical Instrumentation System

A portable instrumentation system has been developed to collect seven channels of temperature data and a voice information channel. This system has been used successfully to monitor the physiologic heat stress experienced by KSC fire rescuemen while performing a simulated rescue in the field. A dual-purpose signal conditioner received temperature information from seven Series 700 Yellow Springs thermistor

probes. Three different types of probes collected skin, body core, and suit temperatures. The signal conditioner, which comprised a special bridge, a buffer, and amplification circuits, covered a range of 20 to 120 °F. In this application, the seven conditioned temperature signals were fed to a TEAC (Model 40) nine-channel instrumentation recorder; the two remaining channels were used for tape speed compensation and voice annotation.

The same circuitry will be used, but at different levels, for a yet-to-be-completed radio telemetry system. In the interim, a simple 49-megahertz, frequency-modulated (FM), voltage-controlled oscillator system was developed to provide real-time recovery of body core temperature during the field testing protocol. This system uses two inexpensive, hand-held FM radios, one of which is carried by the subject. The body core temperature (95 to 105 °F) signal is fed to a voltage-controlled oscillator, which provides modulation of the FM signal. A remote receiver feeds a demodulator, which feeds a frequency to the voltage converter. The resulting temperature data is monitored on a strip chart recorder.

Contact:

D. F. Doerr, 867-3152, MD-ENG

NASA Headquarters Sponsor:

Office of Aeronautics and Space Technology

Orbiter Tire Leak Rate Detection System

An Orbiter's tires are critical to the completion of a successful mission. A system is needed to ensure that the tire pressure will be adequate for landing. This system must be implemented prior to stacking, or it will impact mission schedules.

The objective of this project is to develop a leak rate detection system that will measure the leak rate of an Orbiter's tires in the shortest time possible to minimize

the effects of environmental conditions, such as temperature and barometric pressure changes.

Under normal conditions, all tires leak at some given, exceptionally small rate. It is necessary to determine the actual leak rate of the Orbiter's tires in order to ensure that the tire pressure is above the required safety margins by the end of a mission.

Orbiter tires are currently tested for leak rates using conventional pressure gages and transducers. The allowable leak rate for an Orbiter tire is 0.4 pounds per square inch (psi) per day; a typical leak rate is 0.23 psi per day.

An instantaneous reading of the leak rate would be ideal; however, since it is a rate measurement, some time must elapse between measurements. The accuracy of the measuring device determines how much time must elapse from the initial reading to the final reading in order to accurately discern the pressure change that has occurred. For example, if a 400-psi pressure transducer is used with a 0.1-percent error band, the pressure readings obtained will be accurate to plus or minus 0.4 psi. Typically, a pressure change of 1.6 psi could be measured with this instrument, excluding the errors in the other system devices. This accuracy (0.1 percent) would then require a minimum of four days to elapse between the first and second measurements. This example ignores the effect of the environment on the system and the tire.

Since a leak rate of 0.23 psi per day would only yield a change of 0.000159 psi per minute, it is not practical to measure this rate with a 400-psi device over a short period of time. Environmental conditions must also be taken into account because they can have a marked effect on the absolute accuracy of the leak rate measurement.

Presently, the marketplace is being researched for a leak rate detection sys-

tem. Concurrently, the Engineering Development Laboratory at KSC is conducting experiments on a differential pressure system design to determine if it meets the stated requirements.

Contact:

R. M. Howard, 867-3185, DL-ESS-23

Participating Organization:

Boeing Aerospace Operations, Engineering Support Contract (J. C. Ake and R. T. Deyoe)

NASA Headquarters Sponsor:

Office of Space Flight

Instrumented Torque Wrench System (INTOWS)

Objective

To investigate the development of an instrumented torque wrench system for after-the-fact verification of torque values. The system will automate verifications of noncritical and inaccessible tasks, will free scarce inspection resources to work on more critical tasks, and/or will provide records from which verifications can be made.

Background

Integration, operations, and maintenance activities place great demands on inspection resources, creating a need to develop new assurance technology to more effectively use these resources. In addition, inadequate inspection staffing levels, hazardous operating environments, manloading restrictions, and workspace restrictions create conditions that sometimes preclude real-time verification of torquing activities. This reveals a need to develop an alternate means of verification.

The initial research was conducted under a Small Business Innovative Research (SBIR) Phase I study. Phase I included the evaluation of potential user needs and

the development of a working proof-of-concept model (INTOWS-I) with partial software implementation. Development of a field evaluation version of the system (INTOWS-II) is now under way with SBIR Phase II funding.

Approach

The approach is to use a standard wrench instrumented with strain gages and connected to a hand-held microprocessor. Bar codes will be used to identify task requirements and specifications to the system and to verify items such as operator certification and tool calibration due dates. Inspection personnel now verify such items in real-time. The system will match the operator and the tool to the task and record this information for later retrieval. After task completion, the INTOWS will be returned to the tool control area, where the data will be transferred to a host computer and a report printed for attachment to the record copy

of the work document. The data can be archived for later recovery, and inspection personnel can make task verifications from the printed report.

Results

The hardware and software development is still under way, and field evaluation began in November 1989. Concerns over identification/mapping of fasteners, to link torque data on the report to the actual fasteners on the hardware, may limit the application of INTOWS. Field evaluation should help to determine how much serial processing time will be saved by removal of in-line verifications.

Contact:

B. J. Raymond, 867-7662, RO-ENG

Participating Organization:

ANCO Engineers, Inc. (Dr. Paul Ibanez)

NASA Headquarters Sponsor:

Office of Commercial Programs

Communications and Control

The Fiber Optics and Communication Laboratory

The Fiber Optics and Communication Laboratory provides engineering support for the John F. Kennedy Space Center (KSC) copper and optical-fiber cable plant. The major share of its human and material resources is assigned to the evaluation and application of state-of-the-art fiber optics communication technology. This includes fibers, connectors, splicing tech-

niques, electro-optical receivers and transmitters, and multiplexing. Three other significant laboratory tasks are: maximizing the utilization of the fiber optic and copper cable plant; providing the technical expertise and hardware for the video and photo-optical systems used in support of KSC technical operations; and defining and furnishing test equipment necessary for the maintenance of communications, video, and photo-optical systems.

ORIGINAL PAGE
BLACK AND WHITE PHOTOGRAPH



DC to 150-Megabits-Per-Second Fiber Optic Link Development

A direct current (dc) to 150-Megabits-per-second (Mb/s) single-mode fiber optic test link has been developed at KSC to meet the requirements of space station module checkout in the Space Station Processing Facility and other facilities at KSC. An initial test setup, consisting of a single-fiber data link, was prototyped and tested in the laboratory. An extensive report was written giving the overall performance of the link. The initial test results were reported in KSC's 1988 Research and Technology Annual Report.

The system has been rebuilt and packaged in a field-installable rack-mount chassis. The wire/line driver and receiver circuits, using 100K series emitter-coupled logic (ECL), have been refined; the twin-axial conductors have been eliminated from the system and have been replaced by a 50-ohm coaxial cable. This should help to achieve the design goal of less than 5-percent jitter throughout the system. Activity detector circuits have also been incorporated in both the transmitter and receiver chassis to facilitate troubleshooting the data path between electro-optic transitions in both chassis.

A second fiber channel has been added to allow both clock and data transmission simultaneously over two separate fibers. Field testing of this system is commencing at this time. Both the transmitter and receiver chassis will be installed in the Communication Distribution Switching Center (CDSC) and will use a single-mode fiber test loop to the Vehicle Assembly Building Repeater (VABR) and back, making a 13-kilometer test circuit.

Currently, several transmission schemes that would allow both clock and data to be transmitted over the same fiber are being studied and designed. The eventual goal for this system is to be able to transmit transparently over one fiber from dc to 150 Mb/s. In a transparent system, no input would be necessary from operations personnel if the data transmission rate were to change.

Contact:

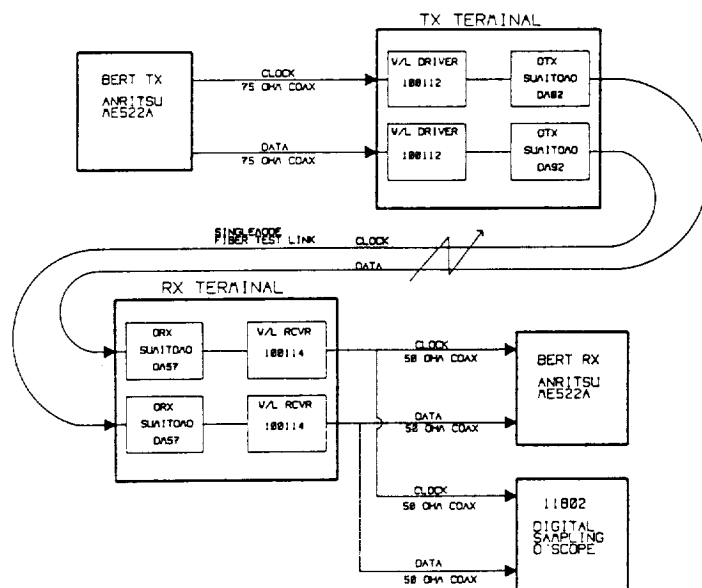
P. T. Huang, 867-2710, DL-ESS-12

Participating Organization:

Boeing Aerospace Operations, Engineering Support Contract (F. H. Galloway and R. W. Swindle)

NASA Headquarters Sponsor:

Office of Space Flight



Two-Fiber, DC to 150-Mb/s, Single-Mode Fiber Optic Test Link

Biosciences

The biosciences research and development effort at the John F. Kennedy Space Center (KSC) is supported by the Environmental Monitoring and Microbiological Laboratory, the Biomedical Research Laboratory, and the Life Sciences Support Facility.

The Environmental Monitoring and Microbiological Laboratory

The Environmental Monitoring and Microbiological Laboratory provides field monitoring, impact assessment, and all clinical and environmental microbiology research at KSC. The facility's equipment includes an automatic colorimeter detector, an atomic absorption spectrophotometer, an automatic microbiological identification system, hydrolaboratory stations, and a microcomputer-based geographic information system.

The Biomedical Research Laboratory

The Biomedical Research Laboratory is a fully equipped and staffed facility capable of performing a wide range of physiological research related to human response to microgravity. The laboratory supports the

preflight and postflight checkout of the Shuttle's bioinstrumentation and systems used in unique life sciences experiments. It also has the capability and skills to accomplish complete testing at temperature extremes on the full range of personnel protective equipment. A clinical laboratory operates within the research laboratory where radioimmunoassay and a variety of blood analyses are carried out.

The Life Sciences Support Facility

The Life Sciences Support Facility is involved in nonhuman life sciences flight experiments for the Shuttle program, in-house and externally sponsored biological research, and the Controlled Ecological Life Support System (CELSS) Breadboard project. The facility provides capabilities for receiving, housing, and caring for animals and growing plants. It contains plant growth chambers, analytical laboratories, preparation areas for food processing and waste studies, and the large CELSS growth chamber for closed system work. Supporting elements include flight animal isolation facilities, surgery and x-ray facilities, and data management and storage.



*Environmental Monitoring and
Microbiological Laboratory*



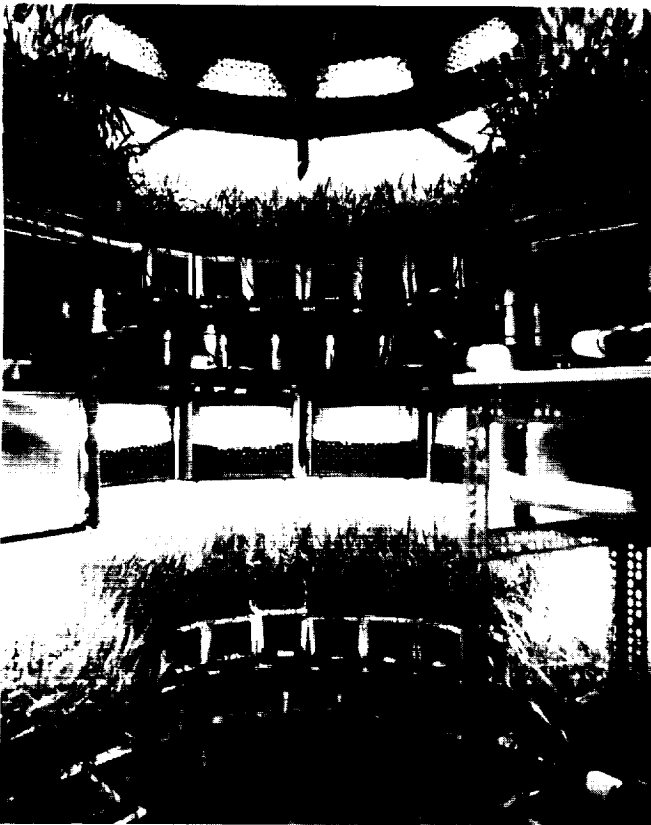
Biomedical Research Laboratory

Life Sciences Support Facility



Controlled Ecological Life Support System (CELSS) Breadboard Project

During the past year, three crops of wheat were grown in the Biomass Production Chamber (BPC). The initial planting was the first test of all four growing levels of the chamber. The second planting also used the entire chamber to determine the effects of position within the chamber and was the first test to incorporate automated pH and conductivity control of the four nutrient delivery systems. In addition, chamber measurements of stand (community) photosynthesis and respiration were taken during the second test. The results demonstrated the potential of the BPC to be used as a tool for studying water and carbon dioxide gas exchange for entire plant communities. Pneumatic door seals were added for the third wheat study, thereby keeping the chamber tightly sealed throughout the duration of crop growth.



Wheat Growing in the CELSS Biomass Production Chamber



The CELSS Biomass Production Chamber

As a consequence, stand photosynthesis and respiration could be logged continuously. The tight closure allowed ethylene gas (emitted from the plants) to build to levels near 100 parts per billion; thus, the first test using tight closure demonstrated the potential hazards from buildup of atmospheric contaminants.

Contact:

W. M. Knott, Ph.D., 853-5142, MD-RES-L

Participating Organization:

The Bionetics Corporation (Dr. C. R. Hinkle)

NASA Headquarters Sponsor:

Office of Space Sciences and Applications

Aquaculture Research

Aquaculture research and development has continued to evaluate the integration of *Tilapia aurea* into Controlled Ecological Life Support System (CELSS) biomass



Tilapia Aurea in an Aquaculture System

production and inedible biomass management. Continuous culture of lettuce and *Tilapia aurea* was accomplished in a combined aquaculture/hydroponic system, demonstrating the potential for including aquaculture in the hydroponic biomass production loop. The computer monitoring and control system was modified to provide more features and increased reliability and was installed on the combined system. A feeding trial to determine the nutritional quality of a blue-green alga (*Spirulina platensis*) as part of a *Tilapia aurea* diet was conducted. A diet that will consist of components from various CELSS inedible biomass streams is being developed. Culture of *Spirulina platensis* in a defined medium and in the combined-system tank water was initiated.

Contact:

J. C. Sager, Ph.D., 853-5142,
MD-RES-L

Participating Organization:

The Bionetics Corporation (P. Hall)

NASA Headquarters Sponsor:
Office of Space Sciences and Applications

Kennedy Space Center Firefighters Occupational Performance Test Validation Program

A study was conducted to evaluate the physiological demands of a three-item test battery for KSC firefighters prior to its designation as an accepted occupational performance standard. This Combat Task Test (CTT) consisted of stairclimbing, a chopping simulation, and a victim rescue simulation.

Twenty male subjects (nonfirefighters and nonsmokers) volunteered to participate. The subjects were matched to the KSC firefighter population for age, height, weight, and percent body fat. Each subject was attired in standard firefighter turnout pants and coat, a helmet, and leather gloves for hand protection. An ISI Ranger 30-minute, self-contained breathing apparatus (pressure demand) weighing 10.4 kilograms (23 pounds) provided the external air supply. Prior to performing the CTT field tests, each subject participated in a variety of standard fitness tests, including a treadmill test (Bruce protocol), CYBEX isokinetic test, Wingate power test, flexibility test, and several other muscular strength and endurance tests.

The mean CTT performance time was 3.61 minutes (plus or minus 0.25), including the transition time between tasks. By 30 seconds into the CTT, the mean heart rate was over 90 percent of the maximum heart rate and hovered between 93 and 97 percent for the remainder of the test; the tasks required 93, 94, and 97 percent maximum heart rate, respectively, for the stairclimbing, chopping, and victim rescue components. A multiple linear regression model was fitted to each parameter: stair-



CTT Victim Rescue Simulation

climbing ($R^2=0.905$), chopping performance time ($R^2=0.582$), victim rescue time ($R^2=0.218$), and total performance time ($R^2=0.769$). Treadmill time was the predominant variable, being the major predictor in two of four cases. Other important predictors were leg power and right and left knee flexion peak torque for the stair-climbing model and arm load, flexibility, and situps for the chopping time model.

These results indicated that CTT performance required near maximal exertion, that certain standardized fitness tests accurately predicted performance on some CTT tasks, that the standardized test predictors were amenable to exercise training, and that the CTT should undergo further refinement prior to its acceptance as an occupational performance standard for KSC firefighters.

Contact:

I. D. Long, M.D., 867-3152, MD-MED

Participating Organization:

*The Bionetics Corporation
(B. Schonfeld)*

NASA Headquarters Sponsor:

*Office of Space Sciences and
Applications/Office of Space Flight*

Tuskegee University Project

Scientists at the Tuskegee University are investigating the physiology of sweet potato storage root formation. This team of scientists has been studying projection methods, processing techniques, and nutritional qualities of the hydroponically grown sweet potato since 1986.

Sweet potato fresh storage root yields of 505 grams for an 85-day growing period and 1,493 grams for 130 days on a per-plant basis were obtained with conventional plant growth chamber environments and a continuously flowing thin-film nutrient delivery system. The team also found it acceptable to harvest the ends of some stems (100 millimeters) every two weeks for making cooked greens. Such treatment did not affect storage root yield under these conditions.

Future investigations will determine the photosynthetic partitioning of light energy with respect to leaf age and position. Response of tuber formation and growth also will be evaluated while the sweet potato plant is supplied water and nutrients by a system that could have application in microgravity.

Sweet potato production is scheduled for evaluation in the KSC Biomass Production Chamber in 1991. Sweet potato production



Harvest of Hydroponically Grown Sweet Potatoes

and utilization databases will continue to enlarge and improve with this goal in mind.

Contact:

R. P. Prince, 853-5142, MD-RES-L

Participating Organization:

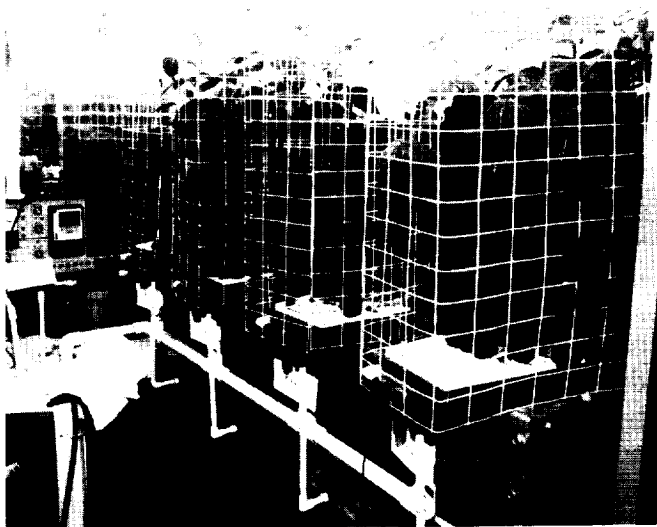
The Bionetics Corporation (Dr. R. Wheeler)

NASA Headquarters Sponsor:

Office of Equal Opportunity Program

Biomass Production Research

Support studies with soybean plants were carried out in standard growth chambers in preparation for tests in the Biomass Production Chamber (BPC). The studies focused on effects of carbon dioxide (CO₂) concentrations on growth and yield and effects of radiant spectral quality from different combinations of electric lamps. The CO₂ studies showed that the best yields could be obtained with concentrations near 1,000 parts per million (ppm)(normal air is 350 ppm). Raising CO₂ above 1,000 ppm tended to lower seed yields; however, the soybean plants grew well and yielded seed even at CO₂ levels as high as 5,000 ppm. A series of tests with high-pressure sodium (HPS) lamps showed that stem growth of soybeans tends to be



Soybean Plants Growing in Hydroponic Tray Culture for the CELSS Program

leggy under pure HPS lighting. By supplementing the HPS lighting with a small amount of blue light, however, the excessive stem growth could be suppressed and plants kept short. This blue-light effect appears to be independent of the photoperiod (day length) effects on stem length that were observed in studies during 1988.

Benchtop studies were conducted with sweet potatoes and peanuts using a nutrient film technique (NFT). The results showed that when peanut "pegs" reached the rooting zone of the trays, normal seeds and shells would develop. Thus, the peanut may prove to be a productive crop for the Controlled Ecological Life Support System (CELSS), using soilless culture techniques.

Contact:

J. C. Sager, Ph.D., 853-5142, MD-RES-L

Participating Organization:

The Bionetics Corporation (Dr. R. Wheeler)

NASA Headquarters Sponsor:

Office of Space Sciences and Applications

Orbiter Environmental Simulator

An Orbiter Environmental Simulator (OES) was developed to support flight research experiments at KSC. The OES is a personal-computer-based data acquisition system that controls a plant growth chamber so the chamber's environmental conditions mimic those observed onboard the Shuttle. The system was used to support a Chromosomes and Plant Cell Division in Space (CHROMEX) ground control experiment. Orbiter environmental conditions, such as carbon dioxide levels, relative humidity, and temperature, were obtained from the Space Transportation System 29 (STS-29) flight Calibrated Ancillary System (CAS) data received in Hangar L at Cape Canaveral Air Force Station. The data were then used by the OES to control the

growth chamber and mimic conditions recorded during STS-29.

Contact:

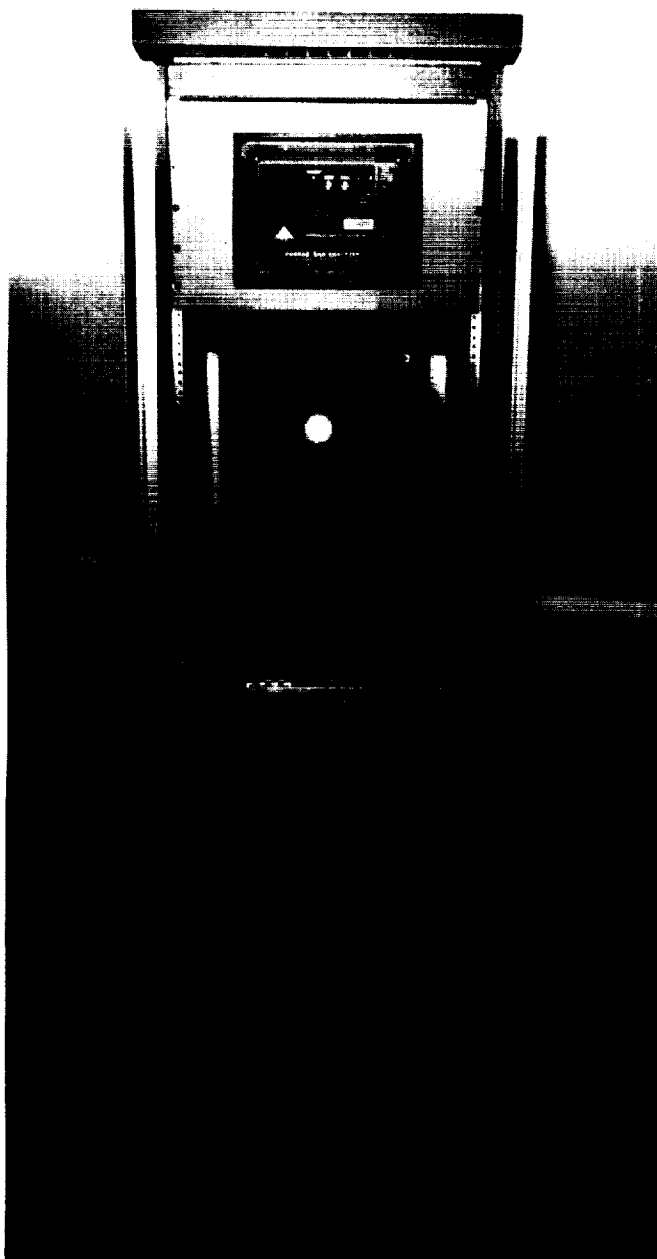
W. M. Knott, Ph.D., 853-5142, MD-RES-L

Participating Organization:

The Bionetics Corporation
(C. Hargrove)

NASA Headquarters Sponsor:

Office of Space Sciences and Applications



Computer Control System for the Orbiter Environmental Simulator

Biomass Processing Research

Development of biomass conversion processes for integration with the Controlled Ecological Life Support System (CELSS) Breadboard Project continued. With the goal of maximal conversion of Biomass Production Chamber (BPC) crop residues from useless, inedible polymers (cellulose and hemicelluloses) into edible products, processes have been selected that can be scaled up within a short time to operate on BPC biomass harvests. The objectives have been to identify and complete the applied development and research needed to design, procure and/or fabricate, install, test, and operate hardware and control systems for these selected processes.

Studies of crop residue pretreatment by extraction of water-soluble organic and inorganic compounds have continued with comparisons of different wheat residue drying and extraction temperatures and of candidate CELSS crop residues (soybean, white potato, sweet potato, and wheat). Production of edible fungal biomass by vegetative mycelial cultures of oyster mushrooms, *Pleurotus ostreatus*, grown on soluble organics extracted from wheat residue, was examined; the determination of the yield coefficient and the maximum specific growth rate has been completed.

Studies continued on the optimization of the production of a cellulase enzyme complex by *Trichoderma reesei* with supplemental addition of beta-glucosidase from *Aspergillus phoenicis*. Culture maintenance, growth, and enzyme production by both organisms were converted from highly purified substrates (that is, alpha cellulose and starch) to more realistic substrates derived from authentic CELSS-BPC residues. Monoculture production of cellulase by *Trichoderma reesei* was studied with emphasis on spore inoculum preparation effects on mycelium production, mycelium inoculum density effects on cellulase production, and residue treatment (with or without strong-base dissolution of lignin



Yield of White and New Potatoes from Hydroponic Tray Culture for the CELSS Program

and hemicelluloses) effects on enzyme production. Monoculture production was also studied with regard to residue strong-base treatments. Cocultivation studies of *Trichoderma reesei* and *Aspergillus phoenicis* to produce the desired mix of cellulose hydrolysis were also continued.

Effects of the following on the enzymatic conversion of BPC wheat residue cellulose to glucose have been studied: residue concentration, enzyme loading rate, hydrolysis physicochemical conditions (especially temperature and pH), and ratio of supplemental *Aspergillus phoenicis* beta-glucosidase to *Trichoderma reesei* cellulase complex. In addition, the evaluation of two commercial sources of cellulase complex (Genencor and Finnsugar) has been initiated in comparison with *Trichoderma reesei* CELSS-produced cellulase. Project management plans have been initiated for breadboard scaleup of processes. The plans include the following reactors:

1. A leachate reactor for aqueous extraction of crop residues.
2. A cellulose conversion saccharification reactor for enzymatic hydrolysis

of particulate residues from the leachate reactor.

3. A *Pleurotus* reactor for production of edible biomass from soluble leachate organics from the leachate reactor and from soluble monosaccharides produced by cellulose hydrolysis in the cellulose conversion saccharification.
4. A mixed microbial community reactor for production of biomass that can be readily incorporated into a *Tilapia aurea* diet and that grows on unused soluble organics coming from the cellulose conversion saccharification reactor and unhydrolyzed particulate organics and spent cellulase enzymes coming from the *Pleurotus* reactor.

Contact:

*D. W. Chamberland, 853-5142,
MD-RES-L*

Participating Organization:

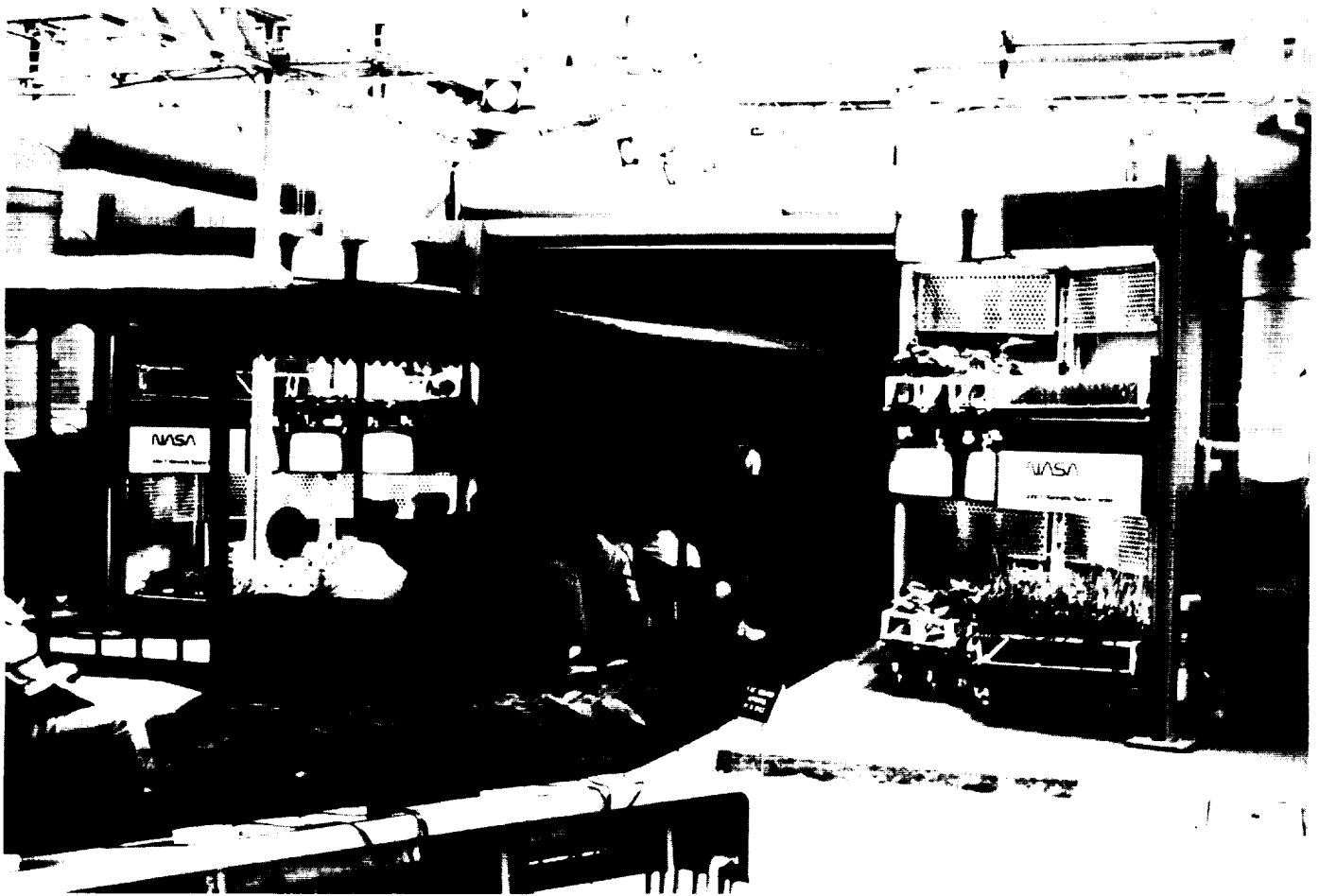
*The Bionetics Corporation
(Dr. R. Strayer)*

NASA Headquarters Sponsor:

Office of Space Sciences and Applications

EPCOT Project

The six hydroponic plant growth display racks at Disney's EPCOT Center have operated continuously since 1987. Visitors to The Land pavilion are introduced to the plant growth methods currently being studied at NASA/KSC as part of the Controlled Ecological Life Support System (CELSS) Breadboard Project. The system was enhanced during 1989 with a state-of-the-art computer control system that controls pH, flow, and temperature of the nutrient solution. This control system was the first prototype of a user-friendly, menu-driven system that will be incorporated into the CELSS Breadboard Project as soon as it has been verified as opera-



Hydroponic Plant Growth System at The Land Pavillion at EPCOT

tionally ready. The interaction with EPCOT has allowed NASA to evaluate this control system under operational conditions using researchers who are unfamiliar with the system to test it, identify problems, and generate growth data on selected crops. Research on plant pathogens in hydroponic systems was initiated this year by researchers at EPCOT. Interaction between these researchers and the NASA staff will transfer some of this expertise to the CELSS Breadboard Project.

Contact:

R. P. Prince, 853-5142, MD-RES-L

Participating Organization:

*The Bionetics Corporation
(C. Hargrove)*

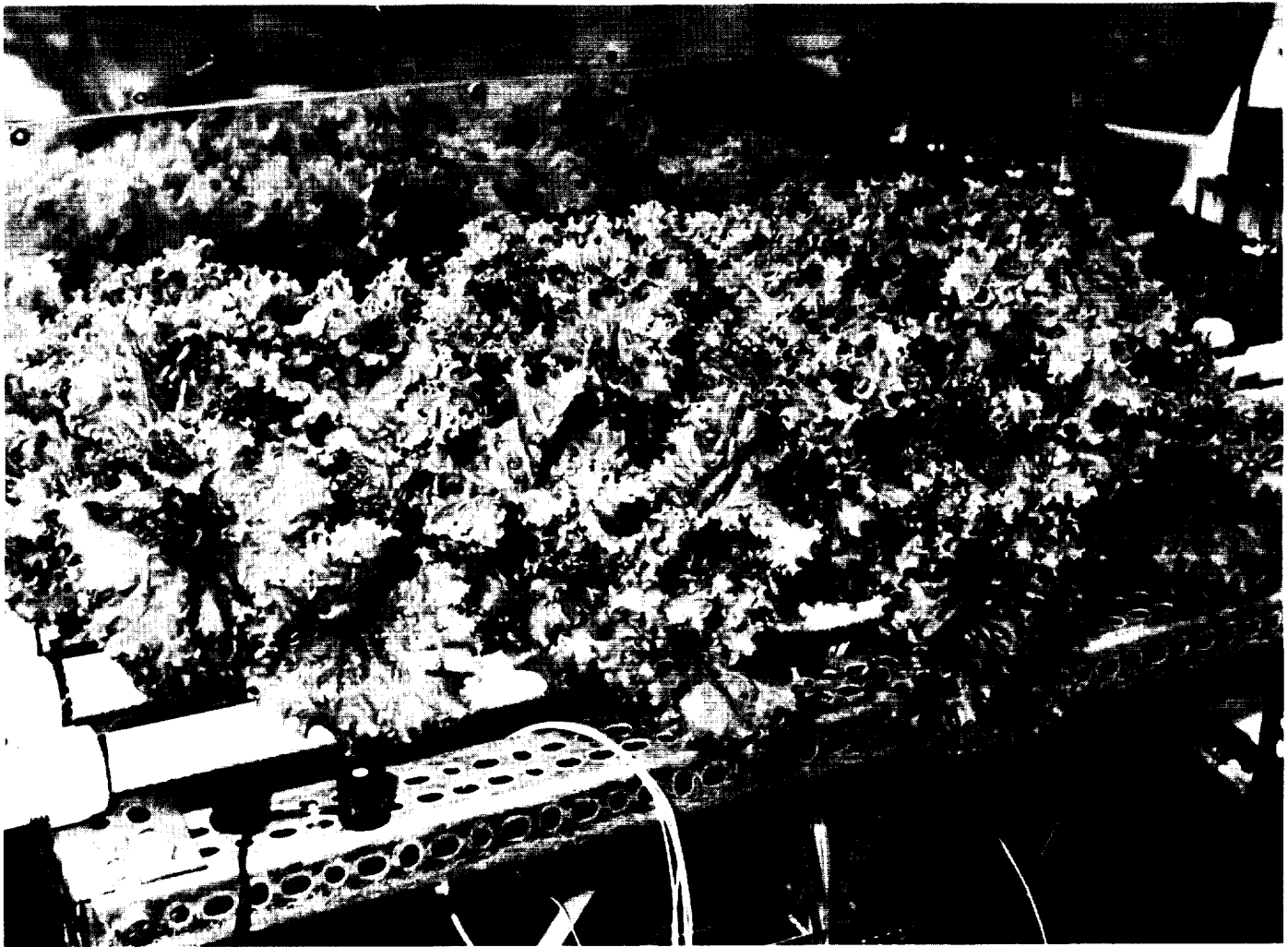
NASA Headquarters Sponsor:

Office of Commercial Programs

Tubular Membrane Plant Growth Unit

Verification and development of the tubular membrane system (TMS) for growing plants in microgravity has continued with the testing of a computer-controlled system and the substitution of microporous tubular ceramic materials to replace the porous membrane tubes used previously. Preliminary tests indicate that the ceramic tube is an adequate substitute for the membrane tube. Wheat and lettuce have been grown in units containing the ceramic tubes with results similar to that obtained in the membrane tube units. The ceramic tubes have a distinct advantage in that they can be cleaned and reused.

A system with a closed bladder for the nutrient solution reservoir has been con-



Lettuce Growing on a Prototype Nutrient Delivery System

structed to test the effects of atmospherically closing the nutrient loop. Preliminary tests and refinements in the design are currently underway. Work to prototype a flight plant growth unit (PGU) nutrient delivery system has continued with the construction of a pump module and a plant growth chamber containing a miniature TMS. These have been mounted within a mockup of the PGU and germination and growth tests with wheat and soybeans are currently being conducted.

Contact:

W. M. Knott, 853-5142, MD-RES-L

Participating Organization:

The Bionetics Corporation (T. Dreschel)

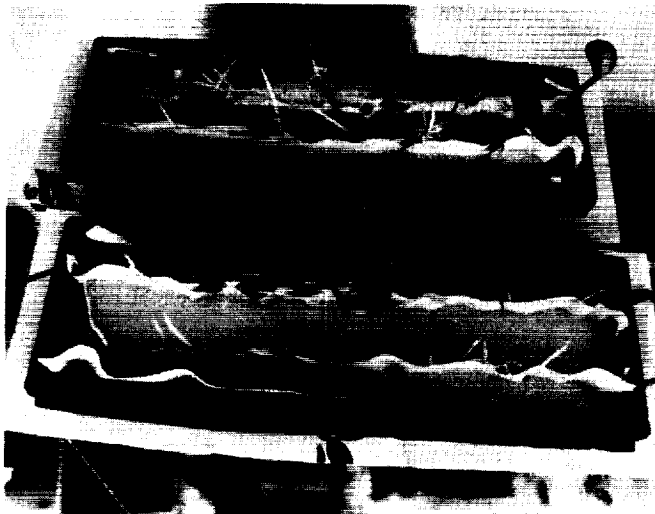
NASA Headquarters Sponsor:

Office of Space Sciences and Applications

Space Biology Plant Research

The Space Biology Plant Research Program at KSC was begun in July 1989. The initial and primary focus is to equip and run a complete plant physiology/biochemistry laboratory. This activity will continue into the next year. The overall goal is to perform original research on the effects of microgravity on plant metabolism. Toward this end, the development of the technology for mounting the Plant Growth Facility II (a mockup of the middeck locker system for growing plants on the Shuttle) on a rotating clinostat for simulation of microgravity conditions is currently underway. This will provide a heretofore unavailable capability for performing essential ground controls for flight experiments, as

ORIGINAL PAGE
BLACK AND WHITE PHOTOGRAPH



Soybean Seedlings With Aerial Roots Due to Clinorotation

well as preliminary investigations prior to flight.

Contact:

W. M. Knott, Ph.D., 853-5142, MD-RES-L

Participating Organization:

The Bionetics Corporation (Dr. C. Brown)

NASA Headquarters Sponsor:

Office of Space Sciences and Applications

A New Technique for the Demonstration of Fiber-Type-Specific Capillarization in Skeletal Muscle

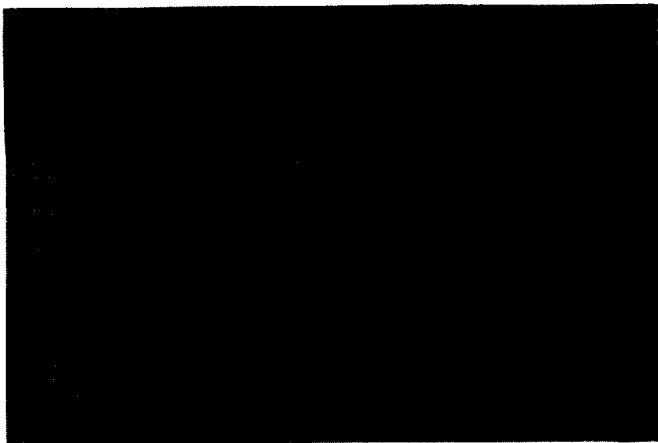
A new technique that allows for the identification of skeletal muscle fiber types and capillaries on the same muscle cross section has been developed at KSC. The histochemical technique is currently being used to evaluate skeletal muscle biopsies from adult male subjects. Skeletal muscle fiber-type composition and fiber-type-specific area and capillarization can be determined.

Skeletal muscle fibers do not have identical properties. They differ in structural, functional, and biochemical characteristics. In addition, histochemical analyses of

skeletal muscle allows classification of fibers into different types that vary according to these characteristics. For example, differences in the pH stability/lability of myofibrillar 5' adenosine triphosphatase (ATPase) allows at least four fiber types to be identified in skeletal muscles (type I, IIA, IIB, and IIC). In general, type I fibers have slow contractile speeds and rely on oxidative metabolism, while type II fibers are fast and rely on glycolytic metabolism. Moreover, alterations in the functional demands placed on skeletal muscle by models of microgravity (for example, bedrest) may selectively influence a given fiber type.

Skeletal muscle of lower mammals is mainly composed of a given fiber type. It has been relatively simple, therefore, to demonstrate fiber-type-specific differences in capillarization. Slow fibers have the greatest number of capillaries. Skeletal muscle of humans has a more heterogeneous fiber-type composition; because of this, most studies of human skeletal muscle have not assessed fiber-type-specific responses. For example, the few reports of fiber-type-specific capillarization have used two different muscle sections: one reacted for myofibrillar ATPase (ATPase) to identify fiber types and the other reacted with periodic acid Schiff (PAS) reagent for the visualization of capillaries. This method is costly and time consuming because the same fiber profile on each of the two separate sections must be matched. This requires elaborate imaging systems or constructing photographic montages.

A histochemical technique, therefore, was developed that allows the simultaneous demonstration of fiber types and capillaries from the same muscle section [see the figure "Transverse Section of a Muscle Biopsy" showing capillary profiles (arrows) and fiber types (I, IIA, and IIB), magnified 550 times]. Simply, a given transverse section of skeletal muscle is serially processed using modifications of standard myofibrillar ATPase and PAS techniques. A preliminary study has compared the



Transverse Section of a Muscle Biopsy

data obtained using the newly developed combined technique (ATPase/PAS) with that obtained using the individual methods (ATPase or PAS). The results indicate that the combined technique does not alter the tissue as evaluated from measures of fiber size, capillary counts, and the identification of type I, IIA, and IIB fibers.

This simple procedure provides the opportunity to examine the histochemical, histological, and morphometric characteristics of a single transverse section of skeletal muscle with a substantial savings in time, energy, and cost.

Contact:

P. Buchanan, M.D., 867-2585, MD

Participating Organization:

*The Bionetics Corporation
(Dr. G. Dudley and Dr. B. Hather)*

NASA Headquarters Sponsor:

Office of Space Sciences and Applications

Environmental Monitoring

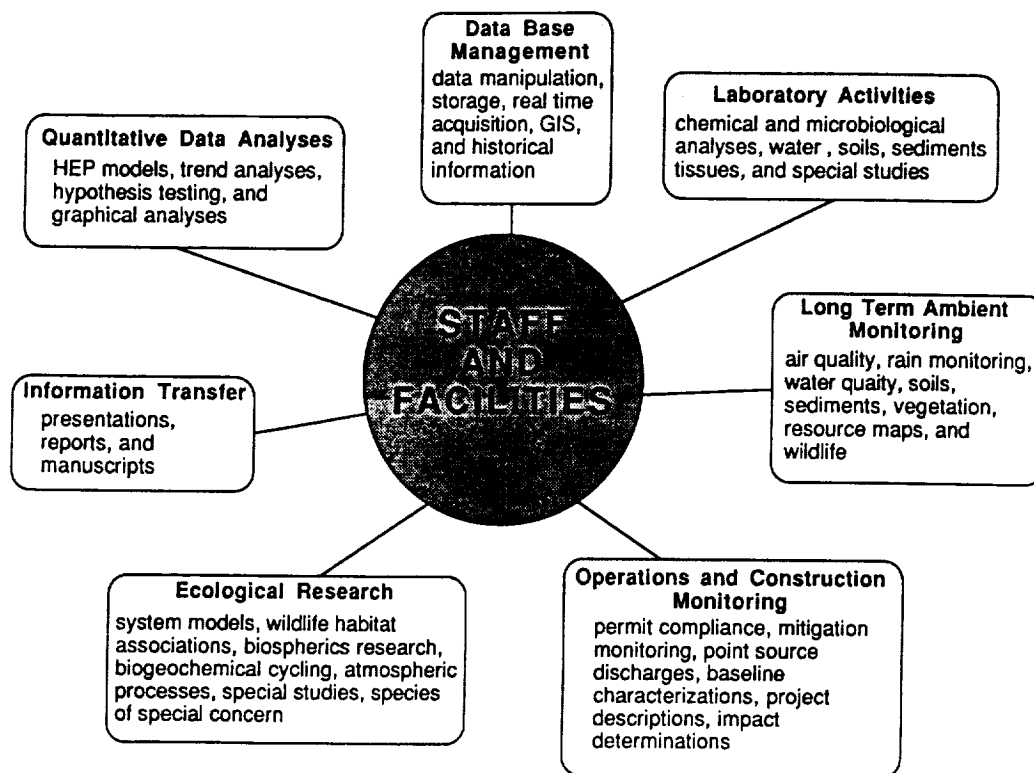
Environmental monitoring at KSC consists of three broad areas of activity, including operations and construction monitoring, long-term ambient monitoring, and ecological research. Operations and construction monitoring focuses on potential environmental impacts produced by development of new facilities and the effects of

existing operations such as launching of the Space Shuttle. Long-term ambient monitoring is utilized to baseline existing conditions and to monitor the range of natural variability that exists in the environment; thus, helping managers separate man-made impacts from natural changes. Long-term databases that support ambient monitoring include air quality, rainfall volume and chemistry, water and sediment chemistry, soil chemistry, vegetation communities, and select threatened and endangered species. Ecological research activities are utilized to develop an understanding of ecological processes and controlling factors that operate in the unique environment at KSC. Information derived through these three areas of the program is incorporated into an Environmental Mapping Assessment and Planning System (EMAPS) for analyses and interpretation using computerized databases and the geographic information system. The ultimate objective is to develop models for the purpose of predicting impacts before they occur and recommend mitigation strategies for those impacts deemed unavoidable.

A major activity during 1989 involved continuation of launch operations monitoring. Field team support was provided for four Shuttle launches (STS-27, STS-28, STS-29, and STS-30) from Pad 39B and one Titan IV launch from Complex 41. For each launch, field surveys were con-



Trapping Scrub Jays at KSC



General Overview of the Major Elements of the Ecological Program

ducted to assess impacts in the surrounding area and to validate the output of the Rocket Exhaust Effluent Diffusion Model. During the days following launch, field surveys were completed and chemical samples were sent to the laboratory for analyses. An environmental effects summary report was developed and distributed approximately 45 days following launch, documenting all findings. To date, only a small area of scrub habitat, located directly in line with the flame trench, has been significantly altered by the launches from Pad 39B. The buffering capacity of the impounded waters impacted by the acidic exhaust is only temporarily depleted at the current launch rate. These findings are consistent with observations made during previous launches from Pad 39A.

Resampling of environmental conditions around Pad 39A was initiated to prepare the database for resumption of launch operations monitoring during the next year. A comprehensive launch-cloud trajectory database was developed on EMAPS that includes nearfield and farfield deposition

for all Shuttle launches. The field activities of a graduate student of the University of Central Florida to evaluate wading bird habitat use in impoundments near Pad 39B were completed. The results of the evaluation are expected to be available early next year. These data will be incorporated into the center-wide waterbird habitat association database for use in future environmental assessment projects.

Long-term ambient air quality monitoring of the Environmental Protection Agency priority pollutants (sulfur dioxide, oxides of nitrogen, carbon monoxide, ozone, and particulates) and recording of local meteorological conditions continued at the permanent air monitoring station (PAMS). The historic trend of increasing ozone levels continued during 1989; the national standard was exceeded twice. Monitoring of atmospheric deposition at the KSC National Atmospheric Deposition Program Site achieved a 99-percent efficiency. Rain fall pH at KSC generally ranged between 4.5 and 4.9 units. Water quality and sediment chemistry monitoring continued,

and support to the Kennedy Atmospheric Boundary Layer Experiment (KABLE) was provided through the collection of hourly water temperature data for the Indian River, Banana River, and Mosquito Lagoon. Resampling of permanent vegetation plots located across KSC in uplands, wetlands, and seagrass beds continued, and a report detailing the climatology and vegetation community composition was initiated. An enhanced climatology database was developed that contains historic information dating to the 1800's. In the EMAPS and remote sensing laboratory, numerous new databases were incorporated into the monitoring program. Examples include watershed boundaries, fire management units, groundwater recharge areas, impoundment boundaries, threatened and endangered plant locations, eagle nest locations, soil types, and U.S. Geologic Survey topographic maps. Monitoring of manatee abundance in KSC waters with aerial surveys revealed that approximately one-fourth of the entire state population aggregates in the KSC security zone during spring. Development of the long-term sea turtle nesting database continued in conjunction with the U.S. Fish and Wildlife Service and the National Park Service. The fourth year of a study evaluating the role of beach nest temperatures on the sex ratio of sea turtle hatchlings continued in conjunction with the U.S. Fish and Wildlife Service's Endangered Species Office. Beach temperatures in the nesting zone are being recorded on an hourly basis throughout the nesting season for the purpose of developing a multi-year database for a major sea turtle nesting area on the east coast of Florida.

Defining functional relationships between wildlife and scrub habitat characteristics continued to dominate activities of the terrestrial wildlife biologists. Radio transmitters were attached to more than 20 gopher tortoises and three indigo snakes for the purpose of developing information on territory size, home range, and habitat preferences for these protected species. The assessment of scrub jay population

size at KSC was published as a journal article, and the study of nesting success and development of habitat maps using EMAPS databases proceeded. The scrub jay research now involves color banding birds and monitoring reproductive success in two major study sites covering a wide range of habitat quality. In addition, the National Park Service requested support for a biological assessment of construction impacts on scrub jays under the Endangered Species Act, allowing KSC Biomedical Office researchers to expand their efforts to a third site for conducting the necessary field investigations. This information will be incorporated into the database, expanding its utility. The second year of the monthly aerial surveys for waterbird distributions in various habitats on KSC was completed. A major woodstork rookery has become established approximately one-half mile south of Pad 39A; and roseate spoonbills continue to successfully reproduce on the center, extending the northern range of the species. The graduate student project evaluating stormwater quality and management options for the KSC industrial area was completed, and a report and model were developed and delivered.

As part of the NASA Biospherics Program, researchers from KSC and Langley Research Center joined forces with members of the local U.S. Fish and Wildlife Service to conduct a second controlled burn to study the effects of fire in wetland ecosystems on the global atmosphere. Preliminary results from this study will be presented at the upcoming Chapman Conference on Global Biomass Burning in Williamsburg, Virginia, in 1990.

Contact:

*A. M. Koller, Jr., D.B.A., 867-3165,
MD-PLN*

Participating Organization:

The Bionetics Corporation (C. Hall)

NASA Headquarters Sponsor:

Office of Space Sciences and Applications / Office of Space Flight

Prototype Devices for Plant Growth

Progress is being made in several areas to develop items essential for computer control of the crop growing process. During the past year through the Small Business Innovative Research Program, three companies have conducted research important to developing this computer control. One company applied fiber optic technology to specific ion detectors. Porous glass and polymer units were fabricated and tested for pH, relative humidity, and ammonia. The plans are to expand the work into commercial units. Another firm developed new nutrient delivery techniques using porous (0.5 micron) stainless steel. Different configurations and control techniques for these systems will be required for the various gravities of the universe. A third company conducted a search for mathematical techniques useful in analyzing the reflectance spectra (400 to 2,600 nanometers) of individual leaves of specific food

plants. This information will be used to permit the control computer to adjust nutrient solution to the plant. It may also assist in determining toxicity of certain minerals.

These prototype developments eventually should enable scientists to study plant response to microgravity and to become more confident about the design and operation of chambers on the Earth, the Moon, and Mars and in microgravity. When the technology has been developed, crop production should become simpler and many tasks will be taken over by robots. In addition, plant yields should increase per unit of energy, area, volume, and mass.

Contact:

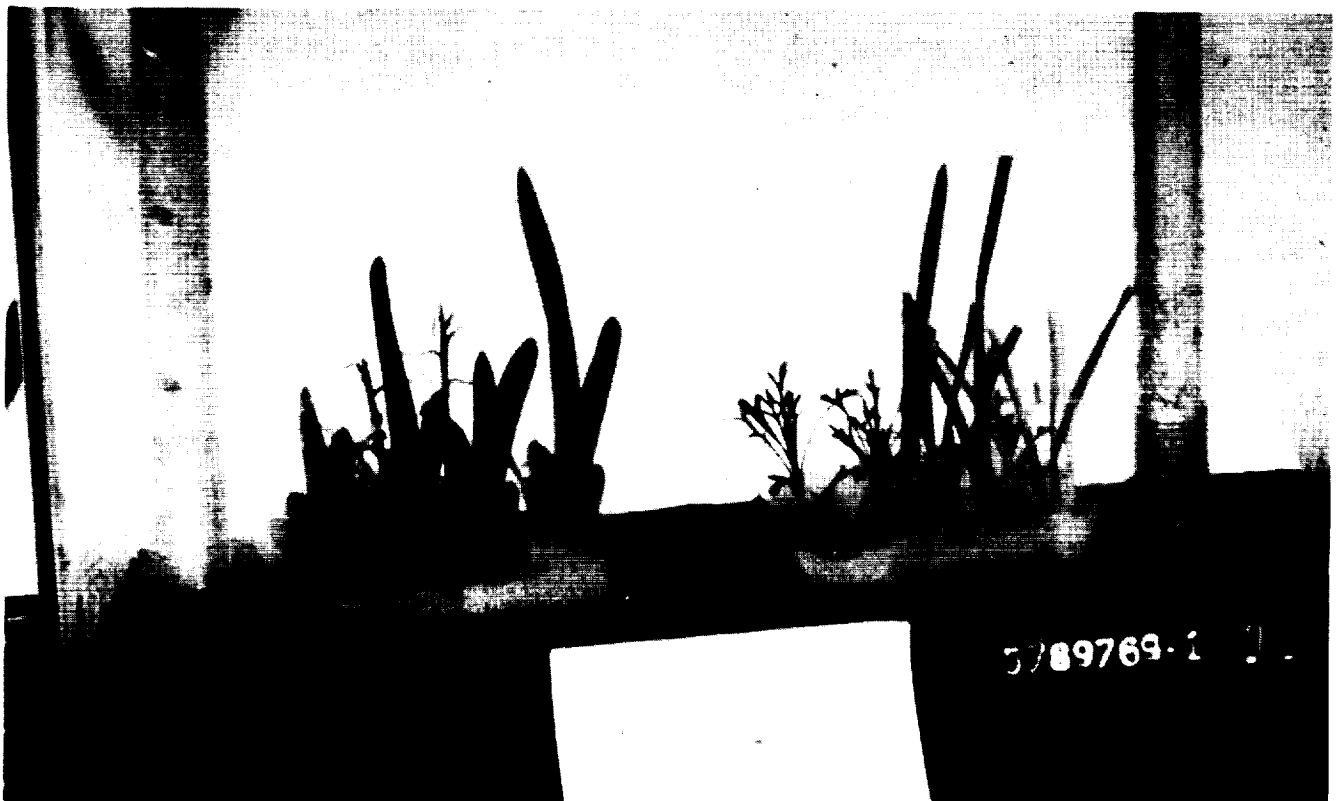
R. P. Prince, 853-5142, MD-RES-L

Participating Organization:

The Bionetics Corporation (T. Dreschel, C. Hargrove, and Dr. R. Wheeler)

NASA Headquarters Sponsor:

Office of Space Sciences and Applications



Example of a Plant Growth Prototype

OPPOSITE PAGE
BLACK AND WHITE PHOTOGRAPH

Human Physiology Research Projects: Blood Pressure Control

The development of low blood pressure during standing (a condition known as orthostatic hypotension) has been documented in both U.S. astronauts and Soviet cosmonauts following spaceflight. The development of effective countermeasures, particularly for long-duration missions, has been difficult since the physiological mechanisms underlying postflight orthostatic hypotension are unclear. Both U.S. and Soviet astronauts drink fluids prior to reentry since dehydration during spaceflight contributes to orthostatic hypotension; however, with flights of longer duration, drinking fluids becomes less effective. New data from actual spaceflight and groundbase studies suggest that the impairment of certain cardiovascular reflexes may contribute to orthostatic hypotension as the exposure to microgravity increases.

One reflex that helps control blood pressure is the carotid-cardiac baroreflex. During standing, this reflex acts to increase heart rate so that blood pressure will not drop; its function is significantly impaired following exposure to simulated microgravity of long duration (30 days). To determine if replacing body fluids (specifically blood volume) would affect baroreflex function, physiologists of the Biomedical Operations and Research Office at KSC measured the response of the carotid-cardiac baroreflex after body fluids were decreased (by diuretics) and increased (by drinking). There was no effect of volume loading or depletion on the baroreflex response. Although acute fluid replace

ment prior to reentry may provide some protection following spaceflight of short duration (days), test results suggest that the fluid countermeasure may not reverse impaired baroreflexes and development of orthostatic hypotension upon return to earth after long duration flights.

Since a protective effect against orthostatic instability following short-term exposure to microgravity has been demonstrated using exercise, KSC physiologists considered the possibility of an acute, intense bout of exercise as a countermeasure for an impaired baroreflex. Acute maximal exercise increased the response of the carotid-cardiac baroreflex for up to 24 hours in a fashion reverse to that reported following exposure to microgravity. From these studies, it seems reasonable to expect that maximal exercise might be effective in reversing the impaired baroreflex that results from microgravity exposure and is associated with postflight orthostatic hypotension.

The results from these studies at KSC are encouraging and provide a physiological basis for future experiments designed to test the effectiveness of acute intense exercise as a countermeasure against postflight orthostatic hypotension following space missions of long duration.

Contact:

*V. A. Convertino, Ph.D.,
867-4237, MD-RES-P*

Participating Organization:

*The Bionetics Corporation
(C. Thompson and D. Tatro)*

NASA Headquarters Sponsor:

Office of Space Sciences and Applications

Hazardous Emissions and Contamination Monitoring

The John F. Kennedy Space Center (KSC) stores and pumps huge quantities of cryogenics, as well as lesser amounts of exotic fluids. The extreme toxicity and volatility of these fluids mandates a comprehensive safety program. Four development laboratories are responsible for implementing the specialized instrumentation hardware and systems that satisfy stringent safety requirements.

The Hazardous Gas Detection Laboratory

The Hazardous Gas Detection Laboratory has the continuing task of implementing systems that are capable of measuring in complex mixtures, gaseous components both qualitatively (specifically, hydrogen, helium, nitrogen, oxygen, and argon) and quantitatively (parts-per-billion range). A typical hazardous gas detection system comprises a mass spectrometer, a sample and calibration gas delivery subsystem, and a data acquisition and control subsystem. The laboratory projects now receiving the most attention are: applying artificial intelligence/expert systems to aid in real-time diagnostics and troubleshooting, operations monitoring and data interpretation, developing a military specification, and flight-qualified miniature detection systems for advanced launch systems.

The Optical Instrumentation Laboratory

The Optical Instrumentation Laboratory develops and tests imaging systems for viewing phenomena that are undetectable to the unaided eye or by normal viewing techniques; examples include hydrogen fires and other thermal emitters and hydrogen and other gas clouds. A recent laboratory achievement is the design and demonstration of a multispectral television camera that is capable of unambiguously imaging and color coding fuel fires in the infrared and ultraviolet spectral emission ranges.

The laboratory is equipped with an optical spectrometer for measuring the emission spectra of an extensive variety of radiating sources.

The Toxic Vapor Detection Laboratory

The Toxic Vapor Detection Laboratory is developing a new series of toxic vapor detectors because the commercial family does not meet the current Government standards for measuring trace amounts of hypergolic fuels and concentrated ammonia vapors in an ambient background. The toxic vapor detection laboratory was set up to bridge this gap between commercial model performance and NASA/KSC requirements. It accomplishes this by sponsoring independent research, evaluating off-the-shelf instrumentation, and designing and fabricating prototypes. All models (commercial or prototype) are rigidly tested inhouse under tightly controlled conditions to determine qualitative and quantitative performance.

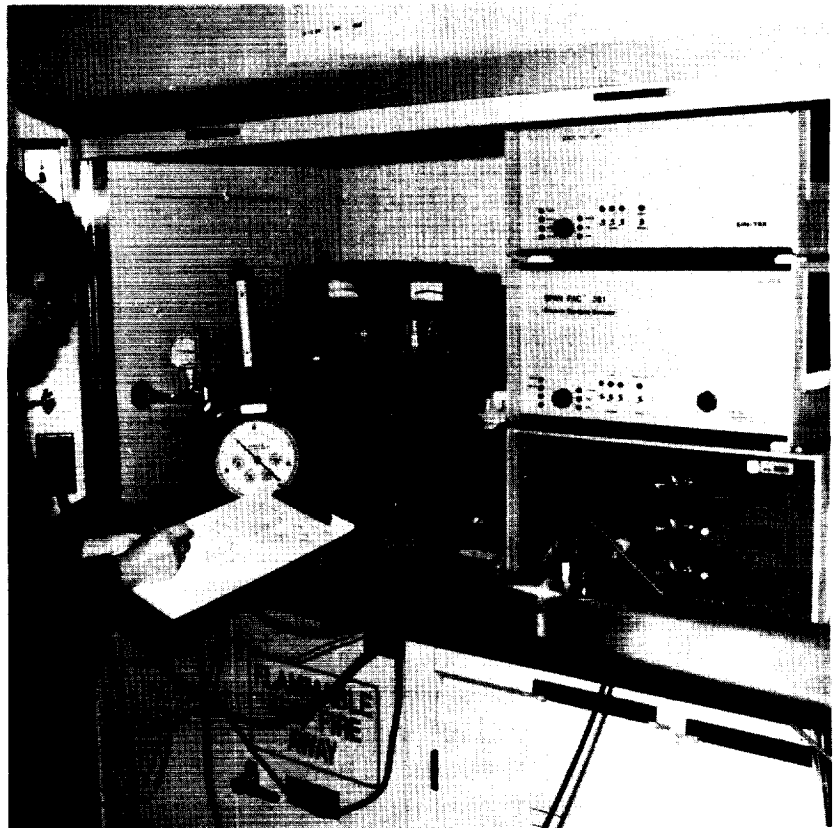
The Contamination Monitoring Laboratory

The Contamination Monitoring Laboratory was established to perform contamination monitoring research and development; develop contamination measuring systems; evaluate commercially available particle counters, hydrocarbon and nonvolatile residue monitors, and other instrumentation; and advance the technology in the areas of real-time nonvolatile residue (NVR), real-time particle fallout monitoring, and contamination monitor calibration methodology. The laboratory is equipped with particle counter systems, personal-computer-based data acquisition and control systems, a pulse height analyzer, a research-grade FTIR spectrophotometer, nondispersive infrared analyzers, and a normal complement of test and measurement instrumentation.

ORIGINAL PAGE
BLACK AND WHITE PHOTOGRAPH



Hazardous Gas Detection Laboratory



Toxic Vapor Detection Laboratory

Real-Time Hydrazine Monitoring Using Surface-Enhanced Raman Spectroscopy (SERS)

Objective

The goal of the Phase I program was to establish the feasibility of real-time monitoring of hydrazine and monomethylhydrazine by Surface-Enhanced Raman Spectroscopy (SERS) and to demonstrate the feasibility of developing a practical SERS-based instrument for monitoring hypergolic vapors during ground-based operations of the Space Shuttle.

Background

In Raman spectroscopy, which measures the vibrational spectra of molecules, approximately 0.001 percent of the intensity of visible light impinging on a molecule is scattered, mostly elastically (that is, no vibrational information at the excitation frequency). However, about 1 percent of the scattered light is at frequencies corresponding to combinations of the exciting light and the molecular vibrational frequencies (the Raman effect). Thus, spectral resolution of the visible scattered light yields a "fingerprint" of the molecule consisting of relatively sharp lines which, like infrared spectra, provide information about bonding that can be used for the qualitative identification of the molecule. The main disadvantage of Raman spectroscopy is its insensitivity. Experimentally, it is difficult to measure spectra at concentrations below 1 percent (10,000 parts per million).

SERS, however, results in a large enhancement of the Raman signal from molecules adsorbed onto roughened surfaces of highly reflective metals. The SERS enhancement is approximately 10^6 compared to the signal of adsorbates on nonactive or smooth surfaces. Detection of less than 0.1 percent monolayer coverage appears feasible from the measurements of SERS enhancements. If a SERS-active

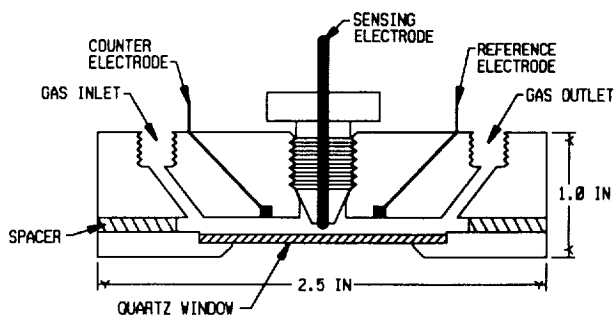
substrate is exposed to an environment containing a mixture of compounds, only those that preferentially adsorb onto the substrate surface will be detected. SERS has been observed on many metal and metal oxide substrates, the most active appear to be silver, gold, copper, silver oxide, and gold oxide.

Approach

The initial work in the Phase I program was devoted to the fabrication and identification of substrates that both adsorb hydrazine and are SERS active. The study included a range of metal, metal oxide, and derivatized substrates. A variety of promising substrates were identified. The substrates were fabricated by both electrochemical and vapor deposition techniques. A detailed characterization of the SERS spectra of hydrazine and monomethylhydrazine was carried out on the SERS-active substrates. Hydrazine concentrations were determined by monitoring the area of the SERS peak due to the N-N stretch of the adsorbed molecule. Hydrazine vapor concentrations were quantitatively measured at concentrations between 60 parts per billion to greater than 35 parts per million. The response time of laboratory sensors was 40 seconds after a step change in the hydrazine concentration. The reversibility of the hydrazine adsorption was found to be dependent on the identity and temperature of the substrate. A lifetime of two weeks was demonstrated with a laboratory sensor.

Results

A schematic of the SERS cell used in all the Phase I experiments is illustrated in the figure "SERS Cell Used in Phase I Research." The cell body was constructed of Teflon to minimize adsorption or reaction of the hydrazine vapors. The optical window consists of a 2.54-centimeter-diameter quartz plate installed in the bottom of the cell body. The cell was completely sealed with respect to the outside environment. The cell design allowed the rapid



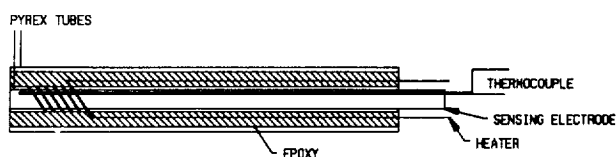
SERS Cell Used in Phase I Research

and reproducible positioning of the substrates.

The substrates used for the Phase I experiments were fabricated from 1-millimeter-diameter silver wire sealed into a glass capillary along with a thermocouple. A high-resistance Ni-Cr wire was wound around the capillary and the entire assembly sealed into a 4-millimeter Pyrex tube with high-temperature epoxy. The end of the substrate assembly was cut and polished to a mirror-like surface with 0.3- and 0.05-micrometer alumina. A schematic of the substrate assembly is shown in the figure "Substrate Assembly Used in Phase I Research."

Silver substrates were electrochemically roughened by potentiostatic cycling between -600 and +200 millivolts in 0.1-molar potassium chloride. The potentiostatic cycling produces a roughened metal surface with the morphology required for SERS activity. The roughened silver surface was converted to the oxide by potentiostatic oxidation in 1.0-molar potassium hydroxide.

Oxide substrates were also prepared by electrochemical deposition of the respective metals or metal hydroxides onto roughened



Substrate Assembly Used in Phase I Research

silver and gold substrates or by sputtering the metal oxides into electrochemically roughened gold and silver or fumed silica substrates.

Spectroscopic and Electrochemical Instrumentation

The Raman spectroscopic instrumentation used during the Phase I program consisted of a triple spectrograph, a tunable excitation filter, a polarization scrambler, and a Raman sample compartment from Spex Industries and an EG&G Optical Multichannel Analyzer with an intensified diode array detector. The excitation source was either a coherent argon ion or a coherent continuous-wave dye laser. The dye laser was operated in the region of 500 to 1,000 nanometers while the argon laser used various laser lines between 450 and 525 nanometers. The SERS spectra data were exported as American Standard Code for Information Interchange (ASCII) files to an 80286-based computer for processing.

All electrochemical procedures for preparing substrate were carried out with a Princeton Applied Research Model 273 potentiostat interfaced to a laboratory computer.

Conclusion

The results of the Phase I program demonstrated the feasibility of developing a SERS-based detector for hypergolic fuel vapors. The major advantages of a SERS-based system include a real-time response, quantitative analysis capabilities, simultaneous multicomponent detection, low detection limits, and intrinsic safety. A SERS-based system for the detection and monitoring of hypergolic fuel vapors would have immediate application for the ground-based operations of the Space Shuttle.

It should be noted, however, that the magnitude of the sensor response decreased during repeated adsorption/desorption of hydrazine. The longest sensor lifetime reported was two weeks. Work in Phase

It will include investigating methods for increasing sensor lifetime.

Contacts:

*P. A. Mogan, R. C. Young, and J. C. Travis;
867-4438; DL-ESS-24*

Participating Organization:

*EIC Laboratories, Inc. (M. W. Rupich and
M. M. Carrabba)*

NASA Headquarters Sponsor:

Office of Space Flight

Hydrogen Sulfide and Ammonia Effects on the ESI 7000 Series of Hypergolic Fuel Vapor Sensors

Objective

To identify a low-toxicity surrogate gas for monomethylhydrazine (MMH) to be used for validation of the Hypergolic Vapor Detection System (HVDS), which is located at Launch Complex 39. The purpose of this project was to examine the suitability of two known interferent gases, ammonia (NH₃) and hydrogen sulfide (H₂S), for this use.

Background

The current HVDS system uses ESI Model 7000 series electrolyzers with dual electrochemical cells. The fuel cells that respond to hypergolic vapors also respond to NH₃ and H₂S. NH₃ is used as a coolant within the Shuttle, and H₂S is used to validate the MMH sample lines to the HVDS cabinets. No documentation is available describing the effect of these gases on the MMH electrochemical cell.

Approach

To determine the ideal gas for use in a surrogate gas delivery system and to determine the signature response of the cells to each gas in the ESI 7000 series, a dilution vessel setup was devised for use in the

NASA Toxic Vapor Detection Laboratory at Complex 34. Both NH₃ and H₂S standards were available for ESI 7660, along with various concentrations of MMH from a Kin-Tek Span Pack permeation apparatus in the carrier air preconditioned to 25 degrees Celsius and 40-percent relative humidity.

Each test began with an exposure of MMH to establish a baseline response. The following tests were performed with the test gases, H₂S and NH₃.

The first test alternated 10-minute exposures of MMH, zero air, and then a test gas into the electrolyzer. This cycle was repeated five times. A strip chart recorded the response from the electrolyzer's electrochemical cells.

The second test exposed the electrochemical cells to an initial 10-minute exposure of the surrogate gas, and then six successive cycles of a 10-minute zero air exposure followed by a 10-minute MMH span. The series was repeated three times. The objective was to examine the cell recovery following exposure to the surrogate gas to determine the effect on sensitivity, response, and recovery times.

The third test examined the response of the cells to the surrogate gas after a 1-hour exposure to zero air. The cycle included 10-minute exposures of MMH, zero air, and surrogate gas followed by a 1-hour exposure to zero air. This cycle was repeated five times.

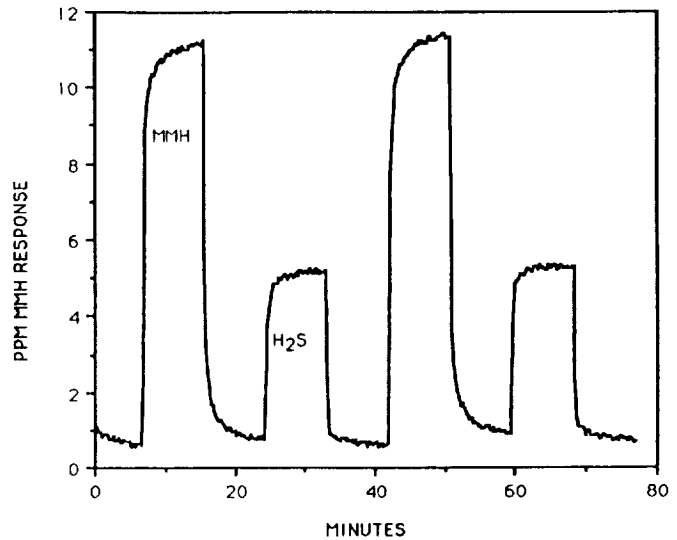
Results

The introduction of NH₃ resulted in an immediate sharp peak followed by a rapid decline within the first 30 seconds of exposure. The response to NH₃ continued its decline gradually for the remaining 9.5 minutes. The response to NH₃ was considerably different from the response to MMH, with each successive response to NH₃ decreasing. The ratio of the average peak height of MMH to NH₃ throughout

the testing was approximately 1:10.

The response of the electrochemical cells to MMH was different following exposure to NH_3 . The MMH response curve did not obtain a plateau after 10 minutes, and the peak was 5 percent lower. Also, the cells required 1.5 to 2 hours to recover from just one 10-minute exposure to NH_3 . The recovery time was independent of whether the cell was exposed to MMH or zero air during that time. These effects indicate a loss of response to MMH. See the figure "NH₃ and MMH Response Curves in an ESI 7660."

The response of the electrochemical cells to H_2S was 15 seconds to 90 percent of peak response, with a plateau achieved almost immediately. The MMH response to 90 percent of the signal was 30 seconds. The H_2S response signature was similar to that of MMH, and the signal intensity did not change throughout the tests. The response to H_2S was more intense than the response to MMH, with a peak response ratio of MMH to H_2S of 2.7:1. Furthermore, H_2S did not alter the response of the cells to MMH or to zero air. See the figure "H₂S and MMH Response Curves in an ESI 7660."



H₂S and MMH Response Curves in an ESI 7660

Conclusion

NH_3 is a poor choice for a surrogate gas to be used for validation of the HVDS because of the following properties: (1) it requires the use of NH_3 above its threshold limit value of 25 parts per million, (2) NH_3 inhibits the response of the sensor to MMH, (3) its response is not repeatable, and (4) the response signature is different from that of MMH.

H_2S is a suitable candidate for use as a surrogate gas for MMH in the HVDS. The response signature is similar to MMH, and the sensitivity of the electrochemical cell to H_2S requires a concentration of less than the threshold limit value of 10 parts per million.

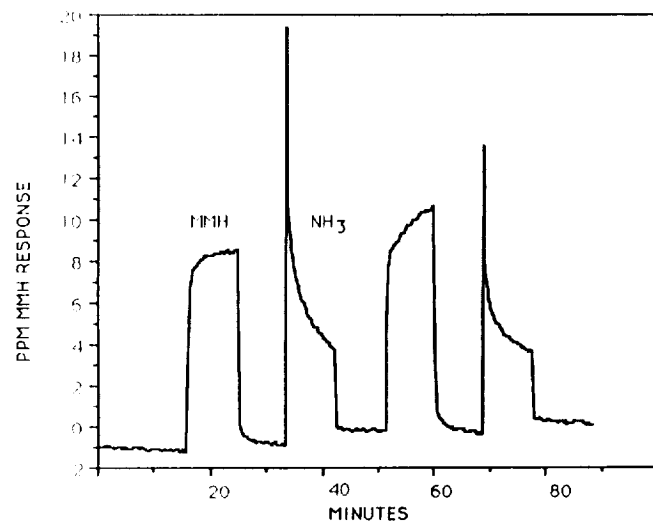
Contacts:

*R. C. Young and J. C. Travis, 867-4438,
DL-ESS-24*

Participating Organization:

*Boeing Aerospace Operations, Engineering
Support Contract (M. J. Beers and
C. B. Mattson)*

*NASA Headquarters Sponsor:
Office of Space Flight*



NH₃ and MMH Response Curves in an ESI 7660

Field Testing of the Citrate Sampler

Objective

Test and evaluate the performance of the citrate sampler in the field to determine the effect of potential interferents and feasibility for use as a personnel and area monitor for hydrazines.

Background

Hydrazines are employed by NASA as hypergolic fuels. The health hazards associated with these chemicals mandate that workers be monitored to ensure exposures remain within safe limits. Personnel of the Naval Research Laboratory and GEO Centers, Inc., developed a badge sampler for the passive collection of ambient hydrazine vapors. After the badge was evaluated in the laboratory, a field test plan was devised and initiated. Samples from outdoor locations revealed an unexpected interferent - sunlight. The field test was postponed until the problem could be solved.

Approach

A modification in the sampling badge was needed to reduce the interference from sunlight. A variety of options was investigated. One option was that ultraviolet absorbers were added to the coating solution in order to act as a sun block for the sampler. Another option was to alter the badge housing to prevent the sun from reaching the citrate-coated substrate. This was originally accomplished by coloring the badge black and later by molding the badge from black polyethylene.

Results

Laboratory testing indicated that the addition of the ultraviolet absorber interfered with the analytical procedures. The second approach, coloring of the badge

black, did significantly reduce the interference effect. The molding of the badge with black polyethylene made a greater improvement. One thousand black badges were ordered from Moldsavers and the field testing was resumed.

The results obtained with the black badge uncovered an additional interferent - tobacco smoke. The effect was noted during monomethylhydrazine quantitation using a coulometric method. No effect was noted using a phosphomolybdic acid colorimetric method. The field test has been completed and the black badge sampler is ready for field deployment.

Contacts:

*J. C. Travis and R. C. Young,
867-4438, DL-ESS-24*

Participating Organizations:

*Naval Research Laboratory (S. Rose-Pehrsson)
GEO Centers, Inc. (P. Taffe)*

NASA Headquarters Sponsor:

Office of Space Flight

Relative Humidity Compensation for an Infrared Total Hydrocarbon Monitor

Objective

To provide real-time relative humidity (RH) correction for the infrared (IR) total hydrocarbon (THC) monitor to be used in the payload transporter canister at KSC. The ground processing of the Hubble Space Telescope at KSC requires monitoring of total hydrocarbon vapor in the payload transporter canister during movement from the Vertical Processing Facility to the Payload Changeout Room at Launch Complex 39. The alarm level selected for this monitor was 5-parts-per-million (ppm) THC measured as methane, and the instrument selected was a Foxboro Miran 101 Specific Vapor Analyzer. The purpose of this test is to quantify and provide compensation for

the response to ambient water vapor (as relative humidity) of the existing THC monitor.

Background

For investigating background conditions at Pad B, an infrared methane monitor similar to the ones selected for support of the Hubble Space Telescope was used to look for THC background over a two-week period, which included the passage of a cold front. The recorded data indicated that the THC monitor reading tracked the reading of the relative humidity monitor during two days of rain followed by cool dry air. (The relative humidity monitor failed in the conditions of 100 percent and condensing, but the THC monitor returned to its lower values after the passage of the front.) The conclusion was obvious that the THC monitor was responding to ambient water vapor content.

While the sensitivity to water vapor is considerably less than to THC, the concentration of water vapor in the air at 70 degrees Fahrenheit (°F) and 45-percent relative humidity is on the order of 1 percent, compared to the alarm level of 5 ppm (or 0.0005 percent) for THC. As a consequence, reasonably expected variations in relative humidity cause significant variations in the THC reading. Furthermore, calibration with dry gas, followed by unattended use in the canister environment, cause the zero THC response to read above the alarm point.

Approach

A linear correction relation for the THC monitor response to relative humidity was developed by delivering to the THC monitor a gas stream with controlled relative humidity and temperature. This was necessary because the actual water vapor content of air is a function of temperature and relative humidity (T/RH). The response of the THC monitor was measured over the expected range of T/RH variation in the controlled environment of the pay-

load canister, and the correction necessary to bring the response back to zero for zero THC vapor concentration was calculated. An average approximation was used to get a plus or minus 2-ppm correction over the entire range.

The controlled T/RH range of the environmental conditions in the payload canister is 71 plus or minus 5 °F and 45 plus or minus 5-percent relative humidity. The test conditions were set up to exceed this range because the approximations necessary for a linear correction are valid only within the range of the data. The test measured the relative humidity response of the THC monitors at each point shown in the test matrix "THC Relative Humidity Response Test Matrix."

*THC Relative Humidity Response
Test Matrix*

Temperature (°F)	Relative Humidities (Percent)			
66	30	40	50	60
70	30*	40	50	60
73	30	40	50	60
76	30	40	50	60
80	30	40	50	60

* Calibration was done at 70 °F and 30-percent relative humidity.

Test Articles and Equipment

The following THC monitors were tested for relative humidity response:

1. Miran 101 IR Analyzer, 3.3 micron, 13.5 meter path, serial no. 205
2. Miran 101 IR Analyzer, 3.3 micron, 13.5 meter path, serial no. 206

The following equipment was assembled to deliver the required control of T/RH conditions to the THC monitors for measurement and compensation of response to relative humidity.

1. Mass flow, temperature and relative humidity (FTH) controller, Miller Nelson Model HCS-301 (modified for computer control)
2. Auxiliary dilution unit (ADU), Kin-Tek
3. Temperature and relative humidity transducer, General Eastern Model 850
4. Strip chart recorder, six pen, Kip en Zonen Model BD 101-6
5. PC with analog input/output boards, IBM PC/XT:

Analog-to-digital board
 Digital-to-analog board
 Multiplexer board
 Relay board

6. Environmental chamber, Hot-Pack Model 417532
7. Span gas, 28-ppm methane in nitrogen, including regulator
8. Zero air, KSC breathing air, high purity specification including regulator

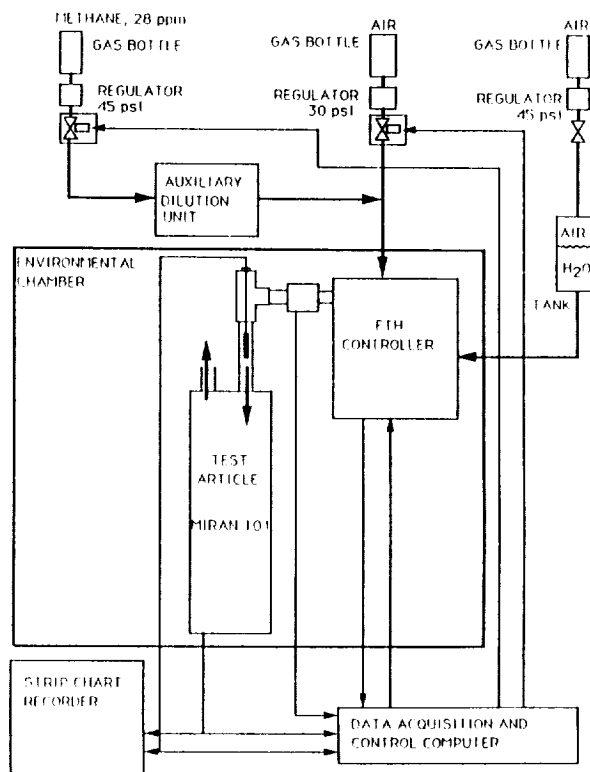
Apparatus

In order to deliver the required range of T/RH to the THC monitor, it was necessary to control the ambient conditions of the test and to control heat gain/loss from the T/RH-controlled gas stream by keeping the transport lines as short as possible. To accomplish this, the FTH controller and the THC sensor were placed side by side on the same shelf inside an environmental chamber. Because the FTH controller can only operate above ambient conditions, the temperature of the environmental chamber was set at 65 °F for all but the 66 °F test runs, when it was lowered to 60 °F.

The sample stream data was collected by a General Eastern 850 T/RH probe in-

stalled in a short, 5/8-inch bore coupling immediately before the THC monitor entrance tube. Thus, the sample is measured and controlled immediately as it enters the THC monitor. The THC monitor is operated normally in the "run" mode, and the exhaust gas is vented to ambient within the environmental chamber. Exhaust T/RH from the THC monitor is not measured.

The overall test setup is shown in the figure "Test Setup for THC Monitor Relative Humidity Response." Note that the difference in supply pressures of the zero air and span gas allows the Auxiliary Dilution Unit (ADU) to be operated with a 15-pound-per-square-inch (psi) pressure drop. It is controlled by an on/off solenoid mixing the controlled flow with the zero air upstream of the FTH controller. The FTH controller sees only a 30-psi gas supply and controls the total flow at 10 liters per minute, whether the span gas is on or off, with zero air providing the balance to 10 liters per minute. The ADU



Test Setup for THC Monitor Relative Humidity Response

was tested in this mode of operation to verify that the meter agrees with a bubble meter measurement vented to ambient pressure, within a 1/2 digit of the ADU mass flowmeter measurement. (This setup can only be used with gasses that do not dissolve in water since the FTH controller humidifies the sample by passing it over heated water.)

Data acquisition and control (DAC) was performed by a personal computer using a 12-bit analog input (analog to digital) board for measurement, and a 12-bit analog output (digital to analog) board for control of the FTH controller. Data was recorded in parallel to the DAC inputs on a six-pen strip chart recorder. The analog-to-digital board was calibrated to the plus or minus 1/2 least-significant bit (out of 12 bits) using a voltage calibrator; the strip chart was calibrated using the same calibrator. The analog-to-digital board was calibrated using a 4-1/2 digit multimeter. The T/RH sensors of the FTH controller itself were not calibrated because the values change in the length of tubing between the FTH controller and the inlet to the THC monitor.

The DAC for this test was programmed in Pascal to provide analog control outputs to the FTH controller and to provide two different types of data files for analysis. One file (slow data) was taken every 15 seconds for the full duration of the test. This provided the electronic equivalent of a strip chart record (or log) of the test. The other file took 120 data points, one per second (fast data), at specific times to record the zero and span readings at each step of stable relative humidity. The fast data zero and span at each step was averaged and used to determine correction factors for the THC monitor response to relative humidity.

Calculations

The key step in determining a correction for the THC monitor relative humidity response is to choose the calibration point

that is low in both temperature and relative humidity so that negative voltage output from the THC monitor is unlikely. This is required because the instrumentation in the canister, as calibrated for the THC monitor, cannot measure negative voltages. If particularly cool, dry conditions should occur, a negative voltage would be read as zero and the artificially high reading would be reported as real THC. A temperature of 70 °F and relative humidity of 30 percent was chosen to give the most accurate compensation over the entire range.

The next step in the process is to determine the optimum slope for the relative humidity correction over the temperature range. This is done by averaging the slopes of both instruments. The slope should represent the best correction in the middle of the canister operation range so that errors are minimized at all of the normal limits and will not exceed plus or minus 2 ppm unless extended beyond the limit by Environmental Control System problems. From the measured response, this was determined to be 0.95×10^{-2} -ppm methane per percent relative humidity.

Next, the temperature compensation coefficient, also in the middle of the relative humidity range of 0 to 30 percent, is determined by plotting the THC voltage versus temperature at constant 40-percent relative humidity. From the measured response, this was determined to be 1.07×10^{-2} ppm per degree Fahrenheit. With this information, the T/RH compensation relation was developed from the following linear approximation for the voltage output of the THC monitor.

$$V = C[V/\text{ppm}] \times \text{THC} [\text{ppm}] + A[V/^{\circ}\text{F}] \times (T - T_0)[^{\circ}\text{F}] + B[V/\%RH] \times [RH - RH_0][\%] \quad (1)$$

where:

V is the output voltage of the THC monitor.

- A is the slope of the response-versus-temperature plot at 30-percent relative humidity. -37.8 : normalizing constant
- B is the slope of the response-versus-relative-humidity plot at approximately 70 °F.
- C is the calibration constant determined at the calibration point of 5.0-ppm methane.
- T is the sample stream temperature.
- T₀ is the calibration temperature (equals 70 °F).
- RH is the sample relative humidity.
- RH₀ is the calibration relative humidity (equals 30 percent at 70 °F).

Equation 1 is solved to obtain the compensated THC concentration as a function of THC monitor voltage output, temperature, and relative humidity. Using these values from the reduced data gives:

$$\begin{aligned}
 \text{THC} = & 36.5 \times V \\
 & -(36.5 \times 1.07 \times 10^{-2}) \times T \\
 & -(36.5 \times 0.95 \times 10^{-2}) \\
 & \times \text{RH} + 36.5 \\
 & \times (1.07 \times 70 + 0.95 \times 30) \\
 & \times 10^{-2} \qquad (2)
 \end{aligned}$$

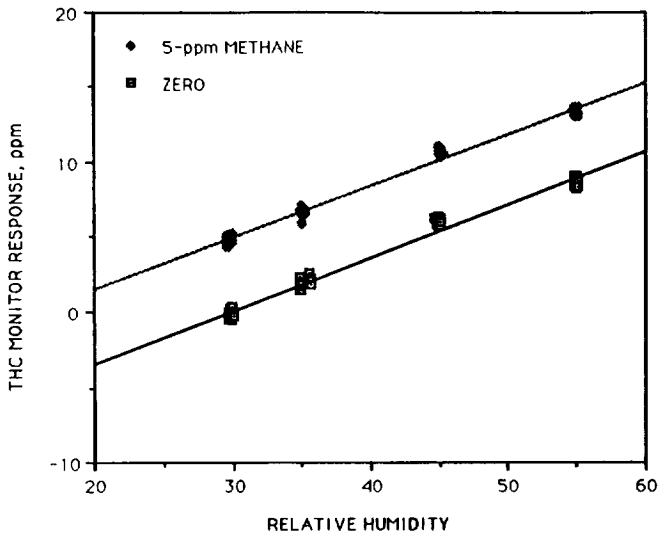
and completing the arithmetic gives:

$$\begin{aligned}
 \text{THC(ppm)} = & +36.5 \times V : \text{uncorrected} \\
 & \qquad \qquad \qquad \text{THC readout} \\
 & -0.39 \times T : \text{linear tem-} \\
 & \qquad \qquad \qquad \text{perature} \\
 & \qquad \qquad \qquad \text{compensa-} \\
 & \qquad \qquad \qquad \text{tion} \\
 & -0.35 \times \text{RH} : \text{linear} \\
 & \qquad \qquad \qquad \text{relative} \\
 & \qquad \qquad \qquad \text{humidity} \\
 & \qquad \qquad \qquad \text{compensa-} \\
 & \qquad \qquad \qquad \text{tion}
 \end{aligned}$$

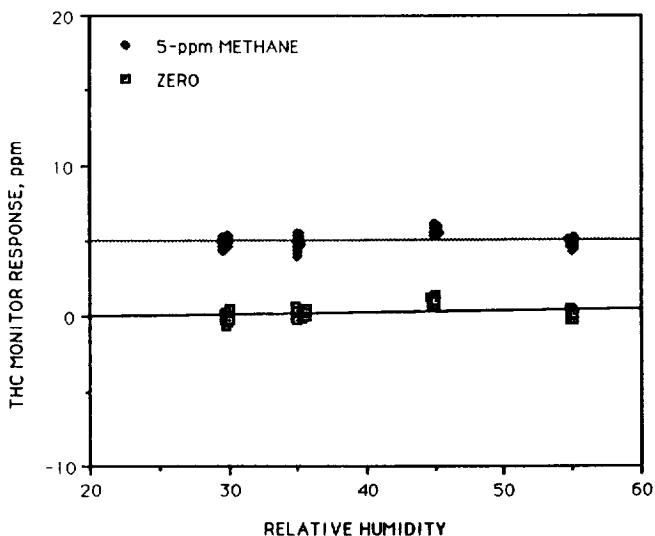
Verification of the correction factors are demonstrated in both THC monitors by running a modification of the THC test program, which has an additional routine to compute the corrected THC readout and to output the corrected voltage to the strip-chart recorder. The graphs in the figure "Demonstration of THC Monitor Compensated for Relative Humidity" show the data from a sample run of a THC demonstration with the uncorrected (top graph) and corrected (bottom graph) readouts at 70 °F. It can be seen from the graphs that the zero offset at 55 percent is approximately 8 ppm and the compensation provided by equation 2 brings it back to zero. The limitation of the linear approximation is seen in the residual zero offset at 50-percent relative humidity, but this is less than 1 ppm.

Another potential source of error in the field is the actual response curve of the relative humidity sensor used for compensation. Most relative humidity sensors (such as the General Eastern 850) are specified to plus or minus 3 percent over the linear range. Each sensor may have a different response within these limits. The worst-case error that can occur from this source is that the sensor used for calibration (to calculate the compensation parameters) would be at the low limit and the sensor in the canister would be at the upper limit. This would add an artificial 6 percent to the relative humidity reading, which would not be compensated; thus, leaving a false residual of 2 ppm in the compensated THC reading. The best way to avoid this problem is to use the same T/RH sensor for calibration and in the canister, so that the response curve will be the same. This cannot be done because the canister sensor is of a different type and cannot be adapted to the calibration setup. This means that the combined effects of the linear approximation and the

UNCOMPENSATED THC MONITOR RESPONSE TO RELATIVE HUMIDITY



THC MONITOR RESPONSE COMPENSATED FOR RELATIVE HUMIDITY



Demonstration of THC Monitor Compensated for Relative Humidity

uncertainty in relative humidity measurement may (or may not) leave a residual, uncorrected error of up to 4 ppm at the limits of the Environmental Control System envelope.

Conclusions

The primary result of the THC monitor response test is that the RH response of the THC monitor can be satisfactorily compensated using a linear approximation to its voltage response (equation 1), provided

that the THC monitor is calibrated at the lower end of the operating envelope of the Environmental Control System of the payload canister. The two THC monitors responded to T/RH variations with enough consistency that an average of the two, over the range of conditions expected, produced one set of coefficients that is sufficient to compensate either or both of the instruments. The compensation equation developed is given in equation 2 and demonstrated in the instrument. In order to apply the T/RH compensation of equation 2, it is necessary to calibrate the THC monitor with zero and calibration gas at a known temperature of 70 °F and a known relative humidity of 30 percent. This is a special calibration requirement and needs special calibration equipment to deliver and measure the T/RH calibration conditions. For best results, calibration should be performed using the same basic apparatus as used for this test.

Contacts:

R. C. Young and J. C. Travis, 867-4438, DL-ESS-24

Participating Organization:

Boeing Aerospace Operations, Engineering Support Contract (C. B. Mattson)

NASA Headquarters Sponsor:

Office of Space Flight

Photoionization Detection of Hydrazine

Objective

To investigate the potential of photoionization detection technology as a means of sensing hydrazine vapors.

Background

Photoionization detectors (PID's) are commercially available for sensing various airborne substances. None, however, have been designed and evaluated specifically for detecting hydrazine fuel vapors in KSC environmental scenarios, such as outdoors

around launch pads and indoors in uncontrolled, industrial-quality air. It was desired to determine through laboratory testing what fundamental problems and tradeoffs may exist in using PID's for such applications, as well as what design configuration would be optimal.

Approach

The first stage in this study consisted of evaluating three commercially available PID's using low-parts-per-million monomethylhydrazine (MMH) vapors. The selected sensors were the Photovac TIP 1, the HNU portable ISIP 101, and the HNU 81-52 GC. After evaluating the preliminary data, the detectors were optimized without major redesign and tested again.

The most promising of the sensors was further modified by installation of an ultraviolet filter on the source lamp. This modification was made to explore detection performance under a tailored ultraviolet ionizing spectrum, which could eventually be used for discriminating hydrazines from other interferents.

The project will culminate in a proposed PID design based on experiences and observations.

Results and Conclusions

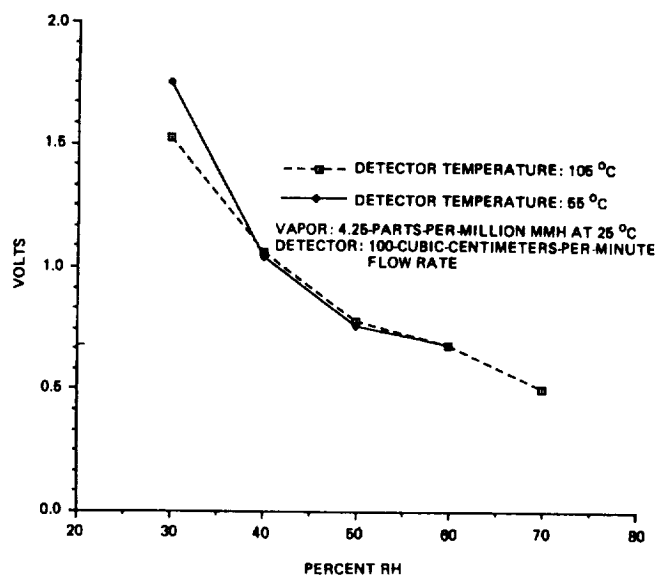
Of the three off-the-shelf detectors tested, the TIP 1 proved to be the most sensitive to MMH vapors. However, its response was also erratic and unstable, which prevented collection of meaningful data. This erratic behavior was thought to be caused by the inherent design of the radio-frequency-pumped ultraviolet lamp.

The HNU portable ISIP 101 detector displayed a relatively limited sensitivity and slower response time, even after being optimized. Its design is not capable of covering the required detection range of 1 to 200 parts per million.

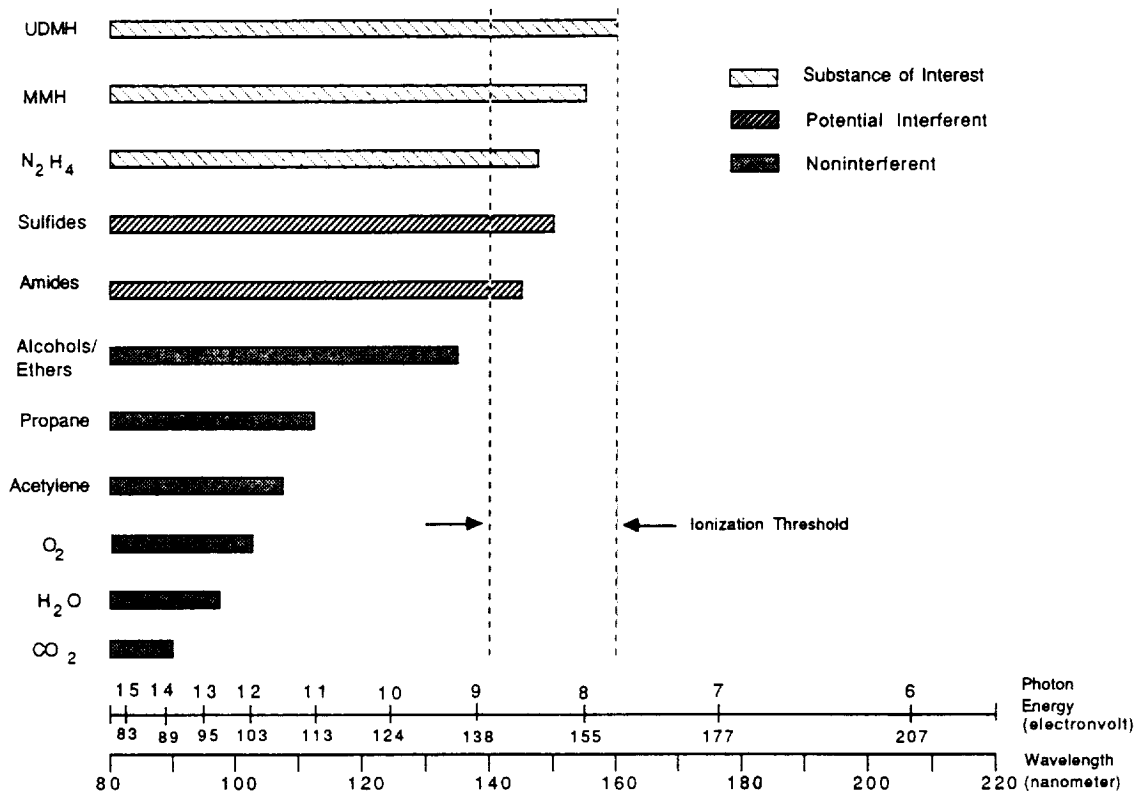
The HNU 81-52 GC detector proved to be the best in terms of sensitivity, repeatability, and response time. Effort was focused on this detector for the latter part of the study.

One major problem encountered with the HNU 81-52 GC detector was that the sample air relative humidity (RH) reduced the PID response; for example, the detector response was 0.7 volts at 60-percent relative humidity versus 1.75 volts at 30-percent relative humidity (see the figure "Effect of Humidity on a 10.2-Electronvolt Lamp"). Another problem was contamination of the ultraviolet lamp window due to prolonged exposure to unfiltered room air. This contamination apparently reduced the ultraviolet flux available for ionization, resulting in the loss of sensitivity.

The figure "Wavelengths, Photon Energies, and Ionization Regions for Various Compounds" depicts the spectral region and ultraviolet photon energies for potential interferents. With this information, the number of potential interferents may be reduced by filtering the spectrum out of the ionization region. With the installation



Effect of Humidity on a 10.2-Electronvolt Lamp



Wavelengths, Photon Energies, and Ionization Regions for Various Compounds

of an ultraviolet filter for selectivity, three problems were encountered:

1. The ultraviolet absorption was severe due to atmospheric air in the sample flow and in the optical path from the lamp window to the ion chamber.
2. The transmittance of typical ultraviolet filters was low even within the spectral band of interest (20 to 40 percent within 145 to 160 nanometers).
3. It is thought, although no exact measurements have been made, that the hydrazine may have a low ionization efficiency, requiring a wide spectral band to generate appreciable ion currents at the electrodes.

This combination of obstacles impeded progress in the attempt to provide conclusive evidence that this technical concept was feasible.

The figure "Comparison of HNU 81-52 GC Responses (With Filter and Without Filter) at Various Temperatures" shows the responses of the HNU 81-52 GC with a filter and without a filter. The loss of signal with a filter clearly depicts the tradeoff between spectral selectivity and sensitivity.

The current HNU 81-52 GC photoionization detector design appears to be acceptable for use in clean-room applications, where the air is controlled at low humidity and negligible contamination. Testing is in progress for overcoming the relative humidity and contamination problems.

Contacts:

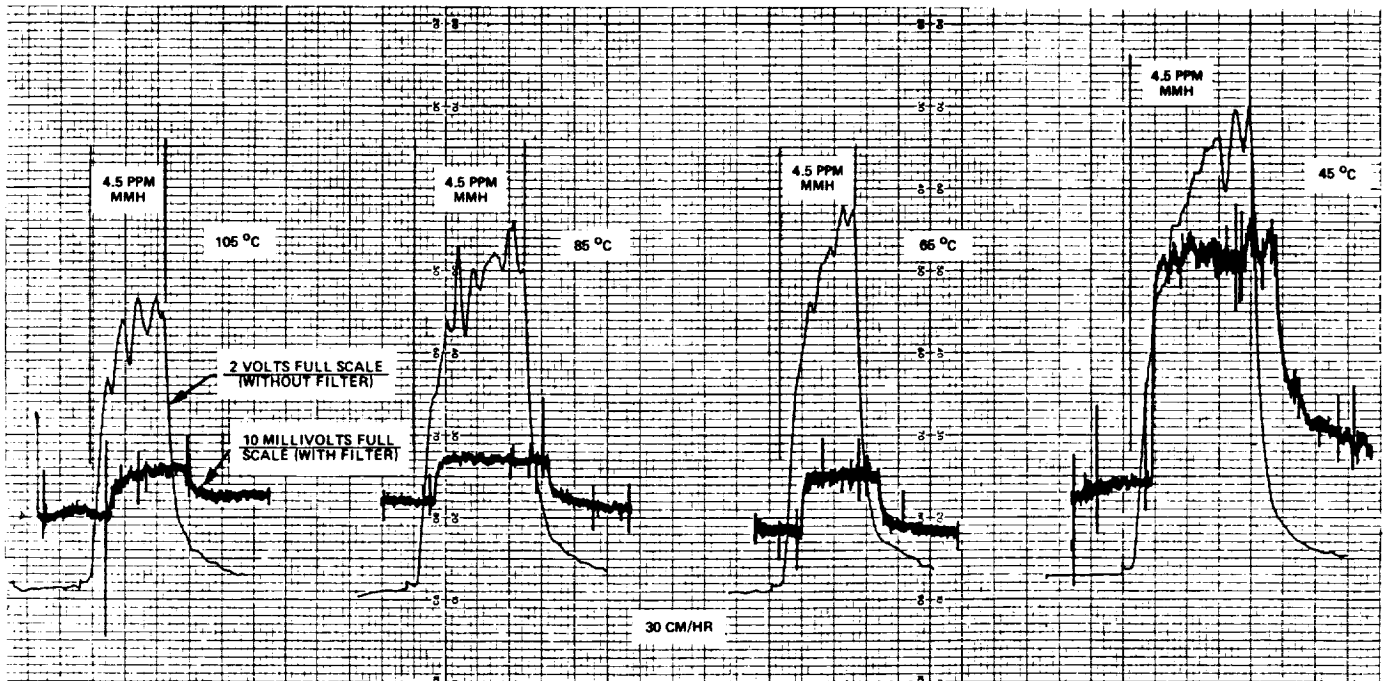
R. C. Young and J. C. Travis, 867-4438, DL-ESS-24

Participating Organization:

Boeing Aerospace Operations, Engineering Support Contract (F. Lorenzo-Luaces and C. B. Mattson)

NASA Headquarters Sponsor:

Office of Space Flight



Comparison of HNU 81-52 GC Responses (With Filter and Without Filter)

Enhancements to the Hypergolic Vapor Detection System

Objective

Perform market survey, laboratory tests, and engineering to design and produce a prototype of a system of health checks (sample flow and detector operation) for implementation into the Hypergolic Vapor Detection Systems (HVDS's) used at KSC.

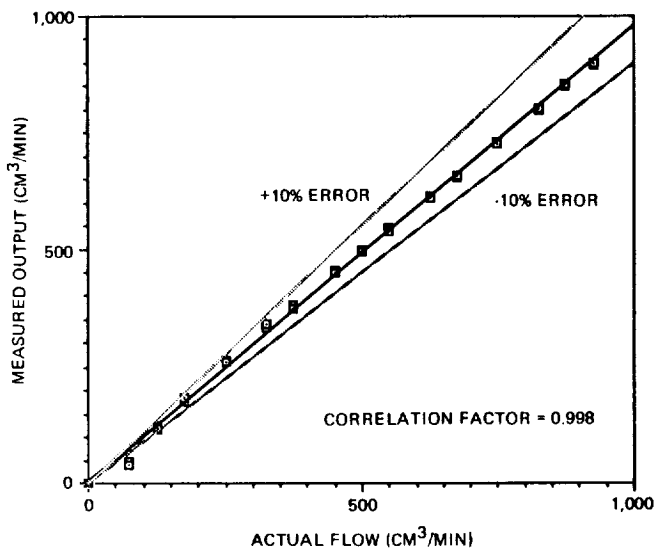
Background

The ESI Model 7000 series of hypergolic vapor detectors used at Launch Complex 39, Pads A and B, experience occasional failures from the sample transport system (pump and sample tubing) or the electrochemical cell (which measures the hypergol concentration). Since this is not a redundant system, these failures (which are currently undetected) result in loss of hypergol detection capability at the sample point being measured. An undetected hypergol leak could result in damage to, or possible loss of, the Orbiter or ground

support equipment. The installation of health checks that could be monitored remotely would provide visibility to the system and would allow measures to be taken to eliminate the problem or use alternative measures to continue operations.

Approach

The new design of the HVDS involved installation of an analog flowmeter with remote output and local display to monitor the sample transport system and a surrogate gas delivery system to provide a functional check of the electrochemical cell. A market survey revealed a limited number of flow sensors were available that met the requirements of size (less than 8 cubic inches), range (0 to 1,000 cubic centimeters per minute, 472 cubic centimeters per minute nominal), accuracy (10 percent of nominal), and power (less than 250 milliamperes at 12 volts direct current). Following extensive evaluation in the Toxic Vapor Detection (TVD) Laboratory, the McMillan Company's Flo-Sensor Model 100-06 was selected to be tested for use. The

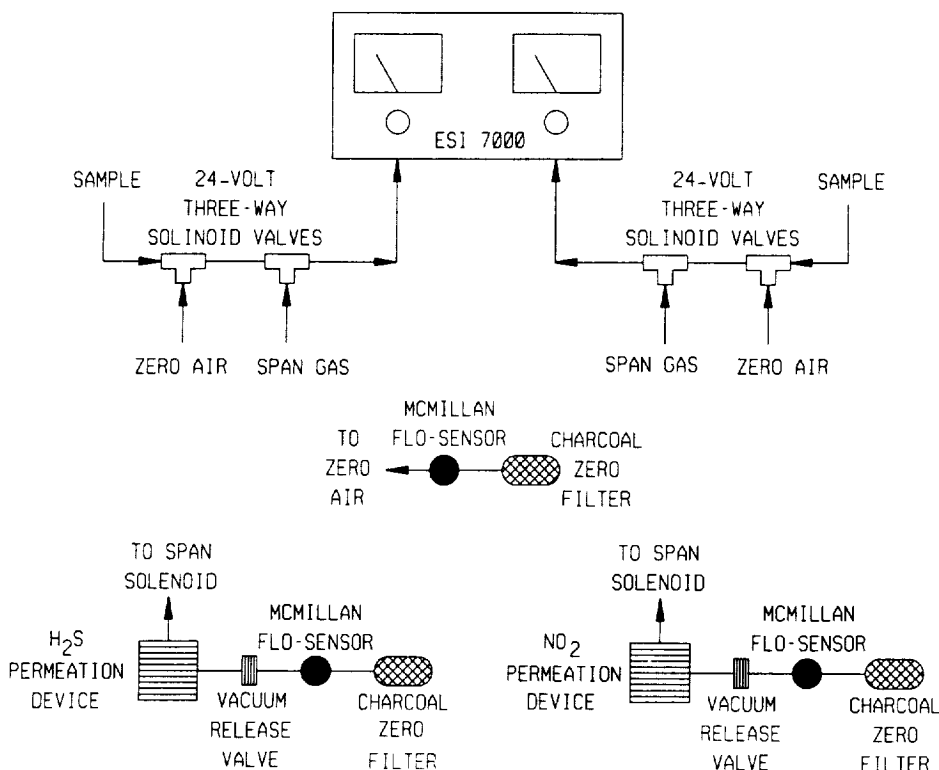


Linearity of McMillan Flo-Sensor Model 100-06

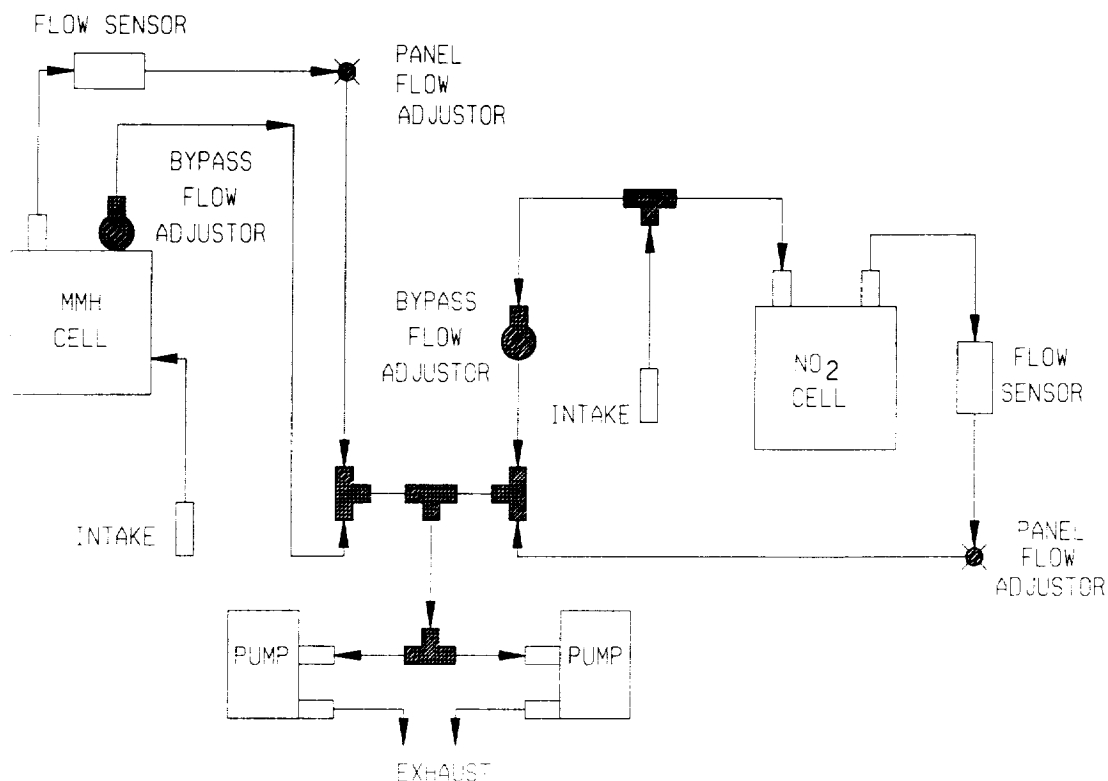
sensor and power supply were mounted on brackets and installed inside the ESI 7000 series without restricting access to electrolyzer components to be serviced during routine maintenance and calibration. The flow sensors were calibrated and then subjected to a series of tests to determine their

linearity, precision, response time, noise level, and temperature effects. A market survey was also conducted to determine the type of display (bar graph, digital, or analog) that was best suited for installation on the ESI 7000 series. Several displays were evaluated against electronic requirements, front panel space restrictions, user choice, and ease of installation.

Since the surrogate gas delivery system could not be installed within the ESI 7000 series, the design required engineering changes to the HVDS cabinet. Factors controlling the design included ease of installation, minimum maintenance, space limitations within the HVDS cabinet, power requirements, and safety considerations. Three designs were developed and tested. Each of the designs used the basic plumbing and solenoid valves, with the difference being the gas delivery methods. One method used pressurized lecture bottles and flow limiters; another system delivered the surrogate gas by bubbling through liquids; the third, and chosen,



Surrogate Gas Delivery Design



Flow Scheme for Redundant Pumping System

method used permeation devices for surrogate gas delivery.

The limiting factors for the surrogate gas system were the compatibility of materials, tubing size, and power. The solenoid valve had to be a three-way valve constructed of Teflon with 1/4-inch national pipe thread (NPT) fittings, to use 24 volts direct current, and to be relatively inexpensive. The market survey revealed a valve manufactured by Galtek Corporation to be the ideal choice. Testing of this valve included a 30-day failure analysis (86,400 cycles) and 96 hours of exposure to 1,000 parts per million of ammonia. Followup testing will include exposure to liquid hydrazine and nitrogen tetroxide.

The ESI 7000 series, which contains two complete detectors within one chassis, currently uses two small displacement pumps (one for each detector). Both pumps have been common single-point failures. To eliminate this problem and provide redundancy to the system, the flow pattern within the ESI 7000 series was

changed to incorporate a vacuum plenum with the pumps connected in parallel and drawing the sample through each sensor.

Results

The McMillan Flo-Sensor Model 100-06 (rated for up to a 1,000-milliliter-per-minute flow rate) provided the required range, accuracy, linearity, and reliability. The sensor utilizes Pelton-type turbine wheels incorporating an electro-optical system to monitor the flow. Noise levels were less than 23.6 cubic centimeters per minute. Although these are not precision flow sensors, they are far superior to the existing rotameters, and they have the required 0- to 5-volt direct current output for remote monitoring.

Electronic and front panel space restrictions determined the final choice for local display of the flow rate. The decision was made to route the analog flow sensor output through a toggle switch to the front panel meter currently used for reading hypergol concentrations. This does not

present a problem for calibration or remote monitoring, and it allows the installer to check each sensor with a proven analog meter. This was also the least expensive solution for the panel meter since no additional meters had to be procured and a minimum of engineering and hardware modifications were required.

The surrogate gas system that was determined to best fit the requirements was one which incorporated permeation tubes filled with dilute solutions of hydrogen sulfide for the hypergolic fuel sensors and nitrogen dioxide for the hypergolic oxidizer sensors. This eliminated the need for high-pressure valves and lecture bottles. The clean air needed for the zero gas could be drawn from within the rack since it is constantly being purged with breathing air and all ESI 7000 series exhaust ports exit to the exterior of the rack.

Contacts:

R. C. Young and J. C. Travis, 867-4438, DL-ESS-24

Participating Organization:

Boeing Aerospace Operations, Engineering Support Contract (M. J. Beers and C. B. Mattson)

NASA Headquarters Sponsor:

Office of Space Flight

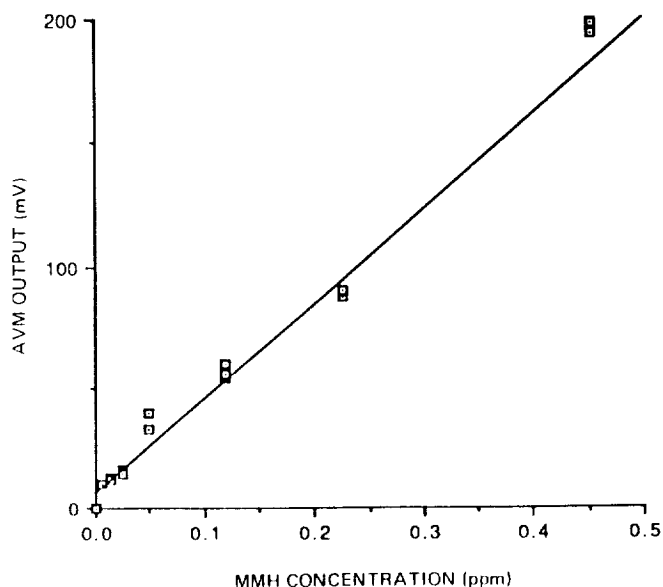
A Feasibility Study of an Ion Mobility Spectrometer (IMS) for Hydrazine Vapor Detection

Objective

To determine the technical feasibility of using an Ion Mobility Spectrometer (IMS) for detecting parts-per-billion (ppb) concentrations of hydrazine (HZ) and monomethylhydrazine (MMH) vapors.

Background

The development of an IMS has been directed toward use for monitoring a variety of chemical compounds. NASA at John

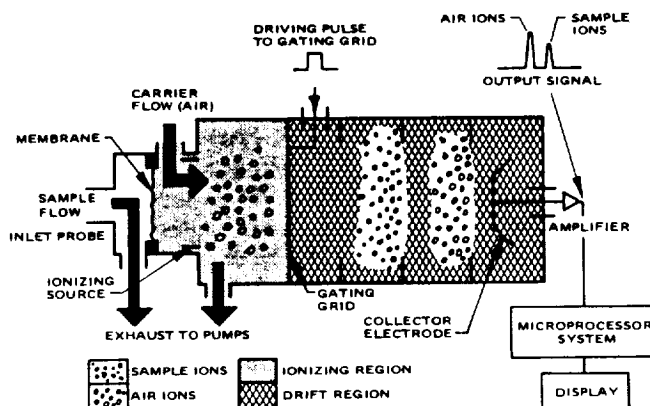


Airborne Vapor Monitor Linearity

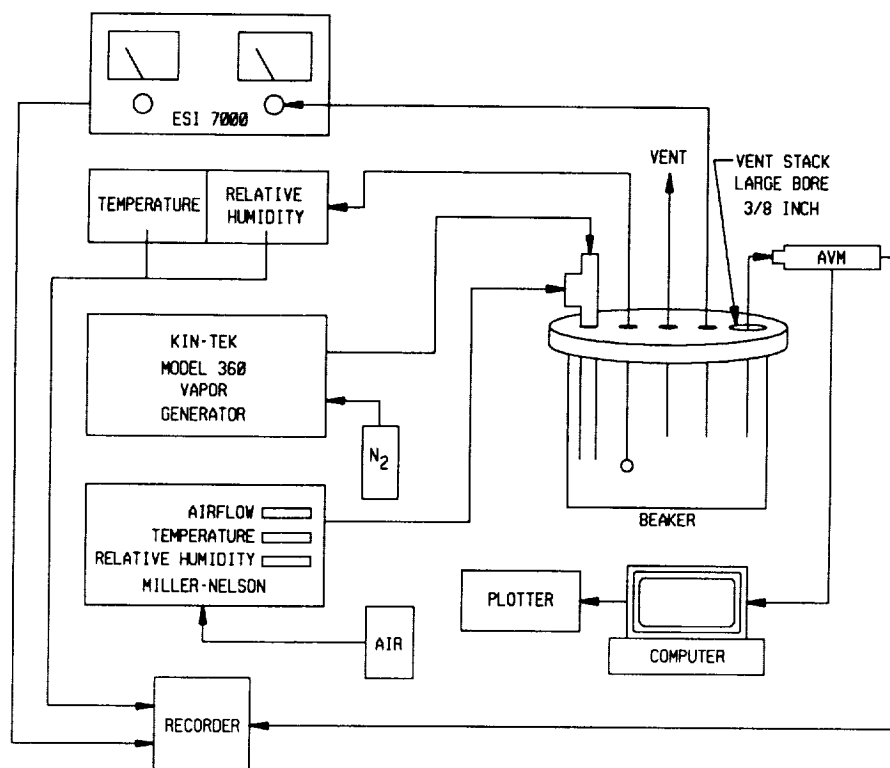
F. Kennedy Space Center has been especially interested in its inherent capabilities of sensing hydrazines at parts-per-billion concentrations. Hydrazines are highly toxic rocket propellants. The American Conference of Governmental Industrial Hygienists intends to lower the permissible exposure limit of HZ and MMH from 100 and 200 ppb, respectively, to 10 ppb in 1990. For the purpose of meeting the 10-ppb permissible exposure limit, an IMS was studied for potential development to be used as a portable personnel safety monitoring device.

Approach

An Airborne Vapor Monitor (AVM) man-



Ion Mobility Spectrometer



Test Equipment Configuration

ufactured by Graseby Analytical, Inc., was used for the study. Concentrated MMH or HZ vapors were generated by the Kin-Tek Model 360 vapor generator. The concentrated vapors were mixed in an insulated beaker with diluent gas (which was temperature and relative humidity controlled) from the Miller-Nelson unit. The test vapor concentrations were validated by collecting the vapor in an absorbing solution and analyzing the solution by coulometric titration. During the test, a recorder continually traced the output from the AVM and a reference sensor, as both sensors were simultaneously exposed to zero air and MMH in air standards in 7-minute iterations. The IMS parameters studied included the detection limit, dynamic linear range, repeatability, response time, effect of relative humidity, interferences, and effect due to air versus nitrogen as the diluent gas.

Results

Test results indicated the detection limit of the AVM was lower than 10 ppb for

MMH vapor. The linear range was approximately 0 to 1,000 ppb for MMH and 0 to 400 ppb for HZ. The AVM was not as repeatable as the ESI Model 7000 series (the reference sensors) due to slow recovery following exposure to MMH. The relative humidity, tested from 30 to 70 percent at 25 degrees Celsius, caused a less-than-15-percent deviation in MMH readings. A preliminary test indicated interferent response to ammonia, but not to isopropyl alcohol, acetone, Freon, and methylene chloride at each respective permissible exposure limit value. The response difference, due to using MMH in air versus MMH in nitrogen standards, was less than 15 percent.

Conclusion

The AVM is the only sensor among 15 sensors tested in the Toxic Vapor Detection Laboratory that is capable of detecting less than 10-ppb MMH vapor. If the recovery time and ammonia interference can be decreased, the AVM should be recommended for development for use as a

portable hypergolic fuel vapor monitor to meet the new 10-ppb requirement.

Contacts:

*R. C. Young and J. C. Travis, 867-4438,
DL-ESS-24*

Participating Organization:

*Boeing Aerospace Operations, Engineering
Support Contract (C. B. Mattson and
Z. G. Laney, Jr.)*

NASA Headquarters Sponsor:

Office of Space Flight

Evaluation of Quick-Response Oxygen Analyzers

Objective

To perform a market survey and to establish an evaluation program for finding a quick-response oxygen analyzer to be used in the Space Station Processing Facility (SSPF).

Background

Processing of Space Station Freedom elements in the SSPF at KSC will require the use of large quantities of gaseous nitrogen and helium, which will be supplied to operational areas by a distribution system located in underground service tunnels. Since some areas in these tunnels have very little airflow, the possibility exists that leaking gas pipes could cause pockets of oxygen-deficient atmosphere.

Personnel exposed to oxygen-deficient atmospheres may suffer severe physiological impairments or unconsciousness in less than 15 seconds depending on the oxygen concentration. Because of this, NASA Safety requires a 10-second response time for the SSPF Oxygen Deficiency Monitoring System. None of the oxygen sensors now in use at KSC meet this requirement; therefore, a market survey and an evaluation program were needed to find a quick-response oxygen analyzer.

Results

With the market survey portion of the program complete, oxygen monitors that are based on various technologies including electrochemical, paramagnetic, and micro gas chromatography, are being procured. Sampling systems have been designed, and an automated data acquisition system has been set up to begin the evaluation portion of the program.

Contact:

P. A. Mogan, 867-4438, DL-ESS-24

Participating Organization:

*McDonnell Douglas Space Systems
Company (H. Allen)*

NASA Headquarters Sponsor:

Office of Space Flight

Development of an Improved Particle Counter Calibration System

Purpose

The primary objective of this project is to develop and qualify a standard aerosol generation system for producing test aerosols in the 0.5- to 5.0-micrometer range with a characteristically uniform size and concentration for use in calibrating optical particle counters (OPC's).

Background

Studies conducted at KSC have demonstrated that OPC's, which are used to monitor airborne particle concentration in clean work areas, exhibit substantial variability. These differences in instrument readings occur not only when instruments from different manufacturers are compared but also between "identical" instruments of the same model.

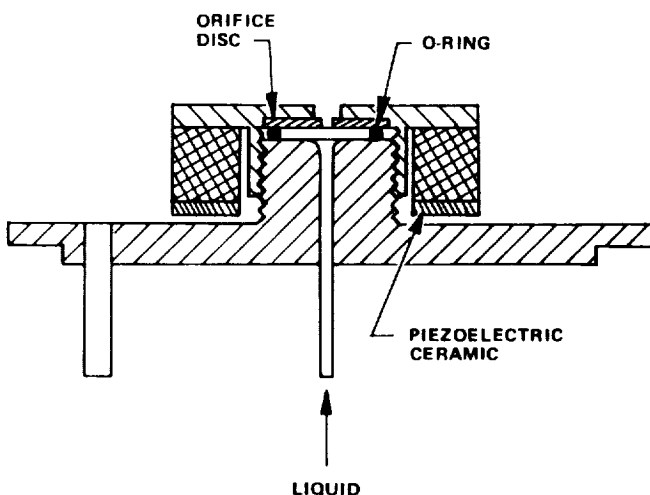
One step in minimizing or at least characterizing instrumental variability is to apply a uniform calibration method to all

OPC's. OPC calibration requires generation and sampling of airborne particles and is currently limited to a size-only calibration. There is presently no standard method for generation and sampling of test particles that is applicable throughout the 0.5- to 5.0-micrometer range.

This project is aimed first at development of a standard methodology for the generation and sampling of particles in the 0.5- to 5.0-micrometer range. Although this technology may eventually lead to a particle concentration calibration technique for particle counters, its primary importance is as a size calibration technology that will allow accurate characterization of the variability between instruments.

Approach

An aerosol particle generation system functions by one of two methods. The first method is the formation of polystyrene latex (PSL) particles from liquid. The second is the formation of a particle stream from premanufactured particles. To create a stream of PSL from liquid, the liquid PSL is injected into the system by a syringe pump. The liquid is then fed through a vibrating orifice, which breaks the stream up into filaments (see the figure "Vibrating Orifice"). The filaments collapse into individual particles. In order to minimize the possibility of these parti-



Vibrating Orifice

cles colliding and sticking together, a nebulizer is used. The particle stream is fed into a sampling plenum where it is diluted and sampled.

The second method of generating aerosol streams, known as nebulization, uses standard size particles purchased from a manufacturer. The particles are then suspended in water or alcohol and placed in a reservoir. The liquid is drawn into the sample stream through a Venturi and impinged on a wall. The larger droplets impact the wall and are returned to the liquid reservoir. The smaller droplets remain in the sample stream and are then fed through a drying chamber into a sampling plenum.

During this project, both types of particle generation systems will be evaluated. It is hoped that nebulization can be used to generate a sample stream with a known concentration of uniform size particles. This method is preferred due to its simplicity.

Commercial nebulizers will be obtained and evaluated for their performance with particles from 0.5 to 5.0 micrometers. An optimal nebulizer will be identified. Evaluation will quantify particle production efficiency versus particle size. Particle sizes will be quantified by use of a particle counter and gravimetric analysis of particles collected on filters. A system for providing clean, dry air to the nebulizer will then be developed using off-the-shelf hardware. Development of a system for diluting and drying aerosol particles will then proceed. The optimum configuration will be identified and used in the overall system design.

Next, the project will develop a sampling system compatible with sample flow rates in the 0.1- to 1.0-cubic-foot-per-minute flow range. This sampling system will be compatible with particle counters of different sizes in order to accommodate many different models of particle counters.

The advantages and disadvantages associated with using water or alcohol as the particle suspension medium will be investigated. The effects of evaporation and particle suspension concentration on performance of the overall generator will be evaluated as part of this task. The best particle suspension medium will be identified and used in the aerosol generation system.

Investigation of premanufactured standard particles will then begin. The effects of different methods of procuring, qualifying, and handling standard latex spheres will also be evaluated in order to develop a methodology for minimizing variability due to these factors. A complete procedure, starting from the point of purchase of test particles and covering qualification procedures and methods for determining the lifetime of the sampling media, will be developed.

Results

This investigation is in its second month. All procurements of test equipment have been received. An appropriate nebulizer has been identified and will be purchased.

Contact:

P. A. Mogan, 867-4438, DL-ESS-24

Participating Organization:

*University of Arkansas at Little Rock
(Dr. A. Adams)*

NASA Headquarters Sponsor:

Office of Space Flight

Multispectral Imaging of Hydrogen Flames

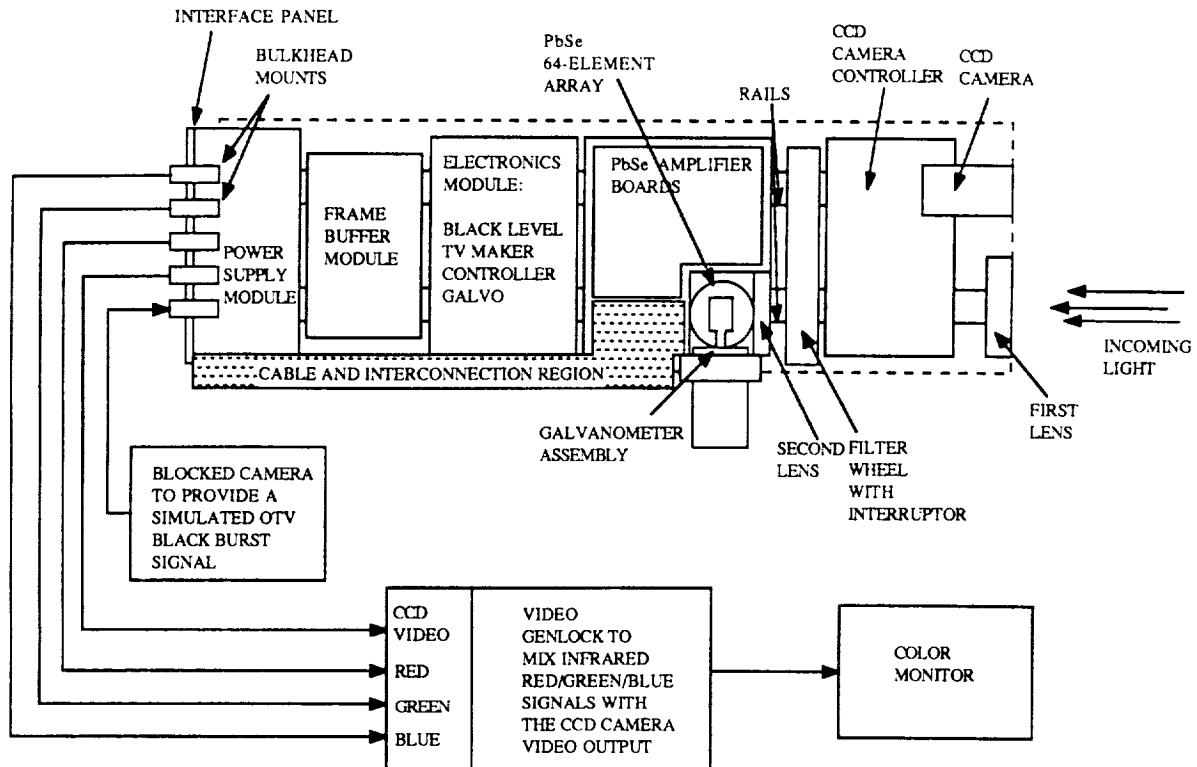
A requirement for a camera that can display normally invisible hydrogen fires was realized during the aborted Space Transportation System 14 (STS-14) launch. Immediately after the on-pad abort, the hydrogen fire detectors went into an alarm

condition. As a consequence of the resulting actions, it became apparent that the ability to image a hydrogen flame was highly desirable.

Hydrogen flames emit insignificant light in the spectral regions (the regions to which the human eye and standard television cameras are sensitive) with most of the emission occurring in the ultraviolet region and in the middle to far infrared regions. Consequently, work began on designing a special camera that could create a video image in one or more of these spectral regions. It was additionally specified that such a camera must meet stringent environmental conditions, must be compatible with the existing operational television (OTV) system, and must be able to resolve interfering phenomena (that is, it must be able to distinguish between a hydrogen flame and other emitters such as thermal sources or solar glint).

After a review of existing technologies, it was decided that an optimal multispectral imaging system for viewing hydrogen flames should consist of a high-quality charge-coupled device (CCD) camera and a low-sensitivity infrared camera operating in the middle infrared region. A search of existing detectors pointed to lead selenide (PbSe) as the preferred detector material - being fast, adequately sensitive, and not requiring cooling. Several PbSe detectors were purchased and tested to validate their use in this proposed system. An infrared spectrometer was used in measuring the middle-infrared emission of various sources (such as, hydrogen flames, incandescent lamps, and hot objects).

After measuring the emission spectra, it became apparent that a high degree of discrimination between hydrogen-based flames, carbon-based flames, and thermal emitters could be achieved by imaging separately in three broadband, adjacent, infrared regions and then by color coding these regions. In other words, by imaging in the infrared in the identical manner that the human eye images (that is, by



Multispectral Television Camera

assigning the colors red, green, and blue to three adjacent spectral regions), a full-color infrared image could be created where hydrogen flames are one color, carbon-based flames are another, and thermal emitters appear as a range of other colors.

A low-resolution, middle-infrared camera was built and tested using only one spectral region. This camera was large and bulky but showed that the general principle was correct. After this, a smaller, higher resolution, three-color camera was constructed and limited field testing was conducted. This second-generation camera (see the figure "Multispectral Television Camera") has demonstrated the discrimination and sensitivity necessary to meet the requirements of a field-usable system. The next year will be spent improving this camera and developing a rugged, compact version compatible with the current operational television system.

Contact:

J. D. Collins, 867-4438, DL-ESS-24

Participating Organization:

Boeing Aerospace Operations, Engineering Support Contract (R. C. Youngquist, S. Gleman, F. Lorenzo-Luaces, J. Moerk, and G. K. Rowe)

NASA Headquarters Sponsor:

Office of Space Flight

Hypergolic Vapor Generation and Validation

Objectives

The first objective of the project is to design and assemble a toxic vapor generation system, which will be used in the evaluation, research, and development of hypergolic vapor detection instrumentation. The system will be reliable, versatile, and flexible. It will be capable of generating a wide range of hydrazine vapor concentra-

tions at the required temperature and relative humidity. Interfaced with a computer, the system will also be automated to deliver hydrazine vapor to the test instrument unattended. The second objective is to validate the vapor concentration. A simple and accurate procedure will be established.

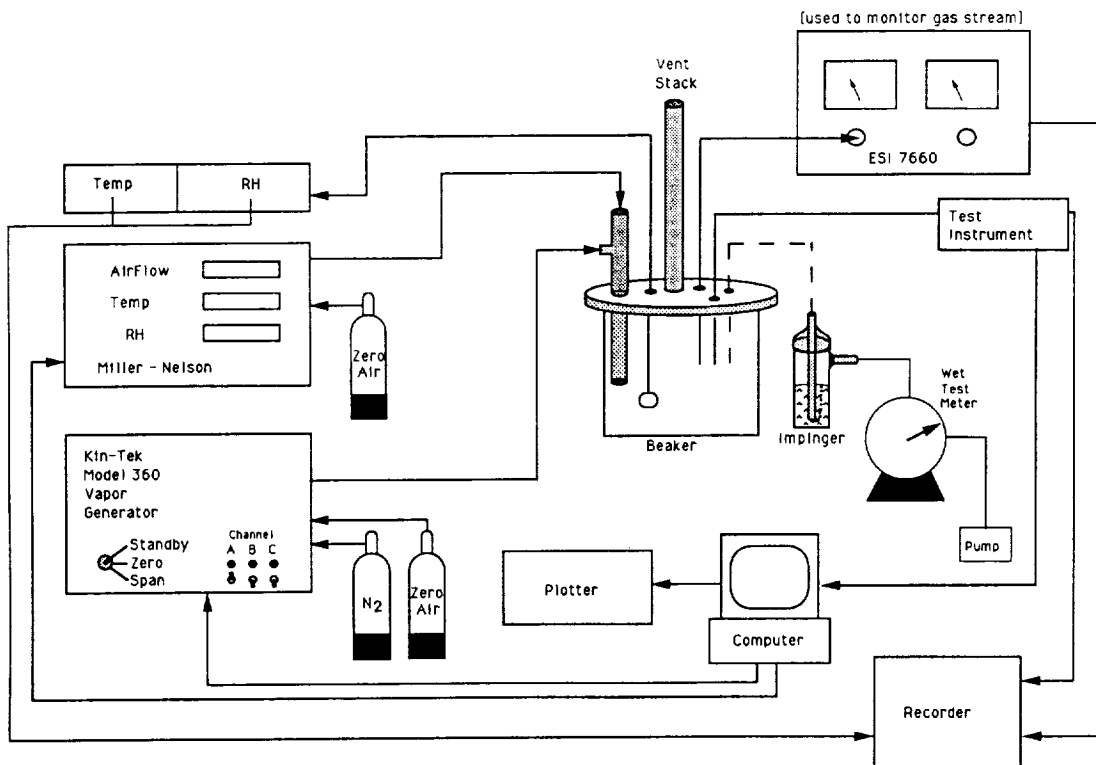
Background

Hydrazine and monomethylhydrazine are used by NASA as rocket propellants. They are toxic, corrosive, and suspected carcinogens. In order to protect the flight hardware and the personnel working on or around the Space Shuttle, two types of detectors are being investigated. These are the parts-per-million (ppm) range, fixed-point leak detectors and the parts-per-billion (ppb) range, portable personnel monitors. The instruments to be used at KSC must meet KSC's accuracy and reliability requirements. The Toxic Vapor Detection (TVD) Laboratory is tasked to provide the capability to measure the

performance of the detectors with consistent, accurate, and safe test procedures.

Approach and Results

The heart of the hardware used in the TVD Laboratory is the vapor generation system. The system was designed and assembled by chemists and engineers with years of experience in the calibration of hydrazine detection instrumentation. The hydrazine vapors are generated from a Kin-Tek Model 360 vapor generator. The vapor generator consists of three permeation devices housed in three ovens with individual temperature control. Each permeation device is a stainless steel dewar containing a length of winding capillary polymeric tube submerged in hydrazine or monomethylhydrazine liquid. The permeation rate of the devices is determined by the temperature of the oven, the length of the polymeric tube, and the type of polymeric material used. Standard hydrazine vapor is generated by first flowing nitrogen through the polymeric tube



Equipment Configuration for Hyperpol Vapor Generation

and then diluting the hydrazine/nitrogen mixture with "conditioned" air from the Miller-Nelson flow-humidity-temperature control unit.

The concentrations of the standard hydrazine vapor are related to the permeation rate of each permeation device, the number of permeation devices activated, and the total flow (that is, the nitrogen flow through the permeation tube and the diluent air flow). Operating in the Span mode, the channel switches located on the Kin-Tek vapor generator control which permeation device or combinations of permeation devices are activated for use. Operating in the Zero mode, the hydrazine vapors from all three permeation devices are vented and zero air replaces the hydrazine vapor which is then combined with "conditioned" air from the Miller-Nelson unit. Thus, by activating the Span or Zero mode in conjunction with activating a combination of channel switches, zero air and hydrazine vapors of concentrations from a few ppb to 20 ppm are routinely obtainable. The concentration range can be expanded to approximately 100 ppm by adding a second Kin-Tek vapor generator to the system. This capability allows the evaluation of an instrument with both a low and high detection range. A temperature range of 25 to 50 degrees Celsius and a relative humidity range of 0 to 80 percent can be provided for conditioning the zero air and standard hydrazine vapors. This capability allows the environmental effect on the instrument response to be evaluated. A sample flow of 5 to 50 liters per minute can be generated for testing several instruments simultaneously. Both the Kin-Tek vapor generator and the Miller-Nelson flow-humidity-temperature control unit have been modified for computer automation. The computer software is modular, with control modules for: (1) gas generation and conditioning, (2) data buffering, and (3) file handling. An automated test is initiated by inputting a sequence of high-level commands to the computer.

The concentrations of the standard vapors are evaluated by trapping the vapor in an impinger containing an acidic-absorbing solution. There are several methods available for analyzing the solution. The TVD Laboratory opted to use a constant-current, coulometric titration method. This method calls for adding a small amount of potassium bromide to the solution. A direct electric current passed through the solution electrolyzes potassium bromide to form bromine. The bromine rapidly reacts with the hydrazine present in the solution. As long as hydrazine is present, the bromine concentration is undetectable. At the moment that all the hydrazine has reacted, the bromine concentration increases to a detectable level, which signifies the end of titration. The length of titration is determined by the amount of hydrazine present in the solution. The concentration of hydrazine vapor is calculated from the result of the titration. For precision and accuracy, the vapor concentration evaluation procedure is performed until triplicate data falls within a plus or minus 3-percent deviation from the mean value. The coulometer, as well as the recorder used to monitor the titration, are checked for accuracy prior to use. Using this method, the TVD Laboratory has verified vapor concentration as low as 1 ppb.

Contacts:

*R. C. Young and J. C. Travis,
867-4438, DL-ESS-31*

*NASA Headquarters Sponsor:
Office of Space Flight*

Preliminary Evaluation of Commercial Hypergolic Fuel Vapor Sensors

Objective

To develop a reliable, low-maintenance sensor for a second-generation Hypergolic Vapor Detection System (HVDS II) to replace the HVDS sensors currently used to support hypergolic fuel loading onto the

Space Shuttle for launch at KSC. The objective of this phase of the project is to locate a commercially available sensor or technology that can meet the goals of long life and reliability and can detect hydrazine (HZ) and monomethylhydrazine (MMH) from 0.5 to 200 parts per million (ppm) with little or no interference from ambient levels of nonhazardous vapors.

Background

Hypergolic rocket propellants are used on the Shuttle for orbital maneuvering and control in space. These propellants are loaded onto the Space Shuttle while it is on the launch pad. Since they are highly flammable and corrosive, a leak during the loading process could cause severe damage to the Space Shuttle or the launch pad if not detected and stopped. To detect any leaks that may occur, NASA uses a system of hypergolic vapor detectors that measure vapors in the air near sources of hypergolic fuels or oxidizers. The system transports the sample vapor through long (up to 120 feet) Teflon tubes to electrochemical sensors where the vapor is analyzed. This system has no redundancy, and the sensors for the hypergolic fuel have a history of operational problems that include early failure of the electrochemical cells, drift of the sensor zero reading, and loss of sensitivity over time. This necessitates frequent calibrations (on a 30-day cycle) and expensive laboratory and manpower support. In order to overcome some of these problems, NASA decided to redesign the entire system, starting with a new fuel vapor sensor.

Approach

The approach chosen was to survey various types of commercially available sensors that use a variety of detection methods. All known technologies were considered, and those evaluated include electrochemical, infrared (IR) absorption, ultraviolet (UV) absorption, photoionization detection (PID), and chemically treated paper tape. Fifteen instruments were procured for test and evaluation, and

preliminary tests have been completed at the NASA Toxic Vapor Detection Laboratory at KSC. Those sensors that performed as well or better than the currently used HVDS sensors in most parameters were selected for more extensive testing or development. The parameters chosen for the preliminary tests included: precision (plus or minus 0.5 ppm), linearity (plus or minus 25 percent of the reading), zero drift (plus or minus 0.5 ppm in 14 days), span drift (plus or minus 1 ppm at 5 ppm in 14 days), response time (60 seconds to 90 percent at 5 ppm), and noise (plus or minus 0.5 ppm).

Results

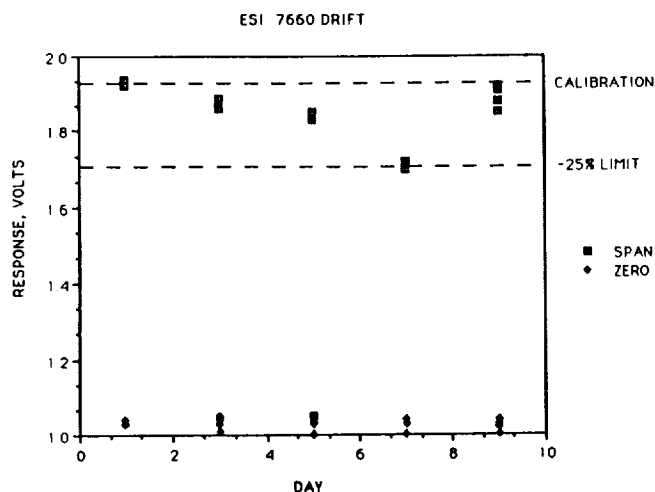
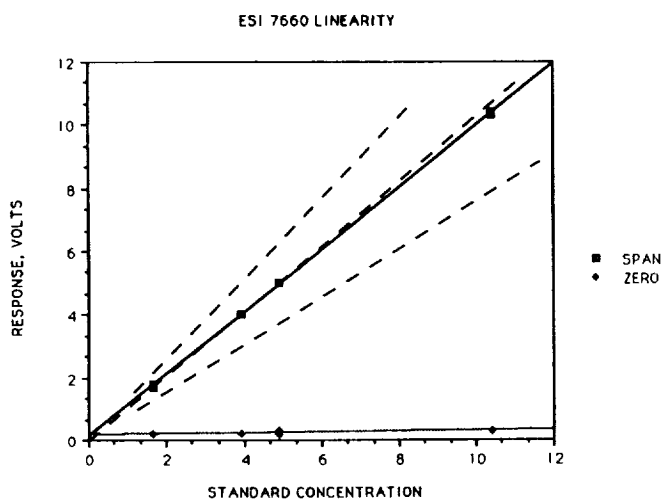
Fifteen commercially available sensors, using four different methods for detection of hydrazines, were tested. Only one instrument passed all parts of the test: one of two ESI 7660 electrochemical cells. The second ESI cell tested showed unacceptable span drift. The next best performance was by the infrared sensors; however, these sensors showed unacceptable zero drift due to changes in thermal conditioning of the sample. The infrared sensors also required approximately 2 hours to stabilize at the test conditions before the zero remained stable. The results of the four detection methods tested were:

1. **Electrochemical Sensors:** The best performance in the screening tests was by the currently used model, ESI 7660. One of two cells tested passed all tests within limits, while the other cell showed unacceptable span drift within the one-week drift test. The ESI 7660 sensor uses a three-electrode potentiostatic cell with alkaline electrolyte and a semi-permeable membrane active electrode.

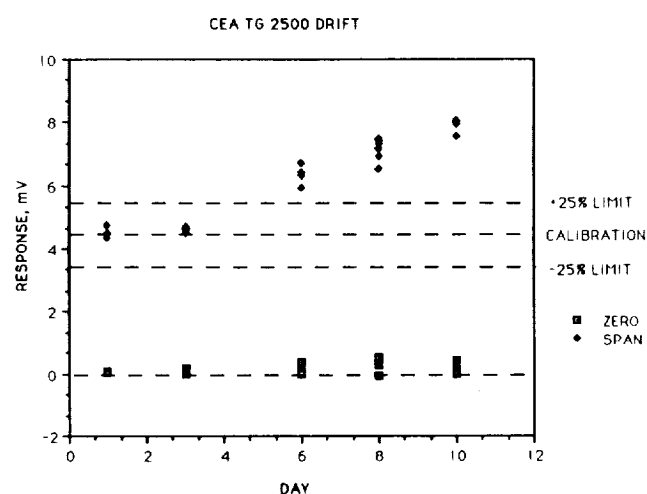
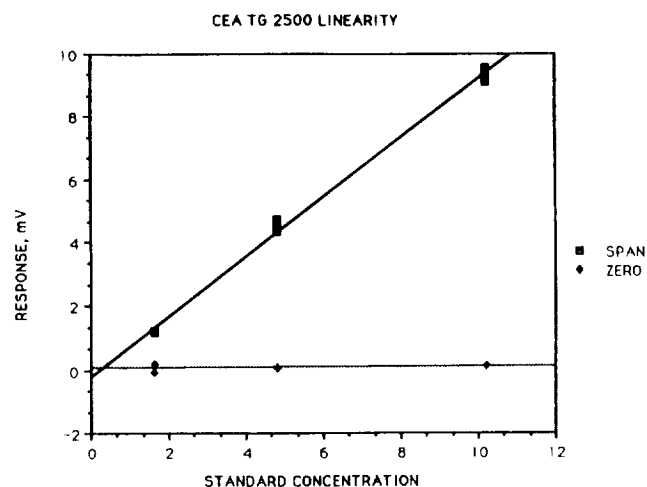
Another type of cell, used by both the CEA and Enmet sensors, was a two-electrode cell using a proprietary metalorganic electrolyte. This cell never reached a stable output when

exposed to MMH, did not have sufficient range (0 to 2 ppm rather than 0 to 200 ppm), and its response times were long (4 to 7 minutes) to 90 percent of the value taken at 10 minutes. See the figures "ESI 7660 Preliminary Test Results," "CEA TG-2500 Preliminary Test Results," and "Foxboro Miran 101 Infrared Sensor Preliminary Test Results."

2. Infrared Sensors: The infrared sensors met most of the requirements for use but took too long to stabilize and tended to drift (zero) if temperature conditions of the sample stream changed. Since this type of problem can be overcome by sample preconditioning (stable flow and temperature control) and is more characteristic of the portable model tested (Miran



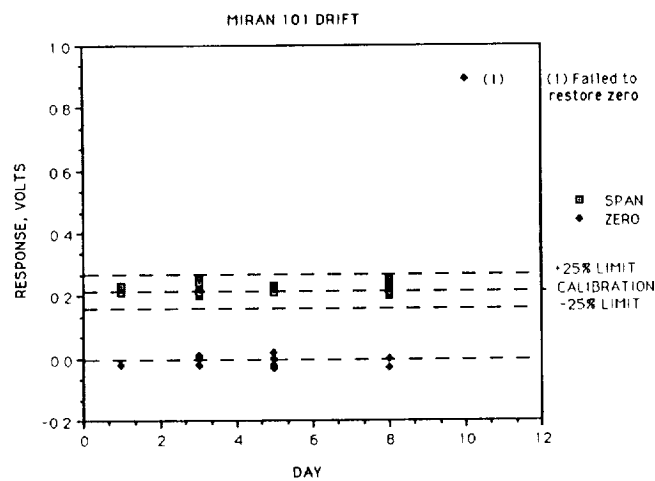
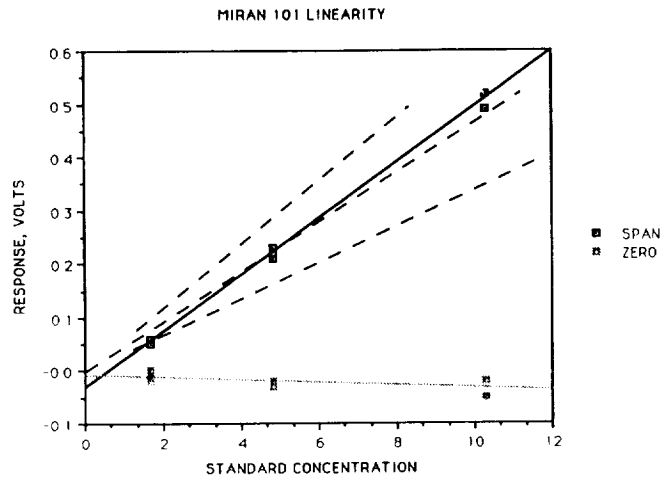
ESI 7660 Preliminary Test Results



CEA TG-2500 Preliminary Test Results

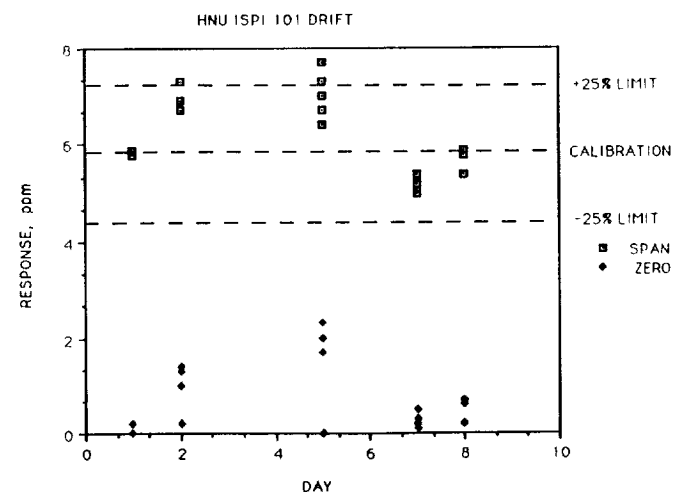
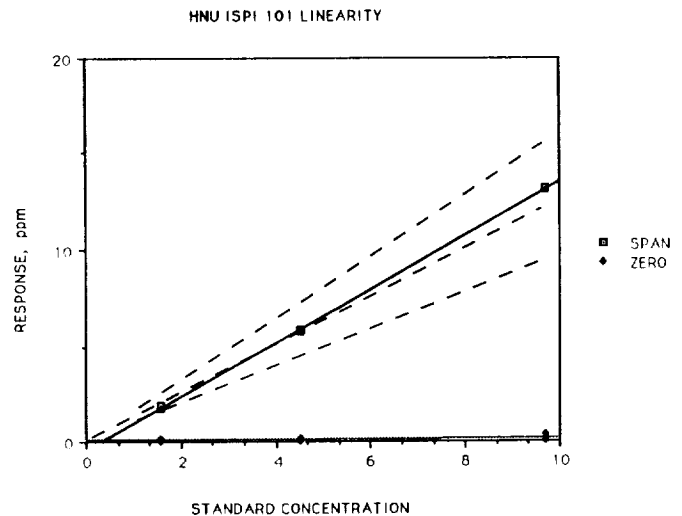
101) than of the infrared technique, the infrared sensors are a candidate for further testing and possible development. One of the infrared sensors also showed unacceptable span drift immediately prior to failure (could not be returned to zero).

3. Photoionization Detector (PID) Sensors: Two portable and one bench PID sensor models were tested at two energy ratings of the ultraviolet lamp. The lamp energy is rated nominally in electronvolts (eV) at approximately the half-power point of the highest photon energy available. Since all the hydrazines of interest have ionization potentials below 8.5 eV, lamps with ratings of



All detectors using the PID method showed a detrimental response to sample moisture content. The photoionization detectors were also very sensitive to contamination of the lamp window and ion chamber with detrimental effect on sensitivity and noise. Details of those problems are beyond the scope of this initial screening test, but should be investigated in detail.

4. Paper Tape Sensors: Hydrazine sensors, using chemically treated paper tape and optical detection of a color change, are among the most sensitive and specific types. While the commercially available units are



Foxboro Miran 101 Infrared Sensor Preliminary Test Results

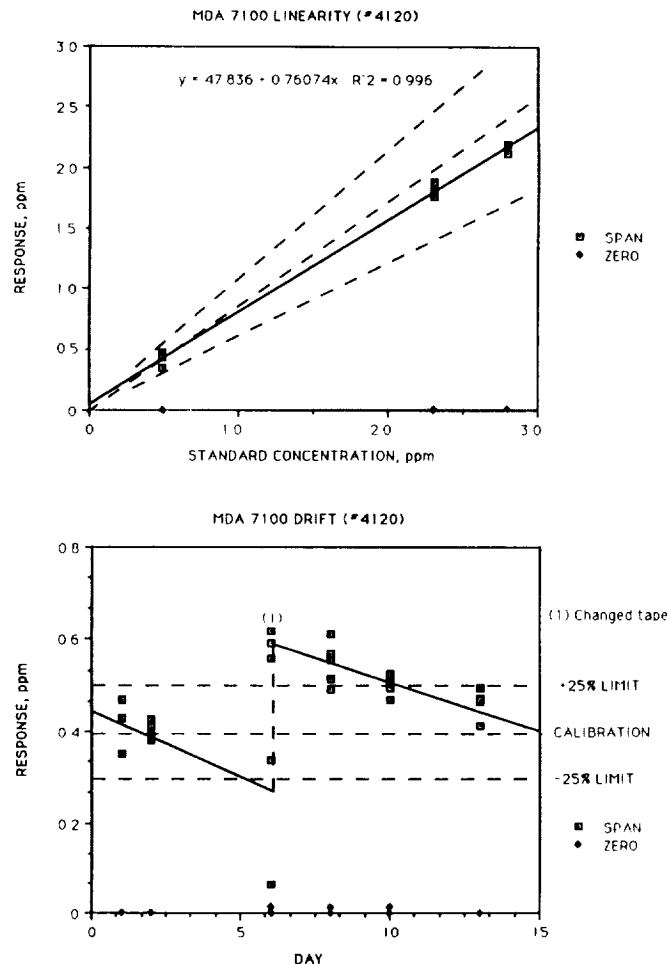
8.4, 9.5, and 10.2 eV were considered good candidates for testing; the 9.5- and 10.2-eV types were included in this test. The photoionization detection method, like infrared, met some of the requirements; though none of the sensors met all of the performance criteria. The most notable failure was a portable Photovac TIP 1, which met only the precision requirement and changed its reading with position (rotation) of the sensor. The HNU ISPI 101, as delivered, was not optimized for hydrazines; it was necessary to increase its signal gain by a factor of about 1,000 to obtain satisfactory response for this test (see the figure "HNU Model ISPI 101 Photoionization Detector Preliminary Test Results").

HNU Model ISPI 101 Photoionization Detector Preliminary Test Results

optimized for detection at the threshold limit value (approximately 0.1 ppm) and the response is saturated at approximately 2 ppm, they were included in the test on the premise that it is easier to reduce sensitivity than to increase it and, if the class of sensor met other criteria, then it might still be suitable for operational use. The primary weaknesses of paper tape sensors are: (1) the long response time required to read 90 percent of the sample concentration and (2) the time to the first indication of a sample is limited by the stepwise nature of the paper tape advance. Chemically treated paper tape also degrades over time when exposed to air and/or humidity (see the figure "MDA 7100 Paper Tape Sensor Preliminary Test Results"). This degradation appears as a loss of span (drift) over the life of the tape. Since the tape must be changed to restore sensitivity, an extra maintenance requirement exists. This was the only class of sensor that had too many intrinsic problems to be considered acceptable for further testing for HVDS II operational use.

Conclusions

None of the sensor models, including the currently used model, passed all of the HVDS II performance criteria. In overall performance, however, the current sensor stands out as the best available at the present time. If another type of sensor is to replace the ESI 7660, it will require further development to overcome weaknesses of the alternate detection methods. In addition, any alternative to the ESI 7660 must result in a significantly more reliable system than the present HVDS to justify the cost of procurement of over 100 sensors plus the cost of pad redesign to accommodate the new sensors. The next



MDA 7100 Paper Tape Sensor Preliminary Test Results

phase of the HVDS II effort will investigate three options:

1. Enhancement of the currently used HVDS system and sensors to provide health checks and redundancy and to improve the individual components for better reliability.
2. Continued testing of new sensors and technologies (such as ion mobility spectroscopy, photo acoustic detection for infrared detectors, pressure-modulated infrared detectors, and new developments in chemiluminescent sensors).
3. More extensive testing and development of the infrared and PID sensors. While these sensors have

limitations, as seen in the test results, they are not necessarily due to intrinsic weakness of the detection methods, and may be overcome with a reasonable development effort.

Contacts:

R. C. Young and J. C. Travis, 867-4438,
DL-ESS-24

Participating Organization:

Boeing Aerospace Operations, Engineering
Support Contract (C. B. Mattson and
Z. G. Laney, Jr.)

NASA Headquarters Sponsor:

Office of Space Flight

Advanced Hazardous Gas Detection System (AHGDS)

The Hazardous Gas Detection System (HGDS), a mass-spectrometer-based system, monitors the Space Shuttle on the launch pads at KSC for potentially dangerous propellant leaks. An improved version of the HGDS is needed to meet the more stringent requirements for the Advanced Launch System (ALS) program. The main features of the AHGDS will be high reliability, high accuracy, high maintainability, self-validation, and operation with a minimal amount of human interface. The system will be configured so it can be used as a prototype replacement unit for the existing HGDS.

The first step in developing the AHGDS was the selection of a mass spectrometer, the heart of the system. The Central Atmospheric Monitoring System (CAMS) has been used by the United States Navy in submarines for years. It has proven to be a reliable and well-supported system. The analyzer from this system was the first choice for use in the AHGDS until the CAMS II analyzer was developed. Research has been performed that suggests that the CAMS II analyzer may be more suitable for the AHGDS than the CAMS analyzer.

The CAMS II is a double-focusing, electromagnetic, scanning mass spectrometer. In testing, it has operated reliably and continuously without recalibration or other adjustments for more than two years. It is capable of measuring atmospheric species from concentrations of a few parts per billion to 100 percent in near real time. A comparison of the characteristics of the CAMS II to the CAMS is shown in the table "Comparison of CAMS and CAMS II Characteristics."

Comparison of CAMS and CAMS II Characteristics

<u>Characteristic</u>	<u>CAMS</u>	<u>CAMS II</u>
Mass range	2 to 135 atomic mass units	1 to 300 atomic mass units
Resolution	1:28	1:200
Detection limit	6 parts per million	0.1 part per million
Electron energy	70 electronvolts	programmable
Monitored gases	8	unlimited

The characteristics of the CAMS II make it more versatile because it can be used to detect any constituent in the mass range of 1 to 300 atomic mass units, which may be necessary depending on the propellants selected for the ALS vehicle. The higher resolution of the CAMS II is also a desirable characteristic.

Tests will be performed in order to determine if the CAMS II can detect the levels of hydrogen (H₂), helium (He), oxygen (O₂), nitrogen (N₂), and argon (Ar) delineated by Shuttle safety requirements. Tests will be performed to determine the optimum configuration of the CAMS II analyzer for AHGDS applications. The ion pump will be replaced with a turbomolecular pump to allow gas measurements in a helium background. The following characterization tests will be performed:

1. The ion beam object slit will be altered to determine the effect on sensitivity.

2. The time required for a scan of 200-parts-per-million levels of H₂, He, O₂, N₂, and Ar will be determined.

The expected results of this testing are that the addition of the turbomolecular pump will enable CAMS II to meet NASA's requirements for leak detection in an He background and to meet NASA's sensitivity requirements.

AHGDS will also possess artificial intelligence capabilities to enable reduction of data flow to the console operator, on-line self-evaluation of data integrity, and self-diagnostics in the event of equipment failure. It would be particularly useful if the AHGDS could perform its own calibration and validation procedures. This artificial intelligence capability is expected to simplify the preparation of the AGHDS for a launch cycle, to reduce manpower requirements, to reduce data flow to the operator, to simplify data interpretation, and to improve reliability through the early identification and mitigation of system failures and out-of-tolerance operation.

Contacts:

*J. D. Collins and F. W. Adams, 867-4438,
DL-ESS-24*

Participating Organization:

*Boeing Aerospace Operations, Engineering
Support Contract
(M. J. Blankenship and S. O. Starr)*

NASA Headquarters Sponsor:

Office of Space Flight

Color Chemistry for Hydrazine Detection

Objective

Investigate the use of vanillin as an indicator in real-time colorimetric detection of hydrazines. The chemistry will be applied in the development of detector tubes, dosimeters, paper tape products, and other analytical techniques.

Background

Hydrazines are employed by NASA as hypergolic fuels for the Shuttle. The health hazards associated with these chemicals and the prospect that the levels of allowable exposures will be lowered significantly in the near future have spurred the need to investigate indicating chemistries. The current color chemistries used in real-time detection either lack sensitivity or have interference problems that render them useless at the low part-per-billion levels.

Early research defined three benzaldehydes that were investigated as potential indicators: paradimethylaminobenzaldehyde (PDAB), vanillin, and para-anisaldehyde. PDAB is known to produce an intense yellow color and is used as an indicator in an established wet-chemical analysis method. These three compounds were examined for reactivity as coatings on substrate materials by exposure to controlled vapor streams of monomethylhydrazine (MMH) and hydrazine. After initial testing of the compounds, it was decided to continue to the next phase (field testing) with the vanillin chemistry.

Approach

The hydrazone formed from vanillin absorbs at 420 nanometers giving a yellow color. From the absorbance reading taken on several standard solutions, it is apparent that the color development is linear. Several substrate materials were considered and tested. The vanillin was successfully coated on silica gel plates and packing, amberlite IRC-50(H) resin, and filter paper. The filter paper is a convenient substrate for laboratory testing and will be used in the field evaluation.

Results

Laboratory testing indicated that vanillin responds to 200-parts-per-billion MMH in approximately 10 minutes. The stain intensity is proportional to the dose. A

color wheel was developed to allow quantitation of the exposure. The badge exposure can be interpolated from a comparison of the badge color with the wheel containing colors equivalent to 0.07, 0.14, 0.48, 1.1, and 3.8 ppm-hours of MMH exposure. The stain is stable for 8 hours or more and, when acidified, is stable for weeks. The color development was retarded in very dry atmospheres; however, once the sample received moisture, the color developed. This effect was mild for the MMH reaction and more pronounced for hydrazine.

A prototype system was developed and incorporated into the citrate passive dosimeter field evaluation conducted at the John F. Kennedy Space Center. This opportunity was taken to evaluate the chemistry for interference effects. No significant problems were detected. The prototype consisted of a vanillin-coated filter paper functioning as a passive colorimetric badge and the color wheel for dose estimation.

Contacts:

*J. C. Travis and R. C. Young, 867-4438,
DL-ESS-24*

Participating Organizations:

*Naval Research Laboratory (S. Rose-Pehrsson)
GEO Centers, Inc. (P. Taffe)*

NASA Headquarters Sponsor:

Office of Space Flight

GMD Badge Test

Objective

To evaluate the performance of the GMD Systems, Inc., colorimetric dosimeters for the detection of monomethylhydrazine (MMH) and hydrazine.

Background

Under Small Business Innovative Research (SBIR) Phase II funding, GMD Systems, Inc., has developed two chemical

systems for passive colorimetric dosimeters. One is the vanillin system invented and patented by GEO Centers, Inc., and the Naval Research Laboratory. The other system, paradimethylaminobenzaldehyde (PDAB), was taken from a known method of wet chemistry for hydrazine analysis.

Approach

A laboratory test plan was devised that evaluated the following performance parameters of the dosimeter for MMH exposures: reproducibility, accuracy, linearity, stain development and stability, humidity effects, and chemical interferents.

An abbreviated test was conducted for hydrazine. It included the same parameters as the tests for MMH, except the interference testing.

Results

The badges contained two sections: one exposed directly to the environment and the other shielded with a diffusion membrane. The membrane was to reduce the amount of MMH that reached the indicator resulting in an extension of the linear range. Initial results indicated that the diffusion membrane did not function properly. The response was not linear with dosage and was affected by humidity. Based on this information, new badges were made that did not have the membrane.

The color standards for the PDAB chemistry did not resemble the actual stain colors. This made it difficult to evaluate the performance. In general, the vanillin was slightly more sensitive than the PDAB and required less time to develop (except when used in less than 10 percent relative humidity). After modifying the color dose estimator for the PDAB, both chemistries performed well in laboratory testing. The field test results have shown that PDAB turns yellow upon exposure to sunlight and vanillin turns purple upon exposure to tobacco smoke. These colors are different

than colors produced by MMH and thus would not produce a false positive. They do, however, affect MMH readings as the dosimeter no longer has a white background and could confuse the user.

Contacts:

*J. C. Travis and R. C. Young,
867-4438, DL-ESS-24*

Participating Organizations:

*Naval Research Laboratory (S. Rose-Pehrsson)
GEO Centers, Inc. (P. Taffe)*

NASA Headquarters Sponsor:

Office of Space Flight

Rocket Engine Leak Detection Mass Spectrometer (RELDMS)

Hazardous Gas Detection Systems (HGDS's) are currently in use in the Space Transportation System (STS) as ground-based monitors for propellant gas leaks. Similar systems are used or are being studied for use in the Expendable Launch Vehicle (ELV) programs. The period of time in which leaks are most likely to occur is during the terminal countdown phase, at the point the engines are fully pressurized. Due to sample transport times and other delay factors, these systems cannot monitor the final countdown phase, which includes engine startup and ends with vehicle lift-off. The RELDMS program was established to develop technology to solve this problem.

The objective of this project is to study, design, fabricate, and test a preprototype RELDMS; to fully characterize its performance and costs; and to identify all issues associated with its use as flight equipment. The products of this project will enable the Government to evaluate the usefulness of RELDMS for the Advanced Launch System (ALS) program.

Substantial gains in launch system reliability and safety can be obtained by the use of an HGDS that can detect leaks in the final countdown phase to allow safe

vehicle shutdown prior to lift-off. The ALS is a joint United States Air Force/NASA program to develop the next generation ELV. This program has stringent cost, turn-around time, and reliability goals. The purpose of this project is to further these goals by demonstrating that a RELDMS can be developed to perform the HGDS function in the final phase of countdown and possibly during a portion of powered flight. The ALS vehicle will be designed to have an engine-out capability; that is, if problems arise in one engine, it may be shut down before a catastrophic event occurs, and the vehicle could achieve orbit with the remaining functional engines. It is possible that information supplied from RELDMS to the flight computers could be used as an aid in making the decision on engine shutdown.

The RELDMS unit will be a lightweight (less than 50 pounds), small (less than 1 cubic foot) mass spectrometer gas analyzer for performing hazardous gas detection in the aft compartment of the Advanced Launch System (ALS) or Space Shuttle or on an umbilical arm connected to the vehicle. The RELDMS will be mounted on or near the ALS engines and draw in gas samples in close proximity to engine fittings most likely to leak. The RELDMS, by being small and close to the engines, will have a very short response time and, thereby, overcome the primary limitation of the present HGDS on the Mobile Launch Platform, which can provide leak detection down to slightly less than T-1 minute. The RELDMS will provide hazardous gas detection from T-60 seconds through the ignition of the engines, thereby improving the chances of performing an on-pad abort in the event of a serious leak. Additionally, the RELDMS will provide vehicle aft-end characterization data during ascent.

The RELDMS will be configured to measure quantities of hydrogen (H₂), helium (He), oxygen (O₂), nitrogen (N₂), and argon (Ar). H₂ and O₂ are propellants, N₂ is a purge gas, He is used for purge and

pneumatic power, and Ar is an indicator of air intrusion. The RELDMS will sample from as many as six areas sequentially.

The technical requirements for the RELDMS will be based on Space Transportation System (STS), Saturn V, and ELV program requirements since the characteristics of the ALS vehicle are not yet defined.

RELDMS could possibly perform one or all of the following missions:

- a. T-60 seconds to T-0 leak detection; compartment averages
- b. T-60 seconds to T-0 leak detection; engine specific
- c. Real-time leak detection during ascent; compartment average
- d. Real-time leak detection during ascent; engine specific
- e. Leak detection during engine refurbishment and checkout
- f. Real-time leak detection during static test firings in the developmental stages of ALS engine design
- g. Real-time leak detection during ascent only for ALS development flight

If RELDMS has localized a leak to specific joints or engine areas, then the time required to fix an on-pad leak could also be significantly reduced. RELDMS will require maintenance; therefore, its maintainability and reliability will be major factors in determining its contribution to reducing overall ALS maintenance costs.

The primary technical challenge of the RELDMS project is to develop a miniature mass analyzer that meets the detection requirements in a high-vibration environment. The project will first develop a larger preprototype that contains a flight-weight mass analyzer to demonstrate that

the concept is sound. The preprototype will then be used in actual engine firings on static test stands to demonstrate its performance in a live firing environment. Based on these demonstrations and cost projections, the United States Air Force will determine if RELDMS will be sufficiently beneficial in meeting ALS goals to make it an ALS requirement.

RELDMS technology has many other potential uses in rocket and jet propulsion systems in detecting leakage in high-vibration environments.

Contacts:

*J. D. Collins and F. W. Adams,
867-4438, DL-ESS-24*

Participating Organization:

Boeing Aerospace Operations, Engineering Support Contract (M. J. Blankenship and S. O. Starr)

NASA Headquarters Sponsor:

Office of Space Flight

Evaluation of Ammonia Sensors for Toxic and Flammable Concentrations

Processing of Space Station Freedom elements at KSC will involve the use of substantial quantities of anhydrous ammonia (NH_3). Since NH_3 is toxic at low concentrations and flammable at high concentrations, it will be necessary to monitor the NH_3 concentrations at each of these levels. Since there has been no significant use of NH_3 at KSC in the recent past and little is known about the performance of various commercially available monitors, this evaluation program should provide valuable information.

Background

Within the Space Station Processing Facility (SSPF), portable ammonia sensor carts will be used near payload elements containing NH_3 . If a leak should occur, personnel will be evacuated from the vicin-

ity. Ammonia vapor concentration will be tracked through remote displays in order to understand the magnitude of the leak. If a significant quantity of NH_3 has leaked, flammable level ammonia sensors will be used to assess the possibility of fires.

In addition to portable sensors, fixed-point ammonia sensors will be mounted at the ceiling level of rooms where NH_3 is used in order to detect any accumulation of ammonia vapors (which are less dense than air). These fixed-point sensors will detect NH_3 at the toxic level for personnel protection.

Approach

The threshold limit value (TLV) of NH_3 is 25 parts per million, and the lower flammable limit of NH_3 in air is 16 percent. Since these two concentrations differ significantly, different instruments will be required. Instruments from each of the different technologies used in NH_3 measurement will be purchased and evaluated for stability, linearity, accuracy, and precision. Instrument technologies to be evaluated include electrochemical cells, semiconductor sensors, catalytic combustion, and

nondispersive infrared.

Because ammonia vapors are unstable, the NASA Toxic Vapor Detection Laboratory has developed the capability to mix ammonia standards from anhydrous NH_3 , using either air or nitrogen. Analysis of ammonia vapors is performed in accordance with ASTM D1426, Part B (Nesslerization).

Results

To date, candidate instruments from each technology have been purchased, and evaluation procedures are being written. Laboratory procedures for mixing and analysis of ammonia vapors have been developed along with corresponding safety plans. Design and fabrication of a sampling system is underway.

Contacts:

*P. A. Mogan, R. C. Young, and J. C. Travis;
867-4438; DL-ESS-24*

Participating Organization:

*McDonnell Douglas Space Systems Company
(H. Allen)*

NASA Headquarters Sponsor:

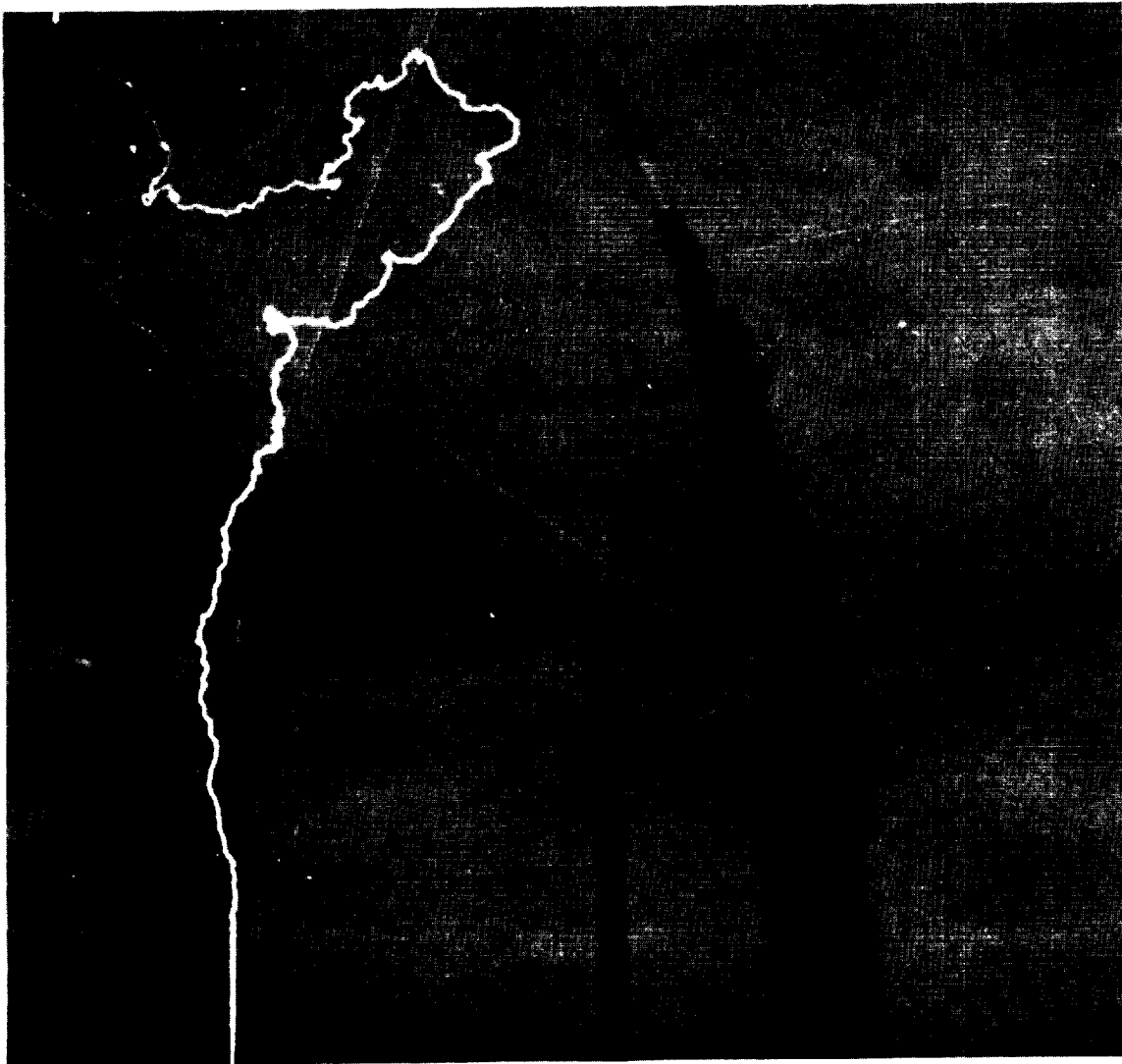
Office of Space Flight

Meteorology

The Atmospheric Science Field Laboratory

The Atmospheric Science Field Laboratory was established at the John F. Kennedy Space Center (KSC) to provide a focal point for thunderstorm and lightning studies. The laboratory has the tools and expertise to delve into all aspects of lightning phenomena, including measurement of

electric and magnetic fields, space charges, and lightning current densities. Data produced by the laboratory's research efforts are used to improve forecasting accuracies, design lightning detection equipment, and optimize lightning protection equipment and systems. The latest and primary research activity supported by the laboratory is the rocket-triggered lightning program.

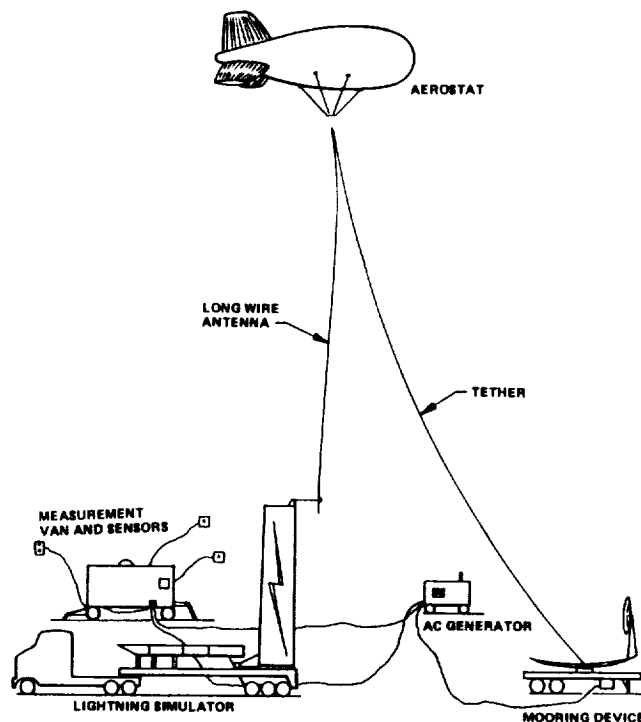


ORIGINAL PAGE
BLACK AND WHITE PHOTOGRAPH

Simulated Lightning for Research Studies

A 6-million-volt Marx generator was recently acquired by KSC on loan from Wright Patterson Air Force Base for use in lightning simulation studies performed jointly by the Eastern Space and Missile Center and KSC (see the figure "Six-Million-Volt Lightning Simulator"). The generator is 9 feet wide, 84 feet long, and 19 feet high in the horizontal retracted position. In operation, it is raised to a vertical position and is about 65 feet tall. It weighs approximately 110,000 pounds. To reduce series inductance, the generator uses two 6-million-volt generators operating in parallel to give a short-circuit current of 60,000 amperes at 6 million volts. The total energy produced is about 150,000 joules.

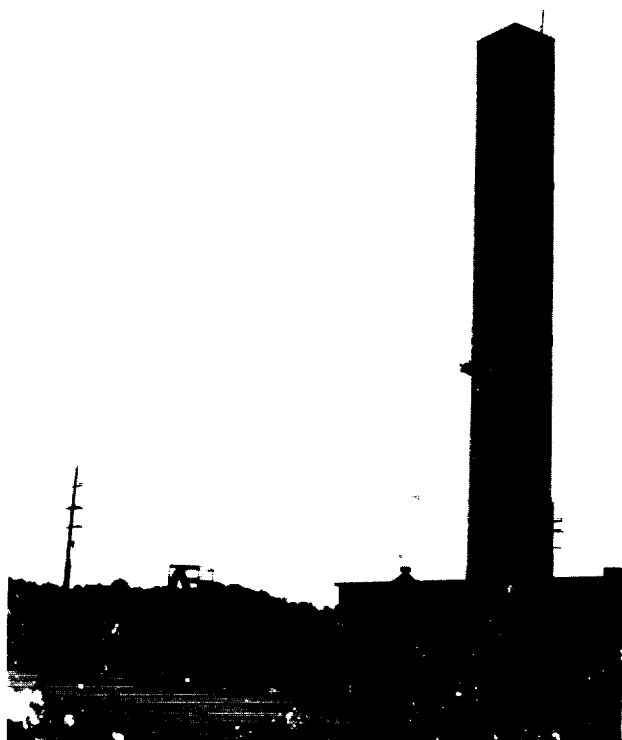
One application for the generator is to produce high voltages and currents in a balloon-supported antenna (see the figure "System Configuration for Generating Electromagnetic Fields") that radiates



System Configuration for Generating Electromagnetic Fields

electromagnetic fields with characteristics similar to those of lightning. The current into the antenna is limited by the antenna impedance, typically of the order of 1,000 ohms. The rate-of-rise of current is limited by the generator inductance of about 80 microhenries. The current moment and waveform period depend on the antenna length. The velocity of propagation is typically the speed of light. The result is a decaying rectangular current waveform with a high rate-of-rise of current over 60,000 amperes per microsecond, with a 6,000-ampere peak, and with a period of about 20 microseconds for a balloon height of 5,000 feet. The electromagnetic radiation will be produced at known locations and used to help calibrate lightning location systems.

Another application for the generator is to inject known currents at typical lightning attach points on facilities thought to be vulnerable to lightning. These facilities usually house operations critical to Shuttle systems where the induced effects of light-



Six-Million-Volt Lightning Simulator

ning could cause serious equipment damage. The currents would be injected at low levels and the results monitored by sensitive electromagnetic measuring equipment to keep the equipment in the facility safe from damage. The measurements would then be extrapolated to full-threat levels and compared with the susceptibility of the equipment housed in the facility. This evaluation would then lead directly to modifications to correct the problems identified, resulting in the elimination of equipment damage and the possible relaxation of work restrictions during lightning warning periods.

Most applications involve equipment or ordnance protection. In a few cases, such as guard shacks, the generator can also be used to identify and correct personnel hazards. The methods of protection and the special hardware that will be developed can be applied to all lightning protection systems and can be made available to the public through the NASA technology transfer.

Contact:

W. Jafferis, 867-4438, DL-ESS-24

Participating Organization:

Boeing Aerospace Operations, Engineering Support Contract (J. R. Stahmann)

NASA Headquarters Sponsor:

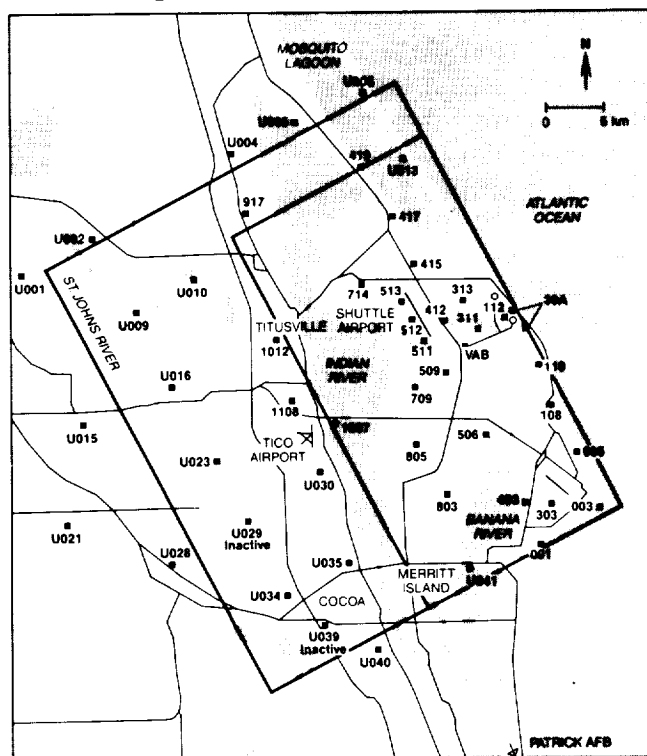
Office of Space Flight

Short-Term Forecasts Using Wind Divergence

In 1987, KSC began operating a mesonet network of wind, temperature, and relative humidity sensors in the St. Johns River Basin for the purpose of evaluating the usefulness of a dense set of data for predicting summer thunderstorm development. Earlier studies had indicated that "forcing" of vertical motion of moist surface air contributed substantially to the growth of clouds of vertical development and that dense measurements of wind velocities at

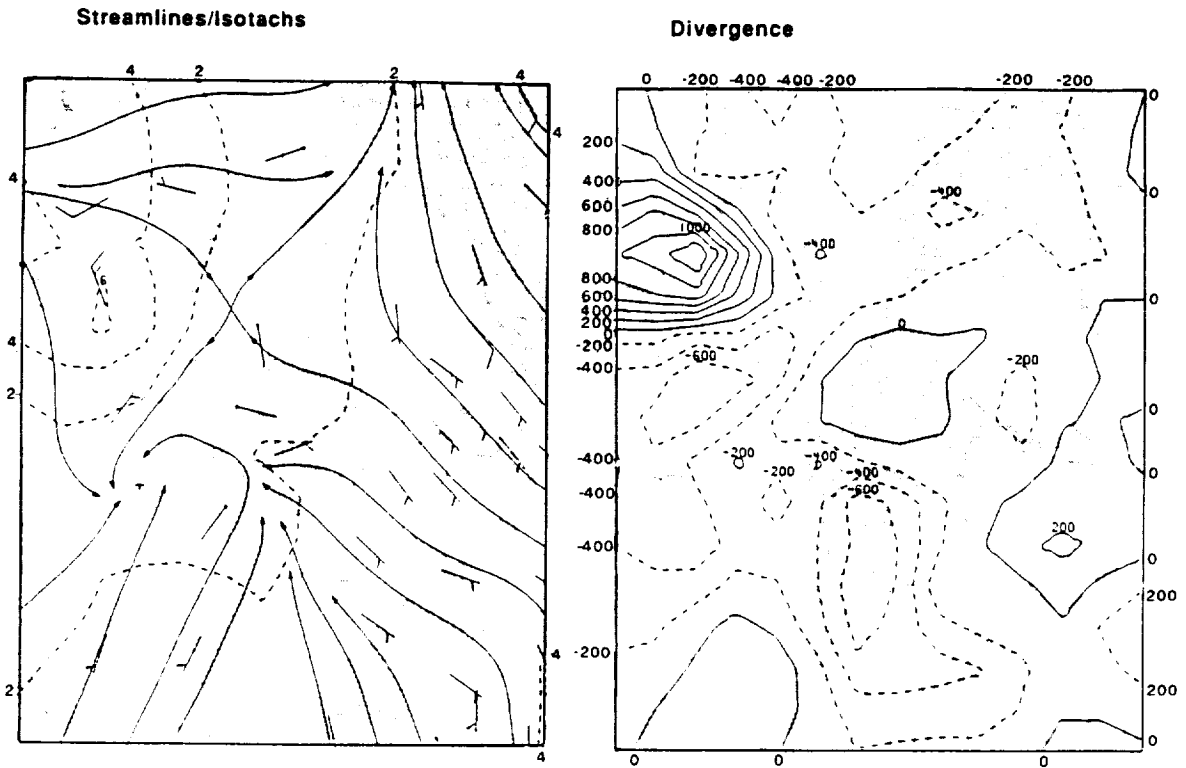
the surface would provide data to quantify this "forcing." The data gathered, when added to the data gathered at KSC and Cape Canaveral Air Force Station (CCAFS) by the Weather Information Network Display System (WINDS), covered an area approximately 35 by 40 kilometers. The figure "Full KSC and Eastern Space and Missile Center Mesonet network" depicts the total network of meteorological sensors. The Mesoscale Research Division of the National Oceanic and Atmospheric Administration (NOAA) National Severe Storms Laboratory has been studying the relationship of wind flow and lightning using data gathered by this network.

A measure of "forcing" the rising of air is called convergence (the negative of divergence) and can be calculated from wind velocities. In the figure "Mesonet network Analyses for 30 July 1987," an area of wind convergence can be seen in the left center of the flow pattern that is depicted in "Streamlines/Isotachs," and the contours of convergence (dashed lines) calculated



Note: The smaller rectangle marks the 1985 to 1986 network boundary. The larger rectangle marks the 1987 expanded mesonet network. Solid squares indicate meteorological stations.

Full KSC and Eastern Space and Missile Center Mesonet network

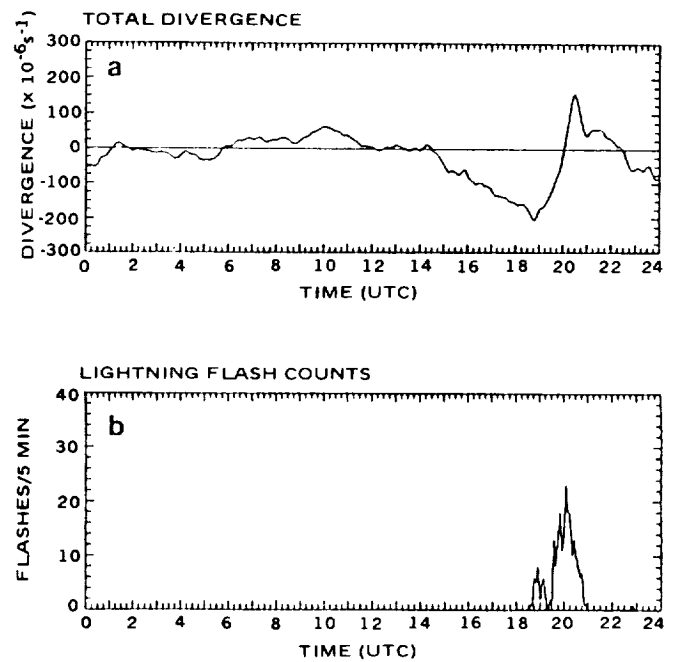


Mesonetwork Analyses for 30 July 1987

from the wind velocities are shown in "Divergence." Both the flow pattern and the contours indicate a concentration of inflowing moist air in the left-center part of the area depicted. A thunderstorm developed in that locale about an hour after the time of the depiction.

An index of the "forcing" of cloud development, called total area divergence, helps to follow the trend in time of the "forcing" over the total area covered by wind sensors. In the figure "Time Profiles of Divergence and Lightning," the trend of this quantity on a summer day is illustrated in "Total Divergence," and the count of ground lightning flashes that occurred within the mesonetwork is illustrated in "Lightning Flash Counts." The downward trend of divergence seen in "Total Divergence" can be idealized as a "signature"; the study indicates that a decrease of 50 units sustained for 15 minutes or longer often precedes the onset of lightning by 30 minutes to 1-1/2 hours. The table "Divergence-Lightning Statistics" displays the results of the study of data for the sum-

mers of 1987 and 1988 (June 1 to September 30). The first row shows the results for all days, irrespective of large-scale wind flow direction.



Time Profiles of Divergence and Lightning

Divergence - Lightning Statistics

Flow Regime	Regime Days	Days With Lightning	Convergence Events	Lightning Events	Average Total Flashes	Δ Divergence ($\times 10^4 s^{-1}$) (All Events)	Δ Divergence ($\times 10^4 s^{-1}$) (Lightning Events)	Lightning Misses	Average Total Flashes per Miss	No. Missed Lightning Events With One Flash
NE	51	14	62	8	6.5	-73	-85	11	7.6	4
SE	62	33	102	32	42.4	-85	-113	27	6.1	13
SW	78	56	99	51	210.6	-107	-130	35	18.8	17
NW	12	4	10	3	38.6	-98	-95	6	4.2	4
Calm	39	12	49	12	139.0	-83	-106	5	2.0	2
Total	242	119	322	106	130.7	-89	-118	84	11.2	40

Note: Based on 1987/1988 KSC expanded mesonetwork data with a divergence threshold of $-50 \times 10^4 s^{-1}$.

The table "The 'If-Then' Rule Statistics for All Cases" shows the application of a simple "if-then" rule, based on the values quoted in the preceding paragraph, which yielded a probability of detection of 0.56 (that is, 56 percent of the ground lightning episodes were predicted). A false-alarm ratio of 0.67 occurred (that is, 67 percent of the cases where blind application of the simple "if-then" rule, if made, would have predicted lightning onset to occur when it

did not). One of several reasons that accounts for this was the fact that the thermal and moisture structure of the atmosphere will sustain or inhibit cloud growth that is "forced" from the surface of the earth. The false alarms arose because of this factor; the matter is addressed in another development project that is under-

"If-Then" Rule Statistics for All Cases

		Lightning Event		Sum
		Yes	No	
Convergence Event	Yes	106	216	322
	No	84	5,402	5,486
Sum		190	5,618	5,808
Probability of Detection				0.56
False Alarm Ratio				0.67
True-Skill Statistic (perfect score: 1.0)				0.52

Notes:

1. The probability of detection is calculated by taking the ratio of the Convergence-Event-Yes and the Lightning-Event-No value and the Convergence-Event-Yes Sum value.
2. False-alarm ratio is calculated by taking the ratio of the Convergence-Event-Yes and Lightning-Event-No value and the Convergence-Event-Yes Sum value.

Convective Triggering Mechanisms

Weather Event	No. of Occurrences*
Seabreeze (Eight events developed on the NW boundary and moved back across KSC.)	24
Gustfront Intersection (Nine events were outflow boundaries intersecting the seabreeze.)	12
Gustfront	10
Maritime Convection	4
Squall Line	3
Mesoscale Convective System (MCS)	2
Trough Passage	1
Other	1
Total	57

* Includes only lightning events of ten or more ground flashes.

way. A hypothetical system that checks every 20 minutes for the presence of the precursor signature in the trend line during the 8-hour period of each day requiring greatest vigilance yields a true-skill statistic of 0.52 (1.0 represents a perfect score). (The reader can appreciate the vigilance required to conduct a weather watch on a Florida summer day by noting that the number of checks for the signature would have totaled 5,808 over the two-summer period.)

The table "Convective Triggering Mechanisms" displays the weather phenomena that produced lightning episodes of ten or more ground flashes per episode during the summer of 1987. "Forcing" due to the sea breeze accounted for a substantial number of such lightning episodes.

Contacts:

*J. R. Nicholson, 867-2780, PT-AST
R. J. Wojtasinski, 867-4993, TE-CID-3*

Participating Organization:

*NOAA/ERL/National Severe Storms
Laboratory (A. I. Watson, R. L. Holle,
and R. E. Lopez)*

NASA Headquarters Sponsor:

Office of Space Flight

Kennedy Atmospheric Boundary Layer Experiment (KABLE)

Objective

The objective of this two-year project is to collect meteorological data during the first year and analyze the three-dimensional structure of the planetary boundary layer (PBL) at Merritt Island/Cape Canaveral during the first and second year. The data were collected from October 1988 to September 1989 and are being used to validate and improve the transport and diffusion algorithms in operational models, such as the Emergency Dose Assessment System (EMERGE) which supports the

Galileo and Ulysses missions and the Rocket Exhaust Effluent Diffusion Model (REEDM) used at KSC and Cape Canaveral Air Force Station (CCAFS).

Background

NASA and the U.S. Air Force have many critical operations occurring at KSC/CCAFS. These operations depend heavily on meteorological conditions; therefore, an understanding of the local meteorology is needed.

Approach

The approach taken by this project is to:

1. Collect data
2. Develop a complete and well-organized database to facilitate data retrieval, distribution, and analyses
3. Analyze data
 - a. Validate the sea-breeze algorithm in EMERGE
 - b. Evaluate the REEDM model

Results

As of this writing, data collected for the fall period of 1988 was analyzed to determine sea-breeze characteristics in the KSC/CCAFS area. Analysis of the data has yielded several useful and interesting results:

1. Detailed characteristics of the sea breeze onset time, depth, propagation speed, inland penetration, and associated stability were determined on several days. In addition to the main sea breeze, a local Indian River breeze was documented by analysis of wind tower and acoustic sounder data. The Indian River breeze was found to have the effect of retarding the main sea-breeze frontal speed across KSC/CCAFS.

2. The stability parameters before and after sea-breeze conditions were evaluated on several days with sea breeze. It was generally found that turbulence in the PBL increased up until the passage of an Indian River breeze or sea breeze; it then decreased the remainder of the day. It was also found that the stability parameter values from wind towers were a good indicator of sea-breeze frontal passage, reaching a peak just prior to frontal passage and decreasing thereafter.
3. Seawater temperature may not be representative of the over-water air temperature. Air temperature at the offshore data buoy should be considered when evaluating the temperature differential required for a sea breeze.
4. KABLE data was used to help evaluate the sea-breeze algorithm in EMERGE. A number of sea-breeze parameters (for example, stability, wind speed, gradient wind, water-to-land temperature difference, and depth of sea breeze) were found to compare favorably with KABLE data; however, there were a few significant exceptions. For instance, the KABLE data showed an average sea-breeze propagation speed of 1 to 3 meters per second, compared to the value of 3 to 5 meters per second used by EMERGE; and the sea-breeze depths, as determined from KABLE data, were somewhat lower than depths used by EMERGE. In addition, the EMERGE sea-breeze algorithm would have terminated the sea breeze sooner than was observed during KABLE. The KABLE data was used to improve the real-time use of the EMERGE during the Galileo launch.

The KABLE analyses will continue until October 1990.

Contact:

A. J. Guerra, 867-4888, RT-SAF-3

Participating Organization:
 Ensco, Inc. (G. E. Taylor, Ph.D.)

NASA Headquarters Sponsor:
 Office of Space Flight

Forecasting Cloud Growth Using Satellite Sounding

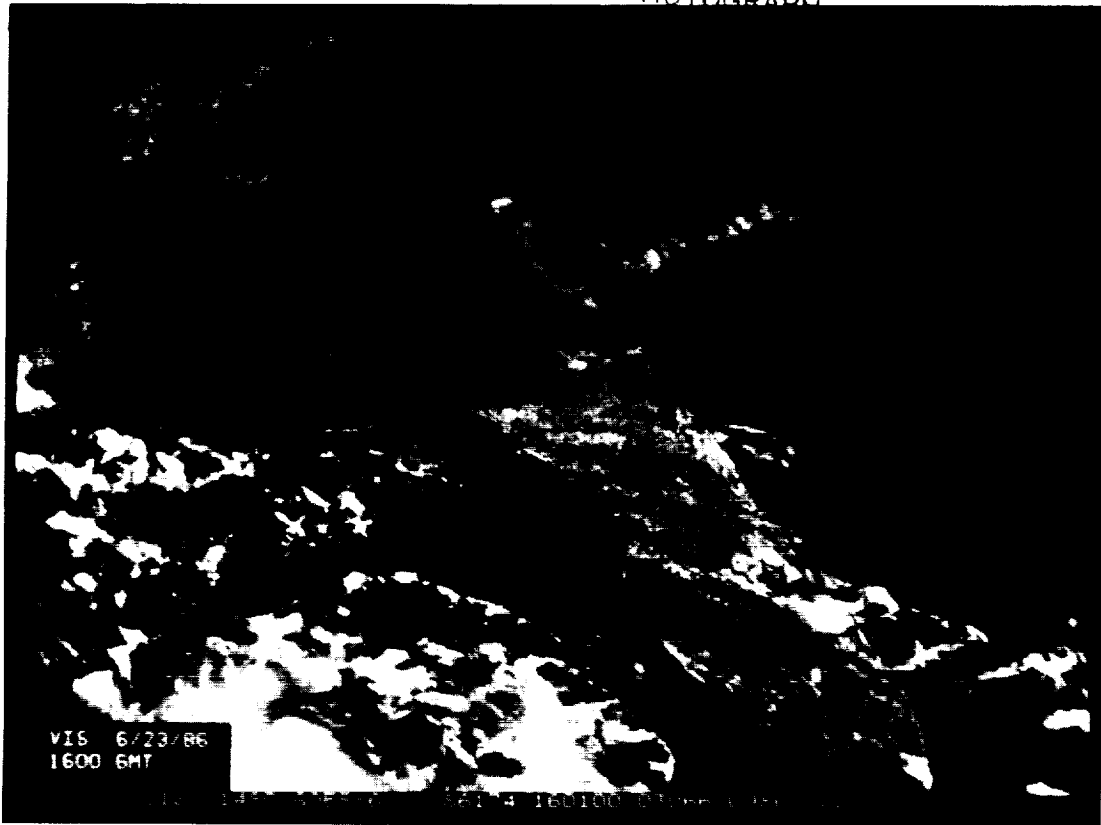
The atmospheric temperature and moisture distribution conditions encountered by a convective cloud after it is initiated will sustain or inhibit the growth of the cloud: very dry atmosphere shortens its life, a temperature inversion layer may limit vertical growth, and an unstable atmosphere sustains its growth.

Temperature and moisture profiles are measured at 12-hour intervals at six stations in Florida. The stations are widely separated. The temporal and spatial resolution of these profiles provides little information concerning the variation of weather parameters across the State. Radiometers aboard geostationary satellites now can provide temperature and moisture profiles at many points and at intervals of 1-1/2 hours. While the profiles lack some of the vertical resolution of conventional soundings, they may provide greater temporal and spatial resolution in the horizontal.

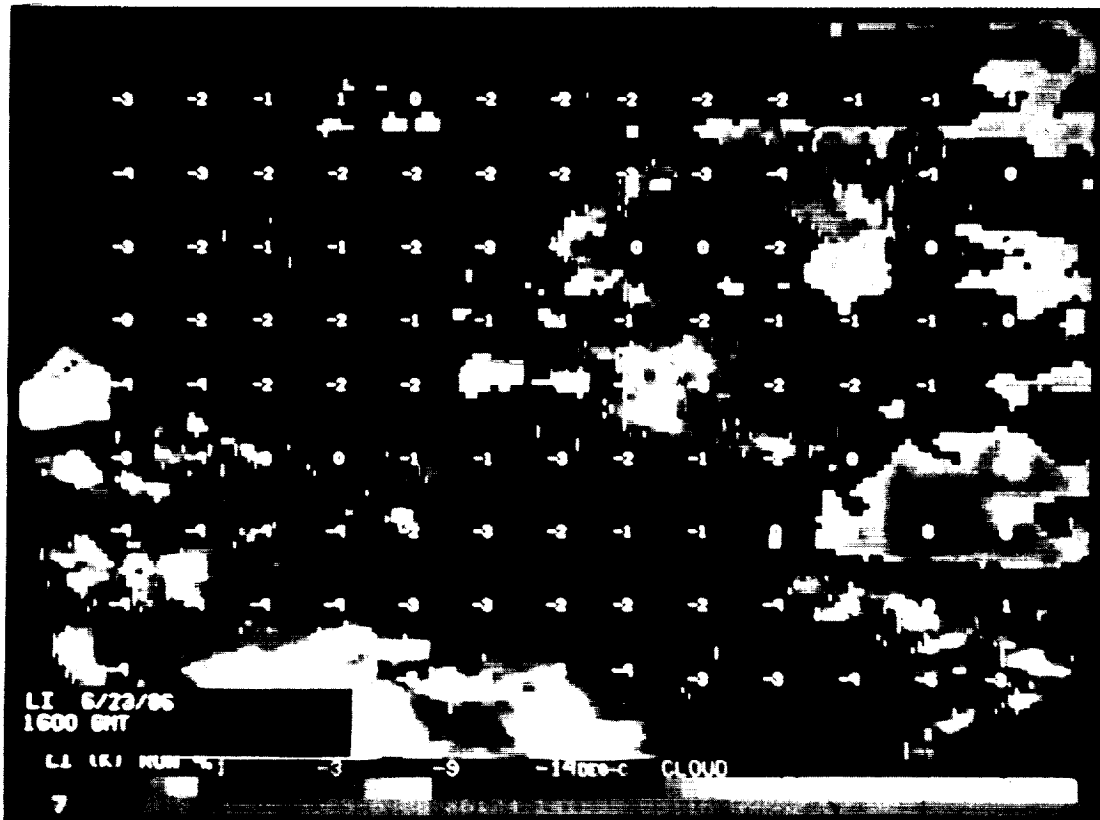
The figure "Satellite View of Clouds Over Florida" shows the cloud distribution over Florida on a summer day. The figure "Florida Locations of Derived Vertical Profiles" displays numbers at locations where satellite profiles of temperature and moisture were acquired. The improvement in density of observations is manifest.

The figure "Profiles Over North-Central Tennessee" displays vertical temperature and moisture profiles from north-central Tennessee acquired during a 3-hour period, shown in Greenwich mean time (GMT). The profile locations in this figure are the circled dots in the figure "Satellite-Derived Contours of Dewpoint Temperature." The

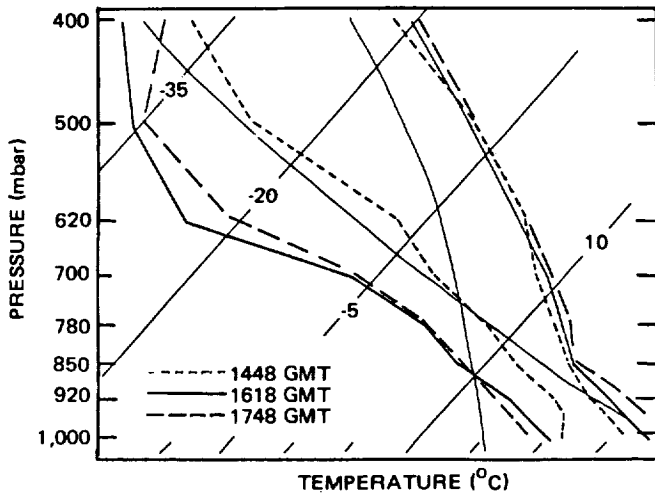
ORIGINAL PAGE
BLACK AND WHITE PHOTOGRAPH



Satellite View of Clouds Over Florida



Florida Locations of Derived Vertical Profiles

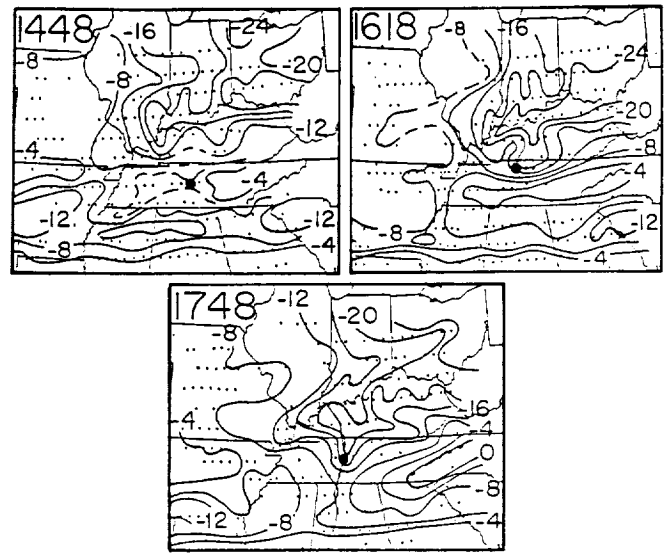


Profiles Over North-Central Tennessee

three left-hand profiles are the moisture profiles. They reveal a distinct decrease of moisture content in time. This information would not have been available from profiles acquired by conventional means.

The figure "Satellite-Derived Contours of Dewpoint Temperature" displays contours of moisture content in the Ohio River Valley region at an approximately 14,000-foot altitude at the times of the profiles shown in the figure "Profiles Over North-Central Tennessee." The dots represent locations of the profiles upon which the analysis is based. The large negative values represent very dry air. Because the analysis includes many profiles not possible to acquire by conventional means, much detail is revealed that would otherwise be lacking.

The application of satellite temperature and moisture profiles to the prediction of convective cloud growth and distribution



Satellite-Derived Contours of Dewpoint Temperature

over Florida is being studied under a grant to Florida State University. Profiles descriptive of important weather cases that occurred during the past summer are being produced. This will demonstrate the effectiveness of the technique required to produce the profiles. It will also permit determination of factors that caused clouds to grow as they did and to be distributed as they were.

Contacts:

*J. R. Nicholson, 867-2780, PT-AST
R. J. Wojtasinski, 867-4993, TE-CID-3*

Participating Organization:

*Florida State University
(Prof. H. Fuelberg)*

NASA Headquarters Sponsor:

Office of Space Flight

010
01000000

Autonomous Systems

Autonomous systems research and development efforts at the John F. Kennedy Space Center (KSC) are focusing on applying artificial intelligence and robotics technology to the Space Shuttle's ground processing and launch operations. The Artificial Intelligence Laboratory and the Robotics Applications Development Laboratory are engaged in this application process.

The Robotics Applications Development Laboratory

The Robotics Applications Development Laboratory is used for prototyping and testing of robotic systems that will be capable of performing many of the mechanical ground processing functions for the Space Shuttle and associated payloads. Elements in the design and evaluation stage include: stereo and structured laser three-dimensional vision systems, real-time reactive and adaptive control systems, and a variety of force/torque and proximity sensors. Some of the applications being investigated are remote umbilical mate/demate operations, hypergolic servicing,

automated Orbiter tile and radiator inspection and maintenance, and plant growth chamber automation.

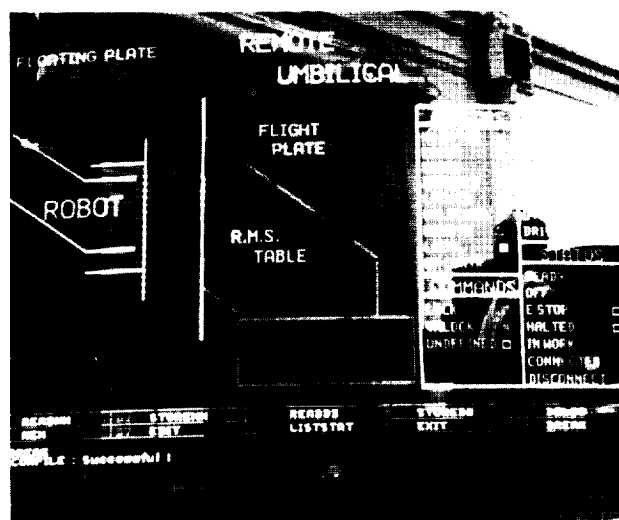
The Artificial Intelligence Laboratory

The Artificial Intelligence Laboratory provides the capability to investigate and develop artificial intelligence/expert systems technology needed by the Space Shuttle program to streamline checkout and launch operations. The laboratory serves as a working environment for systems domain experts and software programmers. It houses specialized computers (10 symbolic processors) and 13 general-purpose personal computers plus peripherals. The laboratory is involved in the analyses or developments of: a launch pad, liquid-oxygen-loading system; a thunderstorm weather forecasting expert system; an electrical field mill network analysis (lightning threat); intelligent launch decision support system (launch feasibility management tool); and a knowledge-based autonomous test engineer (autonomous control, monitoring, fault recognition, and diagnostics for troubleshooting).



ORIGINAL PAGE
BLACK AND WHITE PHOTOGRAPH

Robotics Applications Development Laboratory



Robotics Applications Development Laboratory



Artificial Intelligence Laboratory

Artificial Intelligence Mass Spectrometer (AIMS)

Objective

To show that artificial intelligence (AI) techniques could be applied to the mass spectrometer systems that exist at KSC.

Background

The Artificial Intelligence Mass Spectrometer (AIMS) project was initiated by the Engineering Development Directorate (DE) in an effort to address the problem of adding more mass spectrometers to an already-filled console in the firing room. In addition, consideration was to be given to the problem of maintenance and check-out of these complicated instrument systems in terms of reducing servicing time and operational manpower.

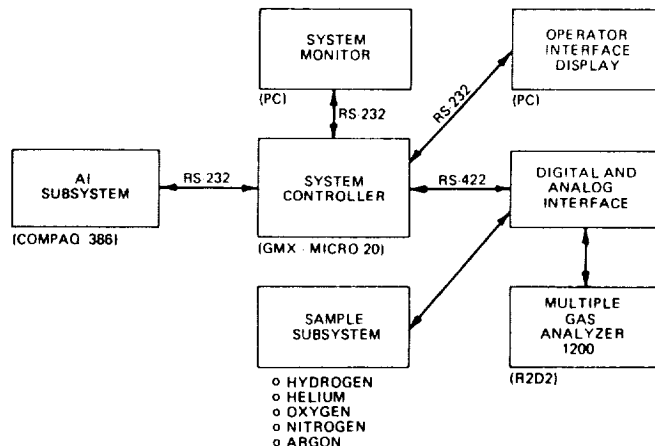
Approach

The goal of the project for 1989 was to model, within reasonable limits, an existing mass spectrometer system and apply AI methods for analysis, control, and operation. Several configurations were considered for use as a test bed; they varied in size and complexity from a software model to an operational and installed system on a Mobile Launcher Platform (MLP). The resources required to program a simulator within the timeframe allowed did not exist at KSC. An MLP could not be made available for temporary changes in configuration and did not provide the flexibility to be used as a test bed.

A laboratory multiple gas analyzer was chosen for the mass spectrometer model and a small representative gas sample system was built and added to the analyzer cabinet. The sample system was a subset of the design used for the Hazardous Gas Detection System (HGDS). The multiple gas analyzer is a Perkin-Elmer unit identical to the type used on the MLP's as part of the Backup Hazardous

Gas Detection System (B/U HGDS). A system controller was assembled from laboratory hardware that was readily available. The system controller was programmed to perform mass spectrometer control functions, provide timing, and act as a communications interface. The AI subsystem and the operator display was connected to the system controller via an RS-232 interface. The multiple gas analyzer and sample subsystem are optically isolated from the system controller. An RS-422 interface was used to pass control and data from the system controller to the optically isolated signal conditioning. The AI subsystem, operator interface display, multiple gas analyzer, and sample subsystem were all connected to each other through the system controller. The operator interface display provides a means for the operator to input commands and retrieve information from the system. This includes the normal data from the system controller and supplemental information from the AI subsystem as it relates to the current mode and configuration of the system.

The AI subsystem was designed to monitor, analyze, display, and pass information to the operator interface display, connected to the system controller. The AI subsystem gathered information from the multiple gas analyzer, sample system, and the operator via the system controller. The AI subsystem applied knowledge-based tech-



AI Mass Spectrometer Architecture

niques to provide information on the system's state, to question the validity of operator commands and sequences, and to provide alarm and warning functions based on the gas selected, the sample location, the concentration observed, and the time frame for the data reported.

Accomplishments

The design and interface of the sample subsystem and multiple gas analyzer to the signal conditioners took about 3 weeks. During this time, a method of controls and interlocks was built in along with additional sensors to allow for expandability for system diagnostics. About 6 weeks were required to write the control software interface for the multiple gas analyzer and sample subsystem. During the initial phases of the project, the information for the AI database was gathered, and operating procedures and parameters for system performance were established.

The operator interface display software was developed in parallel with the software for the AI portion of the project; this, along with timestamping and communications control routines, took about 3 months. A demonstration was held in early October to show that an AI subsystem can be used to monitor and act as an operator's aid in a mass spectrometer system. The AI subsystem can track system configuration, provide alarms to the operator, and warn of commands and situations that are incompatible with the system configuration; this information is based on the recent history of the system. The project was completed using only on-hand hardware and software.

Future Plans

As a result of the AIMS project, experience was gained in several areas, including the difficulties involved in trying to interface AI to a live system, knowledge-based design techniques, the limitations of currently used hardware and software, and

what the capabilities of an AI system can be.

Time will be spent in the months to come refining the definition of what constitutes a useful system configuration. Emphasis will be placed on locating better software tools and identifying the best hardware for this project. The final system must be resident on an MLP, provide for automatic checkout and calibration, aid technicians in troubleshooting, and provide operators with reliable and timely information on mass-spectrometer-based, launch-critical systems.

Contacts:

*J. D. Collins and F. W. Adams,
867-4438, DL-ESS-24*

Participating Organization:

*Boeing Aerospace Operations, Engineering
Support Contract (J. R. Dacus and
S. M. Simmons)*

NASA Headquarters Sponsor:

Office of Space Flight

Remote Maintenance Monitoring System

In its current configuration, the Launch Processing System (LPS) at KSC relies on over 200 ModComp computers to perform launch-critical monitor and control functions between the Space Shuttle and ground support equipment (GSE). While hard failures seldom present troubleshooting challenges, operational ModComp computer history shows that 17.4 percent of the intermittent failures are never found. Due to the system's nature, maintenance of these 200 computers is performed in an off-line environment; thus, making the task of troubleshooting and repairing the system both manpower and time intensive. When fully integrated into the LPS, the Remote Maintenance Monitoring System (RMMS) will function as an automatic maintenance diagnostics system capable of anticipating approaching failures and troubleshooting both hard and intermittent failures down

to the line replacement unit (LRU) level while expending minimum time and manpower.

Spanning a five-year development life cycle, the program schedule includes the development of the RMMS Phase I prototype, RMMS Phase II design and specification work, and RMMS Phase III demonstration and concept validation.

The Phase I prototype focused on the development of a proof-of-concept evaluation unit. This unit demonstrated the ability to implant data acquisition hardware into the ModComp computer, monitor various operating parameters and error conditions, and automatically diagnose the cause of the failure using the artificial intelligence (AI) facilities built into a knowledge-based maintenance diagnostics expert system.

Following the successful completion of Phase I, the start of Phase II represented the beginning of full-scale design and development toward the goal of producing a deliverable maintenance monitor. In its final configuration, the maintenance monitor will be able to capture ModComp data in real-time and subsequently use this information to anticipate failures, diagnose irregular or spurious system conditions, automatically analyze central processing unit (CPU) dump information to determine the source or sources of failure, and provide system maintenance engineers with an interface for performing real-time evaluation of ModComp parameters and processes. Design and development efforts required during Phase II include the specification of a dedicated LISP processor to host the RMMS expert system, an expert system shell to assist in the development of expert system software, and a stand-alone workstation to provide communication and control between the various blocks within the entire system. Additional specifications and designs required to complete Phase II include development work for the logged data monitor (LDM) (which provides CPU dump data logging), the CPU implant

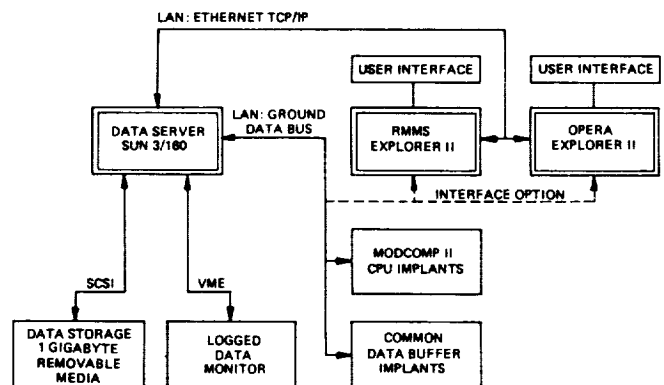
(which provides high-isolation interfaces and ModComp data acquisition hardware), and the common data buffer implant (which provides point-of-failure information following error detection within the buffer). Capable of enhancing the LPS with state-of-the-art technology, the RMMS concept efficiently incorporates continuous real-time monitoring of CCMS hardware, the central integration of various diagnostic data acquisition processes, and the automation of the diagnostic process.

The RMMS system architecture, which defines the major hardware and software components, is complete (see the figure "RMMS System Architecture"). The following is a description of the RMMS hardware components, their functions, and their associated embedded software.

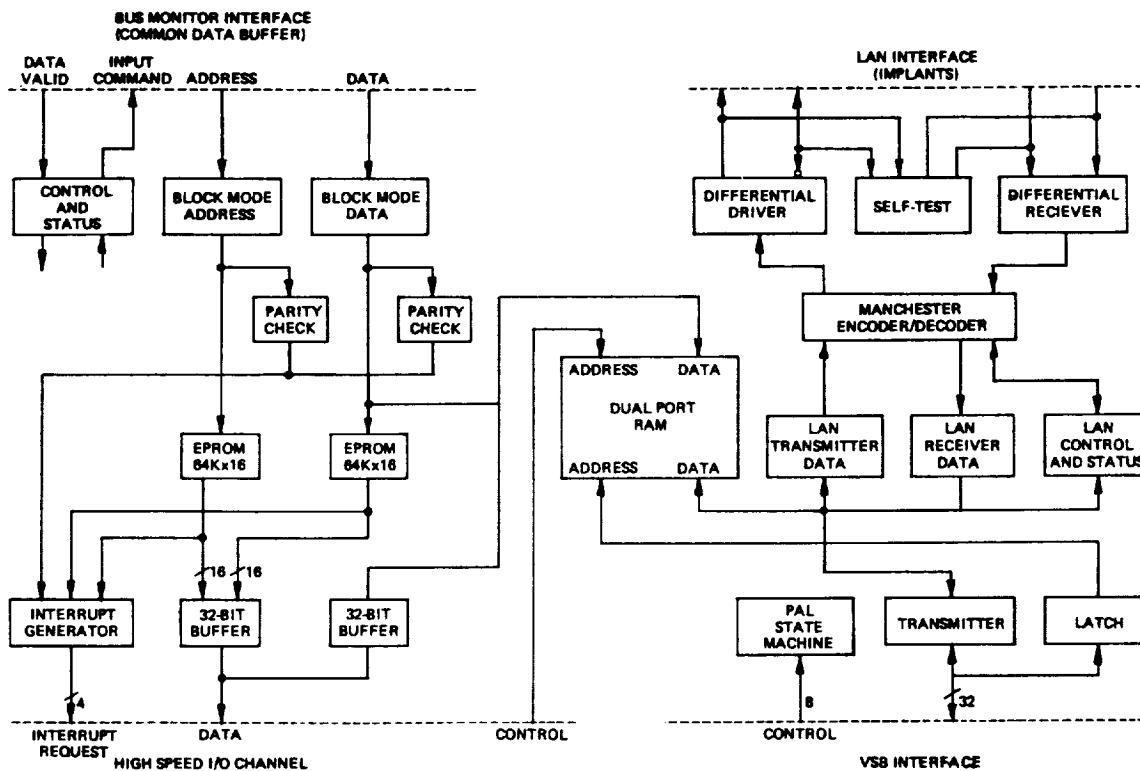
1. Logged Data Monitor

Function: The LDM filters ModComp system messages and data dumps from the common data buffer to the processed data recording (PDR) and shared peripheral area (SPA) information stream and transfers the messages and dumps to the data manager. System messages will be used by the Operations Analyst (OPERA) expert system, while data dump information will be used by the RMMS expert system.

Software: The LDM self-test and acquisition will be written in the



RMMS System Architecture



LDM Input/Output Board

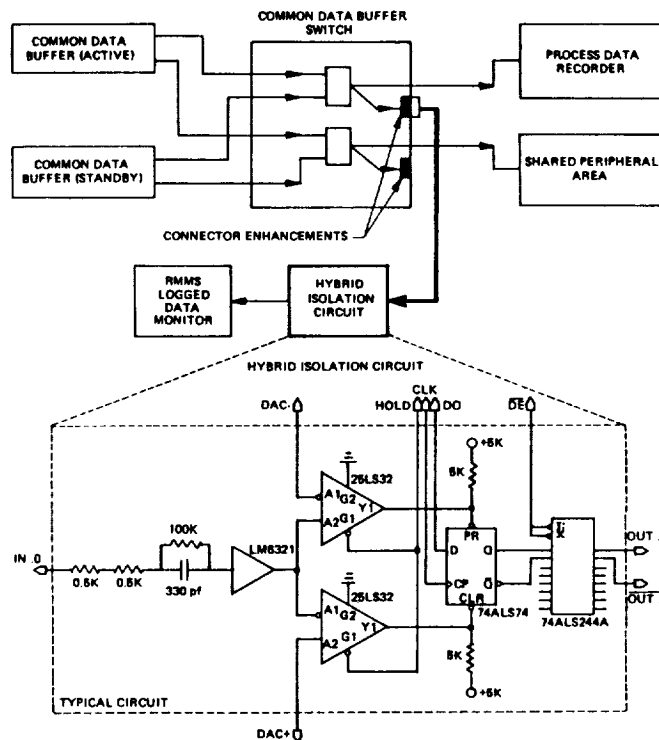
LDM's own microcode set. The command, data retrieval, and communication software will be written in "C" programming language and the 68030 assembly language using the VRTX real-time operating system and the Hyperlink VME backplane communication drivers.

Functional Description: Designed around the Sun 3/160 data manager, the LDM is a dual printed circuit board (PCB) set, which incorporates a CPU on one card and an input/output (I/O) controller on the second card. (See the figures "LDM Input/Output Board" and "RMMS PDR/ SPA Isolated Interface.")

2. Data Manager

Function: The data manager serves as the interface between the implants (data acquisition), the LDM, and the expert diagnostic system (data analysis). In addition, the data manager

serves as the system archiver and implant configuration controller.



RMMS PDR/SPA Isolated Interface

Software: A UNIX-based operating system will be used. The functional programming will be written in "C."

3. ModComp CPU Implant

Function: The ModComp CPU implant monitors and evaluates ModComp memory and register accesses, CPU/option plane handshaking operations, and option plane microcode execution and power supply voltages. It provides failure mode information through images and traces.

Software: The ModComp implant self-test and evaluation will be written in the implant's own microcode set. The command, data, and communication software will be written in the Z8002 assembly language.

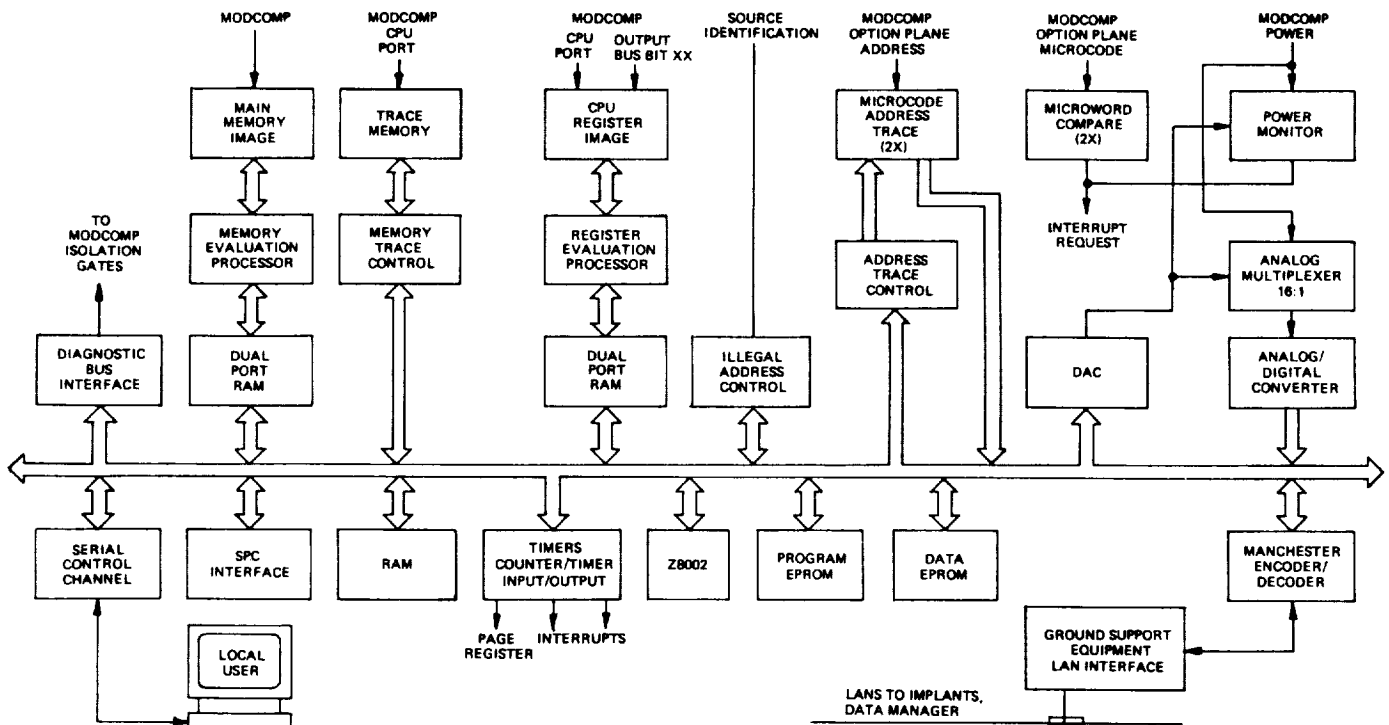
Functional Description: The CPU implant will be configured as a dual-printed circuit board set residing within one of the available card slots in the ModComp. Conceived as a large-

scale data acquisition system, the implant monitors the execution of various ModComp processes to detect impending failures. Subsequently, this enables the implant to create a "snapshot" look at the state of the machine prior to ModComp-detected errors and subsystem autodumps (see the figure "CPU Implant Block Diagram").

4. Expert System

Function: The RMMS expert system interfaces the user with the RMMS system. The expert system allows the user to analyze information from the ModComp implants, common data buffer (CDBFR) implants, and LDM using analyst tools and acquired knowledge from KSC system engineers.

Software: The expert system programming is in common LISP using Intellicorp's Knowledge Engineering Environment (KEE). Intellicorp's KEE is being used to develop the RMMS expert system on a Texas Instrument (TI) Explorer II.



CPU Implant Block Diagram

Functional Description: The RMMS expert system is being developed in three phases.

- a. Phase I will be designed on the TI Explorer II platform with KEE. This phase includes the development of a software tool for system engineers for displaying registers, process states, and tables of a ModComp memory dump that KEE will store as units. These knowledge units will allow the user to access the ModComp information at a higher level. The units have internal knowledge that knows how to locate the data and in what format to present it to the user. The ModComp memory dump display tool developed by MITRE will provide system engineers fast and easy access to ModComp dump information recorded by the data manager through the LDM (see the figure "RMMS Memory Analyst Display"). MITRE will also develop an automated memory dump diagnoser. The diagnoser will use hypothesis-based reasoning from acquired system engineer knowledge. The diagnoser will be capable of stepping through hypotheses generated from initial symptoms. The diagnoser will reject and refine hypotheses until all hypotheses are rejected or refined as far as possible. The system will then recommend further engineering actions (see the figure "RMMS Automated Diagnosis Display").
- b. Phase II will also be designed on the TI Explorer II with KEE. This phase will integrate the Phase I expert system with additional implant data. The expert system will be capable of analyzing memory image, memory trace, address trace, and voltage-level information from the data manager. The knowledge for this analy-

sis will be developed by the RMMS and system engineers.

- c. Phase III will integrate the expert system and the data manager onto one machine with a standard windowing system (X-Windows) and knowledge base [Common LISP Object Standard (CLOS)].

5. Common Data Buffer Implant

Function: The CDBFR implant detects and captures CDBFR-induced errors from the buffer access card (BAC) chassis.

Software: The CDBFR implant self-test and evaluation will be written in the implant's own microcode set. The command, data, and communication software will be written in the Z8002 assembly language.

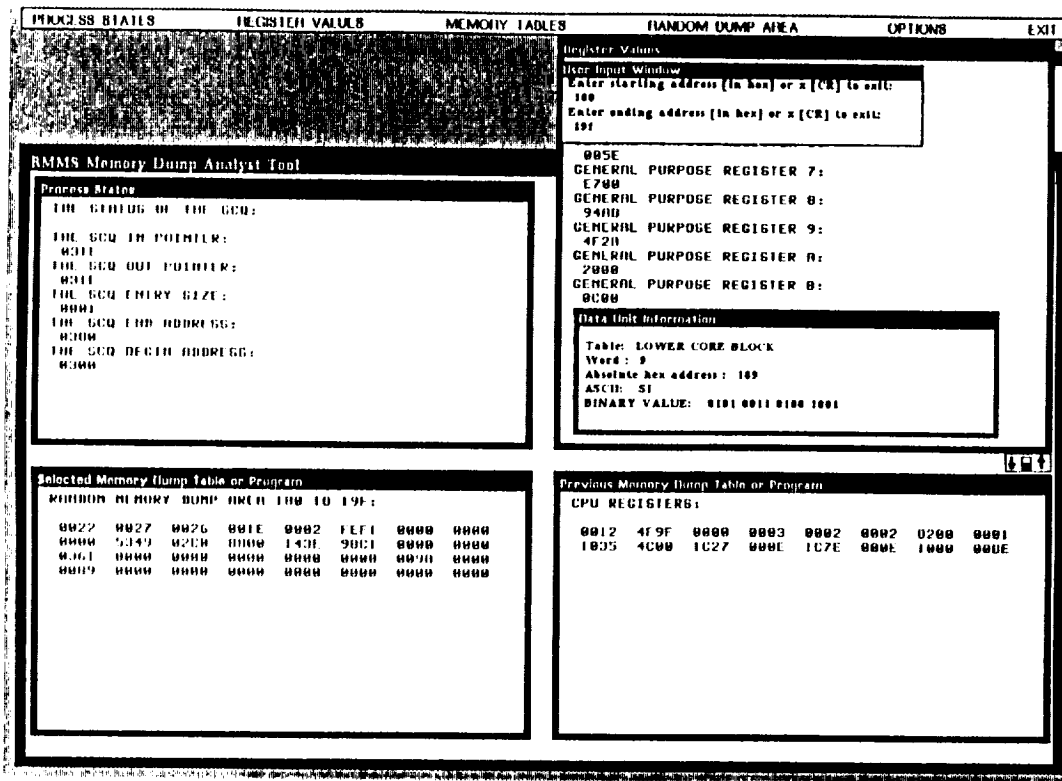
6. Implant Communication Network

Function: The implant communication is a high-speed local communications network for communication of diagnostic data and control information between the data manager and the ModComp and CDBFR implants.

Software: The implant communication drivers will be programmed in the Z8002 assembly language. The data manager driver will be programmed in "C" and the 68030 assembly language on a VME Heurikon card attached to the Sun 3/160 backplane.

Functional Description: The implant data bus is very similar to the Ground Data Bus used on LPS. The network will be daisy-chained together with 1-megahertz differential pair cabling. The network will use the Manchester II communication protocol with 24-bit frames (8-bit address and 16-bit data).

7. Expert System Communication Network



RMMS Memory Analyst Display

Function: The expert system communication network is a high-speed local communications network for transfer of diagnostic data and control information between the data manager and the OPERA and RMMS expert systems.

Software: The communication software will be written in "C" on the data manager and in Common LISP on the OPERA and RMMS expert systems.

Functional Description: The expert-system-to-data-manager communication link will be implemented via a Sun 3/160 network file system (NFS) protocol standard over a 10-megahertz Ethernet communication channel. The Sun 3/160 data manager will be configured as a file server and the TI Explorer II expert system as a client. The TI client will mount onto the Sun 3/160 server to make the Sun 3/160 file system a network drive. The TI client will then have access to the RMMS index file, which lists the complete pathnames to all ModComp auto-

dumps and ModComp diagnostic information. The expert system will use these pathnames to retrieve the pertinent information from the data manager.

Capable of providing enhanced support to the LPS through 1995 with advanced designs, the RMMS concept efficiently incorporates continuous real-time monitoring of the Checkout, Control, and Monitoring Subsystem (CCMS) hardware, the central integration of various diagnostic data acquisition processes, and the automation of the diagnostic process through expert system technology.

Contact:

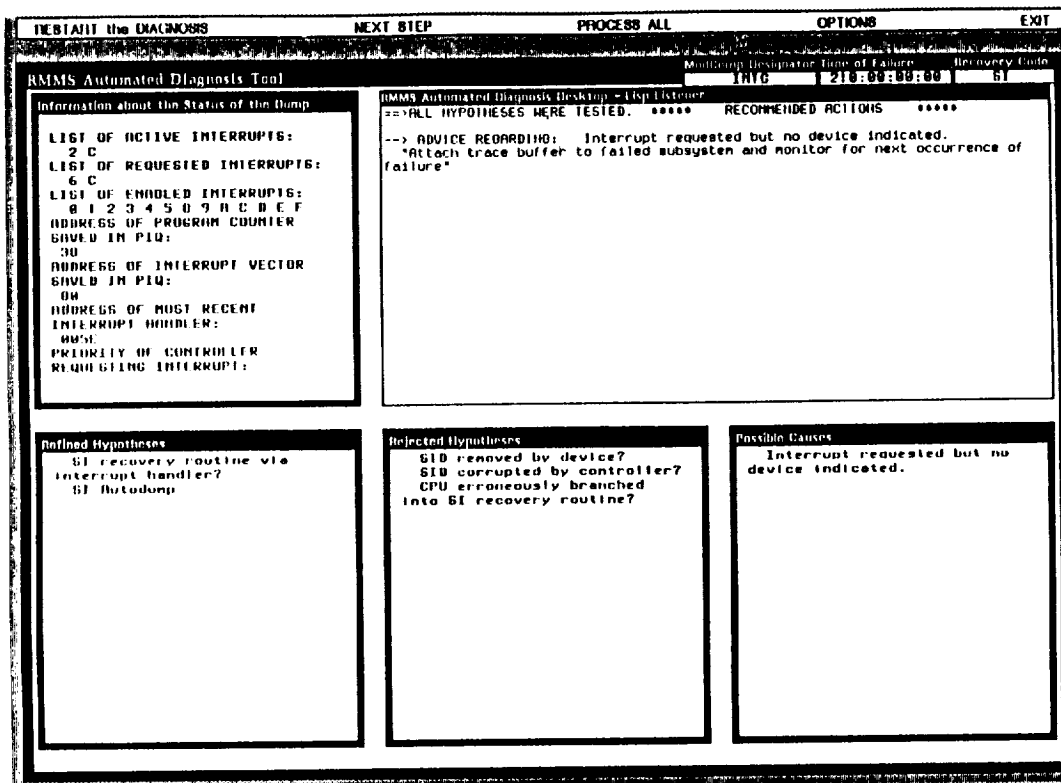
M. Loughed, 867-4946, TE-LPS-13A

Participating Organizations:

*Grumman Technical Services, Inc.
(D. Rochette, H. Austin, D. Priskey,
D. Traturyk, and R. Zorner)
MITRE Corporation (A. Schafer)*

NASA Headquarters Sponsor:
Office of Space Flight

01. FOUR QUALITY



RMMS Automated Diagnosis Display

Intelligent Launch Decision Support System (ILDSS)

The overall objective of ILDSS is to develop prototypes of tools that support decisionmaking by the launch team during Shuttle launch countdowns. The current objective is to support the NASA Test Directors (NTD's) in time management during terminal count beginning at T-9 minutes and holding. The prototype consists of an on-line display with situation annunciation, user-directed "what-if" capability, and advisory capability in terms of situation-action and reactive planning.

The project was originally conceived as a follow-on to the Thunderstorm Weather Forecasting Expert System (TWFES) project. The TWFES project reasoned temporally and spatially about summer thunderstorms in a manner called scenario-based reasoning. This genre of reasoning was deemed appropriate to the Shuttle launch countdown decision process. A feasibility

study was performed in 1988 by an Arthur D. Little, Inc., team. The purpose of the feasibility study was to identify problems during Shuttle countdown to which any knowledge-based software techniques were a viable solution, not just scenario-based reasoning. The use of the word "intelligent" in the project title reflects the intended use of knowledge-based software techniques. Three problems were identified by the feasibility study: management of time, the capture and management of verbal information, and the investigation and management of anomalies. The launch team selected the management of time for prototype development. The project was then staffed by the Engineering Support Contractor in March 1989.

The approach taken in ILDSS has been one of interviews, rapid prototyping, phased development, and accessing related research. Audio tapes and transcripts were made of the interviews. Artifacts used by the NTD's during terminal count were examined during the interviews.

Rapid prototyping has been primarily in Common LISP using Flavors on a Symbolics LISP Machine running Genera 7.2. The first phase of the development has been an integrated time management display (ITMD), which will serve as the substrate for the remaining development. Two additional phases are planned. The second phase will add situation annunciation and user-directed "what-if" capability. The third phase will add advisory capability in terms of situation-action and reactive planning. Some limited capabilities from the second and third phases are present in the first phase.

The interviewing for the ITMD, situation annunciation, "what-if," and situation-action capabilities is substantially complete. A prototype for the ITMD has been developed from the artifacts and designs provided by the NTD's.

Time management by the NTD's simplistically consists of those decisions required by the extension of the T-9 minute hold or invocation of an unplanned hold at one of

the remaining hold points. This requires maintaining mental models of the dynamic state of the countdown and managing the process that determines when to pick up the count.

The figure "ITMD Screen Dump" shows the prototype version of the ITMD. The major features of the ITMD are the clocks [Greenwich mean time (GMT), countdown time (CDT), launch time, window remaining, and hold time remaining], the graphical depiction of time (GMT, CDT, and launch time), windows [launch window, auxiliary power unit (APU) runtime, and collision avoidance (COLA)] and events (ground launch sequencer milestones) correlated in time, the "now" bar, and the T-0 line. This display integrates information currently available on firing room clocks and hard-copy timelines and correlates the information graphically in time.

Implementation and deployment into the launch environment is the responsibility of the launch team. The deployment issues identified by the project are: (1) NTD

ILDSS/TMM STS-XX Demonstration			
Universal Time (GMT)	Shuttle Count (T-Time)	Time to T-0 (L-Time)	Launch Time (T-0 in GMT)
17 12:56:40	-03:20	-03:20	17 13:00:00
12:55:00	T-5m APU Start	L-5m	Hold Time Remaining
12:56:00	T-4m	L-4m	--:--
12:57:00	T-3m	L-3m	Window Remaining
12:58:00	T-2m LHX Pressurization	L-2m	00:20:00
12:59:00	T-1m LH2 Term Replenish	L-1m	APU Time Remaining
13:00:00	T-0 LPS GPC Auto Seq Star	L-0	07:00
13:01:00	T+1m	L+1m	Simulated GLS Control Cancel Pending CD Requests Hold CDT at CDT Hold CDT at GMT Hold CDT Now Resume CDT at GMT Resume CDT Now Set CDT Set Hold Available
13:02:00	T+2m LOX System Safed	L+2m	
13:03:00	T+3m LH2 System Safed	L+3m	
13:04:00	T+4m SRB Separation	L+4m	
13:05:00	T+5m	L+5m	
13:06:00	T+6m	L+6m	
13:07:00	T+7m	L+7m	
13:08:00	T+8m MECO	L+8m	
13:09:00	T+9m	L+9m	
13:10:00	T+10m	L+10m	
13:11:00	T+11m	L+11m	Exit Pause Pause (Data Stream Only) Reset Show Mission Parameters Time Scale Menu What If Menu > Super-Scroll Scroll One He > Super-Scroll Scroll One He > Refresh > Adjust Real-Time Ratio Adjust Update Display Freq Configuration Menu Data Stream Menu Inspect Single Step Countdown Toggle Color/Mono
13:12:00	T+12m	L+12m	
13:13:00	T+13m	L+13m	
13:14:00	T+14m	L+14m	
13:15:00	T+15m	L+15m	
13:16:00	T+16m	L+16m	
13:17:00	T+17m	L+17m	
13:18:00	T+18m	L+18m	
13:19:00	T+19m	L+19m	
13:20:00	T+20m	L+20m	
13:21:00	T+21m	L+21m	

ITMD Screen Dump

ORIGINAL PAGE IS
OF POOR QUALITY

access to the information since there are no computer monitors at the NTD's consoles and (2) sufficiently powerful computing platforms for the more powerful and computationally intensive versions of the prototype.

Contact:

A. E. Beller, 867-3224, DL-DSD-23

Participating Organization:

Boeing Aerospace Operations, Engineering Support Contract (H. G. Hadaller and M. J. Ricci)

NASA Headquarters Sponsor:

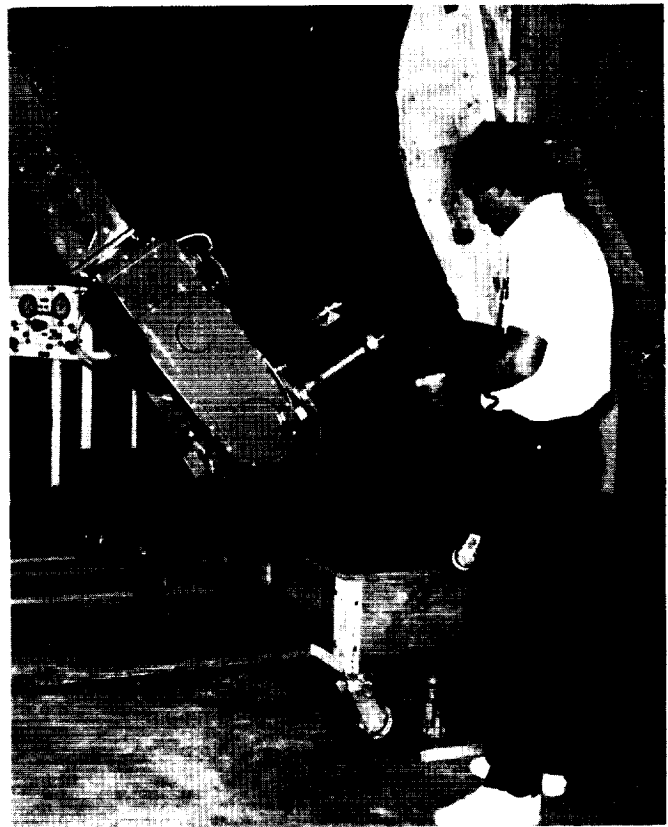
Office of Space Flight

Automated Tile Inspection

The objective of this program is to develop an automated Shuttle tile inspection system. Because tiles are flight-critical components, they must be inspected carefully. Damaged tiles must be refurbished or replaced after each flight. This is a labor-intensive procedure and is on the critical path for the Shuttle processing flow.

The Robotics Applications Development Laboratory (RADL) demonstrated a prototype automated system using a full-scale mockup of a portion of the Orbiter. The system was able to perform the tile inspection process (step-and-gap measurements only) with no human intervention in less than one-tenth the normal manual operating time. This project was approved after testing proved the feasibility of using a robot to position the laser step-and-gap instrument.

Originally, the step-and-gap between individual tiles was measured by feeler gages, and the minimum number of measurements per tile was twelve. With more than 20,000 tiles, the manhours required were significant. A hand-held laser measuring device was developed for measuring the step-and-gap. This device made the use of robotics feasible since a robot could

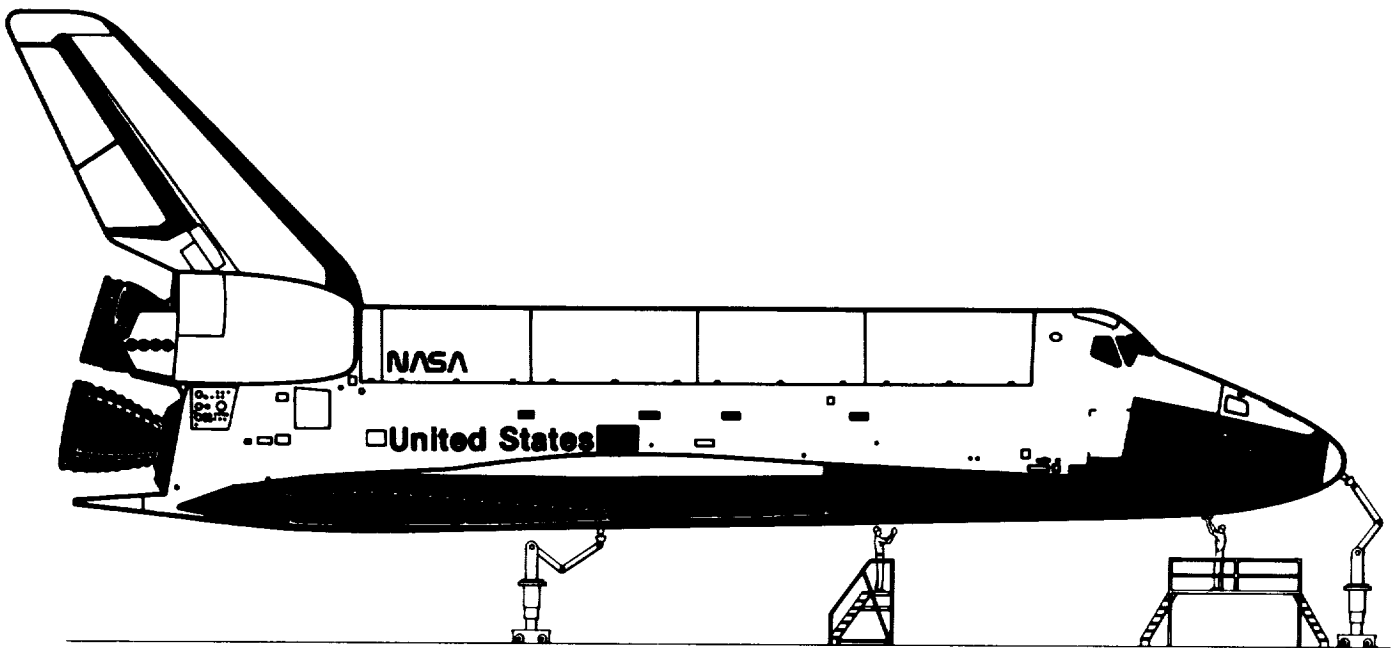


Orbiter Tile Inspection Mockup

manipulate the instrument. By using similar instruments, a robot can make other labor-intensive measurements.

The automated inspection system will use various sensors mounted on a robot to perform detailed inspection tasks during the Shuttle refurbishment cycle. The system will automatically examine regions of the Shuttle that have been defined by a system user; it will search for flaws in the tile surfaces and provide data that can be used for trend analysis. The information will be automatically downloaded to an existing master Orbiter database for future action. In the case of missing tiles or tiles that have been removed due to damage, a sensor will be used to map the cavity and provide dimensional information to the database for a replacement tile.

Studies will be performed to determine the kinematic requirements of the manipulator and the requirements and specifications of the sensors. Additional develop-



Shuttle Tile Robotic Inspection

ment of sensor technology may be needed to meet the system requirements. It is expected that an inspection system will be installed in the Orbiter Processing Facility by 1992. Key technologies being utilized include advanced inspection sensors, accurate positioning mechanisms, and a proximity system for collision avoidance.

Contact:

T. A. Graham, 867-4181, DM-MED-12

Participating Organization:

Boeing Aerospace Operations, Engineering Support Contract (D. W. Chenault)

NASA Headquarters Sponsor:

Office of Aeronautics and Space Technology

Remotely Operated Umbilical System Development

Objective

The Robotics Applications Development Laboratory (RADL) has been involved in a multiyear effort to develop a remotely operated umbilical system to replace the current manually connected umbilical systems. Two technology advancements

required for a successful system are a robot (with its control system) and umbilical connectors. Remote operation connectors have additional requirements over manual connectors of self-cleaning and verification of cleanliness, seal integrity, and electrical continuity of the power and communication connections. This project concentrates on the robot and its controls. The connectors have been considered only to the extent necessary to proceed with robotic development.

Background

Manual umbilicals must remain connected to the space vehicle until the last possible moment to ensure that fuels and oxidizers can be drained should there be a ground abort during the last few seconds of the countdown. This places the highest reliability requirements on the manual system and creates apprehension and concern for the Launch Director and his staff. A system that could be disconnected minutes before lift-off would permit an unhurried disconnect and allow time for verification of a clean disconnect but would, in turn, require a fast-reconnect capability. This is not possible with manual umbilicals because of the time required

for cleaning and verification and the hazardous operating conditions. The development of a remote umbilical capability is an attempt to solve these problems.

The remote umbilical project is the first major project attempted by the RADL. This project will afford the robotics team an opportunity to work with and develop its expertise in advanced robotics mechanisms, sensors, and control systems, since the project requires the integration of numerous subsystems.

The robot used in this project is an ASEA IRB 90.

Approach

Of the numerous requirements a remote umbilical must satisfy, connecting under dynamic conditions and limiting the load on the space vehicle flight plate are the most demanding. A target point on the Shuttle vehicle provided the dynamic criteria for vehicle movement in the horizontal direction of 10 inches at a natural frequency of 0.3 hertz. The maximum allowable force between the ground and flight plates was established at 110 pounds for an umbilical weight estimated at 500 to 1,000 pounds.

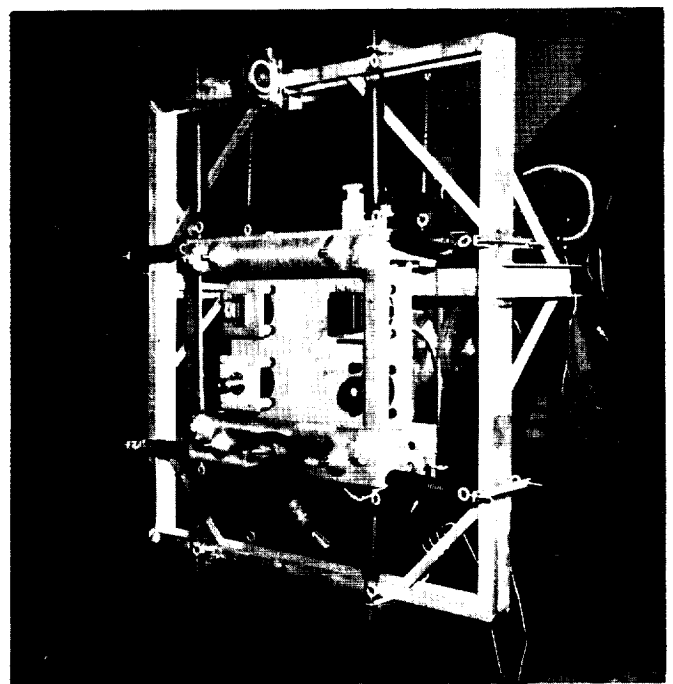
Control of the robot was viewed as two distinct operations requiring two guidance systems. The first being nontactile guidance to move the robot's "ground" plate into synchronous position with the moving vehicle's "flight" plate. The second operation requires tactile guidance to progress to the "connected" position.

A vision system, operable in the visible and/or infrared wavelengths, was selected for the nontactile guidance system. Force sensors were selected as the control input device for the tactile guidance system. The problem with both systems is twofold: (1) the difference between the actual location of the ground plate and its desired position

to detect a required movement and (2) the time delay between detection and actual corrective movement. This called for either a system with very sensitive detectors and high-speed controls and drives or a passive compliance system. A passive compliance system was selected since it offered advantages in testing and was seen as a total solution with the possible elimination of force-sensor requirements.

Due to the inability of the target to simulate orientation changes, plans were established to test the six-degree-of-freedom (6-DOF) vision system using a 3-DOF target motion simulator. This lack of capability was considered insignificant since the passive compliance system would accommodate any unforeseen orientation changes. Test plans called for a progressive-step approach.

Separate tactile test plans were established to determine system speed and the ability to use the robot and controller in this mode.



Remote Umbilical System

Results

Testing of the vision system with passive compliance established it as a viable system. The test demonstrated tracking, mating, and demating. It was, however, only able to do this at 0.15 hertz for the 10-inch amplitude due to the time delay between the vision system's acquisition of the target and the robot's response.

Testing of force sensors to control the robot was less impressive. The first test revealed the same time delay problems encountered with the vision system. A follow-on test to determine if a single-axis motor could be controlled directly by the sensor demonstrated that it is practical.

A separate test was conducted to determine the best location for the sensors. It was found that sensors at the interface points (between ground and flight plates) provided the best signals. This requires the integration of several signals to produce the resultant torque loads but eliminates inertia loads that would be present from the flight plates if the sensors were located between the robot and the ground plate.

The dominant conclusion was that processing speed must be increased to provide a fully usable robotic control system regardless of the guidance system selected. It was also concluded that force-sensor control without the use of passive compliance would push the processing capability to its practical limit.

Future Goals

Three approaches are under way to improve the capabilities of the remotely operated umbilical system. The solution to the problem of slow processing time is the development of a high-speed controller, which is scheduled for completion in March 1990. In addition to improved speed, the controller will allow access to revise the control program, input points, etc. As a backup to the high-speed controller, a

predictive algorithm is being developed; it has not been successfully demonstrated at this time, but work is continuing.

Since the high-speed controller can only reduce processing time, there is a high probability that problems will be encountered with force-sensing control operated through a robot controller. A compensating end-effector is being developed as an alternate solution to force-sensing control problems encountered with the robot. The plans are to develop a 3-DOF compensator (position only) with a single drive for each direction and to mount it between the robot and ground plate with sensors at the plate interfaces. Schedules call for completion in June 1990.

Other work is in progress to add electrical and fluid lines to the ground plate to provide more realistic loads to the robot.

A follow-on project is planned to replace the existing 3-DOF motion simulator with a 6-DOF system. The 6-DOF system will allow better testing and evaluation of the developed systems.

Contact:

*Eduardo Lopez del Castillo, 867-4181,
DM-MED-12*

Participating Organization:

*Boeing Aerospace Operations, Engineering
Support Contract (R. P. Bennett)*

NASA Headquarters Sponsor:

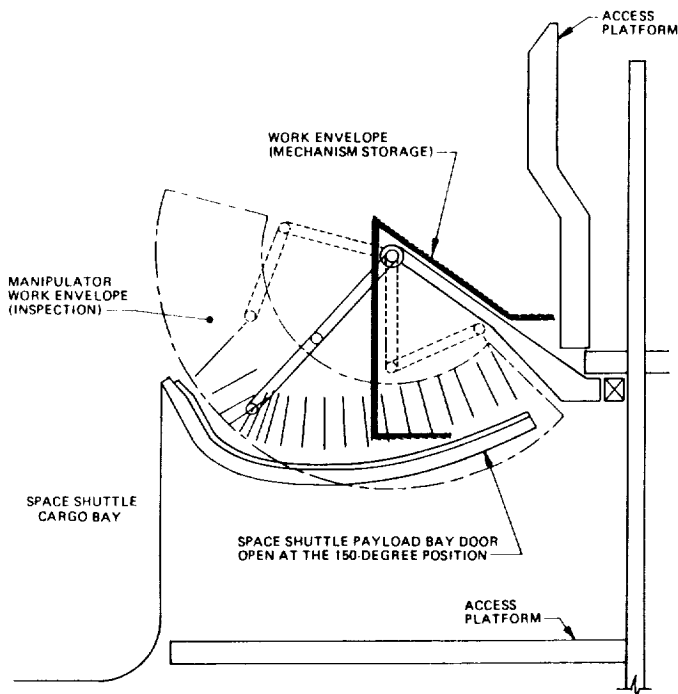
Office of Space Flight

Automated Radiator Inspection

The efficiency of the Orbiter radiators to dissipate radiant heat energy is dependent upon their surfaces being clean and damage free. Currently, the radiators are manually cleaned and inspected during ground processing for damage due to micrometeorite impacts and other causes, and the affected areas are entered into a log. The objective of this program is to develop and integrate a mechanism to automatical-

ly position an inspection sensor above the Orbiter radiator panels. The automated inspection mechanism will incorporate a sensor system developed for NASA to identify damaged areas. The location and extent of the damage will then be automatically entered into a database for further action.

The positioning mechanism will be a four-degree-of-freedom system, cantilevered from access platforms located adjacent to the radiator panels. The cross-section view of the mechanism in relation to the access platforms and Orbiter (see the figure "Orbiter Radiator Inspection Mechanism Schematic and Envelope Analysis") shows the envelopes for performing inspections and for mechanism storage. The mechanism will be capable of positioning the inspection sensor to within an absolute accuracy of 0.10 inch over the entire radiator panel. A control system is being developed to use off-line programming and to automatically perform frame shifting operations to account for imprecise placement of the Orbiter in the Orbiter Processing Facility (OPF). The design and fabrication



Orbiter Radiator Inspection Mechanism Schematic and Envelope Analysis

of the device is being done inhouse, and the system is scheduled for completion and testing in late 1990. Key technologies being utilized include special-purpose automated mechanisms compatible with current OPF equipment, inspection sensors, and database interfaces.

Contact:

Chau Le, 867-4181, DM-MED-12

Participating Organization:

Boeing Aerospace Operations, Engineering Support Contract (D. W. Chenault)

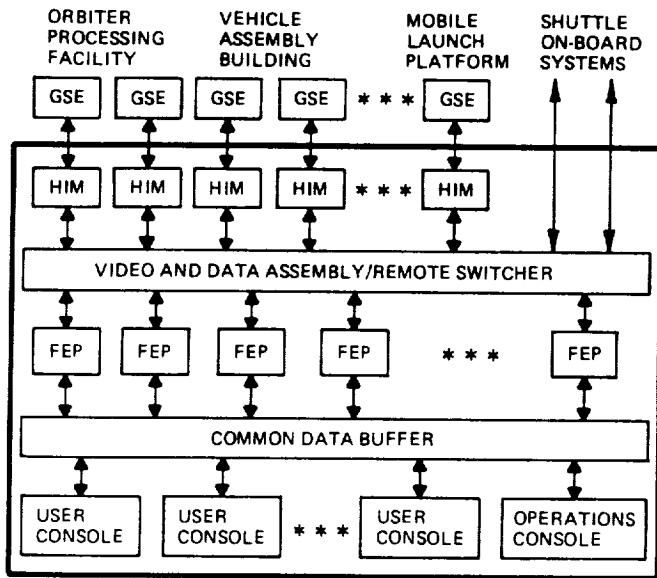
NASA Headquarters Sponsor:

Office of Space Flight

Checkout, Control, and Monitor Subsystem (CCMS) Operations Analyst (OPERA) Expert System

The CCMS is one of three subsystems that constitute the Shuttle Launch Processing System. The CCMS network (see the figure "The CCMS Network") integrates computers, data links, displays, controls, hardware interface devices, software, and microcode. This network provides the only real-time interface between Shuttle engineers and the Orbiter vehicle and its associated ground support subsystems (for example, fuels and environmental controls). Four independent CCMS sets, called firing rooms, are used to process and launch Shuttle vehicles, to train launch teams, and to develop new CCMS software. The CCMS Operations charter is to provide and maintain error-free CCMS configurations to support all user testing requirements, such as launch countdown or Orbiter power-up sequences.

OPERA assists Operations personnel in performing CCMS support tasks, including firing room configuration and management and the detection, isolation, and correction of CCMS set faults. The goal of the OPERA project is to improve existing Operations capabilities by increasing automation and standardizing task performance. Each



FEP = FRONT-END PROCESSOR
 HIM = HARDWARE INTERFACE MODULE
 GSE = GROUND SUPPORT EQUIPMENT

The CCMS Network

expert system in OPERA will act as a consultant, assisting the Operations staff assigned to particular functional task sets (see the figure "OPERA Expert Systems, Operations Staff and Tasks"). The specialized information and skills required to perform these tasks range from expertise concerning the design and behavior of CCMS hardware and software subsystems [central processing units (CPU's) and operating system components] to knowledge of CCMS operating procedures and configuration requirements. OPERA will eventually encompass five expert systems:

Real-Time System Error Management (RTSEM)

Problem Impact Analysis (PIA)

OPS STAFF ROLE \ OPS TASK	TEST CONFIG ROMTS	ERROR DETECT	ERROR EVAL	CPU STATUS/HISTORY	ACTION XQTD	ERROR LOG/TRACK
SET MANAGER	PIA RCES		RTSEM	PIA DBIF	PIA RCES	PIA
TEST CONDUCTOR	PIA RCES	RTSEM	RTSEM	PIA DBIF	PIA RCES	PIA
ANALYST	RCES	RTSEM				
SYSTEMS ENGINEER			RTSEM MBFI	PIA DBIF	PIA	PIA
HW ENGINEER (TECHNICAL)			RTSEM	PIA DBIF	PIA	PIA

OPERA Expert Systems, Operations Staff and Tasks

Problem Reporting and Corrective Action (PRACA) Database Interface (DBIF)

Remote Control Video Switch (RCVS)
 Configuration Expert System (RCES)

Automated Knowledge Acquisition Module (AKAM)

The initial OPERA prototype incorporates two expert systems, RTSEM and PIA. When problems occur in firing rooms, rapid fault isolation and correction are essential in minimizing impacts on user tests and in retaining data integrity. RTSEM and PIA will help the Operations staff to troubleshoot CCMS faults, to restore firing room functionality, and to identify existing related problem conditions. DBIF will supply additional data resources to enhance OPERA's initial troubleshooting capabilities. The RCES will extend OPERA to assist users in planning network configurations that satisfy test and launch requirements and in managing network utilization. The AKAM will help knowledge engineers to compile, input, and validate CCMS system messages.

The primary CCMS fault detection and isolation tools are operating system error messages. These messages are currently manually monitored and interpreted, as generated by interrupt handlers embedded in CCMS operating system components. OPERA's RTSEM expert system operates by reading CCMS-generated system messages, interpreting them, and then evaluating any CCMS problems that may have occurred as identified by the messages. The off-line OPERA prototype simulates firing room configurations. The user can enter specific message occurrences for analysis or can retrieve the message streams from a processed data recording (PDR) tape.

CCMS system messages that come from front-end processors, consoles, the Processed Data Recording (PDR) Subsystem, and the Shared Peripheral Area (SPA) Subsystem are funneled in data blocks

through the CCMS common data buffer and recorded at the CCMS PDR or SPA (see the figure "PDR/SPA Versus OPERA Configuration"). Near real-time data is stored on disk, while historical data is stored on tape. A link between the OPERA computer and the PDR/SPA hardware was necessary to further automate OPERA's capability to process system messages.

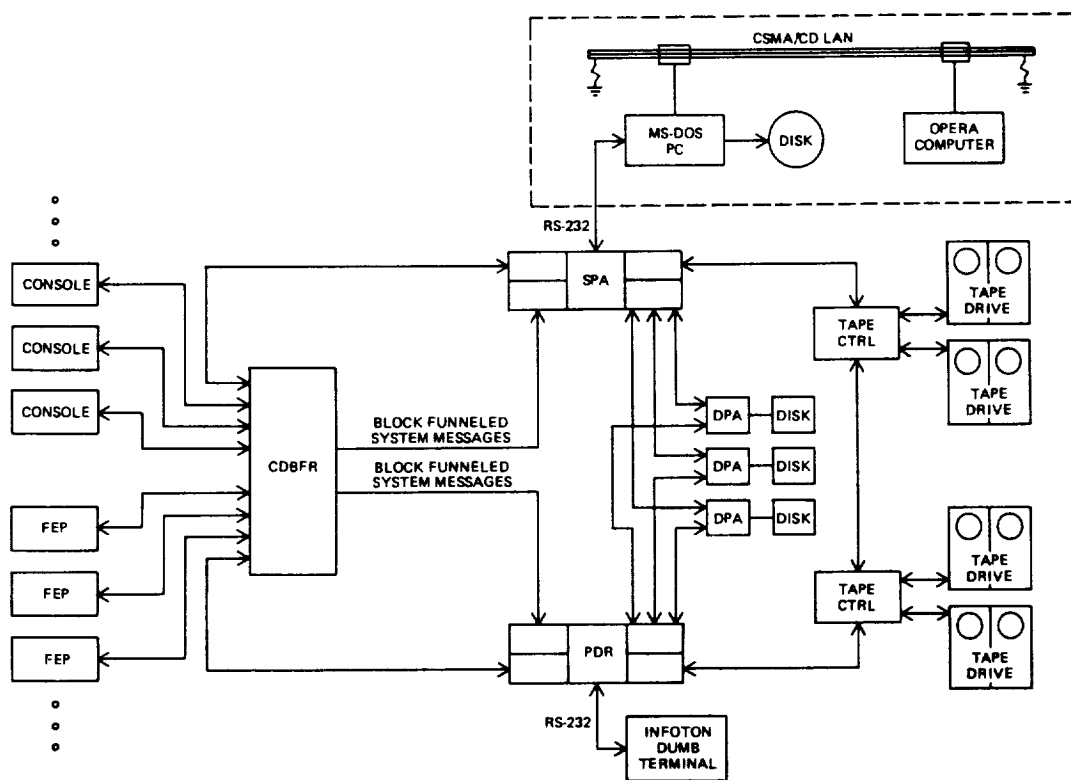
For user input, each PDR/SPA CPU has an Infoton "dumb" terminal without disk storage capability. The terminal communicates over an RS-232 cable. While at the terminal, the user can retrieve and view system messages that have been recorded on tape or disk. It is a simple task to replace the Infoton "dumb" terminal with an MS-DOS-compatible personal computer (PC) having a hard disk drive and a terminal emulator communications software package.

The retrieval program, which displays recorded system messages at the PDR/SPA terminal, is called SPBLOK. While acting as

a terminal, the MS-DOS PC records all SPBLOK output on its hard disk. The format of an SPBLOK output is shown in the figure "Format of SPBLOK Output."

A program written in the "C" programming language was developed that reduces the raw SPBLOK output to an OPERA format. This program runs on an MS-DOS PC and performs two functions. Each OPERA-formatted system message is sent via the PC's network client over the Ethernet to the OPERA host's network server (see the figure "OPERA Off-Line Operation Architecture"). From there, the system message is fed into the OPERA expert system and processed. Each OPERA-formatted system message is also stored in a file that can be used later to run through the interface. The OPERA format is as follows:

```
200:2128/45.061 FEP 135 (GS4) NO
RESPONSE TO THREE SUCCESSIVE
DATA BUS TRANSMISSIONS, OLDEST
ADRS (033400) REMOVED FROM EX-
PECTED LIST,
```



PDR/SPA Versus OPERA Configuration

```

SPBLOK04 INPUT COMPLETE.  DATA PROCESSING STARTING.

SPBLOK                      WT814          FB15-1.1.0.0 PAGE
1
BLOCK FUNNEL LOG DATA RETRIEVAL PROGRAM
USER ID: CCB TCID WT814 8814

SPCOMH01 (SPBLOK) START TIME FOUND.  TIME OF 1ST RECORD= 200:
2127/59.999

CDT= +08:1728/45      GNT= 200:2128/45.061      CPU= M8TR      LOG ID=
SM
0000 0000 4645 5020 3133 3620 2847 5334 2029  ..FEP 136 (GS4 )
0008 204E 4F20 5245 5350 4F4E 5345 2054 4F20  NO RESPONSE TO
0010 5448 5245 4520 5355 4343 4553 5349 5645  THREE SUCCESSIVE
0018 2044 4154 4120 4255 5320 0A0D 5452 414E  DATA BUS ..TRAN
0020 534D 4953 5349 4F4E 532C 204F 4C44 4553  SMISBIONS, OLDES
0028 5420 4144 5253 2028 3033 3334 3030 2920  T ADRS (033400)
0030 5245 4D4F 5645 4420 4652 4F4D 2045 5850  REMOVED FROM EXP
0038 4543 5445 4420 4C49 5354 2C20 908E      ECTED LIST, ..

CDT= +08:1728/45      GNT= 200:2128/45.113      CPU= M8TR      LOG ID=
SM
0000 0000 4645 5020 3133 3620 2847 5334 2029  ..FEP 136 (GS4 )
0008 204E 4F20 5245 5350 4F4E 5345 2054 4F20  NO RESPONSE TO
0010 5448 5245 4520 5355 4343 4553 5349 5645  THREE SUCCESSIVE
0018 2044 4154 4120 4255 5320 0A0D 5452 414E  DATA BUS ..TRAN
0020 534D 4953 5349 4F4E 532C 204F 4C44 4553  SMISBIONS, OLDES
0028 5420 4144 5253 2028 3033 3334 3035 2920  T ADRS (033405)
1 SPCOMH08 (SPBLOK) ENTER 'C' FOR NEXT PAGE

```

Format of SPBLOK Output

200:2128/45.113 FEP 136 (GS4) NO RESPONSE TO THREE SUCCESSIVE DATA BUS TRANSMISSIONS, OLDEST ADRS (033405) REMOVED FROM EXPECTED LIST,

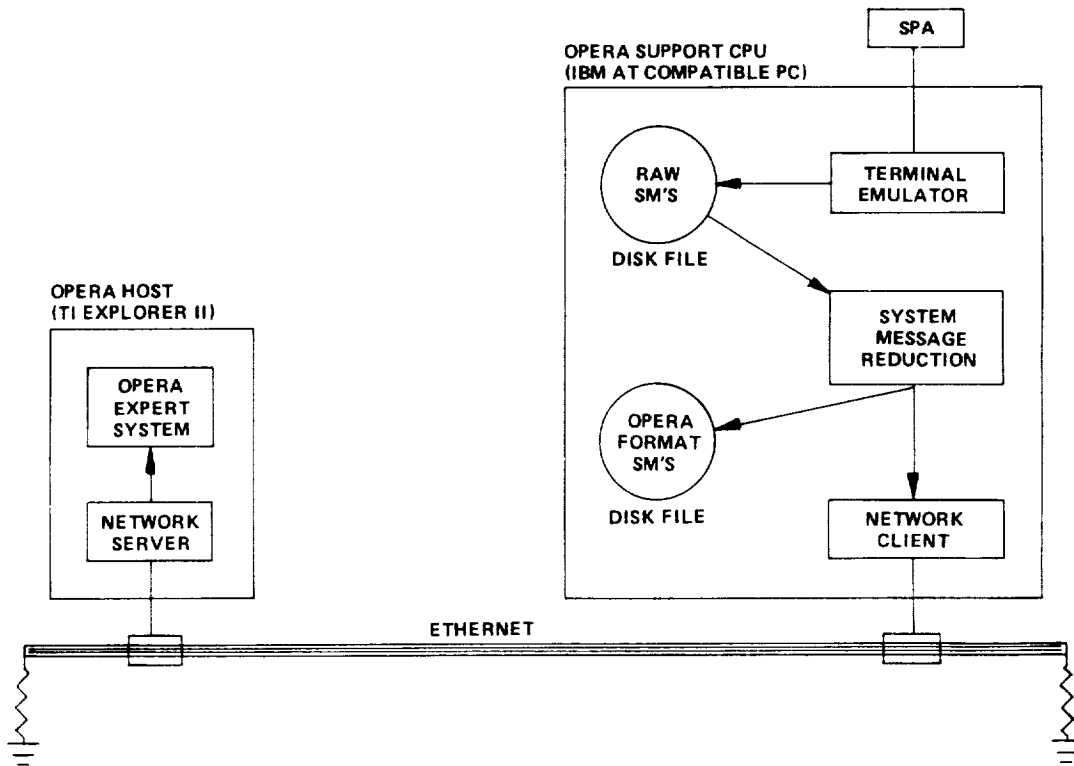
200:2128/45.220 FEP 136 (GS4) NO RESPONSE TO THREE SUCCESSIVE DATA BUS TRANSMISSIONS, OLDEST

ADRS (033414) REMOVED FROM EXPECTED LIST,

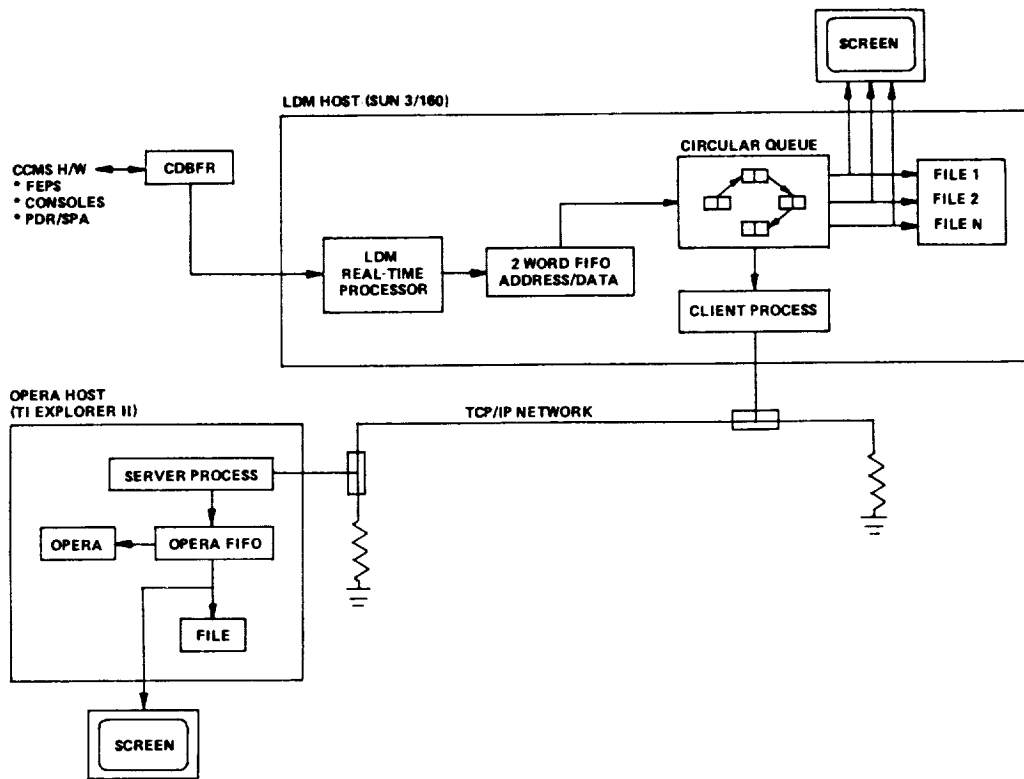
200:2128/45.325 FEP 136 (GS4) NO RESPONSE TO THREE SUCCESSIVE DATA BUS TRANSMISSIONS, OLDEST ADRS (033420) REMOVED FROM EXPECTED LIST,

200:2128/45.425 FEP 136 (GS4) NO RESPONSE TO THREE SUCCESSIVE DATA BUS TRANSMISSIONS, OLDEST ADRS (033424) REMOVED FROM EXPECTED LIST,

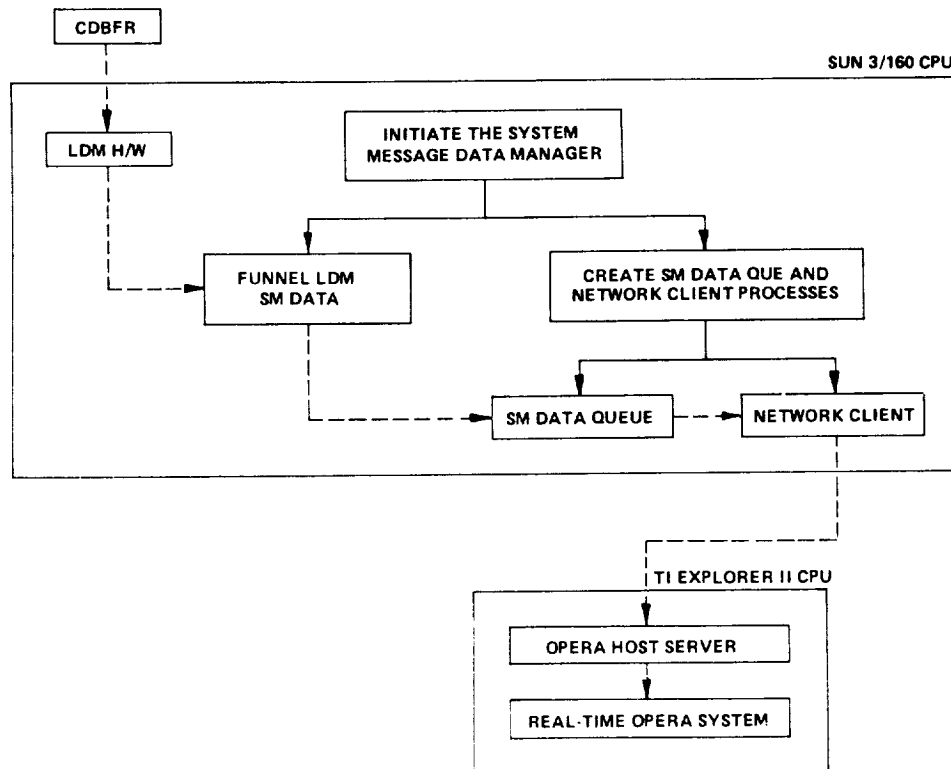
The OPERA real-time operation architecture is a mixture of hardware and software blocks that work together to read system messages from the common data buffer (CDBFR) (see the figures "OPERA Real-Time Interface Architecture" and "OPERA Real-Time Software Operation"). System messages are routed in real-time through the CDBFR and recorded at the PDR on both bulk disk and bulk tape. The hardware link between the CDBFR and the OPERA real-time hardware is



OPERA Off-Line Operation Architecture



OPERA Real-Time Interface Architecture



OPERA Real-Time Software Operation

accomplished by tapping off the bus lines between the CDBFR and PDR. The logged data monitor (LDM), which is under development by the Remote Maintenance and Monitoring System (RMMS) Project, will be used to read and buffer system message data (among other data). Software written on an LDM host will filter out the system message data from the "other data" (which is used by the RMMS expert tool).

System message data is sent through the CDBFR in the form of CDBFR block funnel log address and data. The data consists of a pair of ASCII characters. A complete system message is sent through the CDBFR in the following manner:

```
<CDBFR ID Address/"SM">
```

(Identifies the start of a system message.
16-bit ID address and 16-bit data.)

```
<CDBFR Data Address/ASCII Pair 1>
```

(16-bit data address and 16-bit ASCII pair.)

```
<CDBFR Data Address/ASCII Pair 2>
```

(16-bit data address and 16-bit ASCII pair.)

```
<CDBFR Data Address/ASCII Pair n>
```

(16-bit data address and 16-bit ASCII pair.)

```
<CDBFR ID Address/"$$">
```

(Identifies the end of a system message.)

A problem occurs when multiple Launch Processing System CPU's simultaneously send system messages through the CDBFR. When this situation occurs, a system message from CPU-1 will not necessarily be completed before a system message from CPU-2 is started.

The following is an example of interleaved system messages:

```
<CPU-1 CDBFR ID Address/"SM">
<CPU-1 CDBFR DATA Address/ASCII Pair 1>
<CPU-2 CDBFR ID Address/"SM">
```

```
<CPU-1 CDBFR DATA Address/ASCII Pair 2>
<CPU-2 CDBFR DATA Address/ASCII Pair 1>
<CPU-1 CDBFR DATA Address/ASCII Pair 3>
```

```
<CPU-1 CDBFR DATA Address/ASCII Pair n>
<CPU-1 CDBFR ID Address/"$$">
<CPU-2 CDBFR DATA Address/ASCII Pair 2>
<CPU-2 CDBFR DATA Address/ASCII Pair 3>
```

```
<CPU-2 CDBFR DATA Address/ASCII Pair n>
<CPU-2 CDBFR ID Address/"$$">
```

This example displays a simple case of only two interleaved messages, but the number of interleaved messages may be much larger.

Due to the interleaved nature of the system messages, a circular queue data structure is used to incrementally collect a set of system messages. When a system message has been completed, the message is removed from the circular queue, and a network client process is created which sends the message from the LDM host (SUN 3/160 Minicomputer) to a server process on the OPERA host (TI Explorer II Minicomputer).

Along with the system messages, the LDM keeps track of Greenwich mean time (GMT) from the CDBFR. The GMT is used to time-stamp all system messages. This is necessary due to the numerous time relationships between system message occurrences, which are monitored in the OPERA expert system.

The server process on the OPERA host does one of two things: (1) if the OPERA expert system is idle (waiting for a system message), the OPERA expert system will be initiated by the system message received from the LDM client process or (2) if the OPERA expert system is busy analyzing a system message, the system message received from the LDM client process is put into an OPERA FIFO. When the OPERA expert system has finished analyzing

ing its current message, the top of the OPERA FIFO is used as the next message for analysis by the OPERA expert system.

The expert systems, RTSEM and PIA, are currently hosted on a Texas Instruments Explorer II LISP machine using Intellicorp's Knowledge Engineering Environment (KEE). The systems are integrated by a blackboard architecture that uses an OPERA controller to coordinate the information request and transfer between the expert systems. This same blackboard architecture will be extended as additional expert systems are added to the OPERA system (see the figure "Planned OPERA System Architecture"). In addition, work will begin in 1990 in the area of code optimization for porting the OPERA application to a hardware host that has reduced disk storage and performance capabilities and possibly a non-LISP-based operating system. This would make deployment of the systems in each firing room much less costly.

By applying artificial intelligence technology to CCMS in the form of OPERA's

expert systems, both current and future, it is hoped to capture some of the volatile corporate knowledge of CCMS operations before it is lost to job mobility or employee attrition. The automation of standard tasks and the constant availability of expert consultant capabilities will improve the efficiency and effectivity of CCMS operations. Thus, we can continue to improve our operations without losing the visibility of passed lessons learned.

Contacts:

A. E. Heard and P. P. Pinkowski,
867-3926, TE-LPS-11

Participating Organizations:

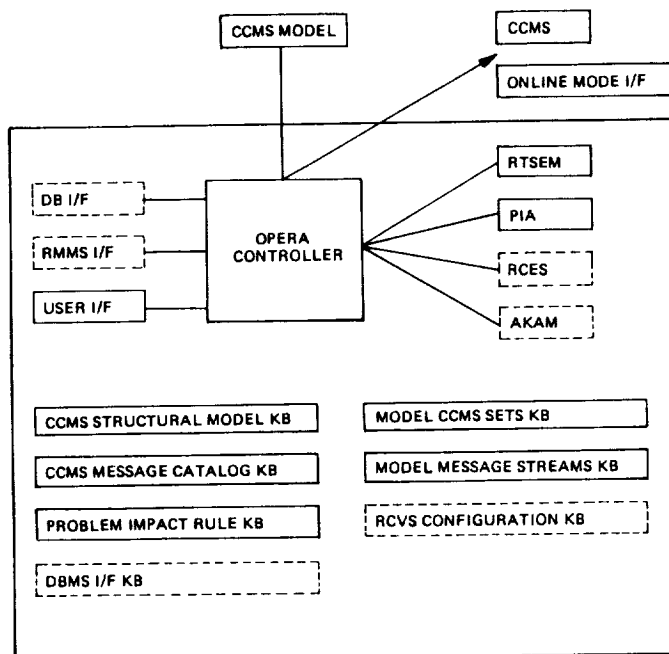
Grumman Corporation (R. B. Hosken)
MITRE Corporation

NASA Headquarters Sponsor:

Office of Space Flight

Automatic Test Expert Aid System Environment (AT-EASE)

The Launch Processing System (LPS) at KSC is made up of over 3,000 individual line replaceable units (LRU's). It is the responsibility of the Intermediate Level Maintenance Facility (ILMF) to test, repair, and verify these components. A large percentage of these components lend themselves to be tested and verified at the ILMF, using automatic test equipment (ATE). Presently, the ILMF uses two major ATE systems to test and verify those components within the LPS that are suited for automated testing. Specifically, these systems are the Genrad 1796 functional printed circuit board test system and a NASA-enhanced Tektronix 3270 system that performs as a functional, high-speed, printed-circuit-board test system. The task of developing the test program sets (TPS's) that these systems use to perform these tests and verifications is both manpower and time intensive. The AT-EASE product facilitates the development of these TPS's. This product is designed to be useful to the seasoned as well as the novice ATE

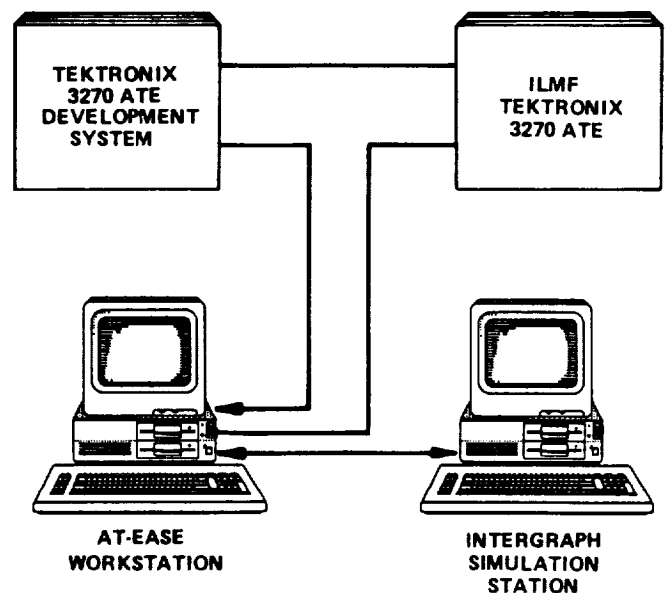


Planned OPERA System Architecture

engineer. The fruits of this project will be a substantial reduction in the TPS development time and more comprehensive, standardized automatic test packages.

Phase I of AT-EASE resides on line with the Genrad software development station as a "smart" front end. The hardware consists of a PC-AT workstation that communicates with the Genrad PDP-8 central processing unit (CPU) through an interface that was designed at KSC. The utilities of this system include an automated, on-line, transferable database of reusable Genrad code; a context-sensitive, full-screen editor; an on-line knowledge base of Genrad automatic test processes; an on-line, automated PDP-8 error code translator; a bidirectional file and data transfer system, and a Genrad TPS development fact and rule base. These databases are controlled by a modern, high-speed, high-capacity, relational database management system called Dataflex. The knowledge bases utilize an object-oriented inference engine called Goldworks. Goldworks also provides for both forward and backward chaining within the knowledge base. The link to the user is a voice-recognizing, menu-driven, windowing package embedded within the editor. The fact base has been completed for Phase I and the workstation has been installed.

Phase II of AT-EASE is an extension of both the hardware and software developed for the Genrad ATE in Phase I. The target ATE system for Phase II is the Tektronix 3270 system. The current TPS development cycle is hampered by the lack of on-line information. The programming language uses a vast number of subroutines and control functions that control hardware or manipulate data within software. These subroutines and functions require multiple variables (such as, values, labels, data, arrays, and limits) in their definition and use. The current method of programming requires the engineer to look up these subroutines or functions in the correct manuals (which are not indexed globally for all manuals) and transfer the



AT-EASE Phase II

information to his/her program. Additionally, program modules created during development that are designed to be reusable are not stored in any central location or catalogued in any standard manner. These modules include mathematical routines, software skeletons, graphical displays, and test routines. Finally, the programs developed for the Tektronix 3270 system utilize data patterns for stimulus. These patterns are created manually. Due to this methodology, there is no accurate quantitative percent fault detection for the circuitry under test. Naturally, these manually generated patterns require long development times, which leads to a limitation in the size and complexity of the LRU's tested on the Tektronix 3270. TPS development selection becomes a function of engineer development time rather than ATE system capability, as it should be.

Phase II of AT-EASE addresses these areas of limitation on the Tektronix 3270. The AT-EASE solution during Phase II is to develop and install two AT-EASE workstations capable of hosting a digital/analog circuit simulator. Using what has been learned and accomplished in Phase I, an interactive, on-line, relational database containing the definition of every subroutine and function necessary to program the

Tektronix 3270 will be created and installed. This database will also contain reusable code that can be accessed, edited, and then downloaded to the ATE via terminal emulation software.

The Intergraph simulation station will run the digital simulator package known as HILO-3 and the analog simulator package C-SPICE. Schematic capture software will allow the engineer to encode the LRU and ATE/LRU fixture circuitry as well as develop the stimulus patterns utilizing mouse-driven graphical entry methods. The patterns would be developed using the same timing cycles that the actual hardware test will use. These stimulus patterns will then be processed through the HILO-3 simulator to derive the expected output patterns and a percent fault detection. The completed patterns (input and output) will then be transferred via a communication link to the AT-EASE workstation and then downloaded to the Tektronix 3270 ATE for application within a TPS. Archiving this code will be done centrally on the AT-EASE workstation with updates and new TPS's being delivered to the ILMF ATE over the same communication link. This will facilitate an efficient software tracking system database. A block diagram of AT-EASE Phase II is provided in the figure "At-EASE Phase II."

Further enhancement to this system will be realized by the continuous growth of the reusable code bank. In addition, this approach to TPS development will be applied to other automatic test systems at the ILMF. These systems will continuously improve test and verification of LPS components at KSC.

Contact:
M. Lougheed, 867-4946, TE-LPS-13

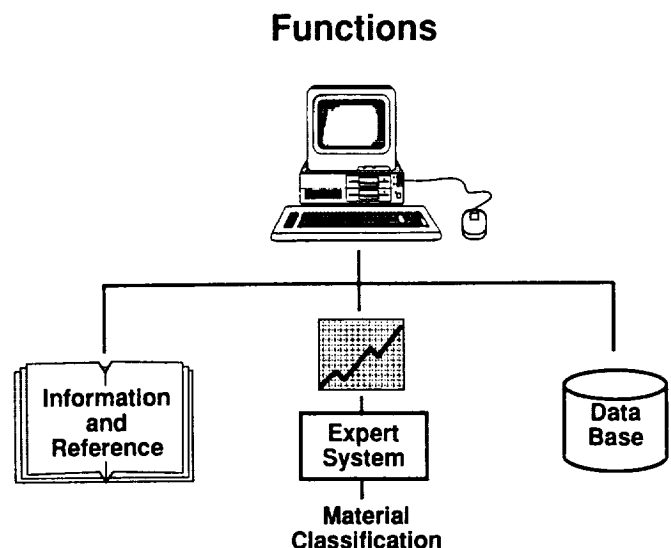
Participating Organization:
Grumman Technical Services, Inc.
(G. Meyer, M. Raney, M. Richardson,
and H. McCoy)

NASA Headquarters Sponsor:
Office of Space Flight

Human Factors and Expert Systems

Research efforts have been initiated to assess the potential for developing systems that can use knowledge bases and rules to mimic the decisionmaking of human experts in high technology work. A joint service (Army, Navy, NASA, and Air Force) pilot project is underway to construct an expert system to accomplish the explosive-hazard classification of energetic materials used for rocket and gun propulsion systems. Employing a unique system of rapid prototypes, researchers are using existing manuals containing standard specifications and procedures, "lessons learned" data, and a directory of recognized experts in the field to build the necessary knowledge and rules. Computer techniques such as hyper-text-sensitive prompting, decision clustering, and contextual menu systems are contributing to the rapid and effective development of information that might otherwise remain unknown, except to one or a few specialists who use it without overt awareness of the complexity of reasoning involved.

Project Capture: Explosive Hazards Classification Expert System



Prototype System Development

If successful, this research may provide insight into the development of innovative methods for mitigating the loss of information resulting from retirement of senior-level scientists and technologists with many years of specialized experience. It may also serve as a pathfinder for developing techniques to better understand the effects of stress and fatigue on performance of critical tasks in an operations environment. Project CAPTURE (Cataloging Advanced Propulsion Technology Utilizing Recognized Experts) has delivered the first prototype system running on AT class computers and will be completed in 1990.

Contact:

*A. M. Koller, Jr., D.B.A., 867-3165,
MD-PLN*

Participating Organization:

The Bionetics Corporation (Dr. S. White)

NASA Headquarters Sponsor:

Office of Space Sciences and Applications

Knowledge-Based Autonomous Test Engineer (KATE)

Kate is a generic, model-based, expert system shell being developed by the Artificial Intelligence Section, Engineering Development Directorate, at the Kennedy Space Center. Its goal is to provide autonomous control, monitoring, fault recognition, and diagnostics for electrical, mechanical, and fluid system domains. KATE incorporates the engineer's reasoning about control and diagnosis of engineering systems in the form of general LISP algorithms. These algorithms are generic in the sense that they do not contain any domain-specific information. The algorithms are then applied to an interchangeable knowledge base (also referred to as a model base), which describes the structure and function of a specific domain using a frame-based representation. This knowledge base is essentially a mathematical model of the particular domain to which KATE is being applied. Using this model,

KATE has the capability to intelligently control, monitor, and diagnose faults for the particular application.

All control and diagnosis is accomplished by the use of a hardware-specific software model. This model produces control operations and expected values for the measurements. In addition, it is used to test diagnostic hypotheses generated as explanations for observed failures. The model is updated as the hardware system is manipulated or degrades. The result is increased machine intelligence in the area of reasoning about and controlling the state of a hardware system.

KATE has been in development since 1985 and was originally applied to and demonstrated against the Shuttle Liquid Oxygen (LOX) System. This early version, the LOX Expert System (LES), has spawned other Shuttle-related projects and two computer-aided design (CAD) Small Business Innovative Research (SBIR) grants.

OMRF ECS Model

During fiscal year 1989, KATE was successfully demonstrated against a scale model of the Orbiter Maintenance Refurbishment Facility's (OMRF's) Environmental Control System (ECS). The OMRF ECS supplies conditioned air to four different compartments of the Orbiter while the Shuttle is in the OMRF. The hardware model of the OMRF ECS contains a purge unit that supplies chilled air to four ducts which, in turn, supply air to the Orbiter. Each duct consists of a heater for maintaining a constant temperature and a motorized flow-control valve for controlling the flow rate. KATE's ability to control and diagnose is being tested and demonstrated against this hardware model. A failure panel has been added to allow for manual failing of various components during testing. An operator can request certain flow and temperature setpoints and KATE will respond by adjusting the valves and heater output to achieve the setpoints.

KATE will also identify and respond to external inputs to the ECS, such as load changes. In addition to control, KATE monitors the system, identifying discrepant measurement values and assigning probable causes. In most cases, control of the system can continue, especially if the failure is determined to be due to a measurement.

Red Wagon

A task to integrate a symbolic processor running the KATE system into the Generic Checkout System (GCS), a complex network of Unix-based equipment, is approaching completion. This version of KATE, referred to as Red Wagon, is scheduled to be demonstrated in February 1990.

The GCS testbed is a physical simulation of a Shuttle water tanking system. KATE/GCS will perform control and diagnosis of fastfill, chilldown, and other processes related to filling the Orbiter's external tank.

Shuttle LOX System

The newest application of KATE is to the Shuttle LOX System. When complete, the KATE/LOX software will operate in an advisory mode only (for example, monitoring and diagnosis during the loading of LOX into the Orbiter while in a launch sequence). Initially, KATE/LOX software will be tested in the Artificial Intelligence Laboratory using real-time Shuttle playback (time-stamped) data from the LOX system. The KATE/LOX software will subsequently be integrated with Launch Processing System (LPS) equipment at the Ground Operations Generic Test Facility (GTF) and demonstrated against the Shuttle Ground Operations Simulator (SGOS) LOX model. Validation of the KATE/LOX software at the GTF will be followed by installation and further testing in Firing Room 2 at the Launch Control Center. A possible extension of this version of KATE will be to the Orbiter Power System.

Space Station Advanced Automation

A KATE/Autonomous Control System (ACS) is being developed under the Space Station Freedom Program. The KATE/ACS project utilizes the GCS architecture previously described, but is intended to supplement and extend the KATE/GCS effort. Major activities for the KATE/ACS task include porting the KATE system software from a LISP processor to an Intel 80386-based Unix workstation in LISP, then reimplementing KATE on the Intel 80386 in ADA. Techniques for translating ANSI Standard Common LISP to Military Standard ADA are being investigated concurrently.

ALO

KATE is also being developed as an Advanced Development Project entitled Autonomous Launch Operations (ALO) as part of the U.S. Air Force's Advanced Launch System (ALS) project. The objective of ALO is to demonstrate an autonomous launch control software system that performs real-time monitoring, fault detection, and diagnosis and control from high-level operations requirements. It is part of an effort to greatly reduce launch crew size and human error. As a step toward a full-scale testbed demonstration, KATE/ALO will be demonstrated on a model that includes both water and liquid nitrogen tanking systems.

CAD

Currently, KATE's model bases are built by engineers who have an understanding of KATE's method of knowledge representation and have access to the electrical and mechanical design schematics and design specification documents for the particular application domain. The manual generation of a knowledge base is a time consuming and tedious task. As a solution, research and development involving the automatic generation of KATE-compatible knowledge bases from CAD and computer-aided engineering (CAE) database files is

currently being performed through two separate projects.

A research grant to the University of Central Florida (UCF) is sponsoring a study to create a tool that can generate knowledge bases from existing CAD/CAE files. Existing databases associated with most engineering drawings are sparse, usually describing only component names, interconnectivity between components, and minimal functional information (for example, a range of values). This information is directly translatable, whereas other information required by KATE must be inferred through the use of intelligent tools. UCF has successfully demonstrated the ability to produce an accurate and fairly robust KATE-compatible knowledge base. This grant has been renewed for its third and final phase.

Prospective Computer Analyst, Inc. (PCA), has been awarded an SBIR Phase 2 contract for a proposed CAD/CAE knowledge-based development tool. The project extends over a period of 24 months and also involves the automatic creation of knowledge bases from CAD/CAE files but is more encompassing in its objectives. The proposed tool will automatically generate KATE-compatible knowledge bases from Intergraph CAD/CAE files using knowledge acquisition methods that will infer a large percentage of the structure and function of the domain from the files. Unlike UCF's

work, however, the information the designer inputs to the CAD/CAE database will be influenced by the tool. Furthermore, in order to capture the knowledge required by the model base that is not directly transferable from the CAD/CAE database, the tool will interface with the system designer during the design phase. The overall objective of the project is to create a tool through which knowledge and information gained throughout the design, development, and operational use of a CAD/CAE-designed project can be retained and utilized to develop and maintain knowledge bases for KATE.

Summary

The development of KATE and its associated concepts is ongoing. With each new application of KATE, software enhancements are made to enable KATE to become more generic and powerful so that it is capable of handling a wider variety of complex engineering systems.

Contacts:

*E. E. New, C. L. Belton, B. Brown, and
P. A. Mullenix; 867-3224; DL-DSD-23*

Participating Organization:

*Boeing Aerospace Operations, Engineering
Support Contract (F. T. Zeviar,
C. L. Walker, B. C. Owen, C. O. Pepe,
R. J. Merchant, R. J. Edwards, C. H. Goodrich,
S. R. Beltz, S. L. Fulton, and T. Gould)*

NASA Headquarters Sponsor:

Office of Aeronautics and Space Technology

Technology Utilization

Congress has charged NASA with the task of stimulating the widest possible use of technology resulting from the space program. Thousands of these applications, known as spinoffs, have been transferred to the public and private sectors of the U.S. economy. This transfer of technology includes spinoffs in medicine, electronics, computer systems, design, and management.

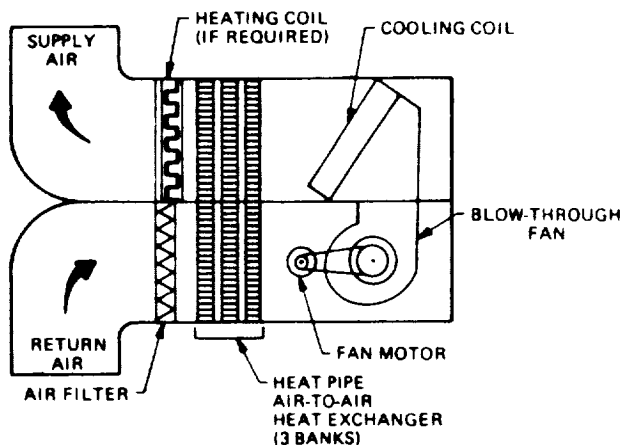
This section of the R&T report describes two such developments of technology at the John F. Kennedy Space Center (KSC); they are a digital hearing aid and heat pipes used as a feedback device to reduce power consumption of air conditioning systems. The technology from these projects has come from the space program and the application has been transferred to industry.

Feasibility Analysis of a High-Efficiency Dehumidifier/Air Conditioner Using Heat Pipes

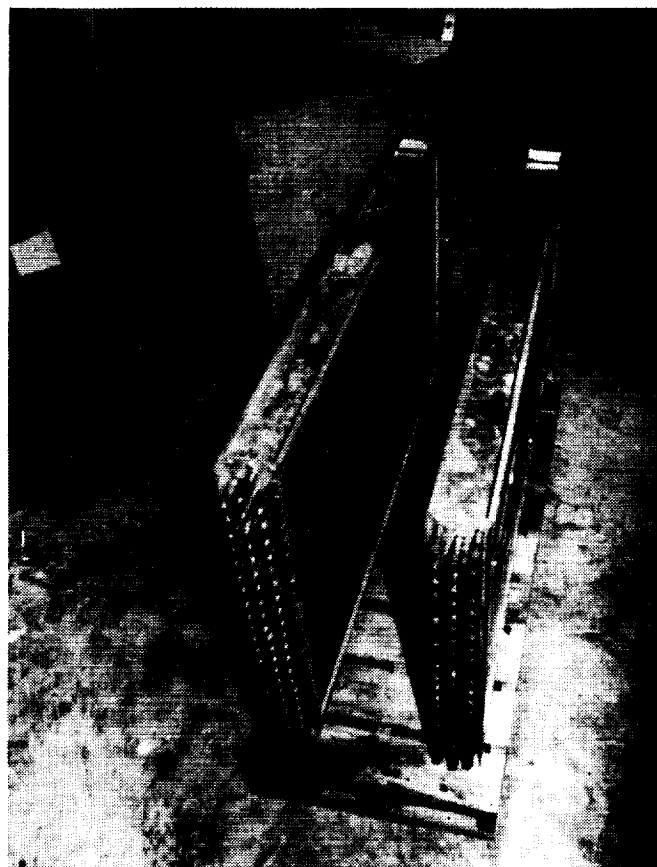
The idea of using heat pipes between the supply air duct and the return air duct in conventional air conditioning units promises to be a cost-effective way to increase the latent heat removal capacity. This design feature is particularly attractive for subtropical climates where humidity control is essential to both industrial processes and human comfort.

The unique aspect of the use of heat pipes is that this method allows efficient removal of sensible heat from the air approaching the evaporator and transfers the heat to the air that has passed through the evaporator, providing reheat. In essence, the heat pipes reduce the sensible load on the evaporator, drop the off-coil temperature, and significantly increase moisture removal. The goal of the project is to demonstrate a latent heat fraction of approximately 60 percent, as opposed to 20 to 30 percent which is typical of conventional units.

The principal contractor for this project is the Florida Solar Energy Center, which installed a heat pipe in a warehouse for Bobs Candies in Albany, Georgia, as a demonstration project. The project, which

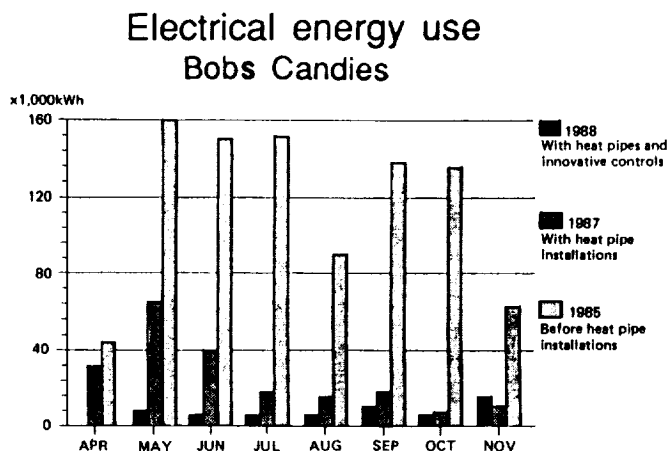


Schematic of an Air Handling Unit With Three Banks of Heat Pipe Air-to-Air Exchange



Prototype of a U-Shaped Heat Pipe

is in cooperation with Georgia Power, has shown a 30- to 50-percent savings of electrical power. In other words, the cost of the project was recovered within the first year of operation.



Comparative Energy Use Before and After Installation of Heat Pipes and Innovative Controls

Off-season variances in energy use in April and November may be attributed to the seasonal variations or control system operation. Further study to resolve these discrepancies is required.

Contact:

J. K. O'Malley, 867-3688, DF-FED-33

Participating Organization:

Florida Solar Energy Center (M. K. Khatter)

NASA Headquarters Sponsor:

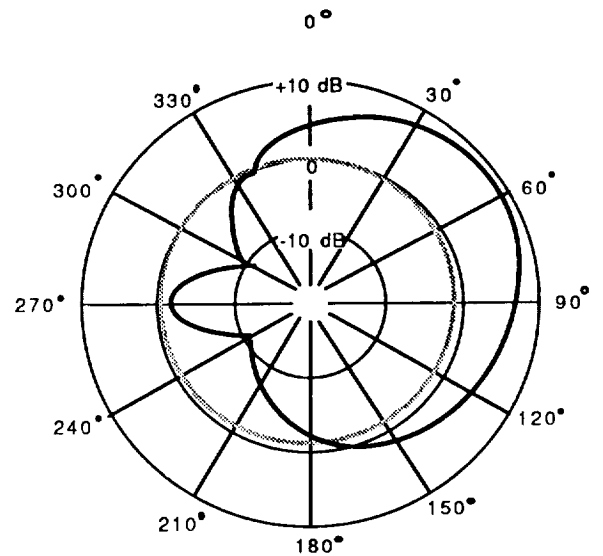
Office of Commercial Programs

Development of a Digital Hearing Aid

The purpose of this project is to develop a digital hearing aid that will lead to improved performance of acoustic amplification for the hearing impaired. Digital hearing aid technology can provide the flexibility of adjustment and control of auditory signal processing required to better compensate for the patient's hearing impairment than is possible with conventional analog technology or even hybrid technology in which analog amplifiers and filters can be adjusted with digital logic.

A key factor in achieving an optimal fit for the patient is the acoustical interaction that occurs between the hearing aid and the patient. By incorporating the hearing aid into the fitting procedure and being able to adjust the parameters of the hearing aid remotely from a host computer (and audiometer) while the patient is wearing the aid, variables such as the acoustics of the earmold, ear, and head can be directly addressed. This allows adaptive fitting procedures that can vary the characteristics of the hearing aid to be implemented during testing.

One example of this acoustical interaction between patient and hearing aid is illustrated in the figure "Directional Sensitivity of a Microphone in Free Field and Near the Right Ear." The hatched curve



..... In Free Field
 ——— Near Right Ear

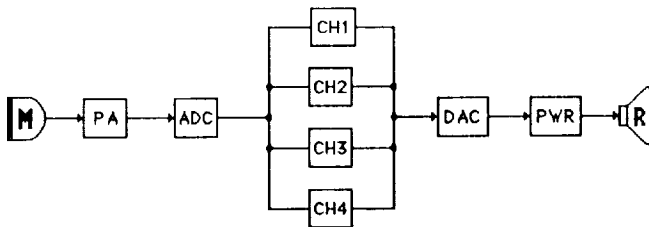
Directional Sensitivity of a Microphone in Free Field and Near the Right Ear

shows the directional sensitivity of a hearing aid microphone for a 2,000-hertz tone for free-field conditions. The solid curve illustrates how the directional sensitivity of the microphone is modified when it is positioned near the head at ear level. Other factors (such as the change in resonance of the ear canal when it is occluded by the ear insert or the acoustic load imposed on the receiver by the ear impedance) also modify the transfer characteristic of the hearing aid. Although some of these factors are systematic, predictable, and time invariant and can be compensated for with fixed-filter shaping, others vary from patient to patient and depend, in part, on the size and shape of the ear insert and its associated acoustic plumbing. These patient-dependent factors can be accounted for if the hearing aid has sufficient adjustment flexibility and if it can be worn and adjusted during the fitting procedure. There are also factors that vary over the short term; for example, sound leakage around the hearing aid back into the microphone, which can produce positive feedback and oscillation at certain frequencies.

The goal, therefore, is to develop a hearing aid that can be adjusted to compensate for a wide variety of hearing losses while taking into account all the factors that can corrupt the prescribed fit. A digital approach was chosen because of the flexibility of design that is afforded, which can include sophisticated adaptive signal processing algorithms. A low-powered, complementary metal oxide silicon (CMOS) chip using very large scale integration (VLSI) technology has been employed to minimize power consumption. In order to use a typical hearing aid battery to power the digital hearing aid, the circuitry is being designed to operate at 1.2 volts and consume less than 2 milliwatts of power.

The figure "Functional Block Diagram of the Digital Hearing Aid" includes a microphone preamplifier and antialiasing filter that provides an input to the analog-to-digital converter (ADC). Following the ADC is a multichannel filter structure that is designed to provide independent adjustment of linear gain and maximum output over four different audio bands of frequencies. The control of maximum output is achieved with a minimum of harmonic distortion by incorporating a filter before and after the limiting operation. The multichannel filter structure is followed by a digital-to-analog converter (DAC) and power amplifier capable of driving the receiver (loud speaker) of the hearing aid.

Several algorithms have been designed to accommodate dynamically changing conditions of signal and ambient noise, thereby extending the operating range of the digital hearing aid over what can be achieved

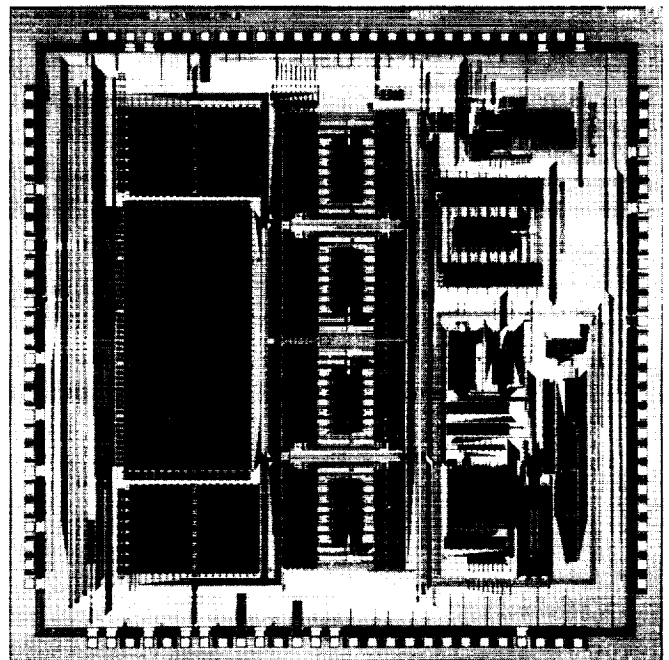


Functional Block Diagram of a Digital Hearing Aid

by conventional means. In addition, a serial port is included for communication between the hearing aid and host computer.

In 1989, work has continued apace towards the ultimate goal of achieving a custom VLSI chip set containing the full-featured adaptive digital hearing aid (ADHA). Most notable is the progress in the development of the digital signal processing (DSP) chip, which has recently culminated in the successful design, integration, and test of the hi-fi Systolic Array of Log Multiplier Accumulator (SALMA) chip. The SALMA chip provides all signal processing for the four-channel model, including all necessary control and per-channel adaptive compressive gain. A photomicrograph of the hi-fi integrated circuit is shown in the figure "Photomicrograph of the Hi-Fi SALMA Chip."

Progress has also been made in the analog design area. Every function needed for data acquisition and reconstruction has been integrated on separate chips, tested,



Photomicrograph of the Hi-Fi SALMA Chip

and verified. The next step in this activity is to modify a few of the circuits and to combine them on a single chip. Adaptive noise cancellation and feedback equalization algorithms that have been demonstrated on the linear benchtop system have been integrated into a building-block chip for further study in a log benchtop system.

Contact:

R. M. Davis, 867-2780, PT-AST

Participating Organizations:

Central Institute for the Deaf, St. Louis, Missouri (A. M. Engebretson, D.Sc.)

Washington University, St. Louis, Missouri (R. E. Morley, Jr., D.Sc.)

NASA Headquarters Sponsor:

Office of Commercial Programs



Report Documentation Page

1. Report No. NASA TM 102150		2. Government Accession No.		3. Recipient's Catalog No.	
4. Title and Subtitle Research and Technology 1989 Annual Report of the Kennedy Space Center			5. Report Date December 1989		
			6. Performing Organization Code PT-PMO		
7. Author(s)			8. Performing Organization Report No.		
			10. Work Unit No.		
9. Performing Organization Name and Address NASA John F. Kennedy Space Center Kennedy Space Center, Florida 32899			11. Contract or Grant No.		
			13. Type of Report and Period Covered Technical Memorandum 1989		
12. Sponsoring Agency Name and Address National Aeronautics and Space Administration Washington, DC 20546			14. Sponsoring Agency Code		
			15. Supplementary Notes		
16. Abstract <p>As the NASA Center responsible for assembly, checkout, servicing, launch, recovery, and operational support of Space Transportation System elements and payloads, Kennedy Space Center is placing increasing emphasis on the Center's research and technology program. In addition to strengthening those areas of engineering and operations technology that contribute to safer, more efficient, and more economical execution of our current mission, we are developing the technological tools needed to execute the Center's mission relative to future programs. The Engineering Development Directorate encompasses most of the laboratories and other Center resources that are key elements of research and technology program implementation and is responsible for implementation of the majority of the projects in this Kennedy Space Center 1989 Annual Report.</p> <p>For further technical information about the projects, contact David A. Springer, Projects Management Office, DE-PMO-5, (407) 867-3035. Thomas M. Hammond, Technology Utilization Officer, PT-PMO-A, (407) 867-3017, is responsible for publication of this report and should be contacted for any desired information regarding the Center-wide research and technology program.</p>					
17. Key Words (Suggested by Author(s)) Research and Technology			18. Distribution Statement Unclassified - Unlimited Subject Category 99		
19. Security Classif. (of this report) Unclassified		20. Security Classif. (of this page) Unclassified		21. No. of pages	22. Price



NASA

National Aeronautics and
Space Administration

John F. Kennedy Space Center

Wallops Flight Complex, MS 00001